

**The Foot-and-Mouth Disease Virus Replication
Complex: Dissecting the Role of the Viral Polymerase
(3D^{pol}) and Investigating Interactions with
Phosphatidylinositol-4-kinase (PI4K)**

Eleni-Anna Loundras

Submitted in accordance with the requirements for the degree of
Doctor of Philosophy

The University of Leeds
School of Molecular and Cellular Biology

August 2017

The candidate confirms that the work submitted is her own, except where work which has formed part of jointly authored publications has been included. The contribution of the candidate and the other authors to this work has been explicitly indicated below. The candidate confirms that appropriate credit has been given within the thesis where reference has been made to the work of others.

The work appearing in Chapter 3 and Chapter 4 of the thesis has appeared in publications as follow:

- *Employing transposon mutagenesis in investigate foot-and-mouth disease virus replication. Journal of Virology (2015), 96 (12), pp 3507-3518., DOI: 10.1099/jgv.0.000306. Morgan R. Herod (MRH), Eleni-Anna Loundras (EAL), Joseph C. Ward, Fiona Tulloch, David J. Rowlands (DJR), Nicola J. Stonehouse (NJS).*

The author (EAL) was responsible for assisting with preparation of experiments and production of experimental data. MRH, as primary author drafted the manuscript and designed the experiments. NJS and DJR conceived the idea, supervised the project, and edited the manuscript.

- *Both cis and trans activities of foot-and-mouth disease virus 3D polymerase are essential for viral replication. Journal of Virology (2016), 90 (15), pp 6864-688., DOI: 10.1128/JVI.00469-16. Morgan R. Herod, Cristina Ferrer-Orta, Eleni-Anna Loundras, Joseph C. Ward, Nuria Verdager, David J. Rowlands, Nicola J. Stonehouse.*

The author (EAL) was responsible for carrying out structural experimental analysis and production of data, and contributed equally to the work alongside Cristina Ferrer-Orta. EAL assisted in the drafting the manuscript. MRH, as primary author, drafted the manuscript and designed experimental work. NJS and DJR conceived the idea, supervised the project, and edited the manuscript.

The work appearing in Chapter 5 of the thesis has appeared in publication as follows:

- *Foot-and-mouth disease virus genome replication is unaffected by inhibition of type III phosphatidyl-4-kinases. Journal of General Virology (2016). 97 (9), pp 2221-2230., DOI: 10.1099/jgv.0.00052. Eleni-Anna Loundras, Morgan R. Herod, Mark Harris (MH), Nicola J. Stonehouse.*

The author (EAL) was responsible for carrying out all experiments and drafting the manuscript. MRH assisted with some of the preliminary experimental work and the drafting of the manuscript. NJS and MH conceived the idea, supervised the project, prepared and edited the manuscript.

This copy has been supplied on the understanding that it is copyright material and that no quotation from the thesis may be published without proper acknowledgement

© 2017 The University of Leeds and ELENI-ANNA LOUNDRAS

The right of ELENI-ANNA LOUNDRAS to be identified as Author of this work has been asserted by her in accordance with the Copyright, Designs and Patents Act 1988.

Acknowledgements

Firstly, I'd like to thank my supervisors Prof. Nicola Stonehouse and Prof. Mark Harris for their guidance and unwavering support throughout my PhD. I'd also like to thank them for pushing me to achieve more than I thought was possible and for having faith in my abilities.

To Morgan, thank you for all your support and help with my research, keeping me thinking critically and remembering all my controls! Thank you for the opportunity to be part of some exciting research. To Joe, thank you for your help with assays and putting up with all my cloning questions (and for overseeing my "little pot of crazy!").

To the rest of the 'Stonelands' and Harris groups (past and present) for all our enlightening discussions and copious amount of coffee. To Kate Loveday, for helping me take my project to new heights, and to Sue Matthews for being my extra pair of hands. To Garstang 8.53, especially Chris: without you guys, coming in everyday to tackle science would have been nigh on impossible!

Last but not least, I would like to thank Charlotte and Lorna, for keeping me sane and standing by me during some of my darkest days. To Mum and Dad, Alexia, and Natalie for believing in me and encouraging me through this endeavour. To Lana and Archer: woof-woof, meow. Finally, to Philip for being my rock: you absolute star, thank you, for everything.



Abstract

Replication of many positive-strand RNA viruses have been shown to occur within intracellular membrane-associated compartments termed replication complexes. Replication of viral RNA occurs within these intracellular compartments as a way for the virus to concentrate the structural and non-structural components into a small area to facilitate replication as well as protecting the virus components from host-cell pathogen recognition and innate immune responses. Using immunofluorescent confocal and electron microscopy, foot-and-mouth disease virus (FMDV) has been shown to dysregulate Golgi and ER-derived membranes, but to date, no distinct membrane-bound replication complex comprised of viral RNA, structural and non-structural proteins, and host-cell proteins have yet to be identified for FMDV.

The FMDV RNA-dependent RNA polymerase, 3D^{pol}, is the primary protein involved in virus genome replication and has been previously shown to form higher-order fibril-like structures *in vitro* in the presence of RNA. These 3D^{pol} fibril structures could act to 'scaffold' replication complex formation. Here, several mutations were made in 3D^{pol} to assess their role in higher-order complex formation. The ability for the different 3D^{pol} mutations to function was assessed biochemically, structurally and in cell culture. The results point towards the necessity for a fully functional (catalytically active) polymerase in the formation of the higher-order structures. Furthermore, complementation studies indicate that 3D^{pol} has two distinct functions necessary for replication within cells.

Additionally, it was pertinent to investigate the role of membrane-associated kinases, such as PI4K, as a number of related viruses utilise this cellular pathway to form an

optimal environment within which viral replication can occur by upregulating the formation of lipids used in the building of intracellular membranes. Investigation of translation and replication of FMDV RNA within cells show that FMDV does not appear to utilise the PI4K pathway. These results highlight differences between FMDV and other related picornaviruses and provide a basis to investigate alternative methods for replication complex formation.

Table of Contents

Acknowledgements.....	iii
Abstract.....	iv
List of Figures	x
List of Tables.....	xiii
List of Abbreviations	xiv
Chapter 1.....	1
Introduction	1
1.1 Picornaviruses	1
1.1.1 Classification and genome structure	1
1.1.2 Aphthoviruses	5
1.2 Foot-and-Mouth Disease Virus	7
1.2.1 History, Taxonomy and Epidemiology	7
1.2.2 Virus Transmission and Control	8
1.2.3 Genome Structure.....	13
1.2.3.1 The 5' UTR	16
1.2.3.2 The 3' UTR	19
1.2.3.3 The Leader proteinase	20
1.2.3.4 Structural proteins 1A-1D/2A	22
1.2.3.5 Non-structural proteins 2A-3D ^{pol}	23
1.2.4 FMDV genome replication	30
1.3 Replication Complex	36
1.3.1 FMDV Fibrils	36
1.3.2 Cellular Interacting Partners in Replication Complex Formation	37
1.4 Aims of the Project.....	40
Chapter 2.....	41
Materials and Methods.....	41
2.1 General Buffers, Media and Solutions	41
2.2 Cell Lines.....	44
2.3 Compounds	44
2.4 Antibodies	45

2.5 Nucleic acid manipulation	45
2.5.1 Plasmids and Replicons	45
2.5.1.1 FMDV Replicon Constructs.....	46
2.5.1.2 Bicistronic Replicon Constructs.....	48
2.1.1.3 CVB3 Replicon Constructs	48
2.5.1.4 HCV Replicon Constructs.....	49
2.5.2 Replicon DNA Preparation	50
2.5.2.1 Transformation	50
2.5.2.2 Preparation of plasmid DNA	50
2.5.2.3 DNA linearisation	51
2.5.2.3 DNA Purification.....	51
2.5.3 RNA Preparation	52
2.5.3.1 T7 In vitro Transcription.....	52
2.6 Cell Culture	53
2.6.1 Cell Culture Maintenance	53
2.6.2 Preparing Cells for IncuCyte Analyses.....	53
2.6.3 Transfection of RNA	53
2.6.4 Preparing Cells for Dual Luciferase Assays.....	54
2.6.5 Transfection of DNA	54
2.6.6 Preparing cells for electroporation	54
2.6.7 Electroporation of RNA	55
2.6.8 Compound treatments.....	55
2.6.9 Cytotoxicity (MTT) assay	55
2.7 Immunofluorescence	56
2.7.1 Preparation of Cells for Immunofluorescence.....	56
2.7.2 Permeabilisation and Antibody Probing.....	56
2.8 Immunoblotting	57
2.8.1 Harvesting Cell Lysates.....	57
2.8.2 SDS-PAGE Gel Electrophoresis	58
2.8.3 Western Blotting	58
2.8.4 Antibody Incubation.....	58

2.8.5 Developing SDS-PAGE membranes	59
2.9 Expression and purification of His-tagged 3D ^{pol}	59
2.10 His-tagged 3D ^{pol} in vitro assays	60
2.10.1 3D ^{pol} Activity Assay	60
2.10.2 3D ^{pol} Crosslinking Assay	61
2.10.3 3D ^{pol} RNA-binding fluorescent polarisation anisotropy	62
2.10.4 Transmission electron microscopy (TEM) negative staining	63
2.10.5 Cryo-electron microscopy (Cryo-EM).....	63
Chapter 3.....	65
Investigating mutations in foot-and-mouth disease virus 3D polymerase in viral replication	65
3.1 Introduction	65
3.2 Mutations of 3D ^{pol}	70
3.3 Purification and validation of mutant 3D ^{pol}	76
3.4 Assessing activity of mutant 3D ^{pol}	81
3.4.1 Incorporation of radiolabelled UTP	81
3.4.2 Determining the structure of non-catalytic mutant GC216/7AA	84
3.4.3 Investigation into RNA binding	87
3.5 Investigation into formation of higher-order complexes	90
3.6 Structural determination of FMDV 3D ^{pol} fibrils.....	96
3.7 The importance of RNA in the formation of fibrils	101
3.8 Is 3CD a catalytically functional precursor?	105
3.9 Chapter discussion	110
Chapter 4.....	115
Investigating the role of foot-and-mouth disease virus 3D polymerase mutants on replicon replication	115
4.1 Introduction	115
4.2 Replicons	117
4.2.1 Replication.....	119
4.2.2 Evidence of protein expression.....	121
4.3 Mutations in 3D ^{pol}	125
4.3.1 Epitope-tagging of replicons	126
4.3.2 Next generation replicons.....	129

4.3.3 Epitope-tagging of replication-deficient replicons	131
4.3.4 Recovery of replication-deficient replicons	132
4.3.5 Cellular localisation of FMDV 3D ^{pol}	135
4.4 Role of structural RNA elements in 5' UTR in replicon recovery	139
4.4.1 Role of mutations the 5' UTR in replicon recovery	140
4.4.2 Is 3D ^{pol} sufficient to recover replication?.....	142
4.5 Discussion.....	147
Chapter 5.....	153
Foot-and-mouth disease virus genome replication is unaffected by inhibition of type III phosphatidylinositol-4-kinases	153
5.1 Introduction	153
5.2 The role of phosphoinositides in virus RNA replication.....	156
5.3 Inhibitors of phosphatidylinositol-4 kinases	160
5.3.1 PIK93.....	161
5.3.2 Compounds 3 and 7	162
5.3.3 Wortmannin	162
5.4 Effect of PI4K on IRES-mediated translation.....	163
5.5 Effect of PI4K on RNA replication.....	167
5.5.1 FMDV replication does not require PI4KIII α or β activity.	173
5.5.2 FMDV replication does not result in upregulation of PI4P lipids.....	175
5.5.3 Involvement of PI3K pathway in FMDV replication	178
5.6 Chapter discussion	180
Chapter 6.....	183
Concluding Remarks and Future Perspectives.....	183
References.....	189

List of Figures

Figure 1.1 Schematic representation of the FMDV genome organisation.....	2
Figure 1.2 Neighbour-joining phylogenetic tree of the aphthovirus genus members...	6
Figure 1.3 Map showing the geographical distribution of the seven different FMDV serotypes highlighted in pools.....	8
Figure 1.4 Schematic of the FMDV genome organisation and capsid protein structure.....	15
Figure 1.5 Schematic depicting the location and organisation of the FMDV 5' UTR..	16
Figure 1.6 Schematic depicting the location and organisation of the FMDV 3' UTR..	19
Figure 1.7 Schematic of the FMDV genome showing the proposed ORFs of each of the viral proteins.....	21
Figure 1.8 Schematic of the relationship of host-cell translation initiation factors and the FMDV 5' UTR.....	31
Figure 1.9 Schematic of the process of FMDV replication.....	33
Figure 3.1 Schematic of the FMDV genome showing the proposed ORFs of each of the viral proteins.....	66
Figure 3.2 Three-dimensional model structure of FMDV 3D ^{pol}	71
Figure 3.3 Schematic outlining the location of the mutations identified in 3D ^{pol}	74
Figure 3.4 Purification of serotype C his-3D ^{pol} recombinant proteins.....	77
Figure 3.5 Mass spectroscopy analysis of his-3D ^{pol} recombinant protein.....	79-80
Figure 3.6 Polymerase activity assays used to determine activity of the 3D ^{pol} recombinant proteins.....	83
Figure 3.7 Crystal structure of mutant polymerase.....	85
Figure 3.8 Fluorescence polarisation anisotropy assay.....	89
Figure 3.9 Glutaraldehyde crosslinking assay.....	92
Figure 3.10 Negative stain TEM of crosslinked polymerase activity assay.....	94
Figure 3.11 Negative stain TEM of crosslinked polymerase activity assay.....	95
Figure 3.12 2D class averaging of fibrils detected by cryo-EM.....	96
Figure 3.13 Intermediate resolution three-dimensional model fibril structure of WT fibril with docked WT 3D ^{pol} crystal structure.....	97
Figure 3.14 Cartoon schematic depicting the proposed arrangement of polymerase molecules.....	98
Figure 3.15 Intermediate resolution cryo-EM structure of FMDV 3D ^{pol} fibrils with crystal structure of WT 3D ^{pol}	100
Figure 3.16 Autoradiograph of glutaraldehyde crosslinking assay.....	101
Figure 3.17 Glutaraldehyde crosslinking activity assay showing the higher-order oligomers treated with DNase I, RNase A and proteinase K.....	103

Figure 3.18 Negative stain TEM.....	104
Figure 3.19 Purification of his-tagged recombinant 3CD protein.....	106
Figure 3.20 Dot-blot of 3CD activity assay.....	108
Figure 3.21 Glutaraldehyde crosslinking assay on recombinant 3CD incubated with RNA over time.....	109
Figure 4.1 Schematic diagrams of second-generation FMDV replicons.....	118
Figure 4.2 Representative data of transfected BHK-21 cells.....	120
Figure 4.3 Western blot analysis of BHK-21 cells transfected with GFP-pac-WT replicon RNA and lysed at incremental time points.....	123
Figure 4.4 Schematic diagram of FMDV replicon.....	126
Figure 4.5 Levels of GFP-expression in BHK-21 cells transfected with GFP-pac replicon RNA.....	127
Figure 4.6 Western blot analysis of BHK-21 cells transfected with 3D ^{pol} epitope-tagged GFP-pac-WT constructs.....	128
Figure 4.7 Schematic diagrams of third-generation FMDV replicon.....	129
Figure 4.8 Representative data of transfected BHK-21.....	130
Figure 4.9 Levels of GFP-expression in BHK-21 cells transfected with ptGFP replicon RNA.....	131
Figure 4.10 Co-transfection of mCherry-WT helper replicon RNA and control tRNA with ptGFP mutant replicon (ptGFP-GNN) or with ptGFP-WT replicon.....	133
Figure 4.11 Levels of GFP expression at eight hours post-transfection of mutant polymerase ptGFP replicons.....	134
Figure 4.12 Dual immunofluorescence analysis showing co-localisation of WT and mutant non-structural proteins.....	137
Figure 4.13 Levels of GFP expression at eight hours post-transfection of mutant polymerase ptGFP replicons.....	141
Figure 4.14 Schematic of the FMDV genome outlining the different regions.....	142
Figure 4.15 Schematic outlining the FMDV replication-deficient mutant ptGFP replicon.....	143
Figure 4.16 Recovery of truncated replicons.....	145
Figure 5.1 Schematic showing the chemical structures of the different PI phosphorylation states.....	158
Figure 5.2 Simplified diagrammatic representation of the localisation of phosphatidylinositol (PI) lipids in the cell.....	159
Figure 5.3 Chemical structures of the PI4K inhibitors used.....	161
Figure 5.4 Schematic of bi-cistronic reporter constructs.....	163
Figure 5.5 MTT cytotoxicity assay of a range of PIK93 concentrations (0-5 μ M) on BHK-21 cells.....	164
Figure 5.6 BHK-21 cells transfected with the bi-cistronic constructs and treated with varying concentrations of PIK93 for 48 hours.....	166

Figure 5.7 Levels of GFP expression as a measure of replication in BHK-21 cells transfected with replicon RNA.....	168
Figure 5.8 Measuring the effect of replication of FMDV replicon RNA in BHK-21 cells treated with PIK93.....	170
Figure 5.9 Measuring the effect of PIK93 on CVB3 replicon RNA replication in BHK-21 cells.....	172
Figure 5.10 The effect of novel PI4KIII α/β compounds on the replication of FMDV and HCV replicon RNA.....	174
Figure 5.11 Effect of PIK93, CMPD (3) and CMPD (7) on the levels of PI4P expression in cells.....	176-7
Figure 5.12 Effect of wortmannin on replication of FMDV replicon RNA.....	179

List of Tables

Table 1.1: Summary of the 35 confirmed genera in the family <i>Picornaviridae</i> ..	3-5
Table 2.1: Summary of GFP-containing replicon constructs.....	47
Table 2.2: Summary of mCherry-containing replicon constructs.....	47
Table 2.3: Summary of bi-cistronic reporter constructs.....	48
Table 2.4: Summary of CVB3 replicons constructs.....	49
Table 2.5: Summary of HCV replicon construct.....	49
Table 3.1: Comparison of the protein sequence alignment of FMDV 3D ^{pol} serotypes O and C.....	73
Table 3.2: Comparison of theoretical and measure masses of his-3D ^{pol} recombinant WT and mutant proteins.....	78

List of Abbreviations

+ve	Positive sense
µg	Microgram
µl	Microlitre
µM	Micromolar
3' UTR	3' untranslated region
³² P	Phosphorus-32
3D	3-dimensional
3D ^{pol}	3D polymerase
5' UTR	5' untranslated region
Å	Angstrom
A	Alanine
APS	Ammonium persulphate
Arf1	ADP-ribosylation factor 1
ATCC	American type culture collection
BHK-21	Baby hamster kidney cells (21 days old)
BSA	Bovine serum albumin
C	Cysteine
CPD	Compound
CO ₂	Carbon dioxide
CPM	Counts per minute
<i>cre</i>	<i>Cis</i> -acting replicative element
CV	Column volume
CVB3	Coxsackievirus B3
D	Aspartic acid
Da	Dalton
DAPI	4',6-diaminido-2-phenylindole
DEPC	Diethylpyrocarbonate
dH ₂ O	Distilled water
DMEM	Dulbecco's modified Eagles' medium
DNA	Deoxyribonucleic acid
Dnase	Deoxyribonuclease
e ⁻	Electron
E1	Envelope 1
E2	Envelope 2
ECL	Enhanced chemiluminescence
EDTA	Ethylenediamine tetra-acetic acid
eIF	Elongation initiation factor
EMCV	Encephalomyocarditis virus
ER	Endoplasmic reticulum
FBS	Foetal bovine serum
Feo	Neomycin phosphotransferase
FITC	Fluorescein isothiocyanate

FMDV	Foot-and-mouth disease virus
FPA	Fluorescent polarisation anisotropy
g	Gravitational constant
G	Glycine
GAPDH	Glyceraldehyde 3-phosphate dehydrogenase
GBF1	Golgi-specific Brefeldin A-Resistant Guanine Nucleotide Exchange Factor 1
GFP	Green fluorescent protein
HA	Haemagglutinin
HCl	Hydrochloric acid
HCV	Hepatitis C virus
HeLa	Henrietta Lacks (cells)
His	Histidine
HIV	Human immunodeficiency virus
HRP	Horseradish peroxidase
HRV	Human rhinovirus
Huh 7.5	Human hepatocarcinoma 7.5
IFN	Interferon
IPTG	Isopropyl β -D-1-thiogalactopyranoside
IRES	Internal ribosome entry site
JFH1	Japanese fulminant hepatitis 1
k	Thousand
kb	Kilobase
Kd	Dissociation constant
kDa	Kilodalton
LB	Luria-Bertani
LC-MS	Liquid chromatography-mass spectrometry
LFU	Luciferase forming units
Luc	Luciferase
M	Molar
mA	Milliamperes
MDA5	Melanoma differentiation-associated protein 5
MDBK	Madin-Darby bovine kidney cells
MHC-I	Major histocompatibility complex I
MEM	Minimal essential medium
MgCl ₂	Magnesium chloride
mins	Minutes
ml	Millilitre
mM	Millimolar
MOPS	3-(N-morpholino)propanesulphonic acid
ms	Milliseconds
N	Asparagine
NaCl	Sodium chloride
NEAA	Non-essential amino acids
NEMO	NF- κ B essential modulator
NF- κ B	Nuclear factor kappa-light-chain-enhancer of activated B cells

ng	Nanogram
nm	Nanometre
nM	Nanomolar
NS	Non-structural
Oligo (dG)	Oligodeoxyribonucleotides (Guanine)
Oligo (dT)	Oligodeoxyribonucleotides (Thymine)
ORF	Open reading frame
p	p-Value
PABP	Poly-A binding protein
PAGE	Polyacrylamide Gel Electrophoresis
PBS	Phosphate buffered saline
PCBP	Poly-C binding protein
PDB	Protein database
PEI	Polyethylenimine
PI	Phosphoinositide
PI(3,4)P ₂	Phosphatidylinositol 3,4-bisphosphate
PI(4,5)P ₂	Phosphatidylinositol 4,5-bisphosphate
PI3K	Phosphatidylinositol-3-kinase
PI4K	Phosphatidylinositol-4-kinase
PI4P	Phosphatidylinositol-4-phosphate
PI5K1	Phosphatidylinositol-5-kinase
PIP ₃	Phosphatidylinositol (3,4,5)-triphosphate
Poly (rC)	Polyribonucleotides (Cytosine)
PTB	Poly-pyrimidine tract binding protein
ptGFP	<i>ptilosarcus</i> Green fluorescent protein
pUpU	Uridylylated
PV	Poliovirus
PVDF	Polyvinylidene fluoride
RdRp	RNA-dependent RNA polymerase
RIG-I	Retinoic acid-inducible gene I
RIPA	Radioimmunoprecipitation assay
RNA	Ribonucleic acid
Rnase	Ribonuclease
RPM	Revolutions per minute
sec	Seconds
SDS	Sodium dodecyl sulphate
SEM	Standard error of the mean
SGR	Sub-genomic replicon
siRNA	Short interfering ribonuclease
ssRNA	Single-stranded ribonuclease
T	Thymine
TBE	Tris-Borate-EDTA
TBS	Tris-buffered Saline
TEM	Transmission electron microscopy
TEMED	N,N,N',N'-tetramethylethylenediamine

tRNA	Transfer ribonucleic acid
UTP	Uridine 5'-triphosphate
V	Volts
v/v	Volume/volume
VPg	Viral protein genome-linked
w/v	Weight/volume
w/w	Weight/weight
WT	Wildtype
ZnCl ₂	Zinc chloride

Chapter 1

Introduction

1.1 Picornaviruses

1.1.1 Classification and genome structure

Picornaviruses are a diverse family of small RNA viruses. The family consists of 35 genera and over 80 species of single-stranded positive sense RNA (+ve ssRNA) viruses as classified by the International Committee on Taxonomy of Viruses (ICTV) in 2016 (ICTV, 2016; Adams et al., 2017). Many of these viruses (summarised in Table 1.1) are significant causative agents of human and animal disease. Members include poliovirus (PV), human rhinovirus, bovine enterovirus, hepatitis A virus and, foot-and-mouth disease virus (FMDV). PV, belonging to the genus *Enterovirus*, is one of the most well-defined viruses; much of the research on the replication processes of *Picornaviridae* is due to the discovery that PV could be propagated in cell culture (Enders et al., 1949) and for review see Racaniello, 2007.

The term “picornavirus” is derived from “*pico*”, meaning small, and “*RNA*”, which refers to the ribonucleic acid contained within the non-enveloped, icosahedral capsid of all picornaviruses. Picornaviruses measure between 18-30 nm in diameter and contain a +ve ssRNA genome between \approx 7.5-8.5 kb in length (reviewed in Racaniello, 2007). Despite being a diverse family, picornaviruses share a very similar genome structure and organisation (as highlighted in Fig. 1.1). The FMDV RNA encodes for a large single polyprotein that can be separated into three regions: P1 (1A-1D) that

encodes for the structural (capsid) proteins, P2 (2A-2C) and P3 (3A-3D) which encode for the non-structural proteins necessary for the replication of the genome and the manipulation of the host-cell environment. The genome is flanked by two highly structured untranslated regions (UTR) located at the 5' and 3' termini of the genome. The 5' UTR is covalently linked to protein VPg, and contains a number of highly-structured RNA elements including an internal ribosome entry site (IRES). The 3' UTR is polyadenylated (Rueckert et al., 1984; Stanway, 1990) and contains two stem-loop structures preceding the poly-A tract. The two stem-loops at the 3' UTR have been shown, through studies using FMDV infectious clones and passaging in cell culture, to be involved in the replication ability of the RNA. Exchanging the 3' UTR with the equivalent region of swine vesicular disease virus, or deleting the 3' UTR region abrogated virus replication (Sáiz et al., 2001). The FMDV 3' UTR has also been shown to be involved in the circularisation of the genome by interacting with structural elements in the 5' UTR (Serrano et al., 2006).

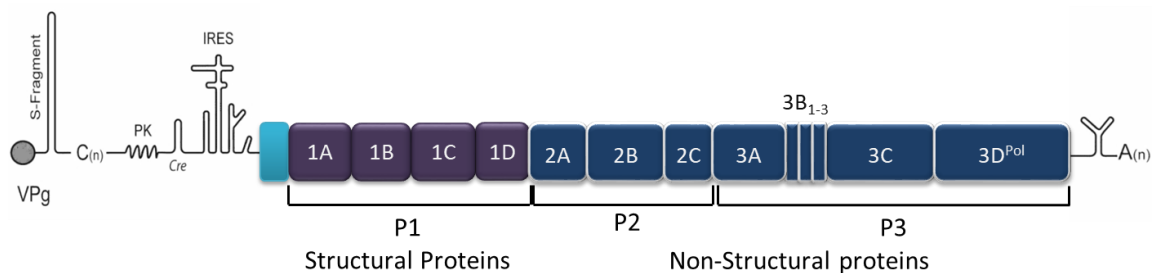


Figure 1.1 Schematic representation of the FMDV genome organisation. Most picornaviruses share a similar genome structure and organisation. FMDV contains a very long 5' UTR, a 'leader' protease (L^{Pro}) coloured in light blue, and three tandem copies of the 3B protein. Adapted from (Forrest et al., 2014).

Upon entry into the cell and after capsid uncoating, the FMDV RNA genome is translated in a cap-independent mechanism using the IRES located in the 5' UTR. Following translation, the polyprotein is cleaved into the structural and non-

structural proteins by two viral-encoded proteases: leader (L^{pro}) (present in some picornaviruses) and 3C, and by a region termed 2A that results in cleavage of the polyprotein through due to ribosome skipping (see section 1.2.3.5.1). 2A cleaves the structural P1 proteins away from the non-structural P2 and P3 regions, and 3C cleaves the remaining non-structural proteins into their active forms (Stanway, 1990; Lin et al., 2009).

Despite sharing a similar genome organisation, a number of picornavirus species differ in some of their genomic constituents. A major difference between some picornavirus family members is located in the 5' UTR. Cardioviruses and aphthoviruses have a significantly larger 5' UTR than enteroviruses and rhinoviruses (1300 bp compared to 600 bp) as they contain a large poly-C tract. Other differences can be found within L^{pro} , 2A and in the number of 3B protein copies they contain (Palmenberg, 1987; Stanway, 1990). These are discussed in more detail in subsequent sections.

Genus	Species examples	Accession number
<i>Ampivirus</i>	Ampivirus (newt picornavirus)	KP770140
<i>Aphthovirus</i>	Foot-and-mouth disease virus	AY593829
	Bovine rhinitis A virus	EU236594
	Equine rhinitis A virus	DQ272578
<i>Aquamavirus</i>	Seal aquamavirus	AY593829
<i>Avihepatovirus</i>	Duck hepatitis A virus	EU142040
<i>Avisivirus</i>	Avisivirus (chicken picornavirus)	DQ226541
<i>Cardiovirus</i>	Encephalomyocarditis virus	KC614703

Genus	Species examples	Accession number
	Theiler's murine encephalomyelitis virus	M81861
<i>Cosavirus</i>	Human cosavirus	FJ438902
<i>Dicpivirus</i>	Canine picodicrovirus	JN819202
<i>Enterovirus</i>	Coxsackievirus A16	AY421760
	Coxsackievirus B3	M88483
	Poliovirus	V01149
	Enterovirus D68	AY426531
	Rhinovirus A	FJ445111
<i>Erbovirus</i>	Equine rhinitis B virus	X96871
<i>Gallivirus</i>	Gallivirus	JQ691613
<i>Harkavirus</i>	Falcovirus	KP230449
<i>Hepatovirus</i>	Hepatitis A virus	M14707
<i>Hunnivirus</i>	Hunnivirus	JQ941880
<i>Kobuvirus</i>	Aichi virus	AB040749
<i>Kunsagivirus</i>	Kunsagivirus	KC935379
<i>Limnipivirus</i>	Carp picornavirus	KF306267
<i>Megrivirus</i>	Turkey hepatitis virus	HM751199
<i>Mischivirus</i>	Mischivirus	JQ814851
<i>Mosavirus</i>	Mosavirus	JF973687
<i>Oscivirus</i>	Oscivirus	GU182408
<i>Parechovirus</i>	Human parechovirus	S45208
<i>Pasivirus</i>	Pasivirus	JQ316470
<i>Passerivirus</i>	Passerivirus	GU182406
<i>Potamipivirus</i>	Eel picornavirus	KC843627
<i>Rabovirus</i>	Rabovirus	KP233897
<i>Rosavirus</i>	Rosavirus	JF973686
<i>Sakobuvirus</i>	Feline sakobuvirus	KF387721
<i>Salivirus</i>	Salivirus	GQ179640
<i>Sapelovirus</i>	Avian sapelovirus	AY563023

Genus	Species examples	Accession number
	Porcine sapelovirus	AF406813
	Simian sapelovirus	AY064708
<i>Senecavirus</i>	Seneca Valley virus	DQ641257
<i>Sicinivirus</i>	Sicinivirus	KF741227
<i>Teschovirus</i>	Porcine teschovirus	AF231769
<i>Torchivirus</i>	Tortoise picornavirus	KM873611
<i>Tremovirus</i>	Avian encephalomyelitis virus	AJ225173

Table 1.1 Summary of the 35 confirmed genera in the family *Picornaviridae* (as of 2016). Adapted from ICTV 2016 Master Species List (ICTV, 2016).

1.1.2 Aphthoviruses

Aphthoviruses are a genus of picornaviruses, members include FMDV, bovine rhinitis A virus (BRAV), bovine rhinitis B virus (BRBV) and equine rhinitis A virus (ERAV), according to the ICTV (Knowles et al., 2012; Knowles, 2017) (Fig. 1.2). FMDV has seven serotypes that are prevalent globally (A, O, C, Asia-1 and South African Territories (SAT) 1, 2 and 3). FMDV is the causative agent of foot-and-mouth disease (FMD) in cloven hooved animals. BRAV has two serotypes, and BRBV only has one serotype. Both infect cattle, as their name suggests. ERAV contains one serotype and is the causative agent of upper respiratory infection in horses (Knowles, 2017). The different aphthovirus members contain a poly-C tract within the 5' UTR, and an L^{pro} sequence marking the start of the polyprotein open reading frame (ORF). FMDV is the only aphthovirus species that contains three non-identical tandem repeats of protein 3B (Stanway, 1990; Knowles et al., 2012; Palmenberg, 1987).

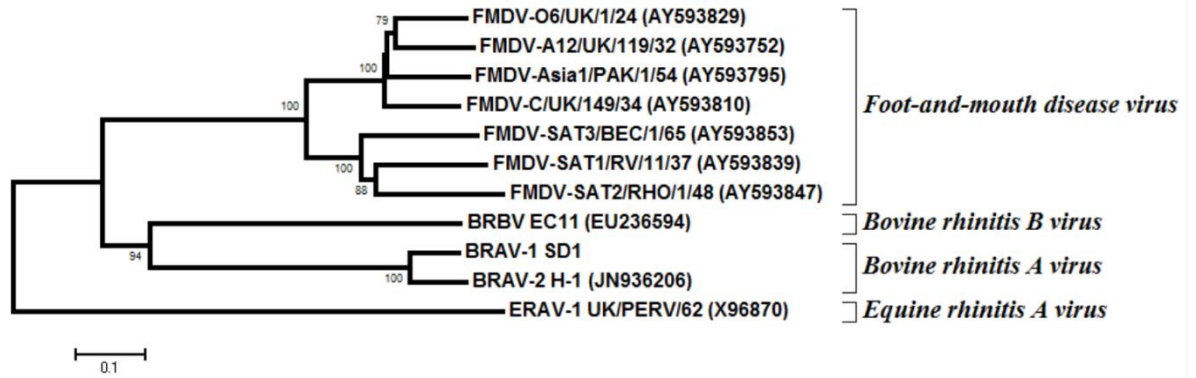


Figure 1.2 Neighbour-joining phylogenetic tree of the aphthovirus genus members. The P1 (1A-1D) amino acid sequences were used to show the relationship between the different serotypes of each species. The FMDV serotypes compared here are O, A, C, Asia-1, SAT1, SAT2 and SAT3. Accession numbers of each serotype is shown. Adapted from (Knowles, 2017).

1.2 Foot-and-Mouth Disease Virus

1.2.1 History, Taxonomy and Epidemiology

Foot-and-mouth disease (FMD) is a highly infectious, vesicular disease of both domestic and wild cloven-hooved animals including cattle, sheep, swine, goats, buffalo and deer (Otto, 1994; Pacheco et al., 2003; Grubman et al., 2004; García-Briones et al., 2006). The first written description of FMD in cattle is believed to have been documented by Hieronymus Fracastorius in 1514, and later published in his major work "*De contagione et contagiosis morbis et eorum curatione*" (Infectious and contagious diseases and their treatment) where he also outlined the concept of epidemic disease in 1546 that identifies the transmission of a vesicular disease in cattle (Grubman et al., 2004). In 1897, at the dawn of the "virology era", German scientists Loeffler and Frosch identified that the causative agent of FMD was filterable. This later led to the characterisation of foot-and mouth-disease virus (FMDV) (Loeffler et al., 1897; Modrow, 1929; Grubman et al., 2004).

There are seven different serotypes of FMDV (A, O, C, Asia-1, SAT1, 2, and 3). The large number of FMDV serotypes contributes to the difficulty in the development of effective FMDV vaccines as there is no cross-protection. There is a global prevalence of FMDV and there is a propensity for regions to be endemic to a number of different serotypes, which can be classified as pools (Fig. 1.3) (Di Nardo et al., 2011; Jamal et al., 2013). Serotypes O, A and C were considered the most widely distributed (Knowles et al., 2005), however, it is believed that serotype C is no longer extant outside of laboratories with the last reported outbreak being in Ethiopia in 2005

(Rweyemamu et al., 2008), and the last reported outbreak of serotype A was in eastern Asia in 2010 (Park et al., 2013). Asia-1, SAT1 and SAT2 have a more limited geographic distribution. SAT3 is only present in pools identified in southern Africa.

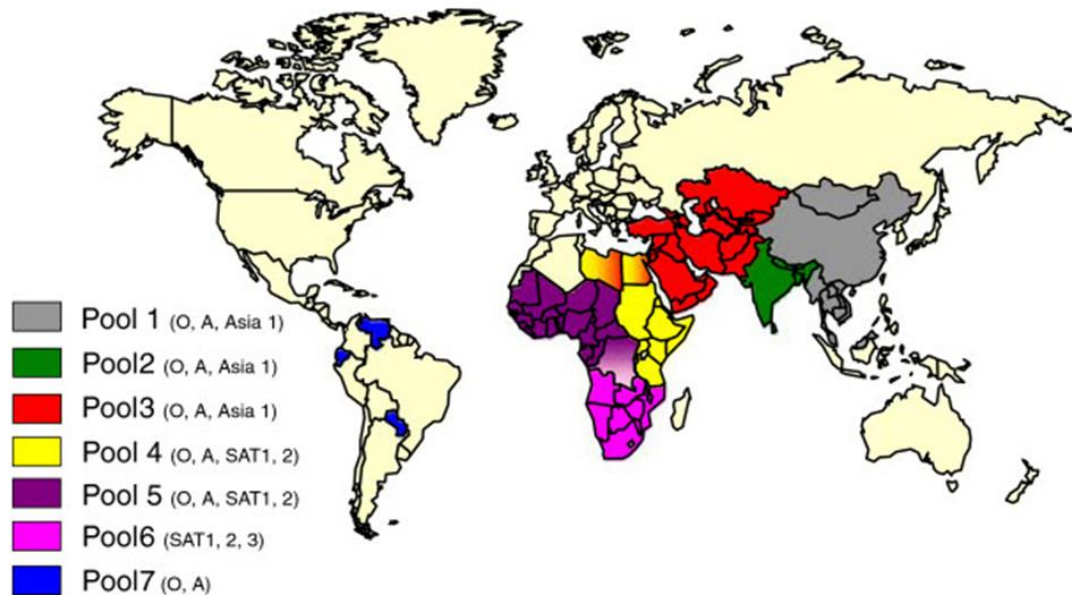


Figure 1.3 Map showing the geographical distribution of the seven different FMDV serotypes highlighted in pools. Map from (Jamal et al., 2013).

1.2.2 Virus Transmission and Control

FMDV is highly contagious and has multiple known routes of transmission. The known routes of transmission are by respiratory transmission, by direct contact of infected animals through the fluid from blisters, blood, saliva and milk, through fomite contact including via agricultural trucks and loading ramps, and from feed containing products from infected animals (reviewed in Grubman and Baxt, 2004; Racaniello, 2007).

FMDV has been classified as a zoonosis, although transmission and manifestation of clinical symptoms in humans are extremely rare. Since the characterisation of the virus in 1897, only one confirmed and 40 unconfirmed human cases of FMDV have

been documented worldwide (Bauer, 1997). The only confirmed case of a human infected with FMDV in the UK was recorded in 1966. The infection resulted in the development of clinical symptoms, virus recovery from the lesions and antibody production (Armstrong et al., 1967). However, humans have been shown to be carriers of the virus; following contact with infected animals the virus was recovered from the nose, throat and saliva of the individuals, however no clinical symptoms were identified, nor was there any increase in antibody production resulting from exposure to the virus (Sellers et al., 2009). Humans are also able to physically transport the virus via fomite transmission to susceptible animals. No human-to-human transmission has been documented (Brown, 2001; Sellers et al., 2009).

The threat of FMDV infection in cloven-hooved livestock is increased by the ability for the virus to replicate rapidly within the target cells, and by the high levels of excreted virions. These characteristics contribute to the production of highly antigenic variability and a quasispecies nature of the virus which poses a challenge to vaccine production. Upon infection, FMDV mediates efficient host-cell protein synthesis shut down by cleavage of the essential cap-dependent translation initiation factor eIF4G. As a result of this shut down, infected cells struggle to mount an effective antiviral response based on *de novo* protein synthesis (Domingo, Escarmís, et al., 2005; Domingo, Pariente, et al., 2005; Summerfield et al., 2009).

Due to the need to produce an efficient vaccine against FMDV, knowledge of the adaptive immune response against FMDV infection has been well-characterised. FMDV has been shown to elicit a rapid humoral response followed by effective clearance through phagocytic cells. Within 3-4 days post-infection high levels of

neutralising antibodies can be detected in infected livestock (McCullough et al., 1988; Doel, 2005). However, the innate immune response to FMDV infection and viral replication is less well understood. Recent studies have attempted to shed light on these interactions particularly when considering novel antiviral strategies (Summerfield et al., 2009).

As with most viral infections, FMDV-infected non-immunological cells induce the production of interferons (IFNs), chemokines and cytokines, however, due to the effective host-cell protein synthesis shut-down mediated by FMDV, the production of IFN, chemokines and cytokines from mRNA is limited resulting in a downregulation of MHC-I-mediated antigen presentation (Sanz-Parra et al., 1998; Ku et al., 2005; de Los Santos et al., 2006; de los Santos et al., 2007). Studies by de los Santos et al. demonstrated that FMDV can also interfere with NF κ B signalling, and result in the down-regulation of the p65/RelA subunits of the molecule even at later times during infection (de los Santos et al., 2007). The generation of a rapid, and well-established adaptive immune response points to an active innate response being present within infected cells.

FMDV was responsible for the slaughter of over 7 million livestock in the UK alone during two major national outbreaks in 1967 and 2001. The spread and control of the virus had an unprecedented economic impact of over £8 billion. Other countries including Taiwan, Ireland, France, South Africa and the Netherlands have had similar outbreaks with comparably devastating effects on their tourism, agricultural and financial economies (reviewed in Sobrino et al., 2001; Sáiz et al., 2002). There are a number of vaccines against FMDV already available, however they are only

economically viable in regions and farms that are endemic to FMDV (Sobrino et al., 2001; Sáiz et al., 2002). There are a number of limitations associated with the vaccines despite their success, making them counter-productive in an emergency outbreak situation. Some of the concerns include the need for a high-containment facility to produce the vaccines and the use of cell suspensions to grow virus for the vaccine. The use of cell suspension for vaccine production can result in a high concentration of contaminating non-structural proteins resulting in the animals producing antibodies against these proteins making it difficult to serologically distinguish between vaccinated animals and infected animals. Modern methods of production of these vaccines have, however, improved and contamination of the vaccine with non-structural proteins has been reduced.

Additionally, the current inactivated vaccines do not induce a rapid immune response and vaccinated animals have the potential to become carriers of the virus and experience long-term asymptomatic infection but still able to shed virus to naïve animals; animals may remain in a carrier-state for up to 4 years (Brown, 2001; reviewed in Grubman and Baxt, 2004). However, recent studies have defined methods such as ELISA-based assays and diagnostic assays targeting non-structural viral proteins, that allow for easier differentiation of vaccine-derived and virus-infected animals (reviewed in Sáiz et al., 2002; Alexandersen et al., 2002). The most widely-used method of containing an outbreak in the UK and the European Union is by the inhibition of movement and the slaughter of infected and in-contact susceptible livestock (Grubman et al., 2004); this could potentially be prevented by the development of therapeutic drugs and alternative vaccine strategies.

There have been recent developments in the field of alternative vaccines that do not require infectious virus. A vaccine using the highly immunogenic VP1 capsid protein (encoded for by 1D) has been developed; however, when tested in a bovine population, the vaccine produced limited protection against a challenge. It is believed that the quasispecies nature of the virus resulted in the selection of antigenic variants as a response to the vaccine, which can make the development of an effective vaccine challenging (Kleid et al., 1981; Taboga et al., 1997; Tami et al., 2003). More recently, studies have shown that the antigenic region of the VP1 (termed the G-H loop) may have been necessary for protection against challenge in cattle. As such, by removing a portion of the VP1 G-H loop, a 'negative vaccine' could be developed which could both protect cattle from challenge as well as differentiate vaccinated and infected animals (through the detection of antibody production against the modified G-H loop sequence) (Fowler et al., 2008; Fowler et al., 2010; Fowler et al., 2011). Live-attenuated vaccines have also been developed and tested, although they provide good protection in the bovine population, there were concerns that the attenuated strains may still be virulent in other host populations (e.g. porcine) in addition to the risk that live attenuated vaccines may revert back to the wildtype phenotype (Beck et al., 1987; Sobrino et al., 2001; Grubman et al., 2004). Empty viral capsids and virus-like particles consisting of the co-expression of the capsid proteins VP0, VP1 and VP3 (encoded for by 1D, 1A-B and 1C, respectively) on a plasmid in *E. coli*, have also been developed for the use as a vaccine. To date, they have been the most successful alternative form of vaccination, inducing complete protection when challenged at seven days (Grubman et al., 2004; Porta, Xu, et al., 2013; Porta, Kotecha, et al., 2013; Xiao et al., 2016).

However, in an emergency situation, a method is needed to rapidly reduce virus shedding and contain an outbreak. To do this, antiviral approaches could be developed. It has been shown that interferon effectively inhibits virus production and induces an innate immune response in the infected cells. If delivered prophylactically and in combination with the current vaccine, the interferon treatment could allow time for the adaptive immune response induced by the vaccine to activate and clear the infection (Ahl et al., 1976; Almeida et al., 1998; Chinsangaram et al., 2001; Grubman et al., 2002). However, trials using interferon in combination with the empty viral capsids failed to completely clear the challenged animals of the virus (Wu et al., 2003).

For a successful antiviral drug to be developed, a better understanding of the innate immune response, particularly in ruminants, needs to be established. The production of an effective antiviral requires a target that is conserved in all serotypes of the virus and inhibit the ability of the virus to replicate and spread to other cells. Key targets include the major viral protease, 3C and the viral polymerase, 3D^{pol}, responsible for the replication of the viral genome and highly conserved among all serotypes. Understanding and inhibiting the function of these proteins could lead to the development of an effective broad-spectrum and fast-acting antiviral therapeutic.

1.2.3 Genome Structure

The FMDV virion is composed of an 8.3 kb +ve ssRNA genome encapsidated in a simple pseudo-icosahedral capsid approximately 25 nm in diameter. The capsid is composed of 60 copies of four structural proteins VP1-4, encoded by 1D, 1B, 1C and 1A, respectively (protomer). VP1, VP2 and VP3 are exposed on the surface of the

capsid, whereas VP4 is internalised (Fig. 1.4). The viral RNA that is packaged within the capsid is arranged in a single ORF, organised like a cellular mRNA, which is translated as a single polyprotein that is co- and post-translationally cleaved by three virus-encoded proteases (L^{pro} , 2A and 3C) into intermediate and mature structural and non-structural proteins (Burroughs et al., 1971; Robertson et al., 1985; Grubman et al., 2004; Jamal et al., 2013; Gao et al., 2016). The viral genome is flanked by 5' and 3' UTRs that contain regulatory elements of replication and translation.

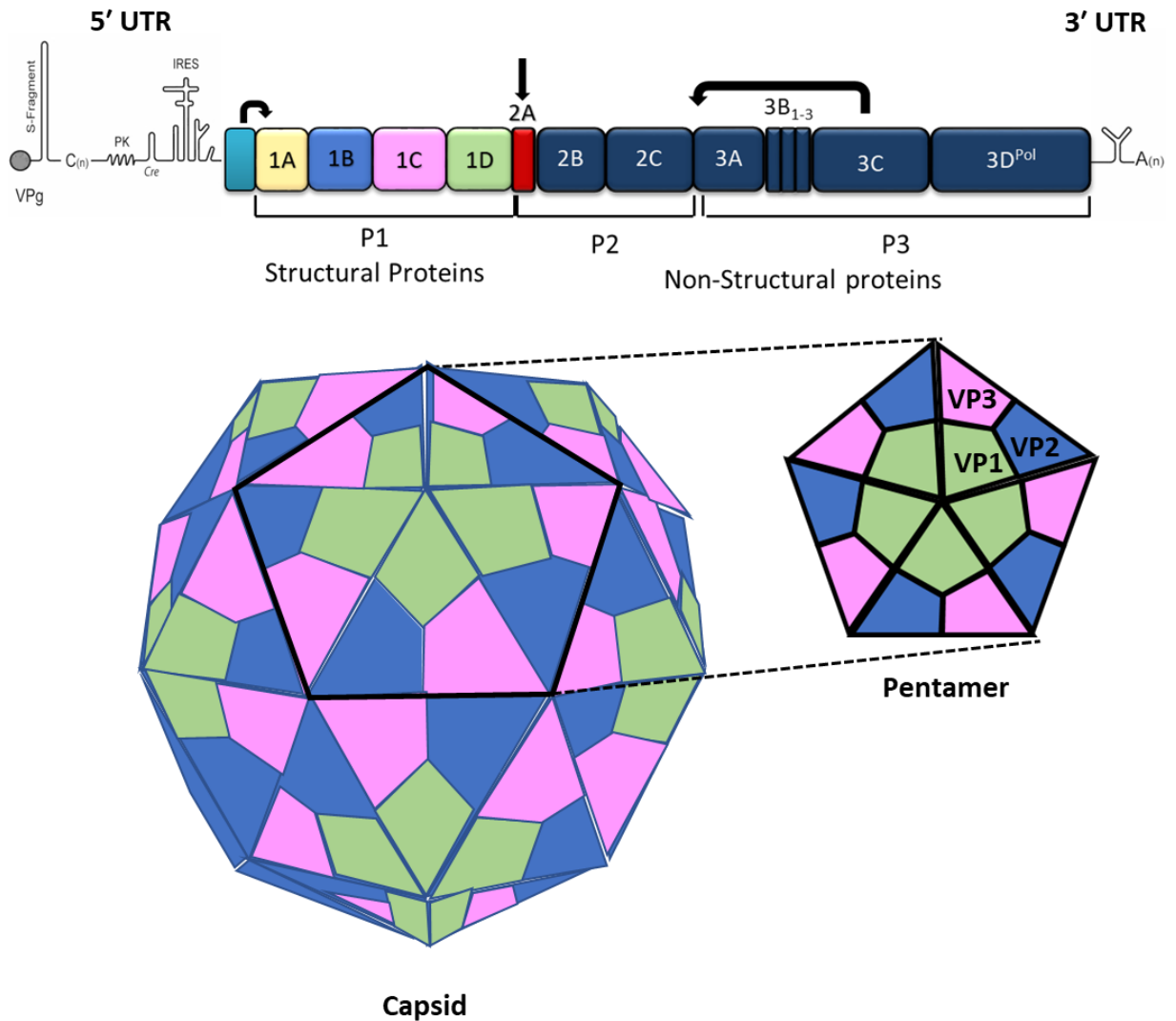


Figure 1.4 Schematic of the FMDV genome organisation and capsid protein structure. The structural proteins 1A-1D encoding for VP1-4 are colour coded in yellow, blue, pink and green, respectively and their organisation within the protomer, pentamer and pseudo-icosahedral capsid are depicted. VP4, encoded by 1A is not visible as it is internalised. Non-structural proteins are depicted in dark blue. Arrows show the major cleavage sites between L^{pro} (turquoise) and the P1 region, 2A between the P1 and P2-P3 region and 3C that cleaves between the non-structural proteins in the P2-P3 region. Adapted from (Jamal et al., 2013).

1.2.3.1 The 5' UTR

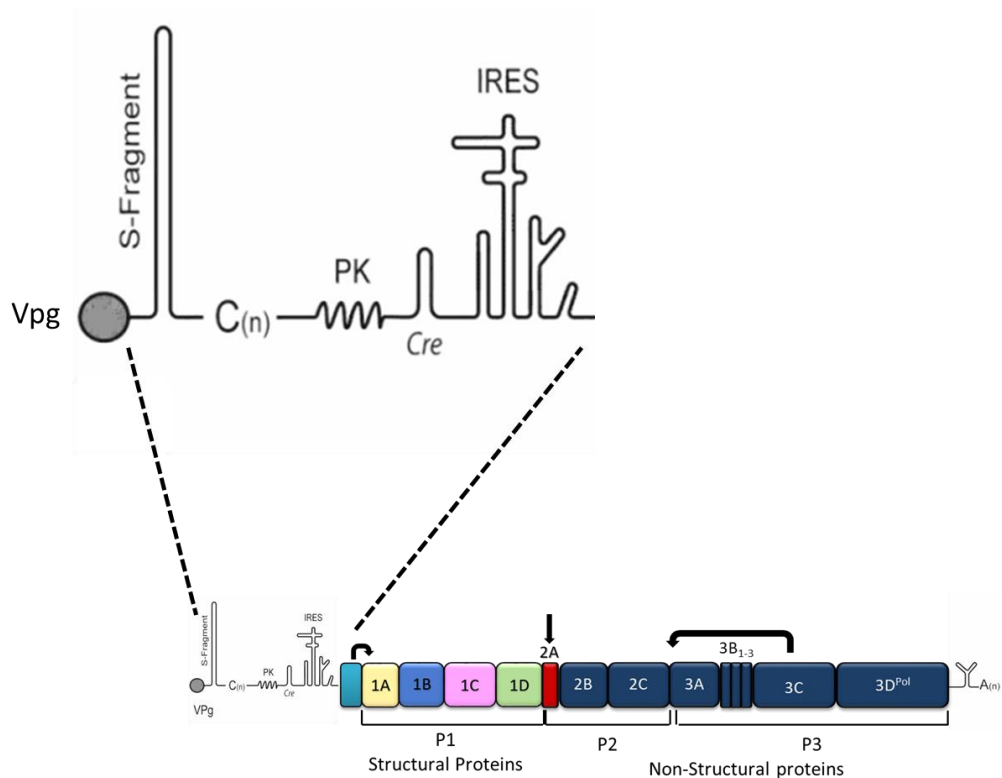


Figure 1.5 Schematic depicting the location and organisation of the FMDV 5' UTR. It is a 1.3 kb region of five highly structured RNA elements. The elements are: the S-fragment, the poly-C tract, two to four pseudoknot structures, the *cis*-acting replicative element (*cre*), and the internal ribosome entry site (IRES).

1.2.3.1.1 The S-fragment

FMDV has a much larger 5' UTR than other picornaviruses containing approximately 1,300 bases (Forss et al., 1984; Grubman et al., 1984; Robertson et al., 1985). The 5' UTR, upstream of the ORF, can be divided into five structural elements (Fig 1.5). The first structural element is the S-fragment, a long, 360 base-pair stem-loop structure believed to be involved in maintaining genome stability, and may play a role in virus genome replication. The S-fragment is found in all FMDV serotypes, some sequence conservation has been observed by digestion with RNase H in the presence of oligo (dG), and use of sequencing gels within this region of the FMDV genome

(Rowlands et al., 1978; Harris, 1979; Harris, 1980; Newton et al., 1985; Belsham et al., 1990; Bunch et al., 1994; Mason et al., 2002; Belsham, 2005; Carrillo et al., 2005; Jamal et al., 2013). Some S-fragment truncations have been reported in the wild within SAT isolates (personal communication Lidia Lasecka, Pirbright Institute; Joseph Ward, Leeds; Valdazo-González et al., 2013)

1.2.3.1.2 The Poly-C tract

Following the highly structured S-fragment is a poly-C tract of variable length (100-200 bp) (Brown et al., 1974; Newton et al., 1985; Black et al., 1979; Costa Giomi et al., 1984) (Fig 1.5). The function of the poly-C tract is currently unknown, however, it has been suggested that it could be associated with virulence, or in regulating the switch from translation to genome replication through a proposed interaction with the cellular poly(rC) binding protein (PCBP). Other studies have suggested that the removal of the poly-C tract had no effect on viral replicon *in vitro* (personal communication, Joseph Ward (Leeds)), or on virus infectivity (Harris et al., 1977; Rowlands et al., 1978; Sangar et al., 1980; Kühn et al., 1990; Rieder et al., 1993; Gamarnik et al., 1997).

1.2.3.1.3 The Pseudoknots and the cis-acting replicative element

At the 3' end of the poly-C tract are a series of two to four RNA pseudoknots of unknown function (Clarke et al., 1987; Rieder et al., 1993; Le et al., 1993; Escarmís et al., 1995; Carrillo et al., 2005), followed by a *cis*-acting replicative element (*cre*) (Fig 1.5). The *cre* is a short (55 nucleotide) stem-loop structure with a conserved motif around the bulge of the loop (AAACA) which is essential for the initiation of RNA genome replication. The *cre* acts as the template for the uridylylation of replication

primer(s) 3B (or VPg) (which then becomes linked to the 5' end of the genome upstream of the S-fragment). In other picornaviruses, for example, in PV, the *cre* is located within the protein-coding region, however, in FMDV this structure is localised to the 5' UTR (Paul et al., 2000; Mason et al., 2002; Mason et al., 2003; Grubman et al., 2004; Belsham, 2005).

1.2.3.1.4 The Internal Ribosome Entry Site

As with all picornaviruses, FMDV does not contain a 5' 7-methylguanosine cap to initiate translation, instead it contains a 450-nucleotide internal ribosome entry site (IRES) structure. The FMDV IRES immediately precedes the AUG translation initiation codons of the genome (Fig 1.5). It is at this site that the ribosome and translation initiation factors bind and drive translation of the viral RNA. (Belsham et al., 1990; Kühn et al., 1990; Pilipenko et al., 1992; Mason et al., 2002; Grubman et al., 2004; García-Nuñez et al., 2014).

The FMDV IRES is classified as a type II IRES structure, shared with cardioviruses such as encephalomyocarditis virus (EMCV). Other types of IRESs include type I (found in enteroviruses and rhinoviruses), type III found in hepatitis A virus, and finally a HCV-like 'type IV' IRES (Beales et al., 2003; Martínez-Salas et al., 2015). As with other IRES, the FMDV type II IRES it is a *cis*-acting highly-structured RNA sequence located at the 5' region of the genome. Despite the lack of conserved sequence and RNA structure, the function of the IRESs of different viruses remains the same. The key differences between the different IRES types are primarily in the number and secondary RNA structure of the domains, and the combination of cellular interacting and binding partners (Beales et al., 2003; Kieft, 2008; Martínez-Salas et al., 2015).

Eukaryotic cells have also been shown to be able mediate translation of up to 85 mRNAs in a cap-independent manner. The first of such IRES-containing cellular mRNAs that was defined encodes for BiP, the immunoglobulin heavy chain binding protein (Sarnow, 1989; Macejak et al., 1991; Hellen et al., 2001; Baird, 2006).

1.2.3.2 The 3' UTR

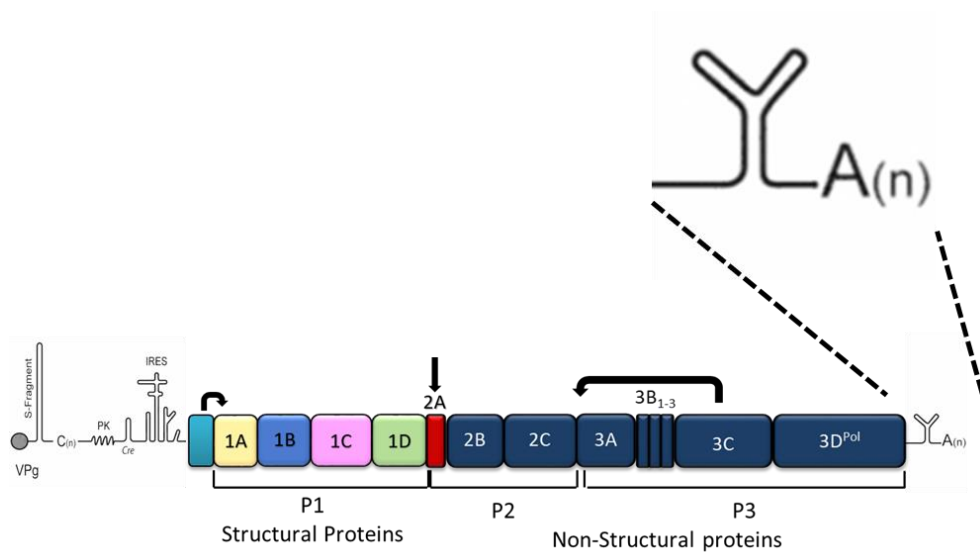


Figure 1.6 Schematic depicting the location and organisation of the FMDV 3' UTR. The region is composed of two stem-loop structures preceding a poly-A tail.

The 3' UTR located downstream of the ORF termination codon contains a sequence of ≈90 nucleotides that forms two stem-loop structures, followed by a poly-A tail (Porter et al., 1978; Belsham, 2005; Serrano et al., 2006) (Fig 1.6). The 3' UTR has been shown by multiple studies to be important in PV and FMDV genome replication and infectivity through the circularisation of the genome mediated by the poly-A binding protein (PABP) and the S-fragment in the 5' UTR (Barton et al., 2001; Herold et al., 2001; López de Quinto et al., 2002; Serrano et al., 2006). The terminal A residues of the poly-A tail also permit for the generation of a negative strand

replication intermediate through the binding of the uridylylated VPg during genome replication (Herold et al., 2001; Barton et al., 2001; Mason et al., 2003). As mentioned previously, the two stem-loops at the 3' UTR have been shown to be involved in the replication ability of the RNA. Exchanging the 3' UTR with the equivalent region of swine vesicular disease virus, or deleting the 3' UTR region abrogated virus replication (Sáiz et al., 2001). Additionally, the deletion of one of the stem-loop structures in 3' UTR has been shown to affect the replication efficiency in virus infected, and in replicon transfected cells (Sáiz et al., 2001; Gao et al., 2016; Fiona Tulloch (Edinburgh), personal communication).

1.2.3.3 The Leader proteinase

The first product of the genome ORF is the leader (L^{pro}) protein, a proteinase unique to *Aphthoviruses*, which contains two in-frame initiation codons (AUG). Two forms of the L-proteinase are generated: Lab^{pro} and Lb^{pro} . Site-directed mutagenesis studies have shown that Lb^{pro} alone was sufficient and necessary for the production of live, infectious virus (Fig 1.7). Deletion of the first AUG (Lab^{pro}) abolished replication of viral RNA, whereas deleting the second AUG (Lb^{pro}) had no effect on replication (Carroll et al., 1984; Sangar et al., 1987; X Cao et al., 1995; Belsham, 2013). Deletion of the L^{pro} from the genome without the spacer function of the leader sequence, rendering it 'leaderless', whilst maintaining the second AUG, affected the virulence of FMDV, but was not necessary for viral replication (Piccone et al., 1995; Grubman et al., 2004). Studies of viruses recovered from infectious clones where the L-proteinase was deleted showed remarkable attenuation in cattle, caused no clinical symptoms, and were unable to spread to other animals despite being able to

replicate at slightly reduced efficiency in cell culture (X Cao et al., 1995; Brown et al., 1996; Chinsangaram et al., 1998).

L-proteinase has been shown to play a role in promoting translation of the virus RNA as it inhibits host-cell cap-dependent mRNA translation and protein synthesis. The L-proteinase cleaves the host-cell translation initiation factor eIF4G (Piccone et al., 1995; Mason et al., 1997). Cleavage of eIF4G effectively shuts off the host-cell translation mechanism and allows for the various translation initiation factors including eIF4A to bind to the virus IRES and interact with the ribosome to drive viral RNA translation but eliminates the ability of eIF4G to bind eIF4E, the cap binding protein (Devaney et al., 1988; Kirchweger et al., 1994; López de Quinto et al., 2000; Saleh et al., 2001).

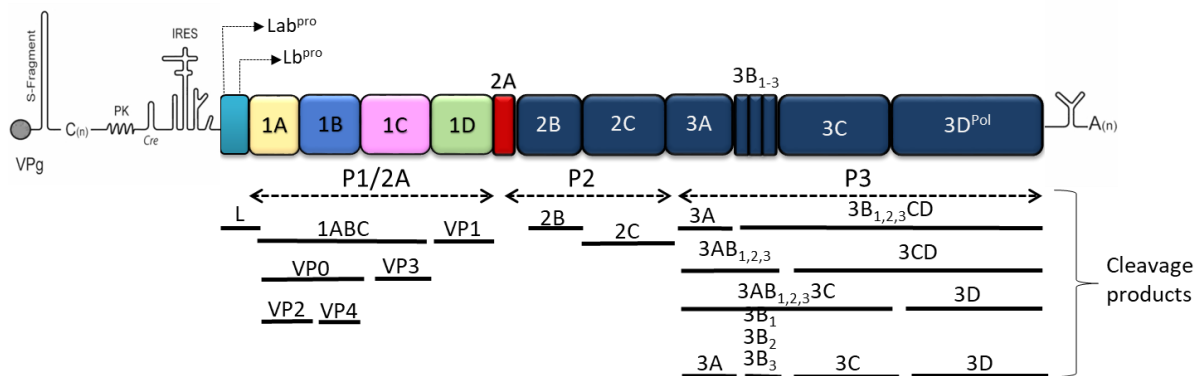


Figure 1.7 Schematic of the FMDV genome showing the proposed ORFs of each of the viral proteins. The 5' untranslated region (UTR) is located upstream of the polyprotein. The leader protease (L^{pro}) is shown containing both transcription start codons; (Lb^{pro}) is sufficient for transcription and translation. The structural proteins are transcribed from segment P1 (1A-1D) and are co- and post-translationally processed to make mature capsid proteins (VP1-4). Segments P2 and P3 encode for the non-structural proteins necessary for replication of the genome (2A-3D). Likewise, both these segments are co- and post-translationally modified into the mature proteins. A poly-A tract at the 3' UTR signifies the end of the genome ORF. Adapted from Forrest et al., 2014.

1.2.3.4 Structural proteins 1A-1D/2A

As highlighted in figure 1.4, the structural proteins of FMDV that form the virus capsid are encoded by the P1 region of the genome. 1A, 1B, 1C and 1D encode for VP2, VP4, VP3 and VP1, respectively (Bachrach, 1968) (Fig 1.7). The capsid is composed of 60 copies of each of the four proteins but is initially assembled into asymmetric protomers consisting of VP1, VP3 and VP0 (precursor to VP2 and VP4). Five protomers associate into a pentamer, and 12 pentamers form into a pseudo-icosahedral capsid containing the ssRNA genome. VP0 is autocatalytically cleaved into the mature structural proteins VP2 and VP4 upon genome encapsidation (reviewed in Sobrino et al., 2001) It is important to highlight that the protomers never exist 'alone'; the smallest stable capsid component is the pentamer.

The three-dimensional arrangement of the structural proteins provides the main antigenic sites used for antibody binding that elicit responses to vaccination or to infection, as well as to mediate receptor binding of the virus to the host cell (Mason et al., 2003). Unlike enteroviruses and cardioviruses, FMDV lacks receptor binding sites formed within surface pockets, or canyons. Instead, FMDV has a protruding loop in the VP1 protein that may comprise of a major neutralisation and receptor-binding site (Hogle et al., 1985; Rossmann, 1989; Acharya et al., 1989).

The FMDV capsid contains a hydrophobic channel located at the 5-fold axis which allows for the penetration of small molecules such as intercalating dyes and caesium ions which results in the inactivation of the virus and capsid instability at pH < 6. It is because of this that FMDV also has a high buoyant density compared to other picornaviruses (Acharya et al., 1989).

1.2.3.5 Non-structural proteins 2A-3D^{pol}

1.2.3.5.1 Proteins 2A, 2B and 2C

The P2 region of the FMDV polyprotein encodes for three mature protein: 2A, 2B and 2C (Rueckert et al., 1984) (Fig 1.7). 2A in FMDV is smaller than its PV analogue, at only 18 amino acids in length (Robertson et al., 1985; Ryan et al., 1997). During the primary polyprotein processing events, the 2A protein remains associated with the P1 region mediating cleavage between the P1 and P2 regions through autoproteolysis, despite a lack of any characteristic protease motifs (Ryan et al., 1994; Ryan et al., 2001). 2A is removed from the P1 region to allow for maturation of the structural proteins by cleavage with another FMDV protease, 3C (Vakharia et al., 1987; Ryan et al., 1989; Ryan et al., 1991). The autoproteolytic property of 2A has been shown to function and mediate cleavage in an artificial system, however for this to occur the 2A-2B boundary needed to remain intact (Ryan et al., 1994; Ryan et al., 1997; Donnelly et al., 2001). This cleavage function of 2A yielded a much higher ratio of proteins upstream to the 2A insertion site, which led to the hypothesis that FMDV 2A was not a traditional protease but was mediating a modification of the translation machinery termed 'ribosome skipping' which allowed for the ribosome to release at 2A but then continue to translate the proteins downstream (Ryan et al., 2001; Donnelly et al., 2001).

Proteins 2B and 2C have been shown to function synergistically as a precursor, 2BC, as well as having distinct functions as individual proteins. One of the functions attributed to the 2BC precursor protein, as defined by immunofluorescence and co-localisation studies, is the blocking of host protein ER-to-Golgi transport which results

in eventual generalised cytopathic events within FMDV infected cells (Mason et al., 2003; Moffat et al., 2005). A similar function is attributed to PV 3A.

2B is thought to function as a viroporin. The 54 amino acid peptide contains two putative transmembrane domains typical of viroporins (Nieva et al., 2012; Ao et al., 2014; Ao et al., 2015). 2B in related picornaviruses including PV and Coxsackievirus has been shown to localise to the ER membrane, thought to be the site of viral replication, but has also been shown to be able to induce damage to the cell membrane resulting in a dysregulation of the calcium ion concentration within the cell and activating autophagy (Bienz et al., 1987; Doedens et al., 1995; van Kuppeveld, Melchers, et al., 1997; van Kuppeveld, Hoenderop, et al., 1997; Suhy et al., 2000; Ao et al., 2015). However, knowledge on the exact function of the protein is limited and much remains to be confirmed for FMDV.

FMDV 2C is a 318 amino acid protein shown to co-localise with membrane-bound replication complexes within infected cells concentrating at the cell membrane and the ER (Tesar et al., 1989; Klein et al., 2000; Teterina et al., 2006; J. Wang et al., 2012; Gao et al., 2016). It is the largest membrane-binding protein of the FMDV genome and is proposed to have a number of functions primarily in the role of membrane rearrangements and the regulation of the cellular immune response, similar to those seen in other picornaviruses such as hepatitis A virus and PV (Troxler et al., 1992; Bolten et al., 1998; Jecht et al., 1998; Gosert et al., 2000; O'Donnell et al., 2011; Gladue et al., 2012).

Studies on FMDV, PV, and on enterovirus 71 2C have shown that it may function as a helicase, unwinding RNA in an ATP-dependent manner, due to the presence of a well

conserved ATPase domain placing 2C within the superfamily III helicases. (Gorbalenya et al., 1990; Mirzayan et al., 1994; Sweeney et al., 2010; Xia et al., 2015). Through inhibition studies on PV and FMDV with guanidine hydrochloride, it has been observed that 2C is essential for virus replication (Saunders et al., 1982; Saunders et al., 1985; Barton et al., 1997; Pfister et al., 1999; Klein et al., 2000). Studies on PV 2C have also identified the necessity for 2C in the initiation of negative strand RNA synthesis, and, as the protein is highly conserved across all picornaviruses, it is believed that FMDV 2C could also share the same function (Barton et al., 1997). Interestingly, the presence of 2C has only been observed within virus replication complexes and not in clarified virus stocks used in vaccine preparation, providing an attractive candidate as a differentiator between 'carrier' livestock (that had been previously infected and had cleared the infection), and vaccinated livestock (Lubroth et al., 1995; Lubroth et al., 1996; Meyer et al., 1997; Lu et al., 2010).

1.2.3.5.2 Proteins 3A and 3B

The 3A protein encoded by FMDV is the largest picornaviral 3A protein (at 153 amino acids in length) compared to the 87 amino acid PV protein (Mason et al., 2003). Using *in situ* protein fluorescent ligation assays and structural data from nuclear magnetic resonance studies, it has been determined that FMDV 3A homodimerizes through interactions between two intermolecular hydrophobic α -helix domains (González-Magaldi et al., 2012; González-Magaldi et al., 2015). Interference of the hydrophobic interface interaction results in a reduction in virus yield in virus-infected cells (González-Magaldi et al., 2015).

The N-terminal domain of 3A is highly conserved amongst the FMDV serotypes and contains a hydrophobic, membrane-associated domain that co-localises to ER and Golgi-derived membranes (O'Donnell et al., 2001; Moffat et al., 2005; García-Briones et al., 2006). In contrast to PV 3A, the C-terminal domain of FMDV 3A is structurally flexible and is prone to a number of deletions and mutations as identified from sequencing data. There were two natural deletion mutants reported in the C-terminal domain, both of which resulted in a change in virulence and host range of the virus (Beard et al., 2000; Pacheco et al., 2013). These deletions in 3A were associated with an increased virulence in swine infected with FMDV, but showed a reduced ability for these viruses to cause disease in cattle, or in bovine-derived cells (Giraud et al., 1987; Beard et al., 2000; Knowles et al., 2001).

FMDV encodes for three non-identical tandem repeats of 3B (3B₁, 3B₂, 3B₃) and is the only picornavirus to do so. Each copy of 3B is 23-24 amino acids in length and encodes the VPg protein. Therefore viral RNA includes VPg covalently linked through the conserved tyrosine residue at position 3 (Tyr3) at the 5' end (Forss et al., 1982; Mason et al., 2003; Pacheco et al., 2003). In order for replication to occur, the VPg is uridylylated into VPg-pU(pU) by the viral polymerase 3D^{pol} (Paul, 2002). Most naturally circulating FMDV strains contain three copies of 3B, suggesting a strong selective advantage (Pacheco et al., 2003; Carrillo et al., 2007), however, studies have observed that, although the presence of all three 3B copies are required for efficient replication, there appears to be a preference for 3B₃ (Falk et al., 1992; Pacheco et al., 2003; Nayak et al., 2005; Arias et al., 2010; Herod et al., 2017). These studies show that deleting 3B₃ resulted in the production of a non-infectious RNA transcript. Studies have shown that the VPg is removed from the genome during translation

(Sangar, Rowlands, et al., 1977; Sangar et al., 1980), but is present at the 5' ends of transcripts.

1.2.3.5.3 Protein 3C

The major protease encoded by FMDV is 3C (Klump et al., 1984). 3C is one of the more well-defined proteins of the species and is responsible for the majority of the processing of the viral polyprotein during replication of the genome. 3C is responsible for the processing of 7 cleavage sites between the non-structural proteins with the exception of the autocatalytic cleavage events occurring between L^{pro} and P1, P1-2A and 2BC, and the maturation cleavage of VP0 into VP2 and VP4 (Vakharia et al., 1987; Clarke et al., 1988; Palmenberg, 1990; Bablanian et al., 1993). FMDV 3C shows greater heterogeneity amongst its cleavage sites being able to cleave between Gln-Gly, Glu-Gly, Gln-Leu and Glu-Ser dipeptides, in comparison to the singular Gln-Gly cleavage site for PV 3C (Robertson et al., 1985; Palmenberg, 1990; Birtley et al., 2005).

Similar to the protease activity seen in L^{pro}, FMDV 3C is able to cleave host-cell proteins as well, primarily cleaving the translation initiation factor eIF4A (Belsham et al., 2000) and the histone protein H3 (Grigera et al., 1984; Falk et al., 1990; Tesar et al., 1990). This function of 3C is thought to be a unique mechanism of FMVD to subvert host-cell translation in favour of viral replication. More recently, 3C has also been implicated in immune evasion by reducing the RIG-I/MDA-5 signalling through the cleavage of the nuclear transcription factor kappa B (NF- κ B) essential modulator (NEMO) (Wang et al., 2012).

3C and its precursor 3CD may also have non-catalytic roles during the FMDV life-cycle, particularly during the initiation of replication and the mediating of VPg uridylylation (Murray et al., 2003; Nayak et al., 2005; Nayak et al., 2006; Steil et al., 2009)

1.2.3.5.4 3D^{pol}

The RNA-dependent RNA polymerase (RdRp) from FMDV, 3D^{pol}, is a 54 kDa enzyme. The main function that has been described for 3D^{pol} is in the synthesis of positive- and negative-strand RNA during viral genome replication. The first description of 3D^{pol} was detailed in a study by Polatnick and Arlinghaus, 1967 where the 3D^{pol} was originally described as the foot-and-mouth disease virus infection-associated antigen (FMD-VIAA) as antibodies against it could be detected in the sera of infected cattle (Cowan et al., 1966) but was unable to antigenically recognise FMDV structural proteins (Morgan et al., 1978). As such, it was subsequently shown to be the viral polymerase (Lowe et al., 1981).

The sequence and structure of 3D^{pol} is highly conserved among the different FMDV serotypes (Villaverde et al., 1988; George et al., 2001). Crystal structure analyses also show a similar structure between all other picornavirus RdRps. The structure resembles a standard 'right-hand', that consists of 'palm', 'fingers' and a 'thumb' domains (Ferrer-Orta et al., 2004). The catalytic domain of these RdRps is located in the 'palm' region. This region has the most conserved structure amongst polymerases and consists of a three-stranded antiparallel β -sheet flanked by three α -helices. This core domain is integral in maintaining correct structure of the enzyme catalytic site (a highly conserved YGDD sequence) and is necessary for the

recognition, binding, and priming of nucleotides for downstream binding to the phosphoryl transferase and subsequent formation of nascent RNA strands (Hansen et al., 1997; O'Reilly et al., 1998; Ferrer-Orta, Arias, Escarmís, et al., 2006). 3D^{pol} is a non-proof-reading polymerase resulting in a high level of mutation and recombination occurring during replication, lending FMDV a quasispecies nature, common across all picornaviruses.

Most of the understanding of the structure and function of the FMDV 3D^{pol} has occurred as a result of studies on PV 3D^{pol} and from recent crystallographic studies. FMDV 3D^{pol} structures have been solved as unliganded or as proteins in complex with RNA. Structures have also been solved showing the interaction of 3D^{pol} along with the VPg (Ferrer-Orta et al., 2004; Ferrer-Orta, Arias, Agudo, et al., 2006; Ferrer-Orta, Arias, Escarmís, et al., 2006; Ferrer-Orta et al., 2009). Additionally, PV 3D^{pol} was shown to function as a higher-order oligomeric structure and form complex fibrils that have been shown by cryo-EM to contain RNA within the active sites (Pata et al., 1995; Beckman et al., 1998; Lyle, Bullitt, et al., 2002). The formation of fibrils within FMDV has also been investigated. These studies have shown that FMDV 3D^{pol} is able to form higher-order fibrils, however, their function is still being investigated (Bentham et al., 2012).

The elongation of nascent RNA chains and replication of the genome catalysed by PV 3D^{pol} has been shown to occur within membrane associated replication complexes (Flanegan et al., 1977; Bienz et al., 1983; Bienz et al., 1987; Bienz et al., 1992). Structures resembling PV replication complexes containing 3D^{pol} and RNA have also been described in FMDV-infected cells (Polatnick and S.H. Wool, 1983; Polatnick and

S. Wool, 1983). However, more recent evidence from the literature shows that the reorganisation of cellular membranes during FMDV infection is different to that seen during infection with other picornaviruses. FMDV infection results in a dramatic condensation and relocalisation of intracellular organelles to one side of the cytoplasm in the perinuclear region (Monaghan et al., 2004) as opposed to the association to specific intracellular membranes.

The highly-conserved structure and function of the FMDV 3D^{pol} make it an attractive target for antiviral therapeutics. Studies using nucleoside analogue 5-fluorouracil have shown it to be mutagenic for a number of viruses including FMDV. A well-defined antiviral, Ribavirin, has also been shown to be able to eliminate FMDV from persistently infected cells due to its ability to enhance mutagenesis (Sierra et al., 2000; Graci et al., 2002; Airaksinen et al., 2003).

1.2.4 FMDV genome replication

FMDV enters cells by binding the α V subgroup of the integrin family of receptors via a highly-conserved arginine-glycine-aspartic acid (RGD) motif located on the VP1 capsid protein (Berinstein et al., 1995; Neff et al., 1998; Jackson et al., 2000; Jackson et al., 2002; Duque et al., 2003; Jackson et al., 2004; O'Donnell et al., 2005). Upon binding to the cellular receptor, the virus is internalised by clathrin-mediated endocytosis (Fox et al., 1989; Mason et al., 1994; Leippert et al., 1997; Berryman et al., 2005; O'Donnell et al., 2005; Martín-Acebes et al., 2007). The capsid is subsequently broken down into pentamers within the low pH environment of the endosomes, and the viral RNA is released into the cytoplasm where replication can

occur (Cavanagh et al., 1978; Baxt, 1987; O'Donnell et al., 2005; O'Donnell et al., 2008).

FMDV RNA first undergoes initial translation mediated by host-cell translation factors once within the cytoplasm. Two of the first host-cell interacting partners that were discovered to be involved in the translation of the FMDV genome were a 57 kDa protein known as the polypyrimidine tract-binding protein (PTBP), and a 45 kDa IRES-specific *trans*-acting factor (ITAF₄₅) protein (Luz et al., 1991; Stewart et al., 1997; Pilipenko et al., 2000). Both of these proteins have been shown to interact with the FMDV IRES and are essential for the formation of the ribosomal translation initiation complex.

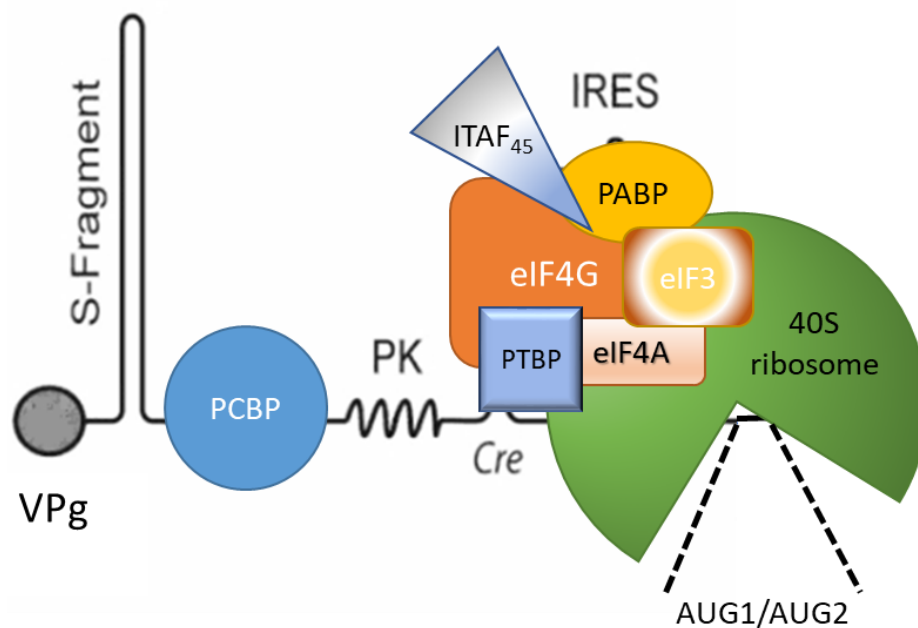


Figure 1.8 Schematic of the relationship of host-cell translation initiation factors and the FMDV 5'UTR. The recruitment of these translation initiation factors allows for the cap-independent translation of the FMDV viral genome. Adapted from (Jamal et al., 2013).

Host-cell translation initiation factors eIF4G and recruited subunits eIF4A, eIF3a and eIF4B, and the 40s-ribosomal subunit, along with cellular co-factors PTBP, ITAF₄₅, the poly-A binding protein (PABP) and the PCBP bind to the IRES element located in the 5' UTR. The binding of the cellular co-factors to the RNA initiate internal translation of the viral RNA genome in a cap-independent manner typical of a number of positive-sense RNA viruses such as pestiviruses, hepaciviruses, aphthoviruses and enteroviruses (Pelletier et al., 1988; Jang et al., 1988; Belsham et al., 1990; Sizova et al., 1998; Niepmann, 2009) (Fig. 1.8). The viral genome is thus translated into a single polyprotein from which the structural and non-structural protein precursors are co- and post-translationally processed into the mature, functional proteins (detailed in section 1.2.3.5) (Blyn et al., 1997; López de Quinto et al., 2002; Rodríguez Pulido et al., 2007; Martínez-Salas, 2008; Yu et al., 2011). The processing of the non-structural proteins is mediated by the action of 3C, and various defined intermediate precursors are formed, as highlighted in figure 1.7, in a defined order (Semler et al., 1981; Pallansch et al., 1984; Lawson et al., 1992; Oh et al., 2009; Cameron et al., 2010; Herod et al., 2017)

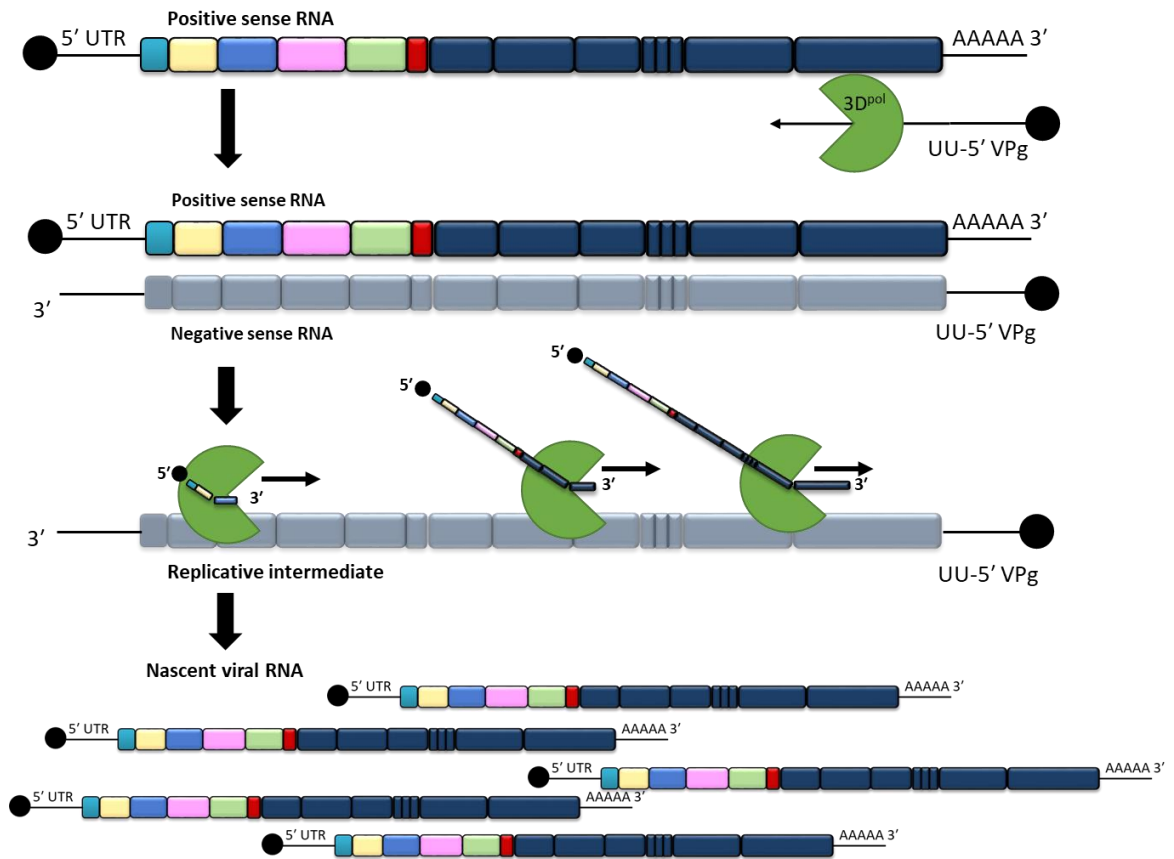


Figure 1.9 Schematic of the process of FMDV replication. Positive strand RNA is used as the template for replication and the synthesis of a negative strand intermediate. This negative strand intermediate is used as the template to form nascent positive strand RNA which can either be packaged into newly synthesised virions or be further used for replication.

Following translation of the genome, replication is initiated. Initiation of both replication and translation has been shown to involve the circularisation of the genome through discrete RNA-RNA and RNA-protein interactions between the 3' UTR, the 5' UTR, cellular host factors, and virus-encoded proteins such as 3D^{pol}, 3A and 2BC. Examples of interactions that have been proposed are the PCBP with the 5' UTR, the PABP with the 3' UTR and the PCBP and the PABP with the S-fragment (Herold et al., 2001; López de Quinto et al., 2002; Serrano et al., 2006). This

mechanism is thought to be widespread amongst positive-strand RNA viruses (Pogue et al., 1994; Gamarnik et al., 1998; Villordo et al., 2010; Park et al., 2013).

Replication of FMDV RNA begins with 3D^{pol}, in the presence of 3CD, mediating the uridylylation the Tyr3 residue of VPg. The template for VPg uridylylation has been shown to be the *cre*, however in PV, the poly-A tail at the 3' end of the genome is also responsible for VPg uridylylation (Paul et al., 1998; Murray et al., 2003). In FMDV, a copy of uridylylated VPg (VPg-pUpU) binds to the 3' end of the template RNA and acts as a primer to initiate replication. It is thus covalently linked to the 5' end of the daughter strand for both positive and negative strand synthesis (Fig. 1.9) (Goodfellow et al., 2003; Murray et al., 2003; Nayak et al., 2005; Nayak et al., 2006; Steil et al., 2009).

The process of replication involves 3D^{pol} binding to the poly-A tail and replicating the RNA template to form a negative strand intermediate from which positive strands can be made and used as templates for translation and to be packaged into nascent virions (Fig 1.9). Translation of the input RNA occurs in a 5' to 3' direction beginning at the IRES located in the 5' UTR, whereas replication occurs in the opposite direction. Therefore, these two functions cannot occur concurrently on the same RNA strand, and it is proposed that a switch must occur for replication to begin, or the two processes of replication and translation occur within different compartments (Harris et al., 1994; Gamarnik et al., 1998; Barton et al., 2001; Paul, 2002; Nayak et al., 2005). In PV, the switch from translation to replication on the genomic RNA is mediated by the binding of the cellular protein PCBP to the cloverleaf. This binding enhances viral translation, while the binding of the viral protein 3CD represses translation and

facilitates negative-strand synthesis (Gamarnik et al., 1998; Serrano et al., 2006). It is possible that in FMDV the S-fragment (section 1.2.3.1) performs the same function as the PV cloverleaf, but this has yet to be elucidated.

1.3 Replication Complex

Replication of viral RNA is thought to occur within intracellular membrane-associated compartments known as replication complexes. Evidence of such compartments have been shown for a number of positive-strand RNA viruses such as PV, HCV and dengue virus (Troxler et al., 1992; Schlegel et al., 1996; Westaway et al., 1999; Gosert et al., 2003; Novoa et al., 2005; den Boon et al., 2010; den Boon et al., 2010). Replication is thought to occur within these compartments as a way for the virus to concentrate the structural and non-structural components into a small area to facilitate replication, as well as to be able to protect the virus components from host-cell pathogen recognition and innate immune responses.

Studies on FMDV have shown that the virus dysregulates Golgi and ER-derived membranes like PV and has been found to concentrate on small membranous vacuoles within the cell (Polatnick and S. Wool, 1983; Schlegel et al., 1996; O'Donnell et al., 2001; Monaghan et al., 2004; Knox et al., 2005). However, no distinct membrane-bound replication complex comprised of viral RNA, structural and non-structural proteins, and host-cell proteins have yet to be identified for FMDV.

1.3.1 FMDV Fibrils

Investigations on the formation of a discrete replication complex during FMDV replication are ongoing. Studies have shown that, like PV, FMDV 3D^{pol} is able to form higher-order fibrils *in vitro*, but only when combined with an RNA template-primer and free nucleotides, suggesting that these structures could be associated with

replication of the viral genome (Pata et al., 1995; Lyle, Bullitt, et al., 2002; Bentham et al., 2012; Wang et al., 2013).

The function of the fibrils in FMDV replication is still to be elucidated, however, it is speculated that these structures may play a role in concentrating the viral replication complex to increase the efficiency of replication, or that these structures may be involved in preventing the formation of double-stranded RNA which could trigger an innate immune response against the virus.

1.3.2 Cellular Interacting Partners in Replication Complex Formation

Viruses have been shown to hijack ER, Golgi and *trans*-Golgi network (TGN) membranes in order to form these factories. Although of particular interest is the composition of the membranes that are formed, the membranes are rich in phosphatidylinositol-4-phosphate (PI4P) lipids, shown to be required for the replication of multiple members of the family *Picornaviridae* and *Flaviviridae*. These viruses enrich the factory membranes with PI4P lipids by up-regulating and selectively recruiting components of the phosphatidylinositol-4-kinase (PI4K) enzyme pathway that phosphorylate phosphatidylinositol lipids into their functional form (discussed in more detail in chapter 5).

There are two types of well-defined families of PI4Ks expressed in mammalian cells, type II and type III. Type III PI4Ks are the larger of the two and are made up of two enzymes PI4KIII α and PI4KIII β , which function in ER and Golgi, respectively (Balla et al., 2006; Konan et al., 2014). Previous studies on PV and Coxsackievirus B3 (CVB3) have identified PI4KIII β as the host enzyme upregulated in viral replication factories (Belov et al., 2007; Hsu et al., 2010; Arita et al., 2011; Altan-Bonnet et al., 2012; Boura

et al., 2015). Depletion of PI4KIII β activity within infected cells by RNA silencing or the use of specific kinase inhibitors, such as PIK93, a selective small molecule inhibitor against PI4KIII β , (Belov et al., 2007; Altan-Bonnet et al., 2012) appeared to block poliovirus RNA synthesis (Hsu et al., 2010; Arita et al., 2011; Greninger et al., 2012). It is thought that the PV 3D^{pol} is able to bind to PI4P lipids and is then either anchored to the viral replication complex, or is stimulated to perform its enzymatic activity (Hsu et al., 2010). A related family of PI-kinases, is the PI3K family of enzymes. These have been documented to be involved in *hepacivirus* replication in a similar manner to the PI4Ks (Altan-Bonnet et al., 2012).

Other lipids have also been shown to interact with related picornavirus replication. Cholesterol is known to be recruited into the enterovirus replication complex by oxysterol-binding protein (OSBP) (Balla et al., 2006; Arita, 2014; Wang et al., 2014). OSBP plays a central role in cholesterol transport and shuttles cholesterol between different cellular organelles in exchange for PI4P (Mesmin et al., 2013). Enteroviruses have been shown to subvert OSBP in order to exchange PI4P for cholesterol at the replication complex (Illynska et al., 2013; van der Schaar et al., 2013; Arita et al., 2013; Roulin et al., 2014; Dorobantu, Albuлесcu, et al., 2015; Albuлесcu et al., 2015). Similar to the studies on PI4K, the chemical inhibition of OSBP disrupts virus replication factory formation, and subsequent RNA synthesis. In PV cholesterol has also been shown to be involved in the processing of the 3CD precursor into mature 3C and 3D^{pol}, however in other enteroviruses (namely human rhinovirus) cholesterol biosynthesis has been shown to have little active role in replication, but to be crucial to support replication, and is enriched in the replication sites (Illynska et al., 2013; Roulin et al., 2014; Berryman et al., 2016).

The involvement of the PI4KIII β family of enzymes, or OSBP and cholesterol, on FMDV replication and translation has yet to be clearly defined, however previous studies on other *Picornaviridae*, and the identification of 3D^{pol} fibril formation, suggest that FMDV may use these mechanisms.

1.4 Aims of the Project

The principal aim of this project was to dissect the role of the FMDV 3D^{pol} in viral replication and to further investigate the formation of 3D^{pol} fibrils *in vitro* in an attempt to understand the relationship between structure and function of these higher-order structures.

In order to investigate this, a number of FMDV 3D^{pol} mutations were made that abrogated function. Structure was investigated using cryo-electron microscopy and x-ray crystallography.

Additionally, it was pertinent to investigate the role of membrane-associated kinases, such as PI4K, as a number of related viruses utilise these cellular factors to form an optimal environment within which viral replication can occur.

Ultimately, by improving our understanding of the formation of the FMDV replication complex, either through the abrogation of intracellular membranes and the pathways necessary for this function to occur, or by investigating the role of the 3D^{pol} fibrils, we will be able to develop better treatments or antiviral therapeutics.

Chapter 2

Materials and Methods

2.1 General Buffers, Media and Solutions

Media/Buffer/Reagent	Recipe
Luria-Bertani (LB) medium and agar	1 % (w/v) Tryptone 0.5 % (w/v) NaCl 0.5 % (w/v) Yeast Extract (Add 1.5 % (w/v) Agar for LB Agar)
1 x TBE buffer (Tris-borate-EDTA)	10 % 10 x TBE buffer (Thistle Scientific) 90 % ml dH ₂ O
1 x Tris-glycine SDS-PAGE running buffer	25 mM Tris 192 mM Glycine 0.1 % sodium dodecyl sulphate (SDS)
1 x Transfer buffer	25 mM Tris 192 mM Glycine 0.1 % SDS 15 % (v/v) Methanol
10 x TBS (Tris-buffered saline)	250 mM Tris 1.37 M NaCl pH 7.5
1 x TBS-T (Tris-buffered saline-Tween-20®)	10 % 10 x TBS 0.1 % ml Tween-20®
Diethylpyrocarbonate (DEPC)-treated dH₂O	0.1 % (v/v) DEPC in dH ₂ O
1 x 3-(N-morpholino)propanesulphonic acid (MOPS) buffer	10 % 10 x MOPS buffer (VWR) 90 % DEPC-treated dH ₂ O
Buffer A (wash)	50 mM Tris 500 mM NaCl 25 mM Imidazole pH 8 with HCl

Media/Buffer/Reagent	Recipe
Buffer B (elution)	50 mM Tris 500 mM NaCl 500 mM Imidazole pH to 8 with HCl
Dialysis buffers (pH 8)	50 mM Tris 500 mM NaCl Buffer 1) 250 mM Imidazole Buffer 2) 100 mM Imidazole Buffer 3) 25 mM Imidazole Buffer 4) 0 mM Imidazole
10 x Elongation assay buffer	300 mM MOPS (pH 7) 250 mM NaCl 50 mM MgCl ₂ 600 μM ZnCl ₂
RNA binding buffer	20 mM Tris-HCl (pH 8) 100 mM NaCl 0.01 % Triton X-100
RIPA buffer	25 mM Tris (HCl) pH 7.6 150 mM NaCl 1 % (v/v) nonidet-P40 (NP-40) 1 % (v/v) sodium deoxycholate 0.1 % (v/v) SDS from 10 % (w/v) stock. 1 mM EDTA 1 x protease inhibitor
4 % paraformaldehyde (100 ml)	4 g paraformaldehyde powder 10 μl 10M NaOH 10 ml 10 x PBS 90 ml ddH ₂ O pH 7
Saponin buffer (100 ml)	10 ml FCS (Foetal calf serum) 100 mg saponin 90 ml 1 x PBS

Media/Buffer/Reagent	Recipe
MOPS-formaldehyde gel	0.32 g Agarose 29.5 ml DEPC-treated dH ₂ O 3.5 ml 10 x 3-(N-morpholino)propanesulphonic acid (MOPS) buffer (VWR) 2 ml 37 % formaldehyde
5 ml 5 % SDS-PAGE Stacking gel (Cold Spring Harbor Laboratory, 2015)	3.44 ml dH ₂ O 0.63 ml 1 M Tris-HCl (pH 6.8) 0.05 ml 10 % (w/v) SDS 0.83 ml 30 % Acrylamide/bis-acrylamide 0.05 ml 10 % (w/v) ammonium persulfate (APS) 0.005 ml TEMED
10 ml 10 % SDS-PAGE Running gel (Cold Spring Harbor Laboratory, 2015)	4.0 ml dH ₂ O 2.5 ml 1.5 M Tris-HCl (pH 8.8) 0.1 ml 10 % (w/v) SDS 3.3 ml 30 % Acrylamide/bis-acrylamide 0.1 ml 10 % (w/v) APS 0.01 ml TEMED
Full MEM	MEM 0.1 % (v/v) NEAA 1 % (v/v) L-glutamine 10 % (v/v) FBS 100 units/ml penicillin 100 units/ml streptomycin
Transfection Minimum Essential Media (MEM)	MEM (Life Technologies) 0.1 % (v/v) NEAA 1 % (v/v) L-glutamine
DNA Transfection mix for 6-well plate	2 µg DNA 10 µl Polythetylenimine (PEI) 700 µl Transfection MEM

2.2 Cell Lines

Cell Line	Derivation	Cell Type	Source
BHK-21	Hamster kidney	Fibroblast	ATCC
Huh 7.5	Human hepatocarcinoma	Epithelial	ATCC
HeLa	Human cervical adenocarcinoma	Epithelial	ATCC
MDBK	Bovine kidney	Epithelial	ATCC (via St. Andrews)
SK-RST	Porcine kidney	Epithelial	ATCC (via St. Andrews)

2.3 Compounds

Compound	Stock conc.	Working conc. range	Source
PIK93	5 mM	1 μ M- 5 μ M	Sigma
Compound 3	40 mM	0.5 μ M – 20 μ M	AstraZeneca
Compound 7	40 mM	0.5 μ M – 20 μ M	AstraZeneca
Wortmannin	2 mM	0.5 μ M – 2 μ M	Calbiochem (Gift from Jamel Mankouri, Leeds)

2.4 Antibodies

Antibody	Species	Dilution	Source	Target
Anti-3A (2C2)	Rabbit	1:2000	Gift from Francisco Sobrino (Madrid)	Primary
Anti-3B (IF8)	Mouse	1:1000	Gift from Francisco Sobrino (Madrid)	Primary
Anti-3C (2D2)	Mouse	1:2000	Gift from Francisco Sobrino (Madrid)	Primary
Anti-3D (397)	Rabbit	1:5000	Gift from Francisco Sobrino (Madrid)	Primary
Anti-His (HRP)	Mouse	1:5000	Sigma-Aldrich	Primary
Anti-FLAG	Rabbit	1:5000	Sigma-Aldrich	Primary
Anti-HA	Mouse	1:5000	Sigma-Aldrich	Primary
Anti-Biotin	Mouse	1:5000	Sigma-Aldrich	Primary
Anti-GAPDH	Mouse	1:5000	Sigma-Aldrich	Primary
Anti-PI4P	Mouse	1:50	Echelon	Primary
Anti-NS5A	Sheep	1:5000	Gift from Mark Harris (Leeds)	Primary
Anti-Mouse (HRP)	Goat	1:2000	Sigma-Aldrich	Secondary
Anti-Rabbit (HRP)	Goat	1:5000	Sigma-Aldrich	Secondary
Anti-Rabbit Alexa Fluor 568	Goat	1:5000	Life Technologies	Fluorescent secondary
Anti-Mouse Alexa Fluor 647	Donkey	1:5000	Life Technologies	Fluorescent secondary

2.5 Nucleic acid manipulation

2.5.1 Plasmids and Replicons

Several plasmids have been designed and DNA or RNA from those plasmids were used in both replication and translation assays. The plasmids can be classed into four types; those based on GFP-pac, ptGFP and mCherry, luciferase, and bicistronic. The bicistronic plasmids contained sequences of FMDV, encephalomyocarditis virus (EMCV), hepatitis C virus (HCV) and human rhinovirus (HRV) IRES.

2.5.1.1 FMDV Replicon Constructs

GFP-pac based plasmid constructs include the FMDV replicon insert replacing the structural proteins 1A-1D with a green fluorescent protein (GFP) reporter gene and a puromycin acetyltransferase resistance gene (pac). ptGFP replicons are the second generation GFP-pac plasmids designed by Fiona Tulloch (St. Andrews) replacing the GFP-pac reporter with a GFP derived from *Ptilosarcus gurneyi* (ptGFP), a bioluminescent sea pen, which is brighter than the *Aequorea* GFP (extracted from the *Aequorea victoria* jellyfish) used in GFP-pac. mCherry constructs have replaced the structural proteins 1A-1D with the mCherry fluorescent report gene (Fiona Tulloch, St. Andrews). Plasmids have also been designed to contain various point mutations or synonymous scrambled DNA sequences to act as experimental controls. These replicons are shown schematically in Table 2.1 and 2.2.

Replicon Name	Designed by	Plasmid backbone
GFP-pac-WT	F. Tulloch (St. Andrews)	pBR3222
GFP-pac-LL	F. Tulloch (St. Andrews)	pBR3222
GFP-pac-Δ3D	F. Tulloch (St. Andrews)	pBR3222
GFP-pac-GNN	F. Tulloch (St. Andrews)/M. Herod (Leeds)	pBR322
ptGFP-WT	F. Tulloch (St. Andrews)/M. Herod (Leeds)	pCDNA

Table 2.1: Summary of GFP-containing replicon constructs. All GFP-pac replicon constructs have been designed with the structural proteins encoded for by 1A-1D have been replaced by GFP-pac reporter cassette. The final ptGFP replicon shows the change from GFP-pac with a simple exchange of the structural proteins 1A-1D to the new ptGFP reporter gene.

Replicon Name	Designed by	Plasmid Backbone
mCherry-WT	F. Tulloch (St. Andrews)	pCDNA

Table 2.2: Summary of mCherry-containing replicon constructs. The mCherry replicon constructs share a similar structure to the GFP-pac constructs; replacing the 1A-1D structural proteins with an mCherry red fluorescent protein.

2.5.1.2 Bicistronic Replicon Constructs

The bicistronic luciferase constructs contain a *Renilla* luciferase reporter gene under the control of a 7-methylguanosine cap, followed by a *firefly* luciferase reporter gene under the control of an IRES from FMDV, EMCV, HCV, and HRV. These constructs were designed in the Hirasawa laboratory (Memorial University of Newfoundland, Canada). These replicons are shown schematically in Table 2.3.

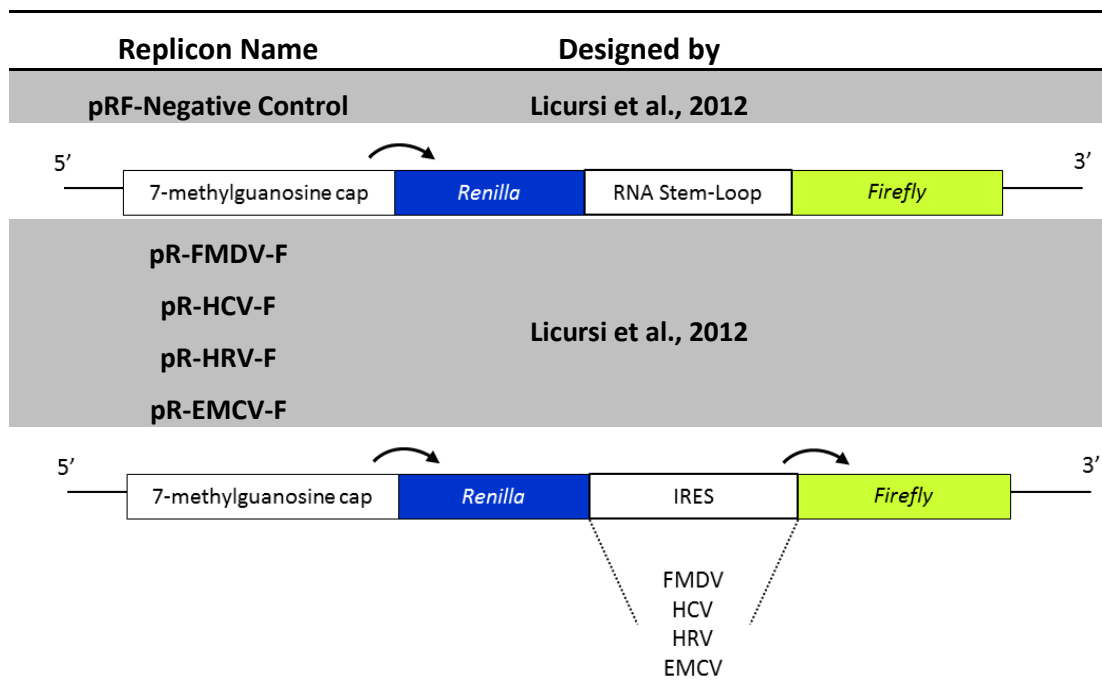


Table 2.3: Summary of bi-cistronic reporter constructs. The constructs described are dual luciferase bi-cistronic constructs. Two different luciferase reporter genes are under the expression of two alternative methods of translation: cap- and IRES-dependent. Luminescence of luciferase depends on the method of translation being utilised.

2.1.1.3 CVB3 Replicon Constructs

The CVB3 plasmids (kind gift from Frank van Kuppeveld, University of Utrecht) encode an ORF for a CVB3 replicon. The structural proteins have been replaced with a luciferase reporter gene. Two plasmids were provided, one encoding a WT CVB3

replicon, and one with a mutation in non-structural protein 3A rendering the replicon replication-defective. The replicons are shown schematically in Table 2.4.

Replicon Name	Designed by
Rib-Fluc-CB3/T7 or CB3/T7-3A	H.Tongren-van der Schaar (Utrecht)

Table 2.4: Summary of CVB3 replicons constructs. The CVB3 replicon constructs, Rib-Fluc-CB3/T7 contain a firefly luciferase reporter gene in place of the structural proteins 1A-1D. A mutant construct was also provided (Rib-Fluc-CB3/T7-3A) which replaced amino acids at positions 6-11 in non-structural protein 3A with 5 alanine residues.

2.5.1.4 HCV Replicon Constructs

The HCV sub-genomic replicon RNA (kind gift from Mark Harris, University of Leeds) termed HCV SGR-Luc-GFP-JFH1, is encoded by a plasmid containing the non-structural proteins of HCV genotype 2a, JFH-1. The structural proteins E1, E2, core and P7 have been replaced with a luciferase reporter gene and a neomycin resistance gene used for stable selection in cell culture. The luciferase reporter gene is under the control of the HCV IRES, and the non-structural proteins NS3-5B are under the control of the EMCV IRES. The replicon is shown schematically in Table 2.5.

Replicon Name	Designed by
SGR-Luc-GFP-JFH1	Jones et al., 2007; Saeed et al., 2012

Table 2.5: Summary of HCV replicon construct. The HCV replicon construct, SGR-Luc-GFP-JFH1 contains a firefly luciferase reporter gene and a neomycin resistance gene in place of the structural proteins E1, E2, core and p7.

2.5.2 Replicon DNA Preparation

2.5.2.1 Transformation

Plasmids were transformed into and DH5 α competent *E. coli* bacterial cells by adding 250 ng DNA to 50 μ l thawed DH5 α competent cells and incubated on ice for 30 mins. Subsequently, the bacteria and DNA were subjected to a heat shock at 42°C for one minute, followed by rapid cooling on ice for two minutes. 500 μ l LB media was added and the transformed bacteria were recovered at 37°C for one hour prior to lawn spreading on LB agar plates containing 100 μ g/ml ampicillin. The plates were incubated for 16 hours at 32°C.

2.5.2.2 Preparation of plasmid DNA

A single colony from the LB agar plates was picked and grown for 16 hours (overnight) in a 32°C shaking incubator in 10 ml LB containing 100 μ g/ml ampicillin. Following the overnight culture growth of the colony in the media, 300 μ l of the culture was transferred to an Eppendorf tube and mixed with 600 μ l 30 % (v/v) glycerol. The glycerol stock of the culture was stored at -80°C for long term storage.

The overnight cultures were subjected to either Miniprep or Maxiprep protocols per manufacturer's instructions (Qiagen), depending on the volume of the culture. Distilled water was used to elute the DNA. The concentration of the eluted plasmid DNA was measured using a nanodrop spectrophotometer and recorded.

2.5.2.3 DNA linearisation

GFP-pac plasmid DNA was linearised with restriction enzyme *HpaI* (New England Biolabs - NEB). ptGFP and mCherry plasmid DNA was linearised with *AscI* (NEB). CVB3 Rib-Fluc-CB3/T7(-3A) was linearised with *MluI* (NEB). HCV SGR plasmid was linearised with *XbaI* (NEB). Linearisation occurred by incubating 1 µl enzyme with 500 ng DNA in a 10 µl reaction. Linearisation was confirmed by resolving DNA by 1 % agarose (1 % (w/v) agarose in 1 x TBE buffer) gel electrophoresis.

2.5.2.3 DNA Purification

Linearised plasmid DNA (500 ng) was phenol-chloroform extracted and ethanol-precipitated by mixing equal volumes of phenol-chloroform with linearised plasmid DNA and centrifuging the sample at approximately 16,000 x g (or 13,300 RPM) for 10 minutes at 16°C. The upper aqueous phase was carefully withdrawn and dispensed into a fresh nuclease-free Eppendorf tube. The aqueous phase was then mixed with an equal volume of chloroform and centrifuged at 16,000 x g (or 13,300 RPM) for a further 10 minutes at 16°C. The upper aqueous phase was once again removed and dispensed into a fresh nuclease-free Eppendorf tube. The aqueous phase was subjected to ethanol precipitation by mixing in 1/10 volume 3M sodium acetate and 2.5 x volume 100 % ethanol. The mixture was gently agitated and placed at -20°C for 20 mins. After precipitation, the mixture was centrifuged at 16,000 x g (or 13,300 RPM) for 30 mins at 16°C. The supernatant was removed and discarded. Equal volume of the supernatant was replaced with fresh nuclease-free 70 % ethanol. The DNA pellet was gently resuspended and the mixture was centrifuged once more at 16,000 x g (or 13,300 RPM) for 30 minutes at 16°C. The supernatant was removed

and discarded and the pellet of purified DNA is resuspended in 18 µl nuclease-free dH₂O. The concentration of the purified DNA was measured using a nanodrop spectrophotometer.

2.5.3 RNA Preparation

2.5.3.1 T7 *In vitro* Transcription

The purified DNA containing the FMDV insert was used as a template for *in vitro* transcription in a T7 *in vitro* transcription reaction. 2.5 µl 10 x T7 transcription buffer, 0.5 µl bovine serum albumin (BSA) (10 mg/ml) and 1.25 µl 20 x RNA Secure were added to the purified DNA and incubated at 60°C for 10 minutes, followed by cooling on ice. Subsequently, 0.75 µl RNase inhibitor, 2 µl ribonucleoside tri-phosphates (RNTPs) from 100 mM stock and 1 µl T7 RNA polymerase was added prior to incubation at 32°C for four hours. Reactions were treated with 1.25 µl RQ1 RNase-free DNase for 30 minutes at 37°C. The RNA was recovered and purified using RNA Clean and Concentrator™-25 (Zymo Research) according to manufacturer's instructions and eluted twice in 25 µl nuclease-free water. The RNA concentration was measured by nanodrop spectrophotometry and stored at -80°C.

Ethanol-precipitated, purified HCV SGR DNA was *in vitro* transcribed using a RiboMAX™ T7 *in vitro* transcription kit (Promega) according to the manufacturer's instructions. The integrity and concentration of the RNA was tested by electrophoresis on a 1 % MOPS-formaldehyde gel (see section 2.1). 500 ng RNA was heated to 85°C for 10 minutes and added to the gel. The gel was subjected to 80 V for 45 minutes.

2.6 Cell Culture

2.6.1 Cell Culture Maintenance

The cell lines used during the project (BHK-21, Huh 7.5 and HeLa) were maintained in DMEM in T75 or T175 flasks (Corning). Cells were passaged every 48-72 hours, or when they were 80-90 % confluent by removing the media and washing the cells in 1 x PBS and detaching the cells using 1 x trypsin-EDTA. Cells were re-suspended in DMEM supplemented with 10 % (v/v) Foetal Bovine Serum (FBS), 100 units/ml penicillin and 0.1 units/ml streptomycin, and passaged at 1:12 dilution. Cells were grown at 37°C in a humidified incubator with 5 % carbon dioxide.

2.6.2 Preparing Cells for IncuCyte Analyses

IncuCyte analyses to measure levels of fluorescence in replicon-transfected cells were undertaken in cells seeded out into 24-well plates at a density of 1×10^5 cells per well and maintained in 500 μ l DMEM for 24 hours.

2.6.3 Transfection of RNA

Cells prepared in 24-well plates were used for transfection with a total of 1 μ g RNA using Lipofectin[®] transfection reagent (Life Technologies) as previously described (Tulloch et al., 2014; Herod et al., 2015). For complementation studies, 0.5 μ g of both ptGFP and mCherry replicon RNAs were simultaneously co-transfected using Lipofectin[®] (Life Technologies) as previously described. Evidence of replication as a result of transfection was monitored using IncuCyte Dual Colour ZOOM[®] FLR for 24 hours.

2.6.4 Preparing Cells for Dual Luciferase Assays

Dual luciferase assays were undertaken in BHK-21 cells seeded at a density of 2×10^5 per well in 6-well plates. These cells were maintained in DMEM for 24 hours until they reach 40-60 % confluency at the time of transfection.

2.6.5 Transfection of DNA

Cells were prepared as described in section 2.6.4. The transfection mix (section 2.1) was optimised as previously described in Licursi et al., 2011; the cells were supplemented in 1300 μ l full MEM and placed at 37°C. After 5-8 hours post-transfection, the media was changed to 2 ml full MEM for a further 48 hours. The cells were lysed in 1 x passive lysis buffer (Promega) and placed at -20°C for at least 2 hours. The cell lysates were collected in Eppendorf tubes, vortexed briefly and centrifuged at approximately 1,000 x g (or 4,000 RPM) for 5 minutes to pellet the cell debris. Following pelleting, 30 μ l of an undiluted lysate sample and a lysate sample diluted to 1/100 in 1 x PBS, and were placed in a white opaque 96-well plate and placed in the luminometer. The Dual-Luciferase[®] Reporter Assay System kit (Promega) was used. The luciferase luminescence in luciferase forming units (LFU) in the neat, undiluted lysate samples and lysate samples diluted 1/100 was measured.

2.6.6 Preparing cells for electroporation

Huh 7.5 cells in a T175 flask (Corning) were washed with 1 x PBS and trypsinised to remove the adherent cells from the flask. The cells were collected and washed three times in diethyl pyrocarbonate (DEPC)-treated 1 x PBS by centrifuging the cells at

approximately 1,000 x g (or 4,000 RPM) for 5 mins at 4°C. Cells were resuspended in DEPC-treated 1 x PBS at a density of 2×10^6 cells.

2.6.7 Electroporation of RNA

5 µg RNA transcripts were transfected into 2×10^6 cells in DEPC-treated 1 x PBS by electroporation using a square-wave protocol at 260 V for 25 ms. Electroporated cells were resuspended in DMEM to 2×10^5 cells/ml and seeded on cover slips in 24-well plates at a density of 1×10^5 cells per well.

2.6.8 Compound treatments

PIK93, Compound 3 and Compound 7, and wortmannin were added to cell cultures either 2 hours prior to transfection, or at the same time as transfection or electroporation at the concentrations described in section 2.3. If the compounds were added 2 hours prior to transfection, the compound was refreshed when the transfection components were added to the cells.

2.6.9 Cytotoxicity (MTT) assay

An MTT cytotoxicity assay of the compounds described in section 2.3 was undertaken prior to experimental use. Cells were plated out into a 96-well plate at a density of 1×10^4 cells per well. Cells were allowed to recover and settle for 24 hours in 100µl DMEM. The compounds were added to the cells at increasing concentrations (ranging from 0 µM up to 20 µM) and allowed to incubate for 24-48 hours. Following the appropriate incubation times, MTT substrate MW414 (Sigma) was dissolved to a concentration of 1 mg/ml in filter-sterilised serum-free medium.

The DMEM and compound were removed from the cells and they were washed in 1 x PBS. 100 µl of MTT solution was added to each well and incubated in the dark at 37°C in a humidified incubator with 5 % carbon dioxide for 30 minutes. Following incubation, the MTT solution was removed from the cells and replaced with 100 µl DMSO. The plate was agitated for 5 minutes at 60 rpm to allow for the purple precipitant to re-dissolve. Any bubbles were removed and the plate was analysed by measuring absorbance at 570 nm using a fluorescent plate reader.

2.7 Immunofluorescence

2.7.1 Preparation of Cells for Immunofluorescence

BHK-21 and Huh 7.5 cells were seeded on to glass coverslips in 24-well plates and transfected with FMDV replicon RNA as described in section 2.6.2 and section 2.6.3, or after electroporation with HCV SGR as described in section 2.6.6 and 2.6.7. Transfected cells were incubated for a range of times (2-8 hours). Following incubation, the media was removed and the cells were gently washed once with 1 x PBS and fixed using 4 % paraformaldehyde for 10 minutes at room temperature. Once fixed, the cells were stored in 1 x PBS at room temperature.

2.7.2 Permeabilisation and Antibody Probing

Cells were permeabilised either in 0.2 % triton X-100 in PBS or in saponin buffer for 2 hours at room temperature on a rocking platform. Permeabilised cells were subsequently washed 3 times in 1 x PBS and probed with the appropriate primary

antibody diluted in 1 x PBS for 2 hours at room temperature, or for 16 hours at 4°C.

Cells treated with the appropriate primary antibody (as listed in section 2.4).

Following primary antibody incubation, coverslips were washed 3 times in 1 x PBS and probed with the appropriate secondary fluorescent antibodies (as listed in section 2.4). The antibodies were diluted in 1 x PBS. Cells were incubated with secondary fluorescent antibodies for 2 hours at room temperature on a rocking platform. Incubation of coverslips with secondary antibody was undertaken in the dark.

Coverslips were washed 3 times in 1 x PBS and mounted on microscope slides after blotting dry with 5 µl ProLong Gold antifade mountant with DAPI (Life Technologies). Mounted coverslips were sealed before visualising by confocal microscope.

2.8 Immunoblotting

2.8.1 Harvesting Cell Lysates

BHK-21 cells were transfected with RNA as outlined previously. Every hour after transfection for 10 hours the cells were lysed by adding 100 µl RIPA buffer and scraped from the well into an Eppendorf tube, vortexed and centrifuge at approximately 16,000 x g (or 13,300 RPM) for 15 minutes to pellet the lysates. The lysates could be stored in -20°C. Lysate samples were subjected to SDS-PAGE electrophoresis on 10 or 15 % resolving gels, with 5 % stacking gel (Cold Spring Harbor Laboratory, 2015).

2.8.2 SDS-PAGE Gel Electrophoresis

SDS-PAGE gels were prepared for electrophoresis of samples (Cold Spring Harbor Laboratory, 2015) . An equal volume of cell lysate sample and 2 x Laemelli loading dye was heated at 95°C for five minutes. The samples were loaded on to the gels. The gels were subjected to 200 V for one hour in 1 x Tris-glycine SDS-PAGE running buffer.

2.8.3 Western Blotting

After electrophoresis, the protein on the gel was transferred onto Immobilon®-P polyvinylidene difluoride (PVDF) membrane (Merck) (activated in 100% methanol prior to transfer) on XCell SureLock Mini-Cell wet transfer apparatus (Life Technologies) in 1 x transfer buffer for one hour 30 minutes at 25 mA. The membrane was subsequently washed in 1 x TBS-T and blocked in 10 % blocking buffer (10 % (w/v) skimmed milk powder in 1 x TBS-T) for one hour at room temperature on a rocking platform.

2.8.4 Antibody Incubation

The membranes were incubated for 16 hours at 4°C on a rocking platform with the primary antibodies (section 2.4), diluted to the appropriate concentration in in 5 % milk (5 % (w/v) milk powder in 1 x TBS-T). Following incubation, the membranes were washed 3 times in 1 x TBS-T and incubated for 2 hours at room temperature on a rocking platform with the appropriate secondary antibody (section 2.4) diluted to the appropriate concentration in 5 % blocking buffer.

2.8.5 Developing SDS-PAGE membranes

The membranes were washed and incubated in combined ECL I and II enhanced chemiluminescence reagents (Pierce) and are exposed on film. The film was automatically developed using the Xograph Compact X4 Automatic Processor to develop the film.

2.9 Expression and purification of His-tagged 3D^{pol}

WT his-tagged 3D^{pol} (kind gift from Esteban Domingo) and mutants constructed by PCR mutagenesis were expressed in Codon plus (+) RiPL competent *E. coli*. For protein production, a 12 ml LB medium containing kanamycin (100 µg/ml) and chloramphenicol (34 µg/ml in 100% ethanol) was grown for 16 hours at 37°C and used as a starter culture. 10 ml of starter culture was used to inoculate 1 L LB broth with 100 µg/ml kanamycin. The cultures were grown at 37°C in a shaking incubator until optical density at 600 nm (OD₆₀₀) was in the range of 0.6-0.8. Cultures were then induced with 1 mM IPTG and grown for a further 3 hours at 37°C. The cultures were centrifuged at approximately 6,000 x g (or 5,000 RPM) for 10 minutes and the supernatant was discarded. The bacterial pellet was resuspended in 1 ml storage buffer (20 mM Tris-HCl, pH 8) and stored at -80°C.

Pellets were lysed with the addition of 30 ml lysis buffer (20 mM Tris-HCl, 500 mM NaCl, pH 8), 200 µl 100 mg/ml lysozyme (Sigma), 15 µl 100 mg/ml DNaseI (Life Technologies), and 1 cComplete EDTA-free protease inhibitor cocktail tablet (Roche) and placed on a roller at 4°C for 30 minutes. The lysed pellets were subsequently sonicated alternating 10 seconds on and 40 seconds off for 6 minutes. The sonicated

lysate was centrifuged at approximately 27,000 x g (or 15,000 RPM) for 20 minutes and the supernatant filtered through 0.22 µm filter.

The filtered supernatant (load) was subjected to nickel affinity chromatography using 1 ml HisTrap HP columns (GE Healthcare) attached to a peristaltic pump. HisTrap columns were prepared by washing with five column volumes (CV) dH₂O, and equilibrating with five CV buffer A (wash). The load was added and collected as flowthrough. The column was washed three times in 3 CV buffer A (wash). Each wash was collected separately. The column was then washed with 5 CV buffer B (elution). The flowthrough was collected in eight 250 µl fractions and the final three ml was collected in fraction 9.

The load flowthrough, washes and eluted fractions (1-9) are analysed by SDS-PAGE and Coomassie (brilliant blue) stain. The typical approximate concentrations, as determined by Bradford assay, of the purified His-3D^{pol} WT, DD388/9NN, DD240/5NN and GC216/7AA mutant proteins were 185 µM, 300 µM, 92 µM and 130 µM, respectively.

2.10 His-tagged 3D^{pol} *in vitro* assays

2.10.1 3D^{pol} Activity Assay

A 100 µl master-mix of 10 µl 10x elongation buffer, 20 µl 500ng/µl poly-A template RNA (GE Healthcare), 2.4 µg oligo-d(T)₁₅ (Promega), 4 mM UTP (Thermo Fisher), and 1 µl [α -³²P]-UTP (250 µCi) (Perkin Elmer) was made alongside 20 µl master-mix for controls which include one without any RNA components, one without poly-A template RNA, one without oligo-d(T) primer DNA, and one without any UTP. 10 µl

of each master mix was aliquoted into an RNase-free Eppendorf tubes (one for each timepoint and for the controls). Immediately before use, a final concentration of 18.52 μM of his-3D^{pol} was added to each reaction tube except for the control tube (that contained no protein). All reactions were controlled for salt concentrations as dilution of individual components (solutes) of the assay were made using the same solvent/buffer.

Reaction tubes were incubated at 30°C for increasing lengths of time (1-120 minutes). Reactions were stopped by the addition of 1.5 μl 500 mM EDTA. 2 μl of each reaction was blotted onto filter paper (Whatmann) and allowed to dry. The dried filter paper was washed by gentle rocking for 2.5 minutes in activity assay wash buffer (200 mM di-sodium hydrogen phosphate, 75.2 mM sodium pyrophosphate) 5 times, followed by once in dH_2O for 1 minute and, once in 100 % ethanol for 1 minute. The filter paper was allowed to dry and was then exposed on to film for 16 hours at -80°C. The film was developed automatically using Xograph Compact X4 Automatic Processor.

The individual dots on the filter paper could then be excised and scintillated with the addition of 3 ml scintillation fluid (Perkin Elmer) and the radioactive counts were measured by ³²P scintillation counts per minute.

2.10.2 3D^{pol} Crosslinking Assay

Individual RNase-free Eppendorf tubes were prepared containing 7.5 μl 1 x elongation buffer and 15 μL 10 mM glutaraldehyde, alongside 80 μl activity assay master-mix consisting of 8 μl 10 x elongation buffer, 16 μl 500ng/ μl poly-A template RNA (GE Healthcare), 2.4 μg oligo-d(T)₁₅ (Promega) and 4 mM UTP (Thermo Fisher). Immediately before use, a final concentration of 18.52 μM of his-3D^{pol} was added to

the master-mix. Controls were also included that substituted each RNA component, protein, or the addition of glutaraldehyde with nuclease-free dH₂O.

7.5 µL of master-mix was added to each individual assay Eppendorf tube before the samples were incubated at 30°C for increasing lengths of time (1-120 minutes).

The reaction was stopped by the addition of 30 µL 2x Laemmli buffer. The samples were then heated for 5 minutes at 95°C. Samples were analysed by gradient SDS-PAGE (12 %, 10 %, 8 %, 6 %, 4 % resolving gels, and 4 % stacking gel (Cold Spring Harbor Laboratory, 2015)), Coomassie (brilliant blue) stain and Western blot probing with primary anti-His or anti-3D antibodies as detailed in section 2.4.

2.10.3 3D^{pol} RNA-binding fluorescent polarisation anisotropy

Using a black opaque 384-well plate (Perkin Elmer), 20 µL of RNA binding buffer (20 mM Tris-HCl (pH 8), 100 mM NaCl, 0.01 % Triton X-100) was added to each well followed by 40 µL of protein to the first well and mixed by pipetting. A serial dilution of the protein was completed across each well by transferring 40 µL of the RNA binding buffer and protein to the next adjoining well and finally discarding 40 µL from the last well resulting in each well containing equal volumes of 20 µL.

Next, 20 µL of 20 nM FITC-labelled 13mer poly-A (from 1 µM stock) was overlaid into each well containing buffer and protein. A control row that contained no fluorescent RNA to establish background polarisation was included. The plate was incubated at room temperature for 1 hour in the dark.

Polarisation was measured using the Tecan plate reader (Darren Tomlinson, University of Leeds) with an excitation filter at 480 nm and S and P channel emission filters at 530 nm.

2.10.4 Transmission electron microscopy (TEM) negative staining

Carbon-coated copper grids were prepared by glow discharge at 25 mA for 30 seconds.

The activity assay master mix was prepared as described for the crosslinking assay in section 2.10.2. Samples were incubated for 30 minutes at 30°C. Reactions were stopped by loading 10 µl onto carbon-coated copper EM grids for 1 minute. The sample was blotted off and the grids washed twice with 10 µl dH₂O for 5 seconds each. The grids were loaded with 10 µl 2 % uranyl acetate for 1 minute and blotted off with filter paper.

TEM was analysed on the Jeol 1400 (Jeol USA Inc.) at 30, 000 x magnification.

2.10.5 Cryo-electron microscopy (Cryo-EM)

Activity assay master-mix was prepared as described in section 2.10.2 and incubated at 30°C for 30 minutes. 10 µl of the master-mix was loaded on a C-flat (protochips) CF1.2/1.3-4C grid (1.2 µm holes) that had been glow discharged at 25 mA for 1 minute. The grids were blotted for 6 seconds at blot force 10, using an FEI Vitrobot Mark IV in chamber conditions at 4°C and 95 % relative humidity.

Initial analysis of the grids took place at the University of Glasgow. 129 micrographs were analysed, yielding 23,700 filament sections by autopicking in Relion 2.0.3. After 2 rounds on 2D classification, 12,521 sections were used in the 3D classifications.

Further cryo-EM analysis involved data collection on the Krios 1 microscope (University of Leeds), using the Falcon III detector in integrating mode. Data was collected at nominal 75,000 x magnification, giving a sampling of 1.05 Å/pixel. The dose rate is 60 e⁻/pixel/second, giving a dose of 54 e⁻/Å²/second. The length of exposure was 2 seconds, with 79 frames in total, giving 1.4 electrons/frame. Collection of data occurred at a defocus range of -1.5 to 2.

Chapter 3

Investigating mutations in foot-and-mouth disease virus 3D polymerase in viral replication

3.1 Introduction

The RNA-dependent RNA polymerase from FMDV, 3D^{pol}, is a 54 kDa enzyme. The main function that has been described for 3D^{pol} is in viral RNA synthesis. 3D^{pol} is a non-proof-reading polymerase resulting in both mutations and recombination occurring during replication, lending FMDV a quasispecies nature, common across all picornaviruses (reviewed in Domingo et al., 2012).

The process of FMDV infection from entry through to egress is extremely quick, completing a single lifecycle in cell culture in 6 hours. In livestock, transmission can result in disease signs being identified as early as 2-3 days post infection (reviewed in Grubman and Baxt, 2004).

Upon entry into the host-cell cytoplasm, the viral RNA genome undergoes initial translation. Host-cell translation initiation factors and ribosomes bind to an IRES element located in the 5' UTR and initiate internal translation of the viral RNA genome in a cap-independent manner typical of a number of positive-sense RNA viruses such as pestiviruses, hepaciviruses, aphthoviruses and enteroviruses (Jang et al., 1988; Pelletier et al., 1988; Belsham et al., 1990; Sizova et al., 1998; Niepmann, 2009). The process of translation is mediated by the binding of translation initiation

factor eIF4G to the IRES. This subunit recruits eIF4A, eIF3a and eIF4B, and the 40s-ribosomal subunit, along with an ever-growing list of cellular co-factors (IRES *trans*-acting factors – ITAFs) including the poly-pyrimidine tract binding protein (PTB), the poly-A binding protein (PABP) and the poly-C binding proteins 1 and 2 (PCBP1, PCBP2) (Martínez-Salas, 2008; Yu et al., 2011; Blyn et al., 1997; Rodríguez Pulido et al., 2007; López de Quinto et al., 2002).

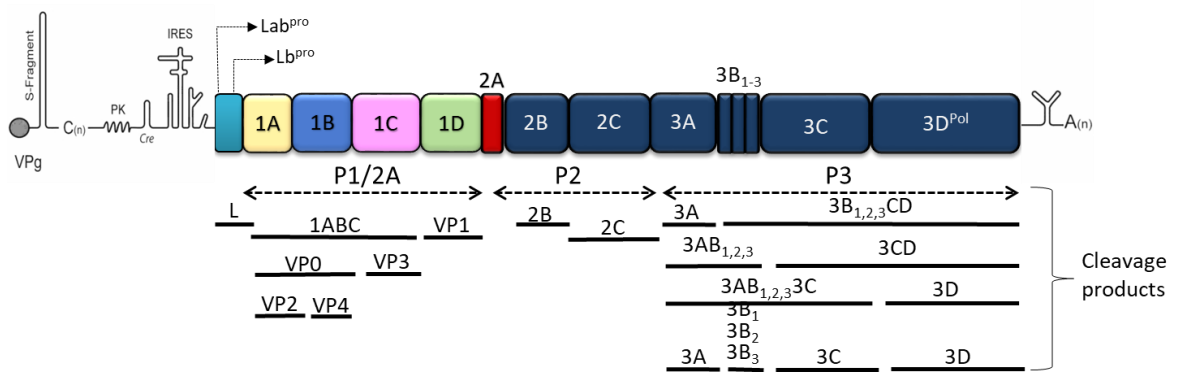


Figure 3.1 Schematic of the FMDV genome showing the proposed ORFs of each of the viral proteins. The 5' untranslated region (UTR) is located upstream of the polyprotein. The structural proteins are transcribed from segment P1 (1A-1D) and are co- and post-translationally processed to make mature capsid proteins (VP1-4). Segments P2 and P3 encode for the non-structural proteins necessary for replication of the genome (2A-3D). Likewise, both these segments are co- and post-translationally modified into the mature proteins. Adapted from Forrest et al., 2014.

The genome is translated into a polyprotein from a single ORF from which the structural and non-structural precursors are co- and post-translationally processed into the active mature proteins (Fig. 3.1). The polyprotein is initially processed into four primary products: L^{pro}, P1-2A, 2BC and P3 (Laporte, 1969; Sangar, Black, et al., 1977; Rueckert et al., 1984). Intermediate polyprotein precursors 2BC and P3 are cleaved into the functional, 'mature' proteins by the virus-encoded protease, 3C via several further intermediates (Doel et al., 1978), including 3AB₁₋₃, and 3CD (Flint et

al., 1997). Further processing releases the 3A transmembrane protein (Moffat et al., 2005; González-Magaldi et al., 2014), three non-identical tandem repeats of primer 3B (3B₁₋₃) (Forss et al., 1982), 3C (Birtley et al., 2005) and 3D^{pol} (Ferrer-Orta et al., 2004).

The process of replication involves the viral polymerase scanning and replicating the RNA template from 5' to 3' direction to form a negative strand intermediate from which positive strands can be made and used as a template for translation and/or to be packaged into virions. Translation of the input RNA occurs in a 5' to 3' direction beginning at the IRES located in the 5' UTR, however, this cannot occur concurrently with replication on the same RNA strand, and it is proposed that a switch occurs for replication to begin (Gamarnik et al., 1998; Paul, 2002; Nayak et al., 2005). However, it is possible that replication and translation can occur concurrently within different cellular compartments.

Initiation of both replication and translation has been shown to involve the circularisation of the genome through discrete RNA-RNA and RNA-protein interactions between the 3' UTR, the 5' UTR, cellular host factors, and virus-encoded proteins (Herold and Andino, 2001; López de Quinto et al., 2002; Serrano et al., 2006). This mechanism is thought to be widespread amongst positive-strand RNA viruses (Pogue et al., 1994; Gamarnik et al., 1998; Kim et al., 2003; Villordo et al., 2010).

Replication of viral RNA commonly occurs within intracellular membrane-associated compartments known as replication complexes. Evidence of such compartments have been shown in HCV, dengue virus, and in other picornaviruses such as PV (Bienz

et al., 1992; Schlegel et al., 1996; Westaway et al., 1999; Gosert et al., 2003; Novoa et al., 2005; den Boon et al., 2010). Replication of viral RNA occurs within these intracellular compartments as a way for the virus to concentrate the structural and non-structural components into a small area to facilitate replication as well as to be able to protect the virus components from host-cell pathogen recognition and innate immune responses. Using immunofluorescent confocal and electron microscopy, FMDV has been shown to dysregulate Golgi and ER-derived membranes in a similar way to PV (Schlegel et al., 1996; O'Donnell et al., 2001; Monaghan et al., 2004; Knox et al., 2005), but no distinct membrane-bound replication complex comprised of viral RNA, structural and non-structural proteins, and host-cell proteins have yet to be identified for FMDV.

Much like PV, where replication is mediated by the binding of 3D^{pol} to the VPg in the presence of 3CD binding to the cloverleaf structure (Harris et al., 1994), replication of FMDV RNA begins with 3D^{pol}, in the presence of 3CD, mediating the uridylylation of the third tyrosine of VPg. VPg is encoded for by non-structural proteins 3B₁, 3B₂, and 3B₃. The template for VPg uridylylation is the *cis*-acting replicative element (*cre*) located in the 5' UTR. A copy of uridylylated VPg (VPg-pUpU) hybridises to the 3' end of the template RNA and acts as a primer to initiate replication. It is thus covalently linked to the 5' end of the daughter strand and is used as a primer for both positive and negative strand synthesis (Murray et al., 2003; Nayak et al., 2005; Steil et al., 2009).

In addition to functioning as the major catalytic protein necessary for viral genome replication, PV 3D^{pol} has been shown, biochemically and by microscopy, to have

another role in creating a support scaffold within which replication can occur. Studies on PV have shown that individual molecules of 3D^{pol} are able to interact with one another and multimerise to form higher-order fibril-like structures (Pata et al., 1995; Lyle, Bullitt, et al., 2002; Spagnolo et al., 2010; Tellez et al., 2011; Wang et al., 2013). Previous work on FMDV has shown, biochemically and by transmission electron microscopy, that 3D^{pol} is also able to form higher-order fibril-like structures, similar to those formed by PV 3D^{pol} (Bentham et al., 2012). This chapter investigates the role of FMDV 3D^{pol} in RNA replication by studying the formation of higher-order structures and the effects of a number of mutant polymerases on their ability to function.

3.2 Mutations of 3D^{pol}

The structure of FMDV 3D^{pol} has been well characterised and there are high-resolution crystal structures of wildtype and several mutant polymerases have been identified (Ferrer-Orta et al., 2004; Agudo et al., 2010; Ferrer-Orta, Ferrero, et al., 2015; Ferrer-Orta, de la Higuera, et al., 2015). These structures have also aided in our understanding of the catalytic domains and the key RNA binding domains, and identified the minimum requirement for nucleotide binding in the polymerase RNA binding site (6 nucleotides).

The model of FMDV serotype C WT 3D^{pol}, as shown in Fig 3.2, has the different motifs outlined. FMDV 3D^{pol} has the standard 'right-hand' structure similar to other template-dependent nucleic acid polymerases (Steitz, 1998). The catalytic domain of the polymerase is located in conserved motif C in the 'palm' region of the structure highlighted in green in Fig. 3.2. The main catalytic residues are two aspartic acid residues located at amino acid positions 388 and 389. These residues have been well characterised as the primary catalytic site in several RNA viruses and is conserved amongst all serotypes of FMDV (Jablonski et al., 1991; Hansen et al., 1997; George et al., 2001; Carrillo et al., 2005). Changing either one or both aspartic acid residues hinders the enzymatic activity of the protein and ability to replicate the viral RNA genome.

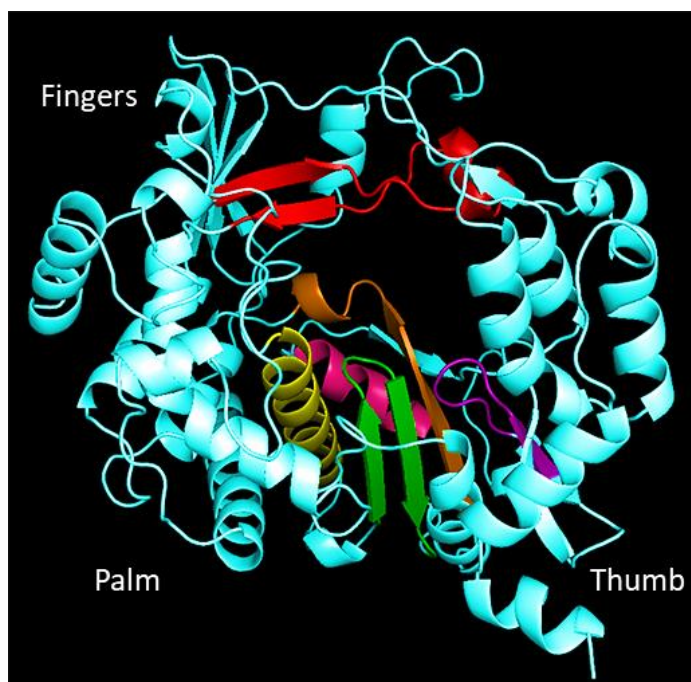


Figure 3.2 Three-dimensional model structure of FMDV 3D^{pol} produced in PyMol based on the structure of recombinant serotype C protein (PDB: 1WNE). The structure shows the protein in the standard right-hand orientation with the location of the palm, thumb and fingers highlighted. The seven conserved motifs are highlighted. Motif A (Orange), Motif B (Yellow), Motif C (Green), Motif D (Purple), Motif E (Pink) and Motif F (Red).

To identify other mutations that affected the function of 3D^{pol}, work by Herod *et al.* identified areas in the genome that could tolerate insertions by random transposon-mediated mutagenesis using an FMDV replicon (Herod *et al.*, 2015). The FMDV replicons that were developed and used have substituted the structural proteins in the P1 region with fluorescent reporter cassettes to monitor replication. These replicons are unable to form infectious virus but can still replicate once transfected into cell culture. The use of transposon-mediated mutagenesis using the FMDV replicon system has been a useful tool to identify key functional regions within viral proteins. By identifying permissive insertion sites, these regions can be further manipulated to include epitope tags for improved downstream studies such as

immunofluorescence (McMahon et al., 1998; Brune et al., 1999; Teterina et al., 2011; Remenyi et al., 2014).

The method of transposon-mediated mutagenesis was used to identify regions in FMDV serotype O 3D^{pol} that could primarily tolerate small genetic insertions but also resulted in the identification of non-permissive insertion sites within the replicon. These non-permissive sites led to the production of replication-defective replicon phenotypes by rendering the polymerase inactive (Herod et al., 2015; Herod et al., 2016). Out of nine mutations in the 3D^{pol} region that were identified, three were chosen to take forward into further studies: catalytic mutations DD388/9NN and DD240/5NN, and non-catalytic mutation GC216/7AA. These mutations were chosen to take forward in the studies as it was expected that the catalytic mutations would affect the ability for the polymerase to function as an enzyme. The phenotype of the non-catalytic mutation was as yet unknown.

Mutant DD240/5NN corresponds to a substitution of the aspartic acid residues 240 and 245 for asparagine, GC216/7AA corresponds to a substitution of glycine and cysteine residues in positions 216 and 217 for alanine and finally DD388/9NN corresponds to a substitution of the two aspartic acid residues in positions 388 and 389 for asparagine. These mutations are represented schematically in Fig. 3.3a. The location of the mutated residues in the polymerase protein in Fig.3.3b is highlighted by differently coloured spheres.

It is important to note that the protein sequences of serotype O and serotype C FMDV 3D^{pol} are almost identical (99 % sequence identity) as highlighted in the sequence alignment in Table 3.1 below. There are four amino acid changes that differentiate

serotypes O and C, the first is located at position 68 from glutamic acid to glycine, the second at position 158 from valine to alanine, the third is at position 170 from leucine to methionine, and the fourth is located at position 294 from glycine to glutamic acid. The amino acids that have been mutated in serotype O (as a result of the transposon mutagenesis studies) are the same as those found in serotype C.

Protein sequence alignment of FMDV 3D ^{pol} serotype O and serotype C	
Serotype-O	GLIVDTRDVEERVHVMRKTKLAPTVAHGVEFNPEFGPAALSNKDPRLNEGCVLDEVIFSKH
Serotype-C	GLIVDTRDVEERVHVMRKTKLAPTVAHGVEFNPEFGPAALSNKDPRLNEGCVLDEVIFSKH

Serotype-O	KGDTKMSEEDKALFRRCAADYASRLHSLVGTANAPLSIYEAIKGVDGLDAMEPDTAPGLP
Serotype-C	KGDTKMSAEDKALFRRCAADYASRLHSLVGTANAPLSIYEAIKGVDGLDAMEPDTAPGLP

Serotype-O	WALQGKRRGALIDFENGTVGPEVEEAALKLMEKREYKFCQTFKDEIRPLEKVRAGKTRI
Serotype-C	WALQGKRRGALIDFENGTVGPEVEEAALKLMEKREYKFCQTFKDEIRPMEKVRAGKTRI

Serotype-O	VDVLPVEHILYTRMMIGRFCAQMHSNNGPQIGSAVGCNPDVDWQRFGTHFAQYRNVWDVD
Serotype-C	VDVLPVEHILYTRMMIGRFCAQMHSNNGPQIGSAVGCNPDVDWQRFGTHFAQYRNVWDVD

Serotype-O	YSAFDANHCSDAMNIMFEEVFRTEFGFHPNAEWILKTLVNTEHAYENKRITVGGMPSGC
Serotype-C	YSAFDANHCSDAMNIMFEEVFRTEFGFHPNAEWILKTLVNTEHAYENKRITVEGGMPSGC

Serotype-O	SATSIINTILNNIYVLYALRRHYEGVELDTYTMISYGDIVVASDYDLDFEALKPHFKSL
Serotype-C	SATSIINTILNNIYVLYALRRHYEGVELDTYTMISYGDIVVASDYDLDFEALKPHFKSL

Serotype-O	GQTITPADKSDKGFVLGHSITDVTFLKRHFHMDYGTGFYKPVMSKTLAAILS FARRGTI
Serotype-C	GQTITPADKSDKGFVLGHSITDVTFLKRHFHMDYGTGFYKPVMSKTLAAILS FARRGTI

Serotype-O	QEKLISVAGLAVHSGPDEYRRLFEPFQGLFEIPSYRSLYLRWVNAVCGDA-----
Serotype-C	QEKLISVAGLAVHSGPDEYRRLFEPFQGLFEIPSYRSLYLRWVNAVCGDAAAALEHHHHH

Serotype-O	-
Serotype-C	H

Table 3.1 Comparison of the protein sequence alignment of FMDV 3D^{pol} serotypes O and C. Nucleotides that were mutated are highlighted in blue, yellow and green. (Carrillo et al., 2005; Ferrer-Orta, Arias, Escarmís, et al., 2006)

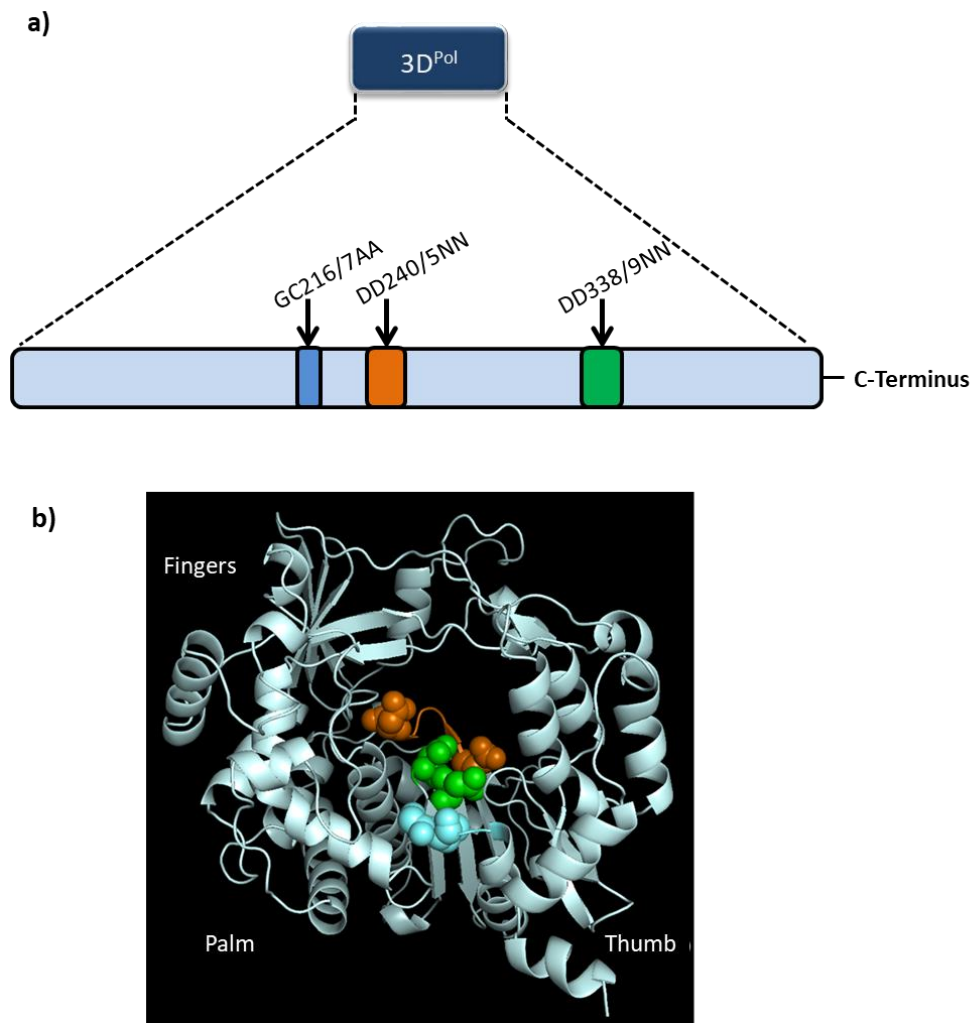


Figure 3.3 Schematic outlining the location of the mutations identified in 3D^{pol}. A) Schematic of the location of the 3D^{pol} mutations, in context of the replicon in which the mutations were initially introduced by transposon mutagenesis. Non-catalytic mutation GC216/7AA is shown in blue, and catalytic mutations DD240/5NN in orange and DD338/9NN in green. B) Shows the locations of the three mutations in context of the recombinant serotype C WT his-3D^{pol} model based on protein sequence with the individual residues highlighted in coloured spheres (produced in PyMol, PDB: 1WNE).

The mutations are located in three different regions of the polymerase molecule. DD240/5NN, in motif A, is categorised as a catalytic mutation as the residues that have been changed are located in the region that interacts with the magnesium ion necessary and integral for enzymatic function of 3D^{pol} during replication (Jablonski et al., 1991; Ferrer-Orta, Ferrero, et al., 2015; Herod et al., 2016).

The DD388/9NN mutation located in the enzymatic active site in motif C, was used as a standard negative control as the phenotypic profile of this type of mutation in these key catalytic residues has been previously defined both in FMDV and in many different viruses such as HCV, PV, EMCV and HIV (Jablonski et al., 1991; Hansen et al., 1997; Krieger et al., 2001; Carrillo et al., 2005; Ferrer-Orta, Ferrero, et al., 2015). In the literature this mutation is commonly termed GNN, or GND when only one aspartic acid residue is substituted for asparagine.

The location of the non-catalytic GC216/7AA mutation is at the double-stranded RNA exit site (Ferrer-Orta et al., 2004; Ferrer-Orta et al., 2007; Ferrer-Orta, Ferrero, et al., 2015) (highlighted in blue spheres in Fig. 3.3b).

3.3 Purification and validation of mutant 3D^{pol}

These mutations (DD388/9NN, GC216/7AA, and DD240/5NN) were introduced into recombinant serotype C his-tagged 3D^{pol} constructs (kind gift from Esteban Domingo, Madrid). The protein was purified by affinity chromatography alongside WT his-3D^{pol} as described in section 2.9. Mutants DD240/5NN and GC216/7AA expressed well (Fig. 3.4a). Purity was assessed by SDS-PAGE followed by Coomassie staining and Western blot (Fig 3.4) using antibodies specific to 3D^{pol} or the his-tag as described in section 2.4. All of the proteins migrated as single species, around the expected molecular mass of the WT protein (54 kDa). There was, however, a clear difference in migration of one of the mutant proteins; DD388/9NN migrated quicker than WT.

To investigate this further, samples of each protein were subjected to analysis by denaturing mass spectroscopy. Samples were dialysed into Tris-NaCl buffer 4 (pH 8) at 50 μ M (section 2.1) by spin column buffer exchange. The LC-MS analysis was performed by James Ault (University of Leeds) and allows comparison of theoretical and measured masses of each protein (Fig. 3.5a-d).

It can be seen that all four mutants have very similar masses within the 54 kDa range, which is close to the expected mass derived from protein sequence, suggesting that there are no additional mutations (Table 3.2). The error range present as part of the measured mass (Table 3.2) was due to the method of mass calculation from the data produced from the spectra. It is possible that there are changes in the local environment of the mutation as a result of two adjacent amino acid changes that result in the slower migration of DD388/9NN by SDS-PAGE.

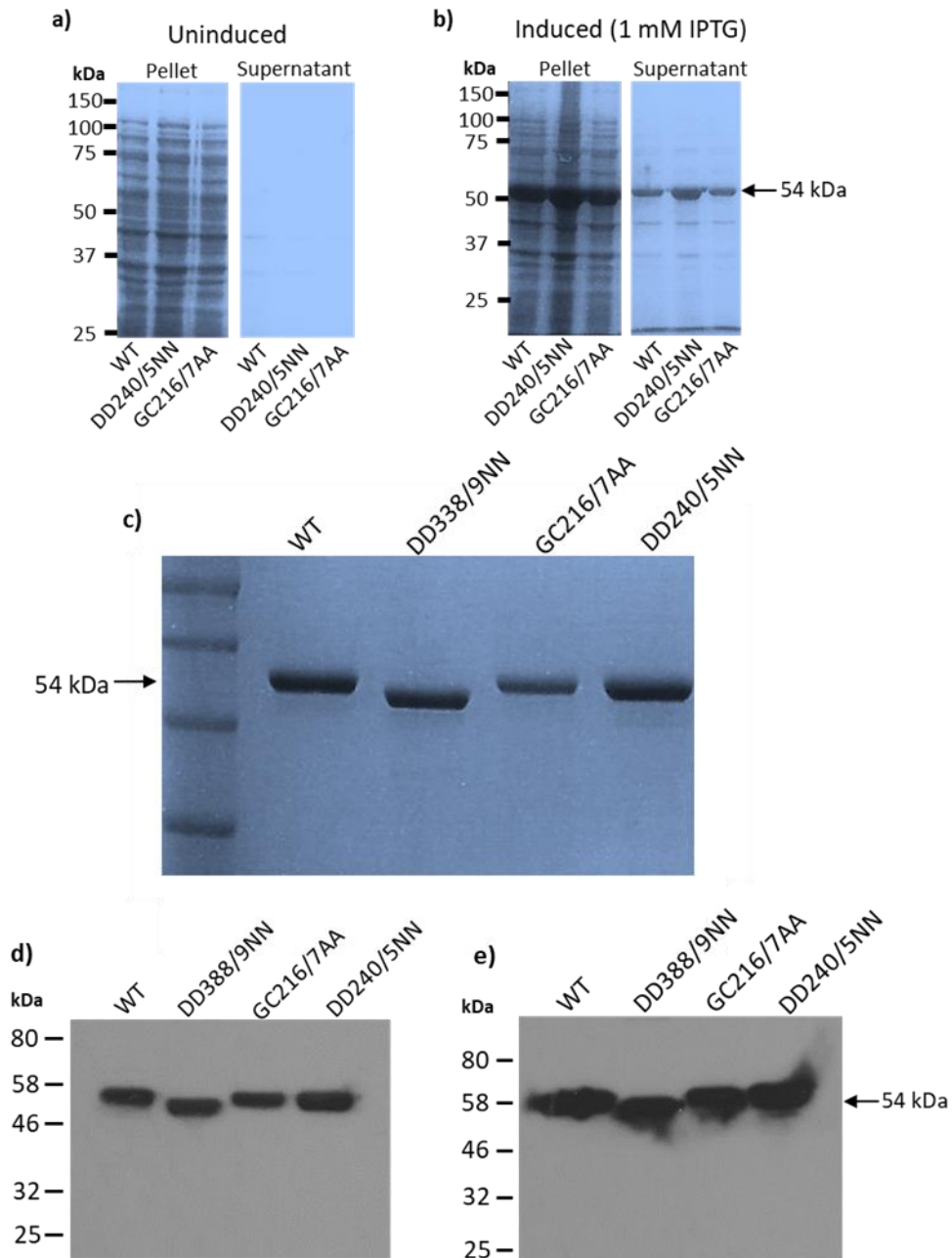
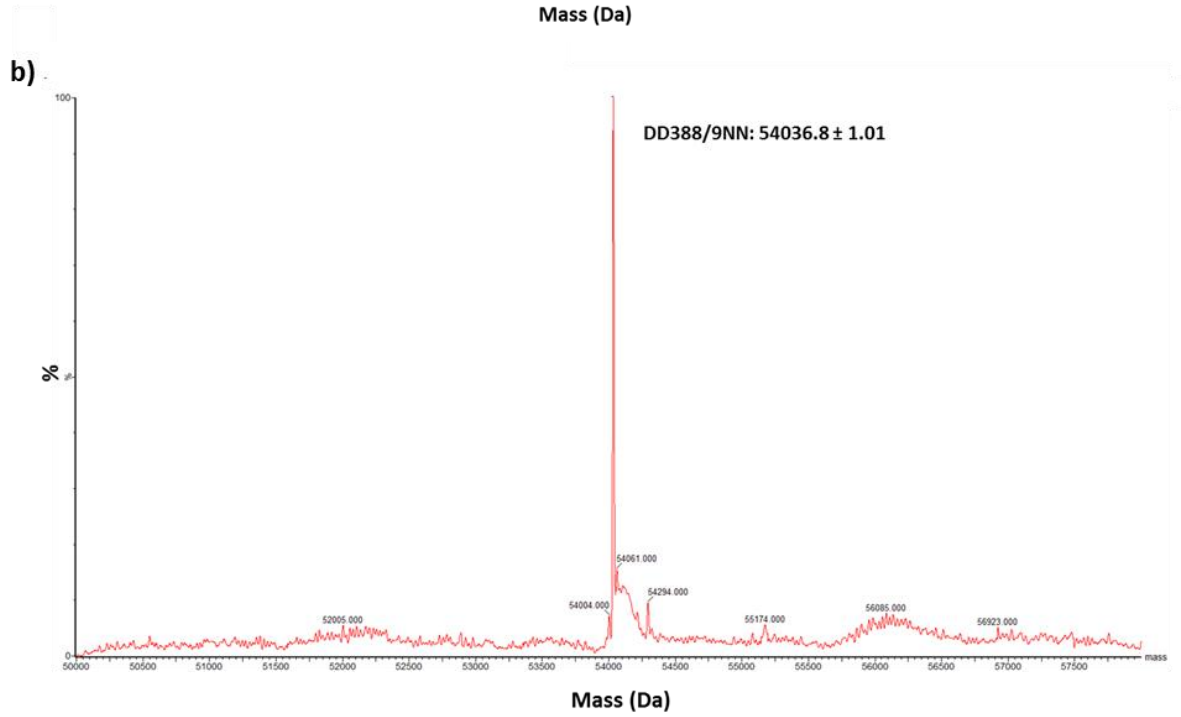
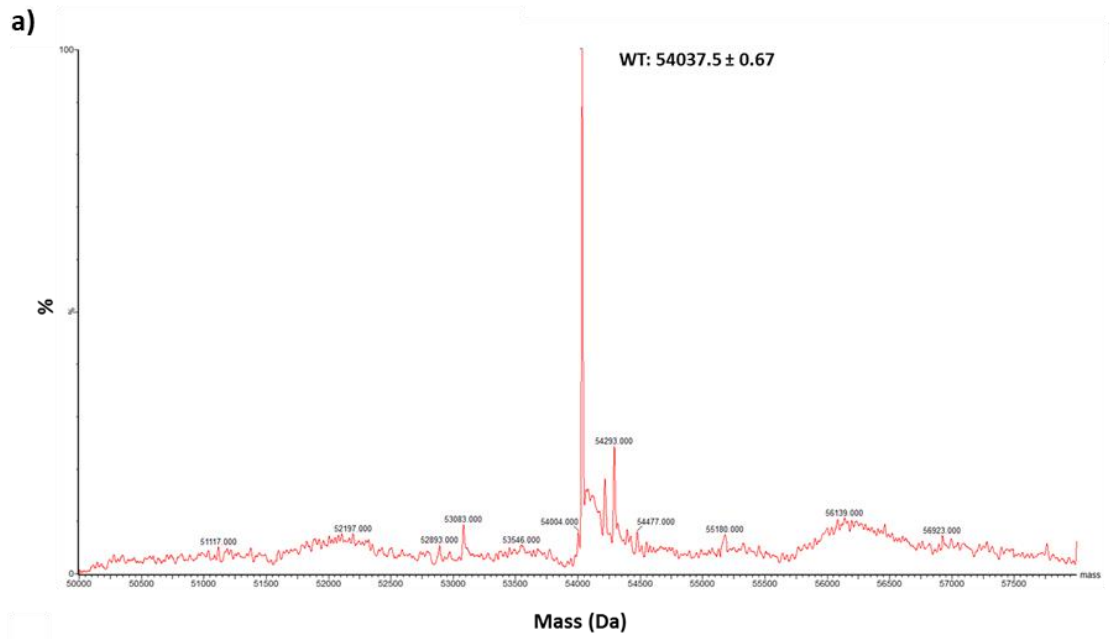


Figure 3.4 Purification of serotype C his-3D^{pol} recombinant proteins. A) Coomassie staining of denaturing SDS-PAGE of uninduced bacterial cell pellet and supernatant during protein expression after 3 hours of incubation at 37°C. B) Coomassie staining of denaturing SDS-PAGE of bacterial cell pellet and supernatant induced with 1 mM IPTG for 4 hours at 37°C during protein expression. C) Coomassie staining of denaturing SDS-PAGE of his-trap affinity chromatography purified hexahistidine-tagged 3D^{pol} recombinant proteins. D) Western blot of purified his-3D^{pol} probed with polyclonal anti-3D (397) primary antibody. E) Western blot of purified his-3D^{pol} probed with monoclonal anti-histidine (HRP) primary antibody.

One explanation for proteins migrating differently than expected can be due to charge differences. However, in this case, both of the 3D^{pol} mutant proteins included DD to NN mutations (DD388/9NN and DD240/5NN) and only the latter migrated the same as WT.

Mutant	Theoretical Mass (Da)	Measured Mass (Da)
WT	54036	54037.5 ± 0.67
DD388/9NN	54034	54036.8 ± 1.01
GC216/7AA	54018	54022.0 ± 7.98
DD240/5NN	54034	54032.8 ± 0.87

Table 3.2 Comparison of theoretical and measured masses of his-3D^{pol} recombinant WT and mutant proteins.



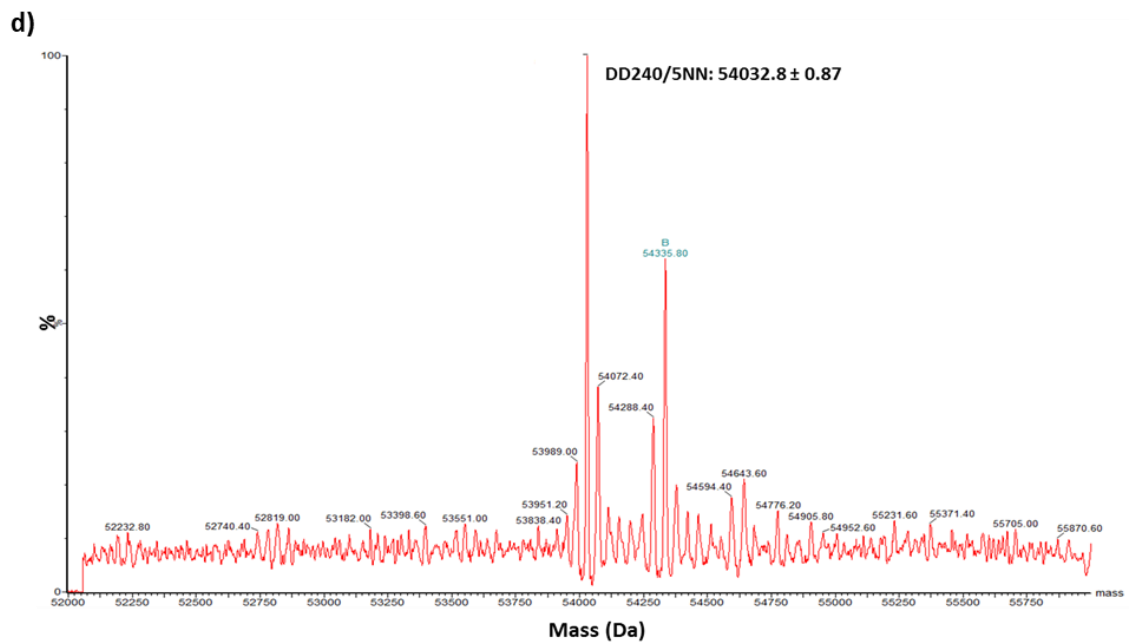
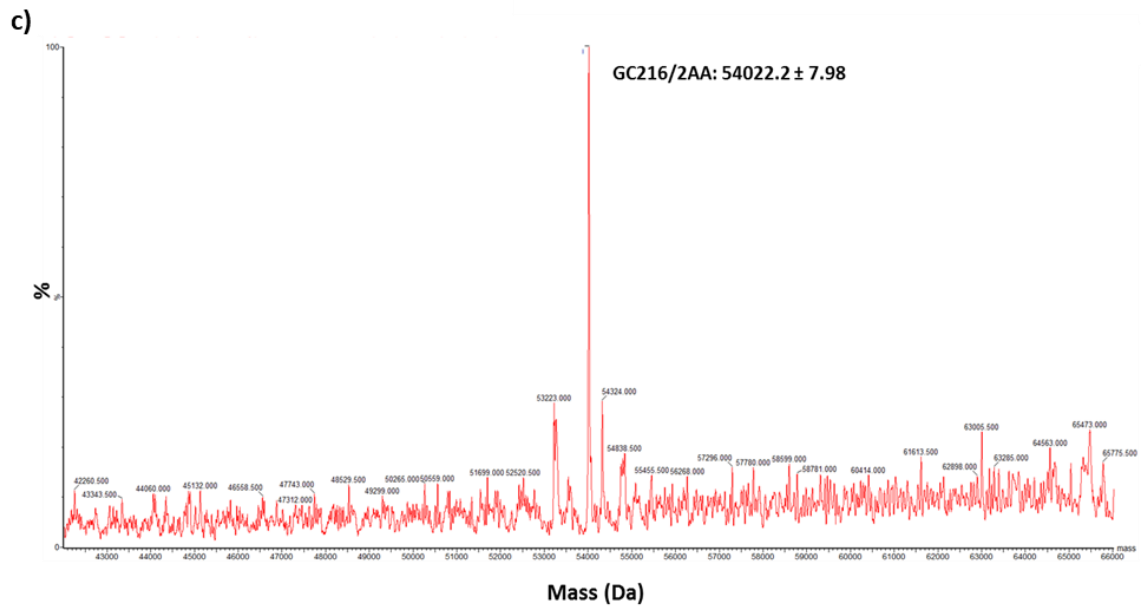


Figure 3.5 Mass spectroscopy analysis of his-3D^{pol} recombinant protein. A) WT his-3D^{pol} LC-MS spectrum. B) his-3D^{pol} DD388/9NN mutant LC-MS spectrum. C) his-3D^{pol} GC216/7AA mutant LC-MS spectrum. D) his-3D^{pol} DD240/5NN mutant LC-MS spectrum.

3.4 Assessing activity of mutant 3D^{pol}

3.4.1 Incorporation of radiolabelled UTP

The phenotypes of the different polymerase mutants were verified using an established polymerase activity (elongation) assay following a protocol originally defined in Bentham et al., 2012, and detailed in section 2.10. The activity of 3D^{pol} was assessed by the ability of the enzyme to incorporate [α -³²P] UTP into a growing strand of RNA, or as part of a larger protein-RNA complex.

The assay utilised 3D^{pol} combined with a poly-A template and an oligo-d(T) primer. This was supplemented with a 5:1 ratio of UTP to [α -³²P] UTP and incubated at 30°C as detailed in section 2.10.1. Polymerase activity was measured by dot-blot and subsequent scintillation counts per minute (CPM) (Fig.3.6a, b). Increased intensity of the signal developed from the dot-blot correspond with higher scintillation counts. Incorporation of radiolabelled [α -³²P] UTP by the polymerase was unable to occur if one or more of the RNA constituents was missing, as shown through the use of controls that had either the template, the primer, or the UTP removed (Fig. 3.6a). These controls had similar intensities on the dot-blot to the control containing no protein (-3D^{pol}), with the exception of the control containing no UTP which showed no dot-blot intensity. Catalytic mutations DD240/245NN and DD388/9NN also showed similar reduced levels of intensity as those of the controls (Fig. 3.6a). It is interesting to note that the intensity of [α -³²P] UTP incorporation of GC216/7AA appears to be greater than that of WT at both 10 and 30 minutes incubation, however

due to the level of 'bleed', it was difficult to determine the difference in intensity and in scintillation CPM accurately (Fig. 3.6a, b).

Normalised scintillation counts quantifying the dot-blot samples incubated for 30 minutes (Fig. 3.6b) show a greater than 10-fold decrease in CPM of the catalytic mutants when compared to the wildtype ($96.7 \pm 0.6 \%$ and $97.8 \pm 1.1 \%$ respectively for DD388/9NN and DD240/5NN). The non-catalytic mutation GC216/7AA is able to incorporate [α - 32 P] UTP to increased levels of efficiency to wildtype ($106.6 \pm 57.7 \%$) (Fig. 3.6a, c). However, the difference in scintillation CPM between WT and GC216/7AA are not statistically significant. Once again, it is difficult to accurately determine this difference due to the level of 'bleed'.

In order to ascertain the difference in [α - 32 P] UTP intensity by dot-blot, a time course of WT and the three different mutants was undertaken (Fig. 3.6c). The time course confirmed the initial study (Fig. 3.6a) that the catalytic mutants DD240/5NN and DD388/9NN did not appear to be able to incorporate [α - 32 P] UTP, as expected. Mutant GC216/7AA was able to incorporate [α - 32 P] UTP to a comparable level to WT 3D^{pol}. The rate of incorporation was also determined by extrapolating the scintillation CPM (Fig. 3.6d). The difference in the rate of total incorporation by WT 3D^{pol} and GC216/7AA is statistically non-significant (Fig 3.6d, e), however, there is a statistically significant ($p = 0.0014$) increase in initial rate of incorporation of radiolabelled nucleotides for mutant GC216/7AA compared to WT (Fig. 3.6f). This suggests that the initial binding of the polymerase to the RNA may occur more efficiently than it does for WT.

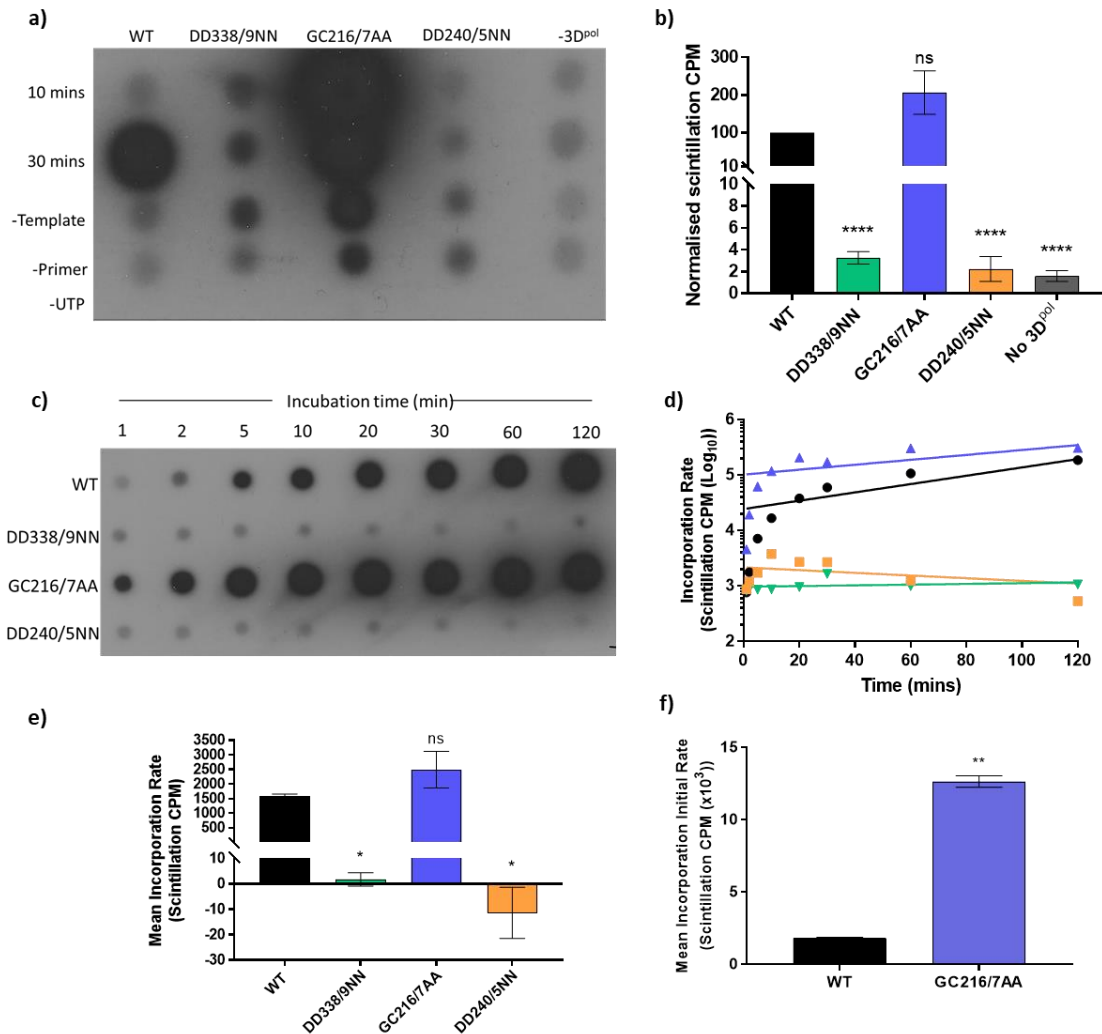


Figure 3.6 Polymerase activity assays used to determine activity of the 3D^{pol} recombinant proteins. A) Dot-blot result of an RNA incorporation assay over time including controls showing that incorporation and polymerase activity is only possible when all RNA components are available. B) Quantification of levels of incorporated radiolabelled nucleotides after 30 minutes incubation by scintillation counts per minute normalised to WT. (n=3, \pm SEM, analysed by two-tailed unpaired t-test). C) [α -³²P] UTP incorporation by different 3D^{pol} mutants over time (minutes) as detected by dot-blot. D) Linear representation of rate of incorporation of radiolabelled nucleotides by 3D^{pol} over time. E) Graph of the mean slope of the rate of incorporation (n=1 \pm SEM). F) mean slope of the initial rate of incorporation (1-10 minutes) (n=1 \pm SEM). Statistical analysis performed using two-tailed unpaired t-test; * p > 0.05, ** p > 0.01, **** p > 0.0001

All the data presented in Fig 3.6 show that WT and non-catalytic mutant GC216/7AA are able to incorporate [α -³²P] UTP. The polymerases with the mutations located in the catalytic domains (DD240/5NN and DD388/9NN) were, as expected, unable to function in this way.

The intensity of the dot-blot for the two catalytic mutants DD388/9NN and DD240/5NN are similar to the controls consisting of samples without either template, primer, or 3D^{pol} (Fig. 3.6a-c). Therefore, the catalytic mutants DD388/9NN and DD240/5NN do not appear to be able to form either protein-RNA complexes, or incorporate [α -³²P] UTP, as expected.

The RNA-protein complex could involve the formation of higher-order oligomers of 3D^{pol}, or aggregates. However, it was not possible to accurately determine the size of the protein-RNA complex that was being retained on the dot-blot filter paper.

3.4.2 Determining the structure of non-catalytic mutant GC216/7AA

The non-catalytic mutation GC216/7AA is located in the double-stranded RNA exit site region of the polymerase. A sample (5 mg/ml) of purified his-tagged 3D^{pol} GC216/7AA was prepared for x-ray crystallography. The crystal structure of GC216/7AA, was solved by Cristina Ferrer-Orta (Molecular Biology Institute of Barcelona) to a resolution of 2.8 Å (Herod et al., 2016) (Fig. 3.7a). The resulting crystal structure, co-crystallised with a 10-nucleotide RNA template-primer duplex (GCAUGGGCCC) in the RNA binding channel, showed that there is a minor change in the structure of the protein located in the loop region opposing the region of the introduced mutation (Fig. 3.6a).

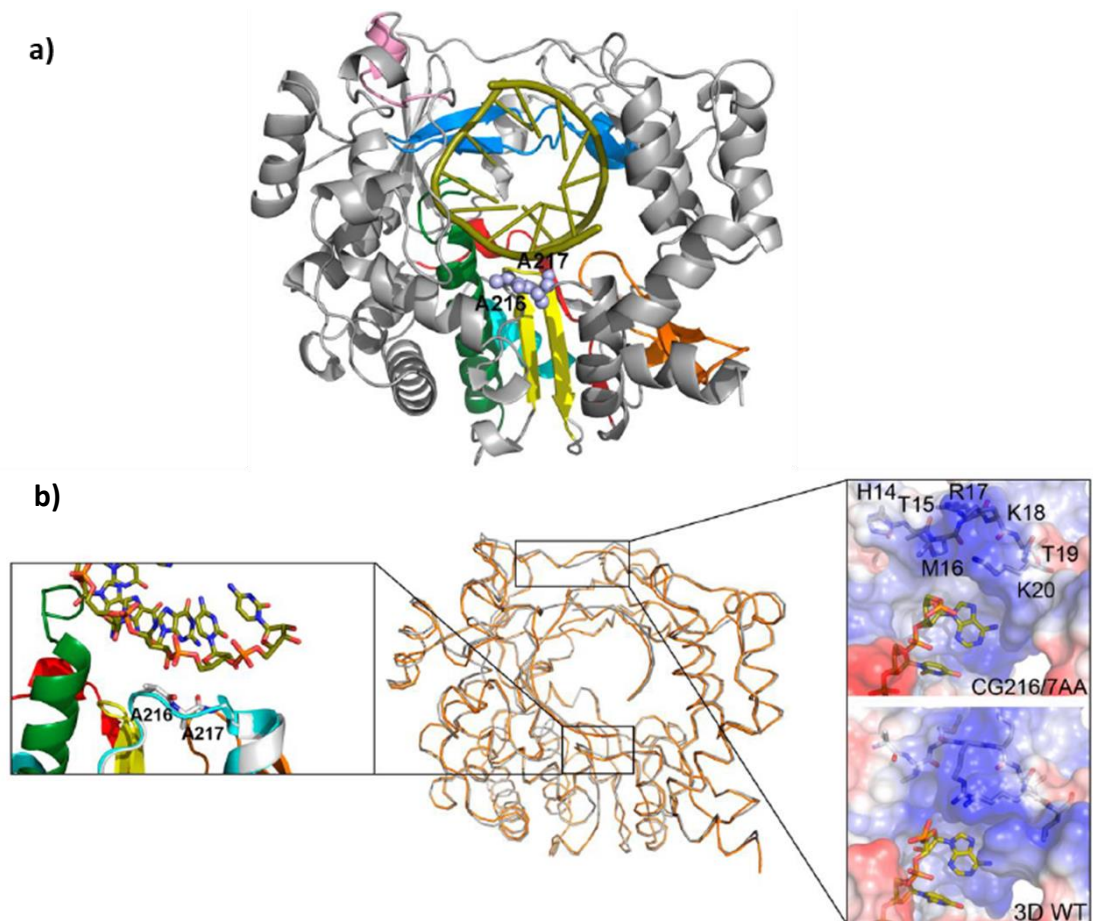


Figure 3.7 Crystal structure of mutant polymerase. A) Crystal structure of GC216/7AA non-catalytic mutant (from Herod et al., 2016) co-crystallised with 10-nucleotide RNA primer-template molecule. The mutated residues are highlighted in grey spheres. B) Centre: Superimposition of WT 3D^{pol} (orange) (PDB: 1WNE) and GC216/7AA 3D^{pol} (grey) (PDB: 5JXS) shows the minor structural changes caused as a result of the residue changes in the non-catalytic RNA exit site. Left inset: detail of mutated region at residues 216 and 217 shows no difference in structure between WT and mutant. Right inset, top: Orientation of M16-R17 region of RNA entry channel in WT 3D^{pol}. Right inset, bottom: Orientation of M16-R17 region of RNA entry channel in GC216/7AA 3D^{pol}. (Note: error in right inset, top: CG216/7AA should read GC216/7AA – figure cannot be edited to correct for the error).

The structural data shown in Fig 3.7b shows the superimposition of wildtype (orange) (PDB 1WNE) and the mutant (grey) (PDB 5JXS) polymerase structures. The structures of the mutant and WT proteins are virtually identical with a slight difference in the loop region containing residues M16 and R17 opposing the region containing the non-catalytic mutations (Fig. 3.7b top right inset) and minor changes in the region containing the GC216/7AA mutations (Fig. 3.7b left inset) (Herod et al., 2016).

The structural changes did not alter the interactions of the RNA with the polymerase at the dsRNA exit site. There was, however, a larger structural change as a result of the mutation at GC216/7AA located at the opposing RNA template entry channel (Fig. 3.7b top/bottom right inset). The segment that is altered the most is the M16-R17 region highlighted in Fig. 3.7b top right inset.

In all known WT polymerase complexes, the R17 basic side chain has been shown to interact with the template nucleotide t+2 (Ferrer-Orta et al., 2007; Ferrer-Orta et al., 2009; Ferrer-Orta, Ferrero, et al., 2015). In these complexes the t+2 nucleotide is orientated towards the active site of the polymerase with the t+1 nucleotide located at the entry of the cavity (Fig. 3.7b bottom right inset). In the GC216/7AA mutant, the M16-R17 region is orientated differently, with the basic side chain of R17 pointed towards the interior of the polymerase molecule instead of towards the polymerase active site. This reorientation has been identified before in three different mutants (3D-K20E, 3D-K18E and 3D-SSI) that affect the affinity of the polymerase with the incoming RNA template molecule and subsequent nucleotide incorporation (Agudo et al., 2010; Ferrer-Orta, de la Higuera, et al., 2015).

It was hypothesised that this mutation in the GC216/7AA that resulted in an alteration in the template RNA entry channel would decrease the ability for the polymerase to transiently bind to RNA (Herod et al., 2016). However, the data shown here supports that the mutant polymerase incorporates the radiolabelled nucleotides with increased efficiency when compared to WT. The affinity of the polymerase-RNA interaction was thus investigated.

3.4.3 Investigation into RNA binding

To address this question of protein-RNA binding affinities, a fluorescent polarisation anisotropy (FPA) assay was used. FPA measures the tumbling rate of a fluorescently labelled molecule, fluorescein- (FITC) labelled RNA (used here). The principle of FPA results in the excitation of a fluorescent molecule by polarised light. The excited fluorophore emits light whereby the degree of polarisation of the emitted light is inversely proportional to the tumbling rate of the fluorescent molecule in solution. The smaller the molecule, the higher the tumbling rate resulting in the depolarisation of the emitted light as the fluorophore reorients in solution during the lifetime of the excitation. Conversely a larger molecule, in this case where fluorescent RNA is bound to the polymerase, the tumbling rate will be slower, and thus less depolarisation of the emitted light will be detected.

The FPA assay here used FITC-labelled 13mer poly-A RNA together with the polymerases as detailed in section 2.10.3 (Fig. 3.8a, b). The K_d values of WT and GC216/7AA were 5.83 ± 0.33 and 6.75 ± 0.52 μM , respectively. The slight decrease in binding affinity seen for mutant GC216/7AA was not significant ($p > 0.063$). In contrast, the K_d values of the catalytic mutants DD240/5NN and DD388/9NN were

1.92 ± 0.17 and 3.50 ± 0.27 μM respectively. The differences in K_d value when compared to WT were highly significant (p > 0.001). The lower K_d values for the catalytic mutants would suggest that they bind the 13-mer poly-A RNA with a higher affinity.

The FPA data support the hypothesis that the mutation in the RNA exit site (GC216/7AA) results in a slight deficiency in the polymerase binding affinity. However, based on the results gleaned from the polymerase activity assay, the structural changes due to the RNA exit site mutation do not appear to affect the ability for the GC216/7AA mutant to incorporate [α -³²P] UTP (Fig. 3.6).

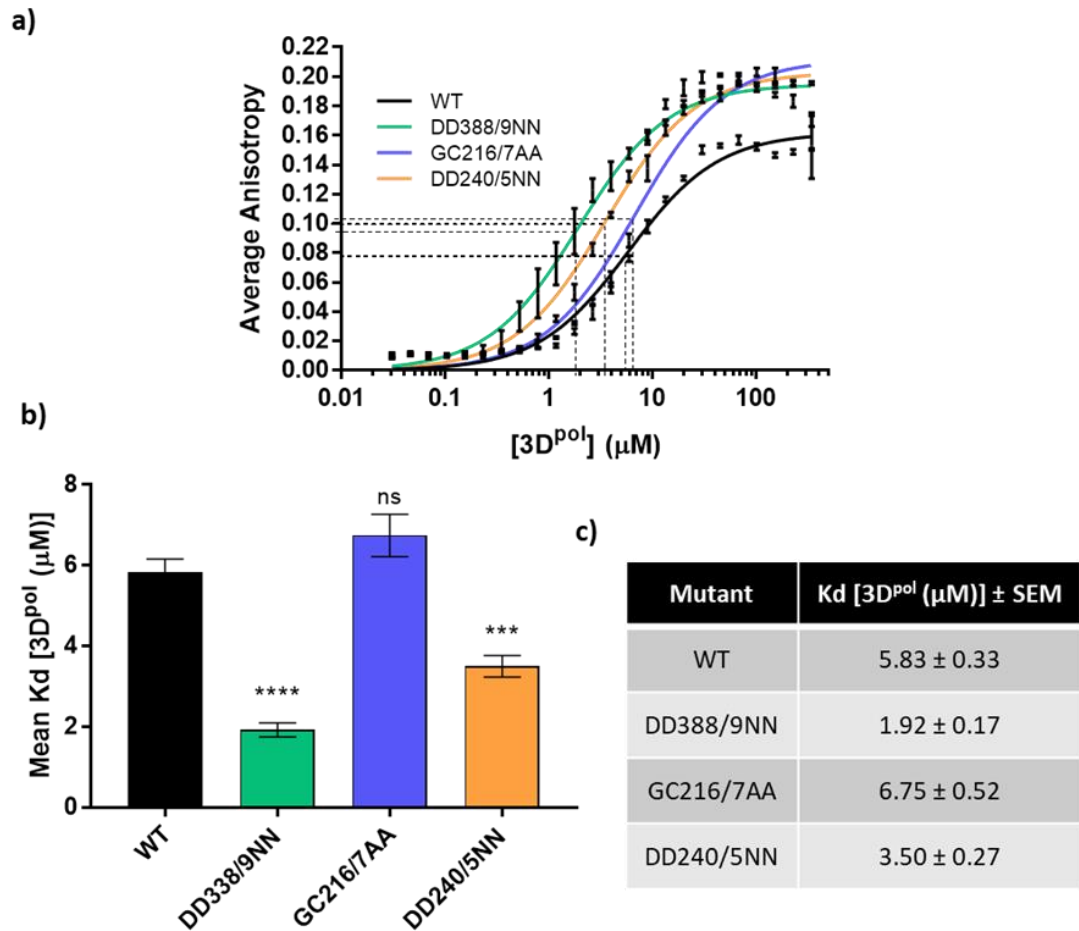


Figure 3.8 Fluorescence polarisation anisotropy assay. A) Graph showing the binding affinity of FITC-labelled 13mer poly-A RNA to each of the recombinant 3D^{pol} mutants. B) Graph showing the mean Kd values for RNA binding affinity compared to WT (n=3, ± SEM, two-tailed unpaired t-test). C) Table summarising the Kd values for each of the mutant polymerases (n=3 ± SEM). Statistical analysis performed using two-tailed unpaired t-test; *** p > 0.001, **** p > 0.0001.

3.5 Investigation into formation of higher-order complexes

Extensive studies on PV polymerase, and previous work on FMDV polymerase, outlined in Bentham et al., 2012, showed that catalytically active polymerase molecules were able to form higher-order lattice or helical structures (Arnold et al., 1999; Lyle et al., 2002; Spagnolo et al., 2010; Tellez et al., 2011; Wang et al., 2013). In the case of PV, these higher-order structures could form *de novo* without the addition of RNA primer-templates (Arnold et al., 1999). In contrast, studies on the oligomerisation of FMDV 3D^{pol} have shown that higher-order structures could only form in the presence of RNA primer-template (Bentham et al., 2012).

The concept of oligomerization of the polymerase molecules and the binding of the RNA to the protein has been shown biochemically to be highly co-operative; multiple molecules interact to facilitate the efficient replication of the viral RNA. Oligomerisation of replication-associated proteins, such as the polymerase, could feature as a functional control by providing stability and protecting the RNA from degradation and denaturation (Ferrer-Orta, Ferrero, et al., 2015). Dimers and higher-order oligomers of polymerase molecules have been reported in a number of positive-strand RNA viruses (Hansen et al., 1997; Luo et al., 2000; Lyle et al., 2002; Hogbom et al., 2009; Chinnaswamy et al., 2010; Spagnolo et al., 2010). In PV in particular, the ability for the polymerase molecules to oligomerise into a planar lattice provides an attractive model for the formation of membrane-associated replication complexes especially when such models suggest the interaction of PV 3D^{pol} with membrane-associated viral precursor protein 3AB and host-cell factors

including phosphoinositides such as phosphatidylinositol-4-phosphate (Lama et al., 1994; Lyle, Clewell, et al., 2002; Lyle, Bullitt, et al., 2002; Hsu et al., 2010). These studies have also shown that PV 3D^{pol} planar lattices are able to fold into helical arrays, termed fibrils (Lyle, Bullitt, et al., 2002; Wang et al., 2013).

Previous work on FMDV polymerase struggled to consistently identify fibril formation by transmission electron microscopy (TEM). It was believed that this was the case due to the transient nature of the fibril formation during the assay. In order to form a more stable and permanent protein-RNA fibril complex, glutaraldehyde, a potent crosslinking agent was added to the assay described here (see also section 2.10.2). Additionally, the inclusion of a crosslinking reagent could allow for the confirmation and resolution of higher-order structure formation by SDS-PAGE.

Purified his-tagged 3D^{pol} (WT and mutants) were incubated at 30°C for up to 2 hours with glutaraldehyde and the RNA template-primer used for the aforementioned activity assay (section 3.4.1). Initially, to characterise 3D^{pol} oligomerisation, non-radiolabelled UTP nucleotide was used. Samples were taken at increasing timepoints, from 1 to 120 minutes, and the reactions were stopped by adding SDS-PAGE 2x Laemmli buffer loading dye as outlined in Chapter 2 (section 2.10.2). The samples were resolved by gradient SDS-PAGE and analysed by Western blot using antibodies either against the hexa-histidine tag or against 3D^{pol} (Fig. 3.9).

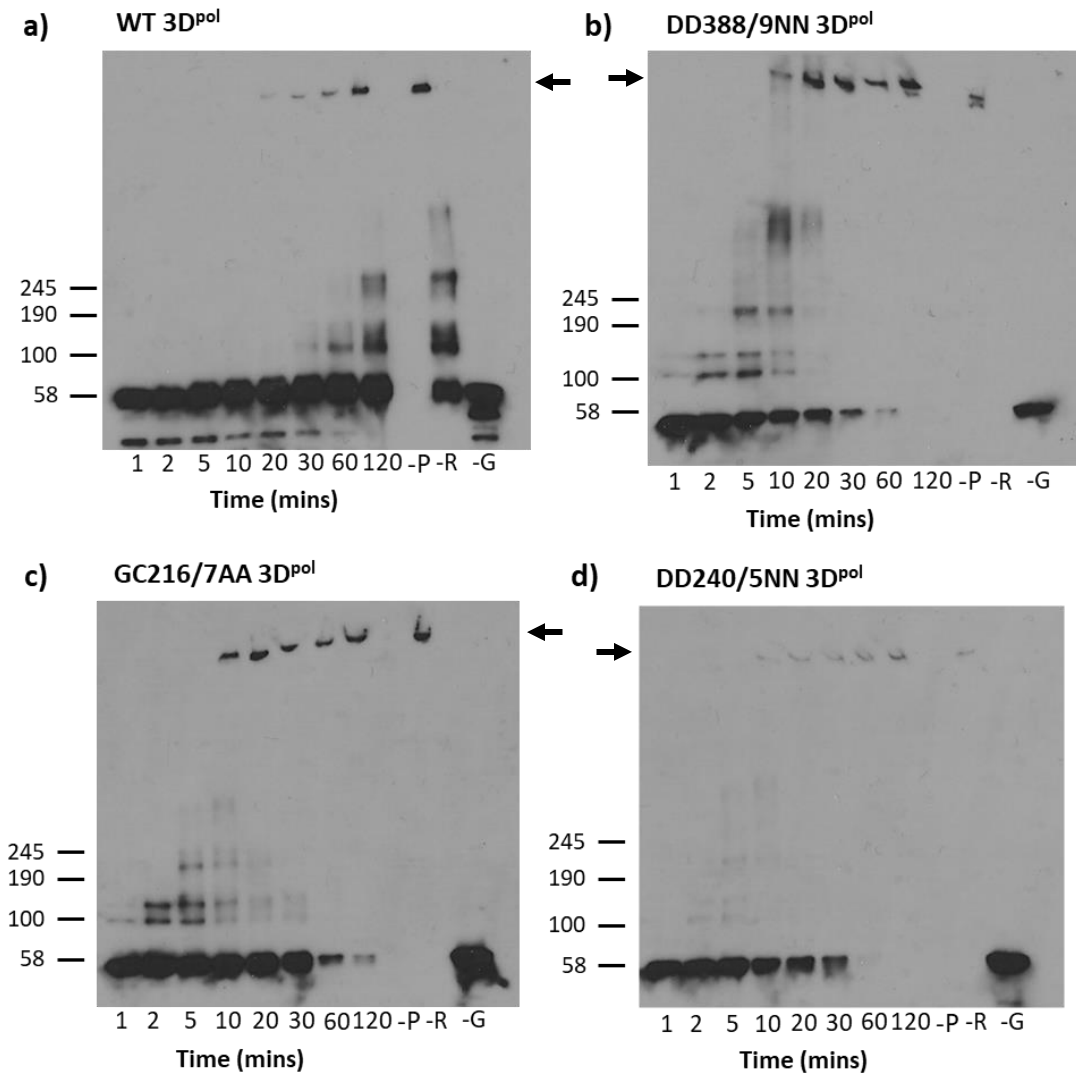


Figure 3.9 Glutaraldehyde crosslinking assay showing the formation of higher-order oligomers by Western blot on denaturing SDS-PAGE gels from a polymerase activity assay (section 2.10.2). A) WT polymerase, B) DD388/9NN, C) GC216/7AA and D) DD240/5NN. Controls include no protein (-P), no RNA (-R) and no glutaraldehyde (-G) all incubated for 30 minutes at room temperature. Arrows denote hypothesised higher-order species. The Western blot was probed with anti-his antibody at the dilution stated in section 2.4.

The SDS-PAGE and subsequent Western blot analysis of the crosslinked protein-RNA complexes showed the gradual increase in oligomer formation over time for WT 3D^{pol} (Fig. 3.9a) before appearing to form oligomers too large to migrate through the gel. Figures 3.9b-d show the resolved crosslinked protein-RNA complexes of the mutant polymerases. It is clear to see that the development of oligomers over time differs slightly to that seen in WT 3D^{pol}. While WT shows a gradual increase over time, the mutants all appear to show oligomer formation during the early timepoints (1-20 minutes) before the complexes became too large to migrate through the gel. However, it is important to note that the rate of UTP incorporation and subsequent oligomer formation was not different between mutants as shown in figures 3.6c and 3.6d. Reactions containing no RNA (template, primer, or nucleotides), no 3D^{pol} and no glutaraldehyde were included as controls. It is interesting to note that WT 3D^{pol} that was incubated without any RNA also appeared to form oligomers after 30 minutes of incubation.

To confirm that the bands of increasing size seen in each polymerase corresponded to the formation of higher-order fibril structures, samples were taken at 30 minutes and the reactions stopped by the addition of 2 % uranyl acetate when the samples were loaded onto carbon-coated copper TEM grids. The grids were analysed under standard TEM by negative stain (Fig. 3.10).

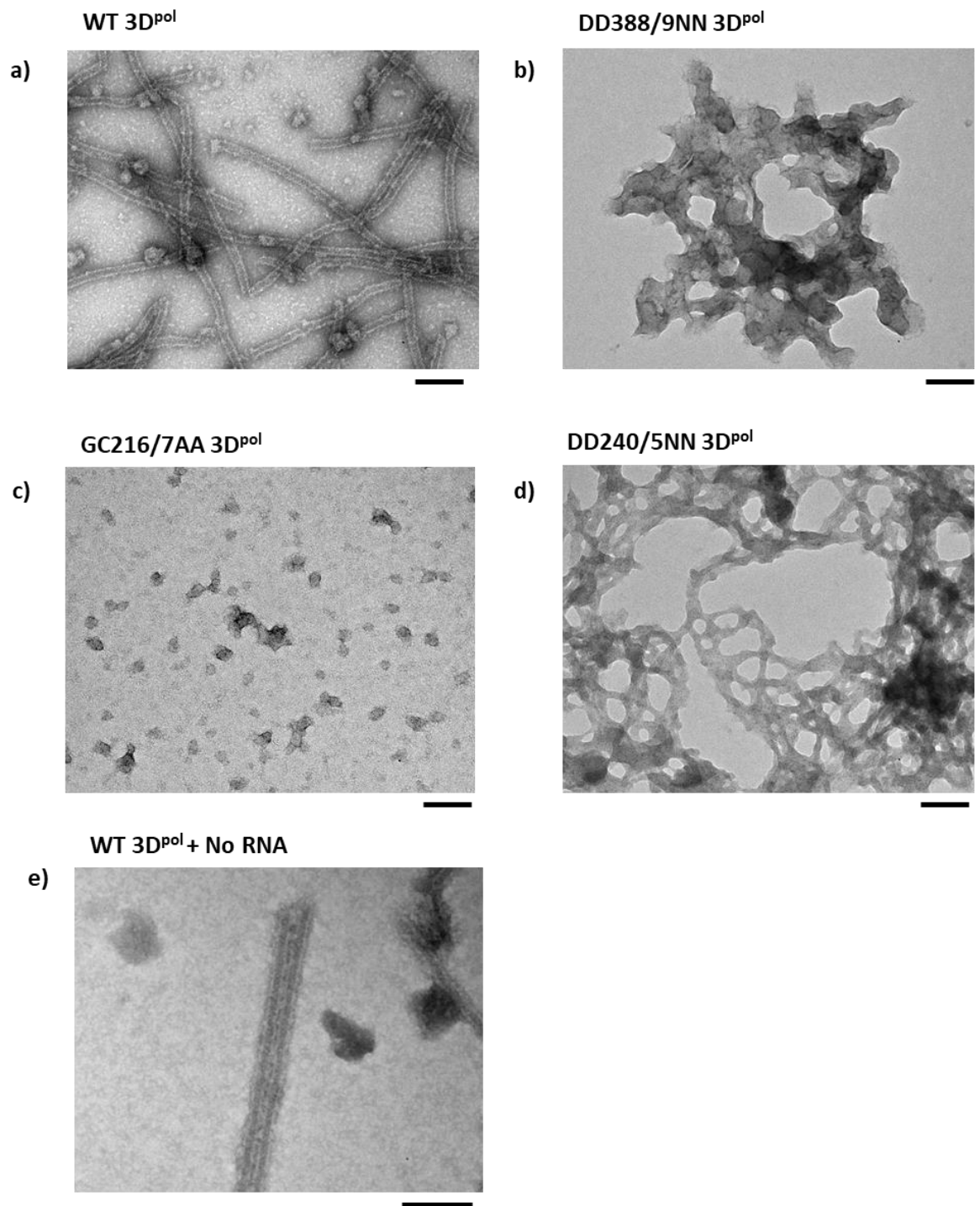


Figure 3.10 Negative stain TEM of crosslinked polymerase activity assay after 30-minute incubation. A) WT 3D^{pol} forms visible fibril formations when incubated with RNA template-primer, B) DD388/9NN, C) DD240/5NN and D) GC216/7AA mutant polymerases do not show any distinct fibril structure formation but protein aggregates. E) WT 3D^{pol} incubated without RNA. Scale bar 100 nm.

Negative stain analysis by TEM showed that WT 3D^{pol} was able to form higher-order fibrillar structures when RNA primer-template and free nucleotides were present (Fig 3.10a). These structures were similar to previous FMDV 3D^{pol} fibrils (produced in the absence of glutaraldehyde) (Bentham et al., 2012). The mutant polymerases were therefore investigated in a similar assay (Fig. 3.10b-d). After 30 minutes of incubation, no evidence of regular higher-order fibrillar were evident, although aggregated protein was visible.

WT 3D^{pol} glutaraldehyde crosslinked assay without any RNA (-RNA) appeared to form oligomers at 30 minutes (Fig. 3.9a). This sample was also analysed by TEM and showed that some fibrils were able to form, however, there was a marked difference in morphology, particularly in the diameter of the fibrils, and in abundance to those formed by WT 3D^{pol} in the presence of RNA (Fig. 3.10e). Early incubation timepoints were also analysed (Fig. 3.11) and revealed that WT 3D^{pol} was able to form fibrils from as early as 2 minutes.

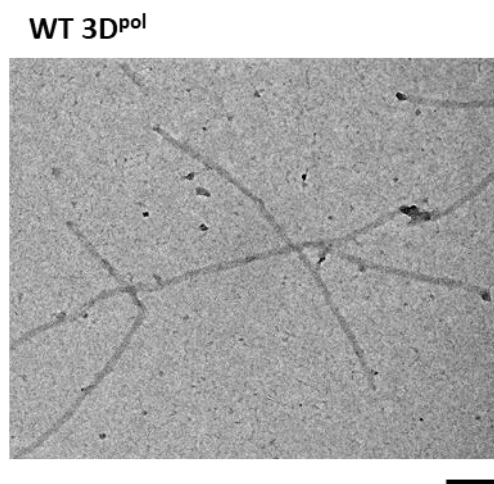


Figure 3.11 Negative stain TEM of crosslinked polymerase activity assay after 2-minute incubation of WT crosslinked 3D^{pol} with primer-template RNA. Scale bar 100 nm.

3.6 Structural determination of FMDV 3D^{pol} fibrils

It has been hypothesised through work on other RNA viruses such as PV and HCV (Hansen et al., 1997; Luo et al., 2000; Lyle, Clewell, et al., 2002; Hogbom et al., 2009; Chinnaswamy et al., 2010; Spagnolo et al., 2010) that these fibrils could reflect part of a 'replication complex'. Therefore, studies focussed on the determination of a higher resolution fibril structure.

WT 3D^{pol} fibrils were produced as detailed in section 2.10.2 and samples were prepared for cryo-EM. Samples were loaded on to carbon-coated C-flat grids and plunge-frozen in liquid ethane, after blotting for 6 seconds, using a Vitrobot (FEI). The preliminary data collection for a medium-resolution structure was undertaken at the Centre for Virus Research at the University of Glasgow with the assistance of Dr David Bhella. Using a T12 cryo-EM, 129 micrographs were taken from a single grid, from those 129, 23,700 fibril sections were used for computational helical reconstruction.

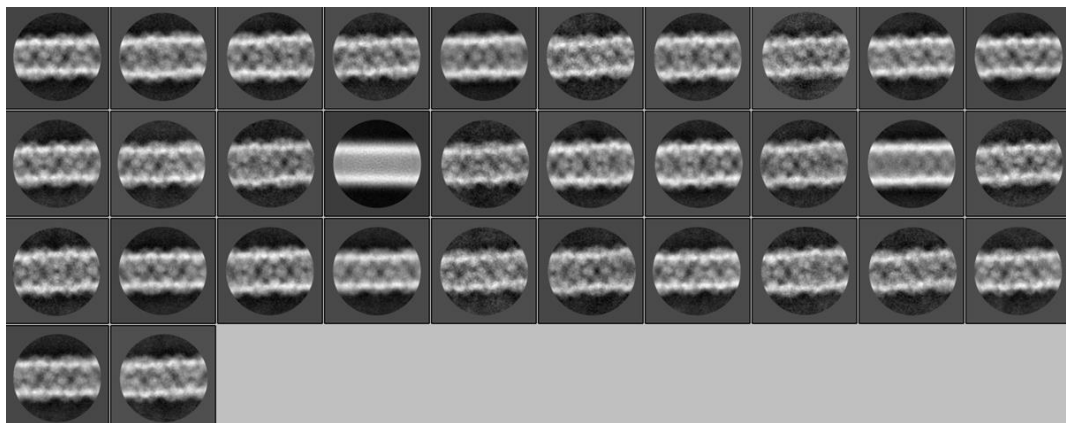


Figure 3.12 2D class averaging of fibrils detected by cryo-EM. From this class averaging of over 200 micrographs and 25,000 fibril segments. The averaging depicted here is from the narrow fibril species with a diameter of 21.6 nm.

The helical reconstruction identified two different species of fibrils of different diameters as identified by class averaging (Fig. 3.12). The narrower fibril species was calculated to have a diameter of 21.6 nm with a maximal distance between peak to peak of 10 nm, the larger fibril species had a diameter of 23.2 nm and a maximal peak-to-peak distance of 12 nm. Both fibril species had a 2-start helical assembly with D2 symmetry. From the class averages a medium-resolution (11 Å) model was determined (Fig. 3.13).

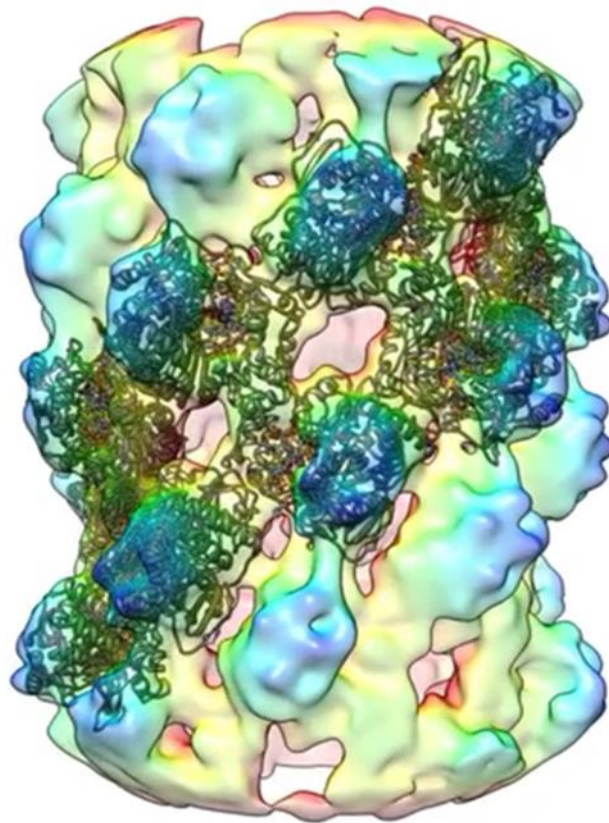


Figure 3.13 Intermediate resolution three-dimensional model fibril structure of WT fibril with docked WT 3D^{pol} crystal structure (PDB: 9EC0). The model is based on helical reconstruction of the narrow fibril species.

The 11 Å resolution model of the narrow FMDV fibrils appears to show a lattice of repeating WT 3D^{pol} dimers (Fig. 3.13). The dimers appear to be oriented in an anti-parallel formation. Using the standard right-hand orientation, the major

intermolecular interfaces appear to lie between the fingers and the thumb, and the palm in adjacent molecules and between fingers only between opposing molecules (head to tail).

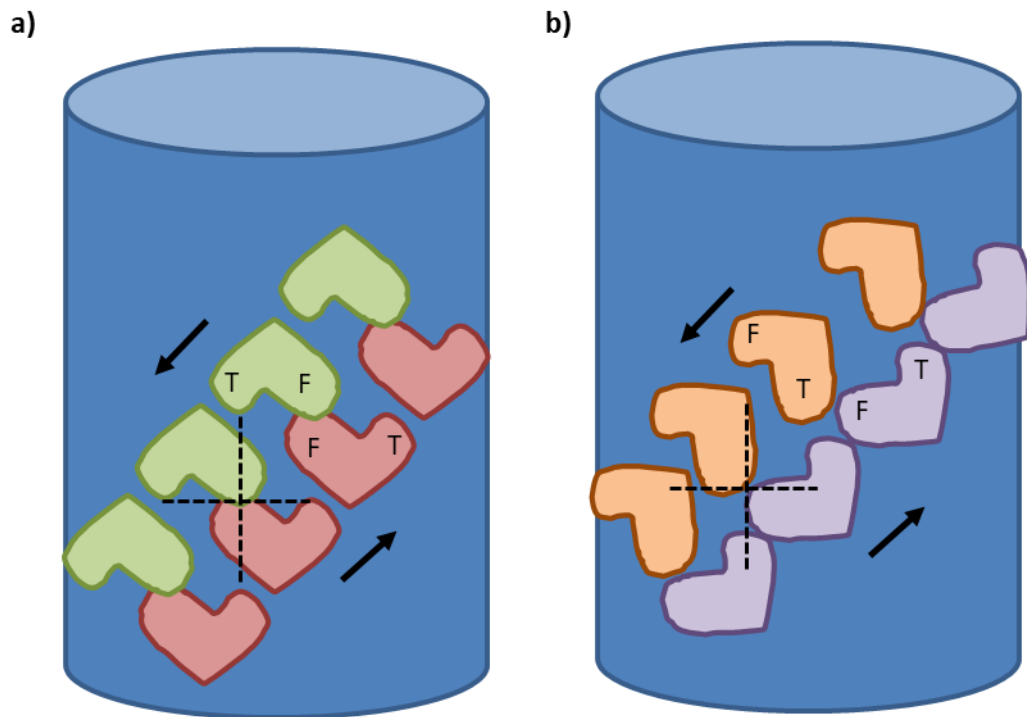


Figure 3.14 Cartoon schematic depicting the proposed arrangement of polymerase molecules. A) Arrangement of FMDV 3D^{pol} molecules forming the fibrils. B) Arrangement of PV 3D^{pol} molecules forming the fibrils (Tellez et al., 2011; Wang et al., 2013). Fingers (F) and Thumb (T) locations are detailed and the arrows (→) depict the direction the individual molecules face highlighting the antiparallel arrangement. Dotted cross placed at interacting interfaces to highlight the differences in orientation of individual molecules between FMDV and PV.

Initial analysis of hypothesised interacting residues between molecules in the fibril show that they are comparable with the PV fibril counterpart (between fingers and thumb in the antiparallel conformation, and fingers and palm between adjacent molecules) especially as both helical fibril structures appear to be formed of antiparallel interacting molecules, however where FMDV 3D^{pol} molecules appear to be mirror images, PV head-to tail dimers are oriented at 90° to each other (Fig. 3.14),

and translated 44 Å relative to the adjacent molecule as a result of the difference in size and flexibility of the helix (Hansen et al., 1997; Wang et al., 2013). PV helical polymerase lattices form a much larger (50 nm) fibril body with a 6-start helix. In PV, a model has been described whereby the RNA molecule travels through the active site which is conveniently located at the head-to-tail interface to fit with the dimer orientation, however, the orientation of the FMDV dimers suggest that the RNA template would need to weave through adjacent molecules.

In order to determine the interacting residues more definitively, and to resolve nucleic acid density, the grids that were prepared in Glasgow were transferred to Leeds, in the Astbury Biostructure Laboratory, to be analysed by the Krios I microscope with the Falcon III detector in integrating mode. Data collection was automated and collected at nominal 75K magnification, giving a sampling of 1.05Å/pixel. The calculated dose rate was 60e⁻/pixel/second resulting in a dose of 54e⁻/Å²/second. The exposure time was 2 seconds with 79 frames in total giving a final 1.4e⁻/frame. Data collection occurred at a defocus range of -1.5 to 2.8 nm. During 36 hours of automated data collection, 3100 micrographs were taken. The data was transferred back to the University of Glasgow for analysis by Dr James Streetley. Analysis is currently ongoing using the same helical reconstruction parameters developed for the medium-resolution model. After further analysis, a higher resolution structure was determined at 9 Å (Fig. 3.15).

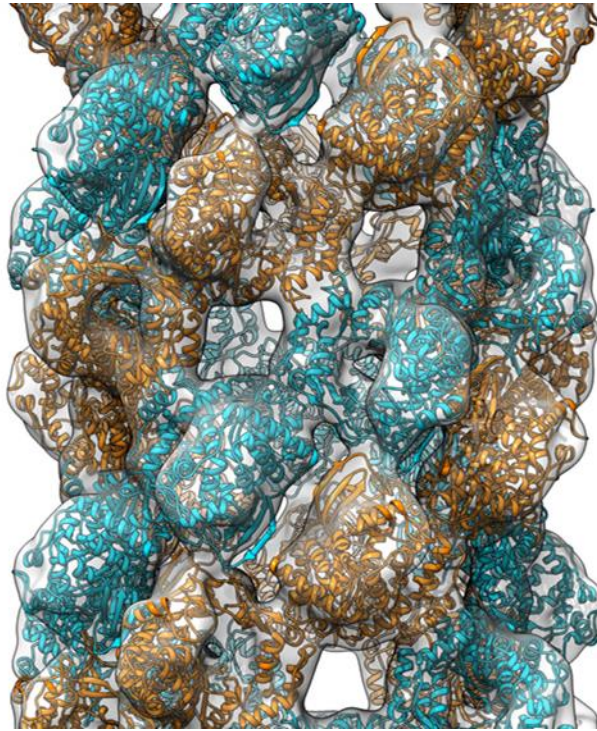


Figure 3.15 Intermediate resolution cryo-EM structure of FMDV 3D^{pol} fibrils with crystal structure of WT 3D^{pol} (PDB: 9EC0) docked into the density.

Despite this, further analysis needs to be undertaken to discern nucleic acid density, as even at higher resolution no RNA can be identified. A reason for this could lie in the level of occupancy of the RNA within the individual polymerase molecules. If only a fraction of the molecules contained RNA, their density may not be easily discernible. The current helical reconstruction data is based on the narrow fibril species. Analysis of the data for the larger fibril species is currently on-going.

3.7 The importance of RNA in the formation of fibrils

RNA appears to be necessary for the efficient formation of regular fibrils, however, the location of RNA within fibrils is under investigation. In order to determine whether higher-order complexes contained RNA, samples from a glutaraldehyde crosslinked polymerase activity assay with [α - 32 P] UTP were resolved by SDS-PAGE (Fig. 3.9). The gels were subsequently dried and autoradiographed to identify if the input RNA used in the activity assay was included within the observed higher-order oligomers forming as a result of the assay (Fig. 3.16).

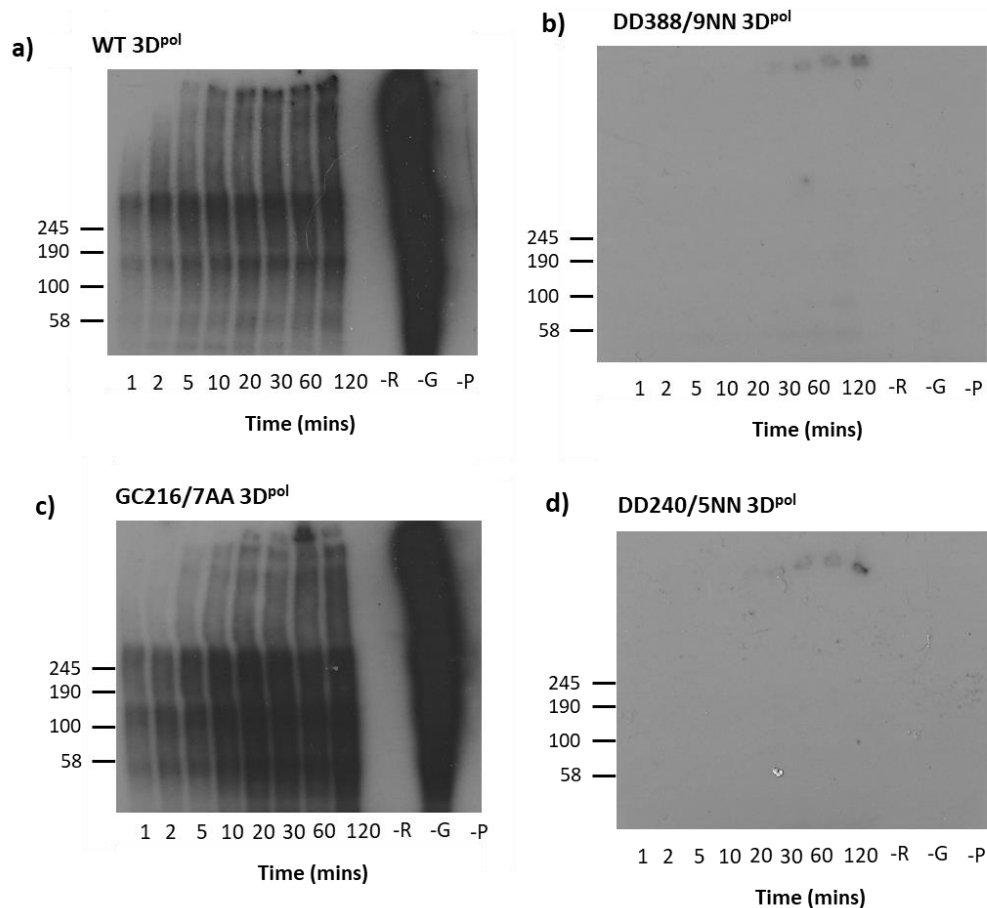


Figure 3.16 Autoradiograph of glutaraldehyde crosslinking assay showing the presence of primer-template RNA and [α - 32 P] UTP within the formation of higher-order oligomers on denaturing SDS-PAGE gels over time. A) WT, B) DD388/9NN, C) GC216/7AA, D) DD240/5NN. Controls include no RNA (-R), no glutaraldehyde (-G) and no protein (-P).

The autoradiograph detecting the radiolabelled incorporated nucleotides show bands of increasing size appearing from as early as one minute after commencing incubation for both WT 3D^{pol} and GC216/7AA 3D^{pol}. The pronounced bands appear at approximately 54 kDa, 150 kDa, and at greater than 245 kDa (Fig. 3.16a, c). Three pronounced bands of similar sizes appear in the crosslinked WT 3D^{pol} oligomeric species bands seen in the Western blot of the activity assay (Fig. 3.9a). From this data, we can infer that the higher-order species of WT and GC216/7AA identified by Western blot are likely to contain RNA.

There was no evidence of RNA in the 3D^{pol} oligomers for the catalytic mutants DD388/9NN and DD240/5NN (Fig. 3.16b, d). This is consistent with these proteins being unable to incorporate [α -³²P] UTP as seen in figures 3.6a and 3.6e, and in figures 3.9b and 3.9d.

With the evidence that RNA may be included in the oligomers, or aggregates, we sought to investigate whether the RNA is protected within the fibril helix. It is hypothesised that because PV fibrils and FMDV fibrils appear to be oriented differently in the model and structure, it may also be hypothesised that instead of the RNA running through the groove made by interactions between the different 3D^{pol} molecules as seen in PV, the RNA may be weaving in and out of neighbouring molecules in this FMDV structure. As such, the RNA may be protected by the protein as well as providing a scaffold for the polymerase to multimerise around.

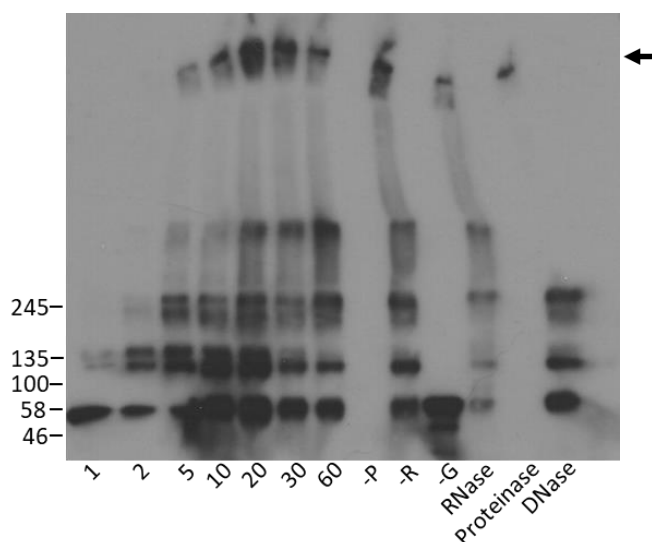


Figure 3.17 Glutaraldehyde crosslinking activity assay showing the higher-order oligomers treated with DNase I, RNase A and proteinase K. Higher-order oligomer formation of WT his-3D^{pol} analysed by Western blot on a denaturing SDS-PAGE gel. Controls include no protein (-P), no RNA (-R) and no glutaraldehyde (-G). The crosslinked samples were also treated with RNase A, proteinase K and DNase I after 30 minutes of incubation at 30°C. Arrow denote hypothesised higher-order species.

The products of a crosslinked activity assay were treated with either DNase I, RNase A, or proteinase K after incubating the assay for 30 minutes (Fig. 3.17). The data showed that there may be a minor effect on oligomer formation (by Western blot) when treated with RNase A suggesting that the RNA may not be completely protected. When treated with RNase A, the apparent quantity of higher-order species is reduced, particularly those species at very high molecular weights (highlighted by the arrow). However, these results may not be definitive as the reduction in higher-order species may also be due to an error in initial loading of the sample. When the assay containing WT 3D^{pol} and primer-template RNA components was treated with DNase I a reduction in higher-order oligomerisation was seen, suggesting that there may have been some RNase contamination of the DNase I. When treated with proteinase K, no evidence of oligomers remained, as expected.

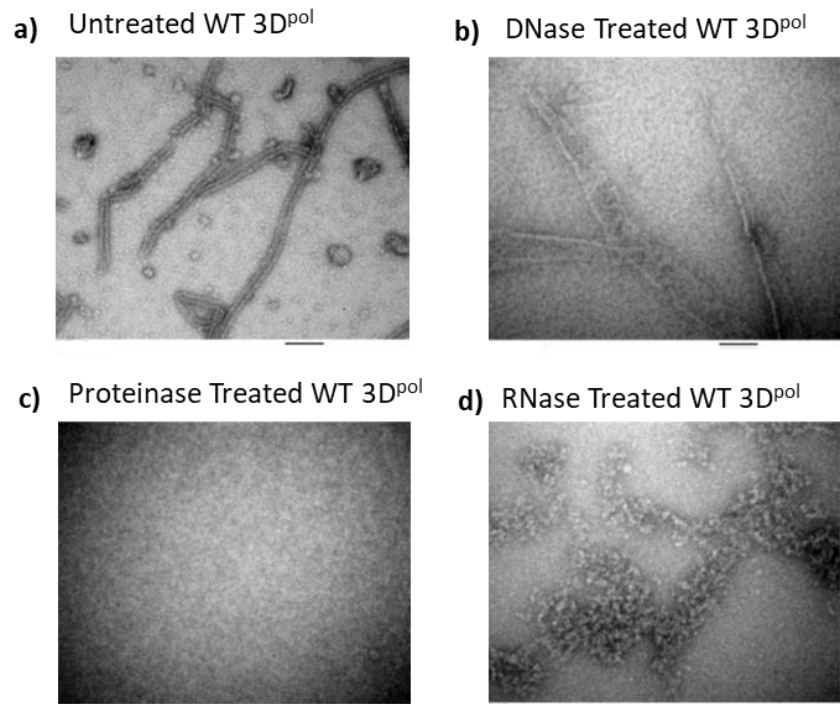


Figure 3.18 Negative stain TEM of A) his-3D^{pol} fibrils when products of a glutaraldehyde crosslinking assay were treated with B) RNase A, C) proteinase K and D) DNase I after 30 minutes of incubation. Scale bar 100 nm.

Samples of the treated crosslinked activity assay were visualised by TEM in order to directly observe the differences in fibril formation when the samples were treated with RNase A. The micrographs (Fig. 3.18) show that when treated with RNase A, no evidence of higher-order oligomers can be detected by TEM. This is consistent with previous results (in the absence of glutaraldehyde) (Bentham et al., 2012). Interestingly, treatment of the samples with DNase I appears to have a slight effect on fibrils consistent with the data in figure 3.17. Endoribonuclease RNase A was chosen as it preferentially cleaves the 3' end of unpaired C and U (pyrimidine) residues in RNA (Cuchillo et al., 2011), and can also cleave dsRNA or RNA/DNA hybrids at low salt concentrations (Myers et al., 1985). This makes it an appropriate choice for endoribonuclease as the nucleotide incorporation due to polymerase activity is of UTP.

3.8 Is 3CD a catalytically functional precursor?

3CD is a precursor of 3D^{pol} and has several documented roles in the lifecycle of FMDV. Previous data shows that 3CD contains a potential nuclear localisation signal (García-Briones et al., 2006; Sanchez-Aparicio et al., 2013). Other roles of 3CD include functioning as a potential initiator of viral replication in formation of a complex for uridylylation (Murray et al., 2003; Nayak et al., 2005; Nayak et al., 2006; Steil et al., 2009). Here, the oligomerisation of 3CD was investigated.

3C is the FMDV major protease involved in the processing of the viral polyprotein during replication of the genome (Klump et al., 1984). 3C has also been shown to be able to cleave host-cell proteins such as the translation initiation factor eIF4A and histone protein H3, as well being involved in immune evasion (Grigera et al., 1984; Belsham et al., 2000; Wang et al., 2012). 3C was used as a control in the investigation of 3CD oligomerisation alongside 3D^{pol}.

To determine these potential functions, samples of recombinant his-tagged 3C and 3CD were purified (plasmids were kind gifts from Stephen Curry, Imperial College, London and Esteban Domingo, Madrid) as described in chapter 2. The optimisation of the purification of his-3CD was undertaken by Sue Matthews, University of Leeds. Optimisation of his-3C purification was performed by myself and experimental results were obtained by an undergraduate project student (Kate Loveday) under my supervision (Fig. 3.19). Production of purified recombinant his-3C was undertaken in order to assess whether the function of 3CD could be recapitulated by incubating 3C and 3D^{pol} concurrently.

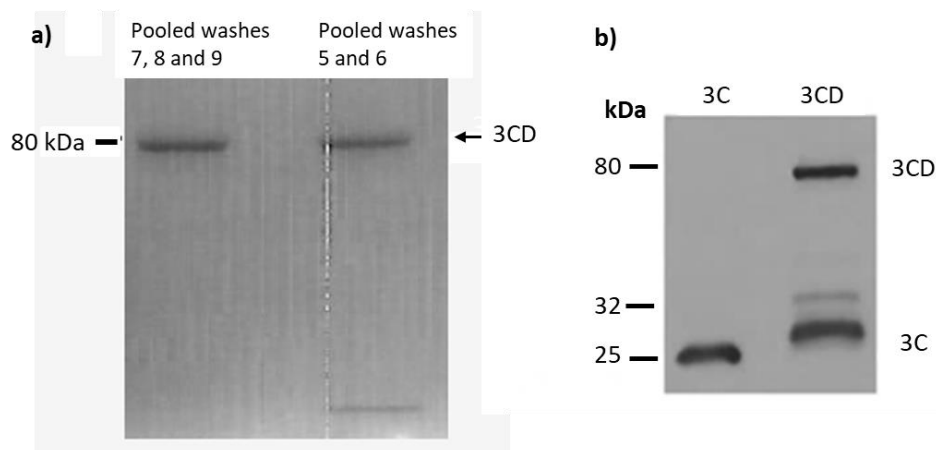


Figure 3.19 Purification of his-tagged recombinant 3CD protein. A) Coomassie stain of purified 3CD. Initial eluates were pooled and dialysed prior to resolving by SDS-PAGE. B) Western blot analysis of purified his-tagged 3C and 3CD probed with a monoclonal anti-3C antibody.

Purification of the his-3C protein was more complicated than expected due to its propensity to aggregate and precipitate out of solution at high concentration. The recombinant protein contained three mutations from the catalytically active cysteine residues in order to inhibit protease activity and improve protein solubility (C95K, C142L, and C163A). It should be noted that such mutations may have a downstream effect on the ability for the protein to function in the proposed assays.

His-3CD, however, did not have any mutations that affected the solubility of the protein, but the active site of the protease was mutated to disable its function as a protease. Once again, this may play a role in the downstream functional assays. It is interesting to note that although Coomassie staining of purified 3CD (Fig. 3.19a) shows a band at 75 kDa (the expected size of 3CD), the subsequent Western blot (Fig. 3.19b) shows a number of smaller protein products possibly representing aberrant cleavage products, most likely as a result of bacterial proteases during protein expression, or the presence of 3D* at approximately 35 kDa. 3D* is thought to be a

fragment of incorrectly processed 3CD. Studies on PV have observed a similar aberrant processing event (Lawson et al., 1992; Parsley et al., 1999).

As his-3CD is a precursor to 3C and 3D^{pol}, it was hypothesised that the recombinant precursor protein would still be able to interact with RNA, or at least be able to bind nucleotides, particularly as it is believed to be involved with VPg uridylylation. A dot-blot activity assay was used to determine the ability for 3CD to bind to, or incorporate [α -³²P] UTP. An RNA primer-template and [α -³²P] UTP, as described for his-3D^{pol} activity assays (section 2.10) was used, and the complex was incubated at 30°C for increasing lengths of time from 0 to 10 minutes. The samples were blotted on to filter paper. Samples incubated for longer than 10 minutes resulted in the formation of aggregate too large to be resolved by SDS-PAGE, therefore it was decided to limit the length of the reaction times to match the trends observed in 3D^{pol} crosslinking assays. Figure 3.20a shows that his-3CD is unable to incorporate nucleotide, as expected.

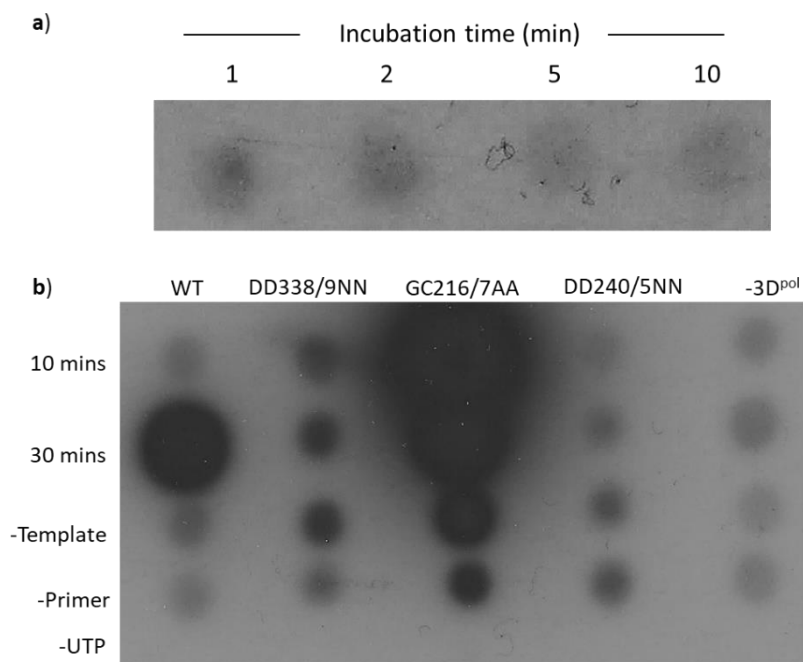


Figure 3.20 Dot-blot of 3CD activity assay. A) Incorporation activity dot-blot assay with purified recombinant his-3CD protein over time (minutes). B) Dot-blot of his-3D^{pol} activity assay from figure 3.5 with the controls (No template, no primer, no UTP) for comparison. The his-3D^{pol} and his-3CD assays were undertaken on the same day with identical controls.

3CD was subjected to the same glutaraldehyde crosslinking assay as was used for 3D^{pol} in an attempt to capture the formation of potential higher-order structures, or fibrils. The crosslinked assay was resolved by gradient SDS-PAGE (as described in section 2.10.2) and analysed by Western blot using anti-His, polyclonal anti-3D 397, and anti-3C 2D2 antibodies as outlined in section 2.4.

Similarly to the his-3D^{pol} recombinant proteins mutants, 3CD appears to form some higher-order oligomeric structures by Western blot, despite being unable to incorporate [α -³²P] UTP (Fig. 3.21). However, TEM of these early timepoint oligomers show aggregate formation instead of any distinct higher-order structure formation (Fig. 3.21d) similar to the results of the 3D^{pol} mutants (Fig. 3.10 b-d).

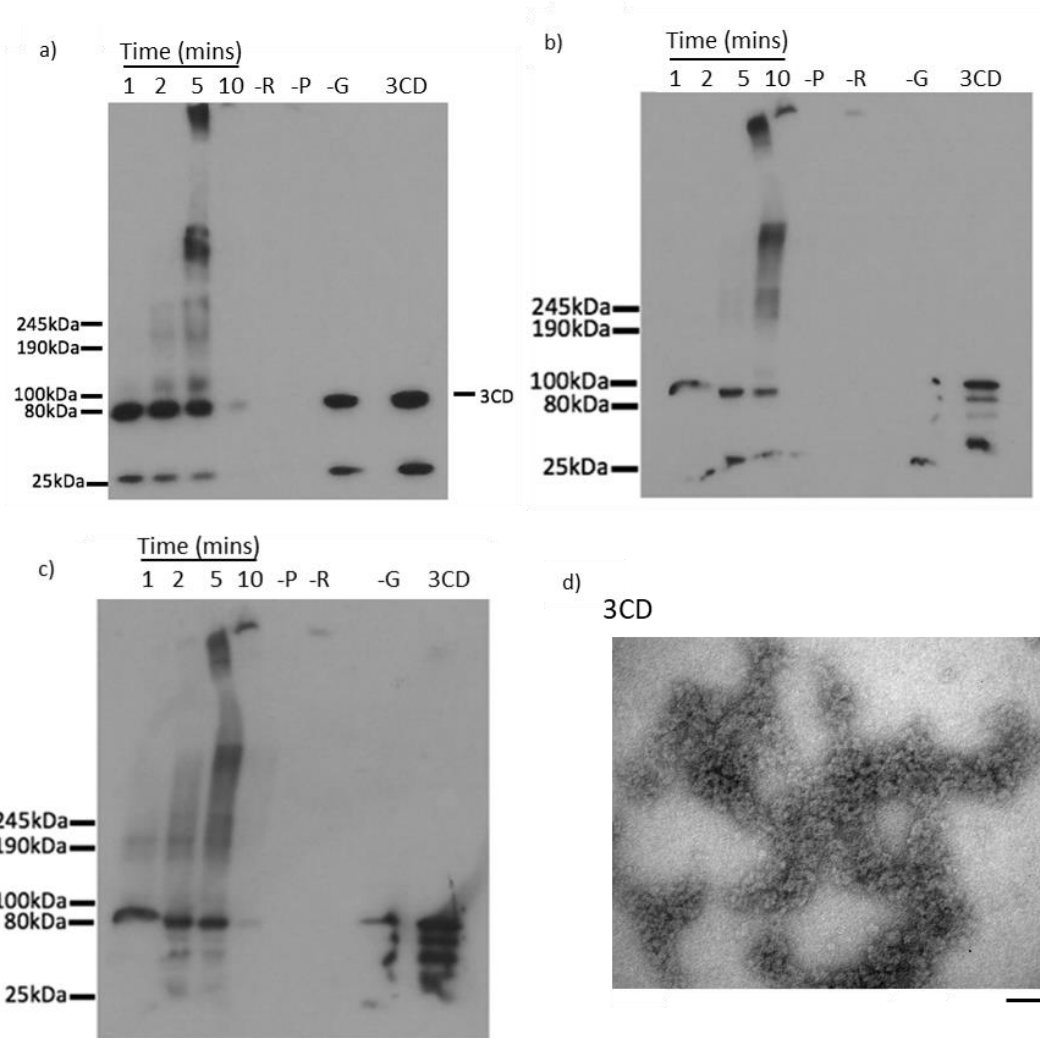


Figure 3.21 Glutaraldehyde crosslinking assay on recombinant 3CD incubated with RNA over time. A) Western blot of crosslinking assay probed with monoclonal anti-3C antibody. Control lanes with no RNA (-R), no protein (-P), no glutaraldehyde (-G), and purified 3CD not subjected to the crosslinking assay (3CD) were also included (n=2). B) Repeat of the glutaraldehyde crosslinking assay with 3CD probed with monoclonal anti-3C antibody, C) Repeat of the glutaraldehyde crosslinking assay with 3CD probed with polyclonal anti-3D antibody (n=1). D) Negative stain TEM of 3CD with RNA primer-template incubated for 10 minutes. 3CD does not show any distinct fibril structure formation but shows the formation of protein aggregates (n=1).

3.9 Chapter discussion

The RNA-dependent RNA polymerase, 3D^{pol}, was one of the first proteins to be characterised both in PV (Baltimore et al., 1962) and in FMDV (Polatnick et al., 1967). In both viruses one of the initial findings showed that the polymerase was not sensitive to actinomycin D (Baltimore et al., 1962; Black et al., 1969), but was able to incorporate nucleoside triphosphates into virus RNA. Both PV and FMDV polymerases were also shown to mediate replication of the virus genomes by binding to VPg (Paul et al., 1998; Nayak et al., 2005). Recent biochemical, microscopic, and structural studies on PV and FMDV 3D^{pol} have also shown that they are both able to form higher-order structures *in vitro* in the form of fibrils (Pata et al., 1995; Lyle, Bullitt, et al., 2002; Tellez et al., 2011; Bentham et al., 2012; Wang et al., 2013).

Here, we have confirmed previous data, showing that FMDV fibrils can only form if the polymerase is catalytically active and replication-competent. Mutations located in the catalytic active sites and in the non-catalytic dsRNA exit site of the protein abrogated protein function *in vitro* and in context of the RNA replicon. All three mutations that were tested: DD388/9NN, DD240/5NN, and GC216/7AA, were unable to form fibrils, even in the presence of primer-template RNA, as was shown for WT (Bentham et al., 2012). The non-catalytic mutant GC216/7AA was able to bind RNA with a similar affinity to WT, despite incorporating RNA nucleotides at a faster rate than WT. However, GC216/7AA was unable to form fibrils. The catalytic mutations DD388/9NN and DD240/5NN bound RNA with low affinity and were unable to incorporate RNA nucleotides or form fibrils. This is in contrast to data for PV (Arnold et al., 1999), where fibrils form spontaneously. These data would suggest that the

formation of the fibrils in FMDV replication is functional in addition to providing support and protection, contrary to the function suggested for PV fibrils (Tellez et al., 2011; Wang et al., 2013).

All three FMDV 3D^{pol} mutations were able to form oligomers as detected by Western blot, however mutant DD240/5NN appeared to aggregate more readily instead of forming distinct higher-order structures unlike DD388/9NN. This would suggest an aberrant protein-protein interaction occurring. For non-catalytic mutant GC216/7AA and WT, the ability to incorporate [α -³²P] UTP would also suggest that, in addition to there being a protein-protein interaction, protein-RNA interactions are involved, however they only lead to the formation of fibrils for WT. In PV, a number of different polymerase mutations that affected catalytic function were analysed and it was suggested that some, despite resulting in a non-functional, non-catalytically active protein, were still able to provide structural support to the planar lattice and result in helical fibril formation (Spagnolo et al., 2010; Tellez et al., 2011).

The crystal structure of non-catalytic mutant GC216/7AA showed that the mutation in the double-stranded RNA exit site had minor effects on the structure of the polymerase when compared to WT (Herod et al., 2016). The differences in the structure of the molecule are predicted to have a minor effect on the incoming nucleotides which leads to the non-replicative phenotype of the mutant. From the cryo-EM structure, the residue changes do not have any effect on the regions on the molecule that could be involved in inter-molecular interactions with neighbouring polymerases. The structural changes in the DD240/5NN and DD388/9NN mutants are also predicted to have no effect on the inter-molecular interactions. These structural

predictions suggest that the formation of fibrils is linked to the enzymatic function of FMDV 3D^{pol}. Work is currently ongoing to dock the crystal structure of the GC216/7AA mutant into the fibril cryo-EM model to verify that the mutation does not affect the protein to form intra-molecular interactions necessary to form fibrils. Further work to establish the interacting residues between polymerase molecules is necessary to establish additional regions of the FMDV polymerase that are essential for fibril formation. Identifying these residues could help elucidate the function of the fibrils *in vitro* and *in vivo*. It is predicted that similar residues are involved as those found in PV fibril intra-molecular interactions. These regions are found predominantly in the finger regions of the molecules (Lyle, Bullitt, et al., 2002; Wang et al., 2013) and those regions that are located towards the N-terminus of the molecule (Lyle, Bullitt, et al., 2002).

The importance of the enzymatic ability for 3D^{pol} to form fibrils can also be seen in the assays with 3CD. Here, a mutant 3CD was used in which the 3C active site within his-3CD was abrogated and thus the protease was unable to function and cleave correctly to release 3D^{pol}. 3CD is unable to form higher-order structures. This supports the model that 3CD has an independent, non-catalytic function in replication. However, more work needs to be undertaken to identify the exact role of 3CD and interactions with components of the replication complex. Additionally, it would be prudent to identify the reason for the aberrant cleavage events occurring post-purification in 3CD as seen in the Western blot in figure 3.19b. These cleavage products equate to sizes larger than 3C but smaller than 3D^{pol} suggesting that

cleavage is occurring in a location within 3D^{pol}. However, it appears that this truncated 3D^{pol} cannot form fibrils.

The formation of a classical intracellular, membrane-associated replication complex for FMDV has yet to be identified within infected cells. Studies have shown, that like a number of related positive-strand RNA viruses, FMDV is capable of dysregulating cellular membranous organelles such as the Golgi and the ER, but no distinct complexes composed of viral structural, non-structural and host-cell proteins have been identified unlike PV (Schlegel et al., 1996; O'Donnell et al., 2001; Monaghan et al., 2004; Knox et al., 2005).

The formation of 3D^{pol} fibrils provides a plausible model for a replication complex in FMDV. However, the lack of RNA in the current fibril structure was unexpected. The model proposed here is based upon the ability for FMDV 3D^{pol} to be involved in protein-protein interactions mediated by RNA binding. The ability to form fibrils could be as a result of a conformational change mediated by the binding of 3D^{pol} to RNA. The conformational change would then allow for the binding of further polymerase molecules in a regular pattern to form a fibril-like structure. The catalytic mutants were unable to bind or incorporate RNA and therefore may not be able to change conformation. They would therefore be unable to form structured fibrils and aggregation could result instead. The non-catalytic mutant GC216/7AA, although able to bind and incorporate [α -³²P] UTP was still unable to form fibrils suggesting that the mutation may be unable to adapt the correct conformation or to form the correct interactions necessary for fibril formation.

The precursor 3AB has been found to associate with PV 3D^{pol} fibrils (Spagnolo et al., 2010). Further work needs to be undertaken to establish if other non-structural proteins, such as 3CD, 3A and 3B_{1,2,3}, are also able to interact with the FMDV 3D^{pol} fibrils. Apart from providing an enclosed, protective environment within which replication can occur, one could speculate, in the context of a cellular replicon complex, that the polymerase molecules could coat newly synthesised negative-sense intermediate and prevent the formation of double-stranded RNA, a potent innate immune response trigger. By avoiding the double-stranded RNA formation it would also allow for a more energetically favourable replication process.

Finally, it would be important to identify if fibrils are able to form when FMDV template RNA is used instead of poly-A, particularly to determine if RNA secondary structure hinders the ability for 3D^{pol} to form fibrils. The use of FMDV genomic RNA would also allow for the development of a more physiological environment to assess any other hypothesised protein-protein interactions that could occur, such as with cellular PABP and PCBP2 and with other viral proteins such as 3B_{1,2,3} and 3CD.

Chapter 4

Investigating the role of foot-and-mouth disease virus 3D polymerase mutants on replicon replication

4.1 Introduction

Upon entry of the FMDV into the host-cell cytoplasm, the viral RNA genome undergoes initial translation by host-cell translation initiation factors and the 40s ribosomal subunit by binding to the IRES element in the 5' UTR. (Belsham et al., 1990; López de Quinto et al., 2002; Rodríguez Pulido et al., 2007).

FMDV has a much larger 5' UTR than other picornaviruses, containing approximately 1,300 bases (Forss et al., 1984; Grubman et al., 1984; Robertson et al., 1985). It can be divided into five functional elements comprising of a 360-base stem-loop structure called the S-fragment, followed by a poly-C tract of variable length, between two and four RNA pseudoknot structures, the *cre*, and a type II IRES (Newton et al., 1985; Belsham et al., 1990; Rieder et al., 1993; Bunch et al., 1994; Escarmís et al., 1995; López de Quinto et al., 2002; Mason et al., 2002; Carrillo et al., 2005). The functions of the S-fragment, poly-C tract, and the pseudoknots have yet to be elucidated.

The genome is translated into a polyprotein from which the structural and non-structural precursors are co- and post-translationally cleaved into the active proteins.

L^{pro} autocatalytically cleaves itself from the polyprotein. Intermediate polyprotein precursors 1A-2A and 2BC separate themselves from the P3 intermediate through a process known as ribosomal skipping due to the sequence of 2A (Ryan et al., 1994). Both 2BC and P3 are further cleaved into the mature proteins by the virus-encoded protease, 3C, via several intermediate precursors: 2B, 2C, 3AB₁₋₃, and 3CD (Flint et al., 1997). The P3 region (3A-3D) undergoes further processing to produce mature 3A, 3B₁₋₃, 3C and 3D^{pol} (Forss et al., 1982; Flint et al., 1997; Ferrer-Orta et al., 2004; Birtley et al., 2005; Moffat et al., 2005; González-Magaldi et al., 2014).

Replication of FMDV RNA begins with 3D^{pol} binding to a copy of uridylylated VPg (VPg-pUpU) that is covalently linked to the 5' end of the negative strand intermediate genome and acts as primer for both positive and negative strand synthesis (Murray et al., 2003; Nayak et al., 2005; Steil et al., 2009). 3D^{pol} replicates the genome in a 5' to 3' direction via a negative sense intermediate which acts as a template for the positive sense RNA that can either be packaged into new virions or translated into viral proteins.

4.2 Replicons

The development of FMDV replicon systems based on the genome of FMDV serotype O (O1/Kaufbeuren/FRG/66) have provided the opportunity to study the replication of a high-containment pathogen under low-containment (McInerney et al., 2000; Tulloch et al., 2014; Forss et al., 1984) and have allowed for the study of separate stages of the virus life cycle such as replication and packaging. The replicon systems that have been developed have substituted the structural proteins in the P1 region with chloramphenicol acetyltransferase (1st generation replicons) or with green fluorescent reporter gene and antibiotic resistance fusion protein, puromycin-*N*-acetyltransferase (GFP-PAC) (2nd generation replicons) (McInerney et al., 2000; Tulloch et al., 2014; Herod et al., 2015). These FMDV replicons are unable to form infectious viruses, but are still able to replicate within a host cell when transfected as RNA. The inclusion of a fluorescent protein (in the second generation GFP-PAC replicons) (Fig. 4.1) has allowed the monitoring of viral RNA replication in real-time (Forrest et al., 2014).

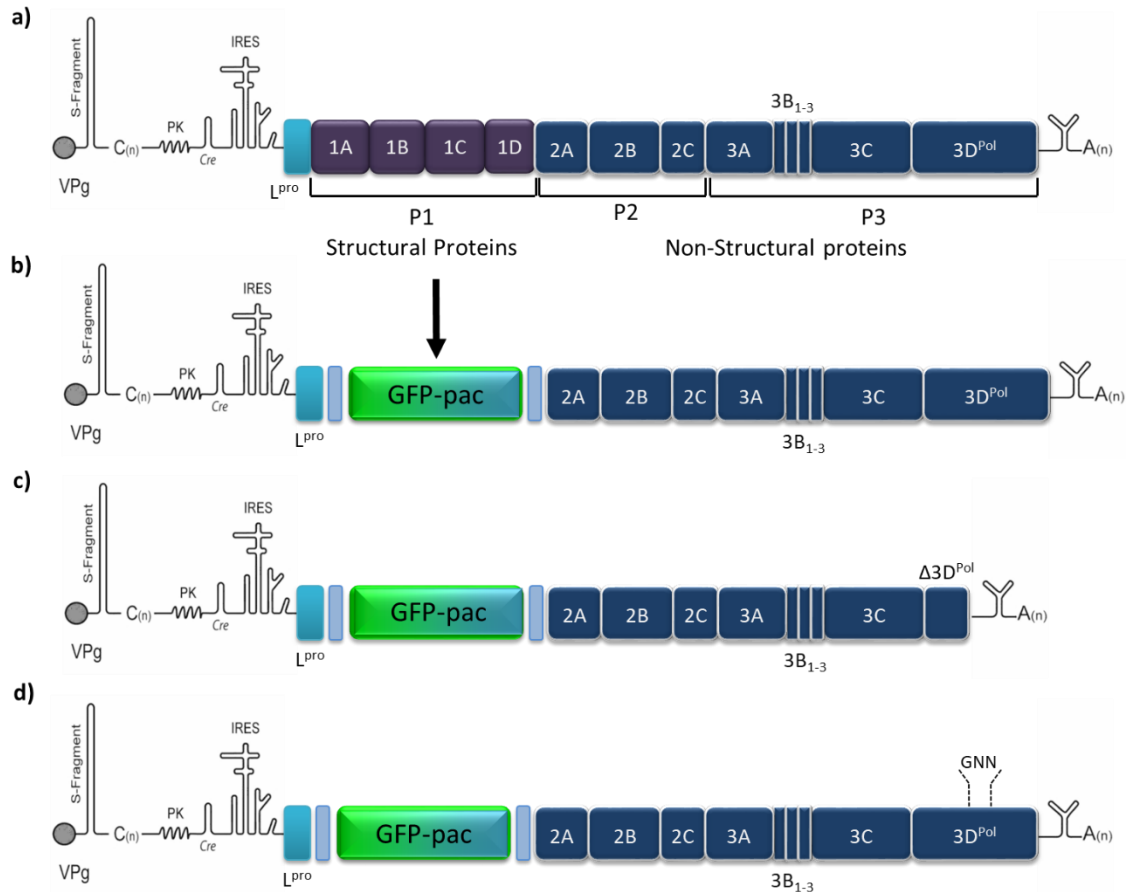


Figure 4.1 Schematic diagrams of second-generation FMDV replicons. A) Schematic of infectious viral genome containing structural proteins 1A-1D in the P1 region. B) Schematic of WT replicon showing the substitution of structural proteins 1A-1D with GFP-PAC reporter cassette (GFP-pac-WT). C) Schematic of replicon showing the substitution of structural proteins in P1 with GFP-PAC reporter cassette. This replicon contains a large deletion in the polymerase protein encoding region (3D^{pol}) and is termed GFP-pac-Δ3D. D) Schematic of replicon showing the substitution of structural proteins in P1 with GFP-PAC reporter cassette. This replicon contains two point mutations (GNN) in 3D^{pol} that renders the polymerase enzymatically inactive (GFP-pac-GNN).

Here we have investigated the effect of the catalytic and non-catalytic mutations within 3D^{pol} previously described in Chapter 3, in context of an FMDV replicon, and the ability to recover the function of the mutated polymerases within cells by co-transfection with WT functional helper replicons. The process of co-transfection and the ability to recover replication-deficient replicons in *trans* has been well

established in PV as well as in HCV (Ryan et al., 1994; Xuemei Cao et al., 1995; Teterina et al., 1995; Towner et al., 1998; Lyons et al., 2001; Tiley et al., 2003; Appel et al., 2005; Jones et al., 2009; Herod et al., 2014).

4.2.1 Replication

In order to determine the replicative ability of the GFP-expressing FMDV replicons, GFP-pac-WT, GFP-pac- Δ 3D, and GFP-pac-GNN RNA was transfected into BHK-21 cells. The number of GFP-positive cells, which correlated with the efficiency of GFP-expression, following transfection reflected the replicative ability of the replicon construct (Fig. 4.1). It is important to note that the replicons containing the mutation termed GNN are the same as the active site catalytic mutation DD388/9NN used in the activity assays in Chapter 3; the mutation is referred to as GNN here for simplicity. To establish the correct conditions for the transfection reactions, experimental conditions were optimised. Reassuringly, the optimum conditions were identical to those previously identified (Forrest et al., 2014). The conditions that produced the best GFP expression in all three of the GFP-pac RNAs were found to be: 0.5 μ g RNA with 2.5 μ l Escort transfection reagent in 250 μ l total volume of MEM per well in a 24-well plate reaction (section 2.6.3).

Transfected cells were imaged at regular intervals over 16 hours post-transfection in an IncuCyte FLR Zoom kinetic imaging system (Essen Bioscience); a fluorescence microscope, housed inside an incubator at 37°C/5 % CO₂. The images were analysed by measuring the number of GFP-positive cells per well, indicating translation and subsequent replication of the GFP-containing replicons, using the IncuCyte imaging processing software.

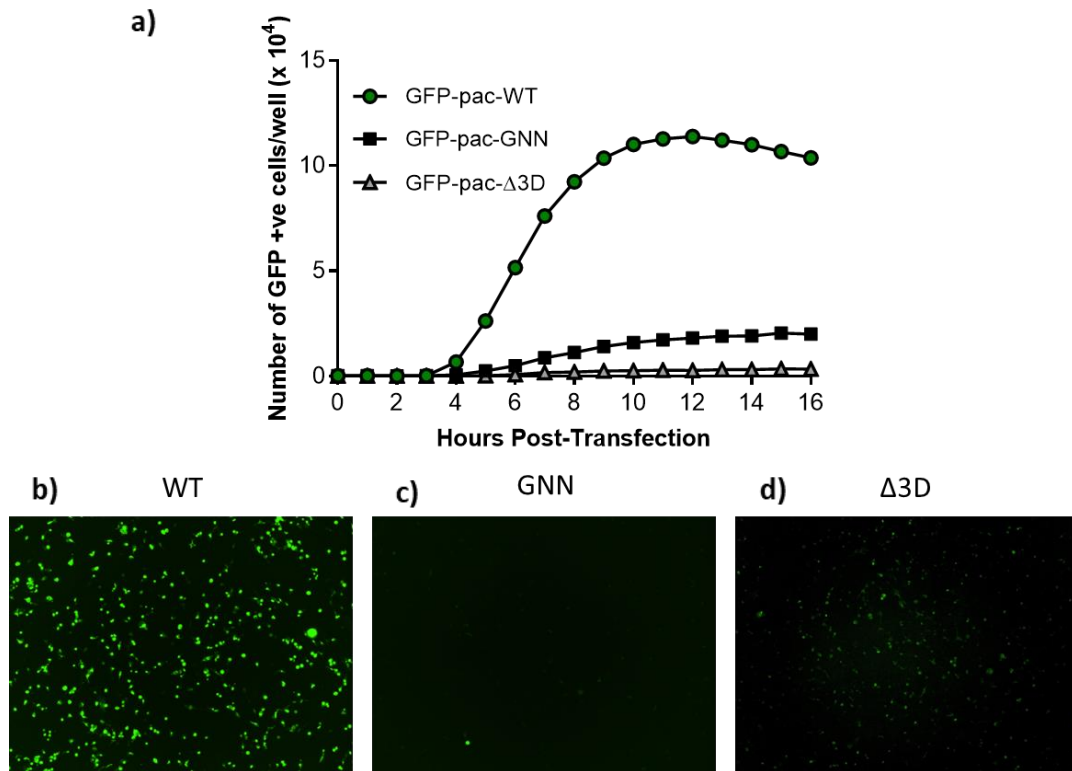


Figure 4.2 Representative data of transfected BHK-21 cells. A) graph showing the mean number of GFP-expressing BHK-21 cells over time (hours) after transfection with GFP-pac replicons (WT, GNN and $\Delta 3D$). $n=3$, error bars removed for clarity. B) IncuCyte image showing representative levels of GFP expression in BHK-21 cells transfected with GFP-pac-WT replicon at 10 hours post-transfection. C) IncuCyte image showing representative levels of GFP expression in BHK-21 cells transfected with GFP-pac-GNN replicon at 10 hours post-transfection. D) IncuCyte image showing representative levels of GFP expression in BHK-21 cells transfected with GFP-pac- $\Delta 3D$ replicon at 10 hours post-transfection.

Data collected on the IncuCyte were analysed using two different methods; by enumerating the total number of cells expressing the fluorescent transgene (e.g. number of GFP-positive cells per well) and by measuring the total fluorescent intensity per well using the integrated software. It is important to note that there was no difference observed when the data were analysed either as total cell counts of total fluorescent intensity. The data presented here represents the total number of fluorescence-positive cells per well unless otherwise stated.

The results from the IncuCyte analysis of the optimisation reaction defined the optimum levels of GFP expression for each of the replicon RNAs (GFP-pac-WT, - Δ 3D and -GNN). Figure 4.2a shows the results of a representative assay. The graph represents the expression of GFP over time post-transfection. Expression of GFP began at 4 hours post-transfection. As expected, GFP-pac- Δ 3D and GFP-pac-GNN had very low GFP counts per well suggesting that the fluorescence measured reflected input RNA translation only, as expected. These replicon constructs can thus be used as controls in further replication assays. Expression of GFP from the construct GFP-pac-WT peaked at 10-12 hours post-transfection. Representative images of peak GFP expression for each replicon are shown in figure 4.2 b-d.

4.2.2 Evidence of protein expression

To complement the IncuCyte analysis, a Western blot analysis of BHK-21 cells transfected with GFP-pac-WT replicon was undertaken. Cells were lysed with RIPA buffer and harvested as described in section 2.8.1. Lysates were subjected to SDS-PAGE and membranes were probed with antibodies against three FMDV non-structural proteins: 3A, 3B and 3D (described in section 2.4 and 2.8.4) (Fig. 4.3).

The results from the Western blot analysis showed the presence of each of the three viral proteins with the appropriate antibody. A band at 54 kDa corresponding to the expected size of 3D^{pol} was visible in figure 4.3a when probed with the rabbit anti-3D 397 polyclonal antibody as specified in section 2.4. The antibody also seemed to identify the 3CD precursor at \approx 75 kDa and the P3 precursor at \approx 110 kDa at later time points (Fig. 4.3a). The mouse anti-3A 2C2 monoclonal antibody used to probe cell lysates transfected with GFP-pac-WT (fig. 4.3b) that was used was very non-specific

which resulted in the detection of non-specific, background bands on the blots. However a band at ≈ 20 kDa visible after 7 hours may indicate the presence of 3A expression. Analysis of the blots identified a darker band located at approximately 26 kDa from the lysates transfected with GFP-pac-WT. It is possible that this band may be corresponding to the expected size of a 3A-3B precursor (Fig. 4.3b). Figure 4.3c shows the presence of at least 5 bands when the cell lysates were probed with a mouse anti-3B 1F8 monoclonal antibody. The sizes of individual 3B bands do not correspond to the molecular weight of the proteins suggesting that the bands represent a variety 3B precursors, however the identities of the precursors have yet to be determined.

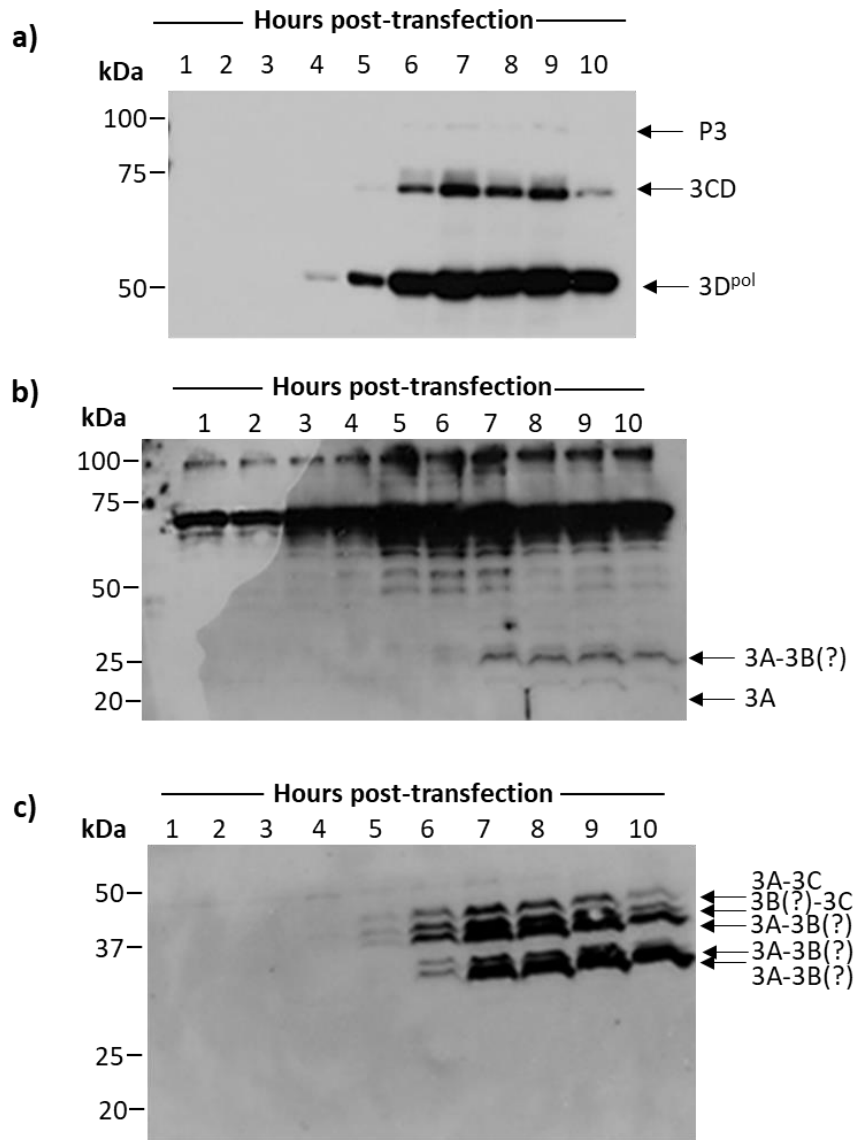


Figure 4.3 Western blot analysis of BHK-21 cells transfected with GFP-pac-WT replicon RNA and lysed at incremental time points. A) Blot probed with anti-3D (397) antibody showing levels of protein expression corresponding to 3D^{pol} (54 kDa), 3CD (75 kDa) and P3 (110 kDa). B) Blot probed with anti-3A antibody showing levels of protein expression corresponding to 3A (20 kDa) and a 3A-B precursor (\approx 27 kDa). C) Blot probed with anti-3B antibody showing levels of protein expression over time corresponding to 3B precursors (\approx 30-50 kDa).

The Western blot data supports the IncuCyte transfection data shown in figure 4.2. However, FMDV non-structural protein expression in the cell lysates occurs at earlier time points, i.e. beginning as early as 4 hours and peaking at 7-9 hours for GFP-pac-WT transfected lysates, instead of peaking at 10-12 hours as seen in figure 4.2. The

earlier expression times of the non-structural proteins seen in the cell lysates could be due to the different modes of measuring replication. In figure 4.2, replication was measured by analysing the number of GFP-positive cells per well, whereas in figure 4.3, protein expression was measured by probing with the appropriate antibody. The difference in expression times could be due to the rate of GFP synthesis and degradation within the cell, and may need longer to accumulate enough to induce a measurable signal within transfected cells.

4.3 Mutations in 3D^{pol}

It has been previously discussed in Chapter 3 that work by Herod *et al.* identified areas in the genome that could tolerate insertions by random transposon-mediated mutagenesis (Herod *et al.*, 2015). Transposon-mediated mutagenesis identified key functional regions within viral proteins, particularly within 3D^{pol} that were both permissive and could be further manipulated to include epitope tags for improved downstream studies such as immunofluorescence, and also non-permissive, which resulted in the production of replication-defective replicon phenotypes (McMahon *et al.*, 1998; Brune *et al.*, 1999; Teterina *et al.*, 2011; Remenyi *et al.*, 2014; Herod *et al.*, 2015; Herod *et al.*, 2016).

Out of nine mutations in the 3D^{pol} region that were identified, three were chosen to take forward into further studies: catalytic metal ion-interacting site DD240/5NN, dsRNA exit site GC216/7AA, and classical replication-deficient motif C mutation GNN (also known as DD388/9NN) (Jablonski *et al.*, 1991; Hansen *et al.*, 1997; Ferrer-Orta *et al.*, 2004; Carrillo *et al.*, 2005; Ferrer-Orta *et al.*, 2007; Ferrer-Orta, Ferrero, *et al.*, 2015; Herod *et al.*, 2016). These functional 3D^{pol} mutations (characterised in the context of recombinant proteins in Chapter 3) were introduced into FMDV replicons here. The schematic in figure 4.4 summarises the location of the mutations in context of the replicon.

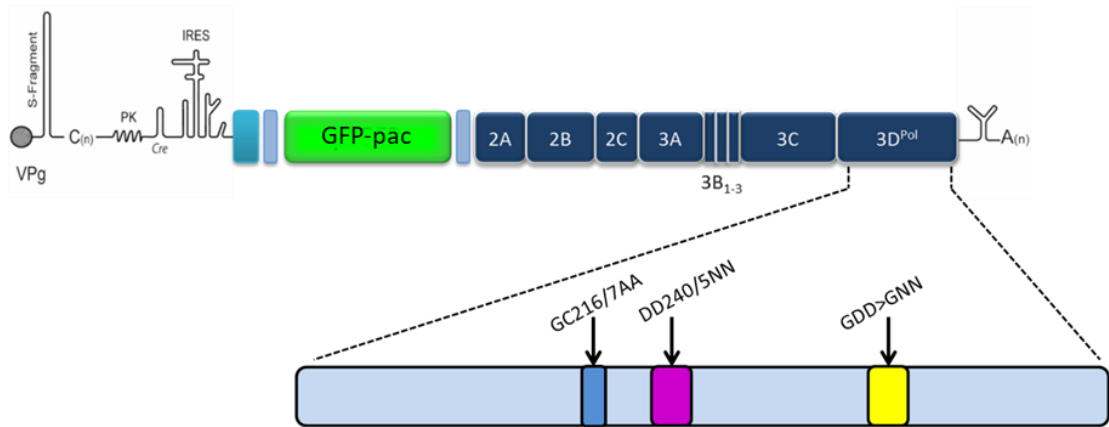


Figure 4.4 Schematic diagram of FMDV replicon highlighting 3D^{pol} diagrammatically showing the location of the three non-replicative mutations in 3D^{pol} identified by transposon mutagenesis.

4.3.1 Epitope-tagging of replicons

Recognition of replication-competent insertion sites by transposon-mutagenesis allowed for the identification of potential locations for insertion of epitope tags such as FLAG (DYKDDDDK) and haemagglutinin (HA; YPYDVPDYA). Herod et al., 2015 identified two locations in non-structural protein 3A and one in 3D^{pol} that could tolerate insertions by transposon-mutagenesis and demonstrated high levels of replication in BHK-21 cells (Herod et al., 2015). As a result of this, FLAG and HA epitope tags were cloned into these sites. The 3A epitope tag-containing insertion sites replicated to the levels of WT, whereas the epitope-tagged 3D^{pol} insertion site was unable to replicate.

Due to the inability of the original epitope-tagged 3D^{pol} insertion to replicate, the FLAG and HA epitope tags were cloned into the C-terminus of 3D^{pol}, in an identical location to the his-tag in the recombinant protein described in Chapter 3. It was believed that although the C-terminus was not identified by transposon mutagenesis as a permissive location, it would not affect the function of the WT protein, thereby

not affecting the replication ability of the replicon due to flexible nature of that region of the protein. The hypothesis was tested by transfecting GFP-pac-WT replicons containing FLAG and HA tags at the C-terminus of 3D^{pol} into BHK-21 cells as described in section 2.6.3 (Fig. 4.5). FLAG- and HA-tagged GFP-pac-WT replicons were able to replicate to the level of the unmodified GFP-pac-WT replicon.

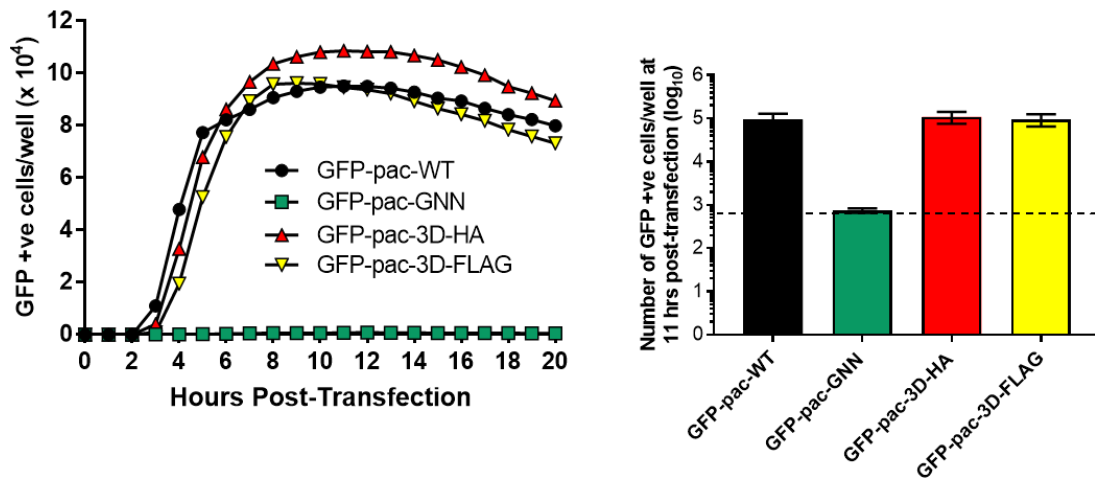


Figure 4.5 Levels of GFP-expression in BHK-21 cells transfected with GFP-pac replicon RNA. A) Levels of GFP-expression at 11 hours post-transfection in BHK-21 cells transfected with GFP-pac-WT, GFP-pac-GNN, GFP-pac-WT-FLAG and GFP-pac-WT-HA replicon RNA. B) Mean levels of GFP-expression in BHK-21 cells transfected with GFP-pac-WT, GFP-pac-GNN, GFP-pac-WT-FLAG and GFP-pac-WT-HA replicon RNA over time. n=2, ± SEM. Error bars on the graph have been removed for clarity.

To ensure that the epitope-tagged replicons had been successfully cloned and were not structurally altered, transfected BHK-21 cells were lysed as described in section 2.8.1, resolved by SDS-PAGE, and then analysed by Western blot (Fig. 4.6). The Western blots were probed with rabbit anti-3D 397 polyclonal antibody, anti-FLAG, and anti-HA antibodies. As the antibodies were able to detect the protein (3D^{pol}) and the appropriate tags at 54 kDa it can be assumed that the insertion of the epitope tags did not alter the native folding of the protein or obscure the antigenic site,

providing support that the insertion of the epitope tags did not affect the function of the replicon, or polyprotein processing.

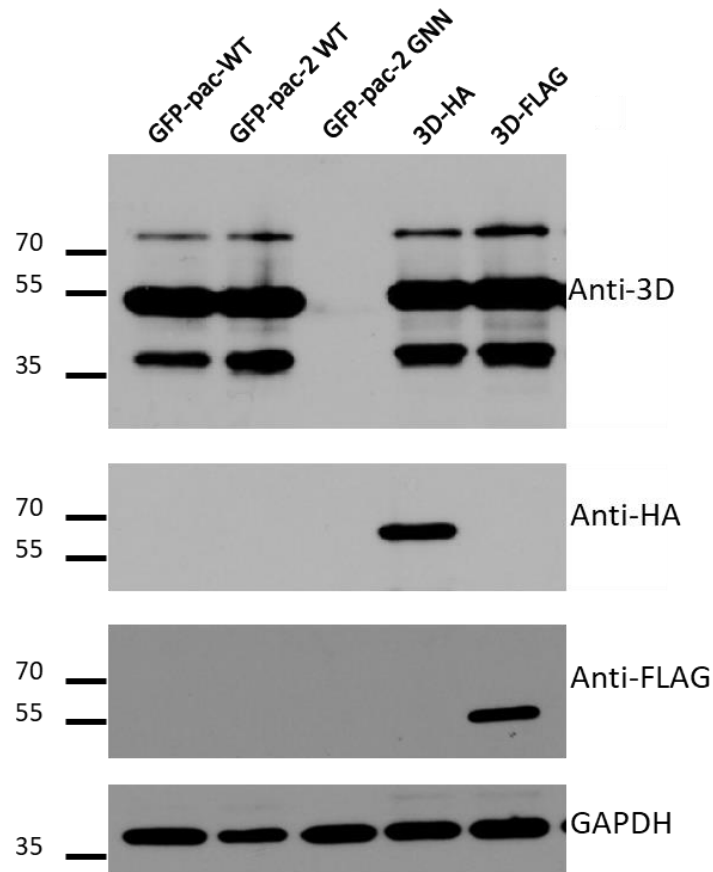


Figure 4.6 Western blot analysis of BHK-21 cells transfected with 3D^{pol} epitope-tagged GFP-pac-WT constructs in addition to controls (unmodified GFP-pac-WT and unmodified GFP-pac-GNN). Protein lysates were prepared at eight hours post-transfection and probed by Western blotting for FLAG and HA expression and 3D^{pol}. Glyceraldehyde 3-phosphate dehydrogenase (GAPDH) was used as a loading control.

The appearance of extra bands in the samples probed with anti-3D 397 antibody was expected due to the polyclonal nature of the antibody. This resulted in the detection of additional bands upon Western blot analysis at 75 kDa and a doublet band located at approximately 35 kDa. It is thought that the band located at 75 kDa is 3CD, and the band at approximately 35 kDa is a non-specific interaction of the antibody with a

fragment of incorrectly processed 3CD, termed 3D*. A similar observation has been made in studies on PV (Lawson et al., 1992; Parsley et al., 1999).

4.3.2 Next generation replicons

A third generation of WT and GNN replicons were also developed replacing the GFP-pac reporter cassette with either mCherry red fluorescent protein or with a new GFP report gene from *Ptilosarcus* sea pen (ptGFP) (Herod et al., 2015, F. Tulloch, G. Luke, J. Nicholson and M. D. Ryan, unpublished data) as shown in figure 4.7.

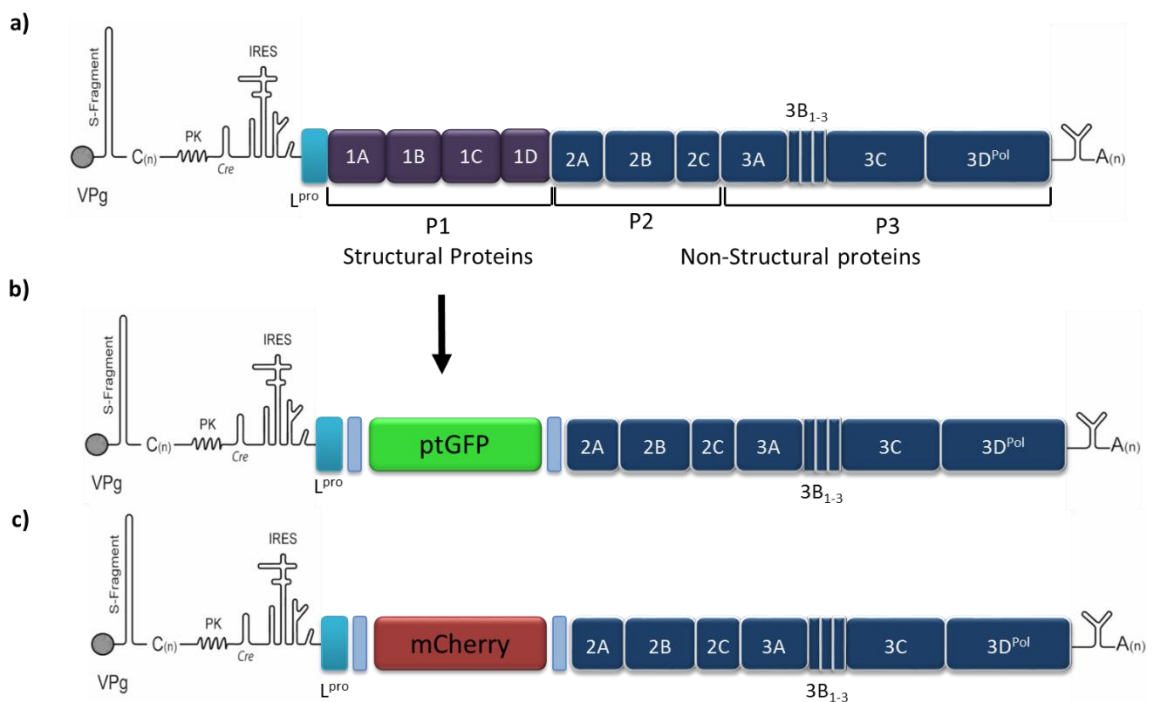


Figure 4.7 Schematic diagrams of third-generation FMDV replicon. A) Schematic of infectious viral genome containing structural proteins 1A-1D in the P1 region. B) Schematic of WT replicon showing the substitution of structural proteins 1A-1D with ptGFP (ptGFP-WT). C) Schematic of WT replicon showing the substitution of structural proteins 1A-1D with mCherry (mCherry-WT).

ptGFP is a GFP that has been described as having higher absorption peak (495 nm), and an emission peak at 508 nm, than the corresponding enhanced GFP (eGFP) or *Aequorea* GFP used in the GFP-pac replicons (absorption at 395 and 470 nm and

emission at 507-510 nm). The emission curve of ptGFP show that the molar absorbance of ptGFP is higher, and the excitation and emission peaks are nearly symmetrical, unlike those of *Aequorea* GFP, and is therefore brighter (Bryan et al., 2001; Environmental Sciences Inc., 2015; Hicks, 2002). Particularly as *Aequorea* GFP has two excitation peaks and current green fluorescence filters are largely inadequate for detection of both (Hicks, 2002). Negative control ptGFP-GNN and mCherry-GNN replicons were also prepared (mutagenesis performed by Morgan Herod, University of Leeds). A representative replication assay (Fig. 4.8) shows the expression of both ptGFP and mCherry over time in BHK-21 transfected cells. The trend in fluorophore expression is similar to that seen in GFP-pac replicon-transfected cells (Fig. 4.2), however, the expression of ptGFP appears earlier in transfected cells (from 3 hours) and peaks at an earlier timepoint (7-9 hours). Expression of ptGFP is not thought to occur at a faster rate, but is detected sooner due to the increase brightness when compared to GFP-pac.

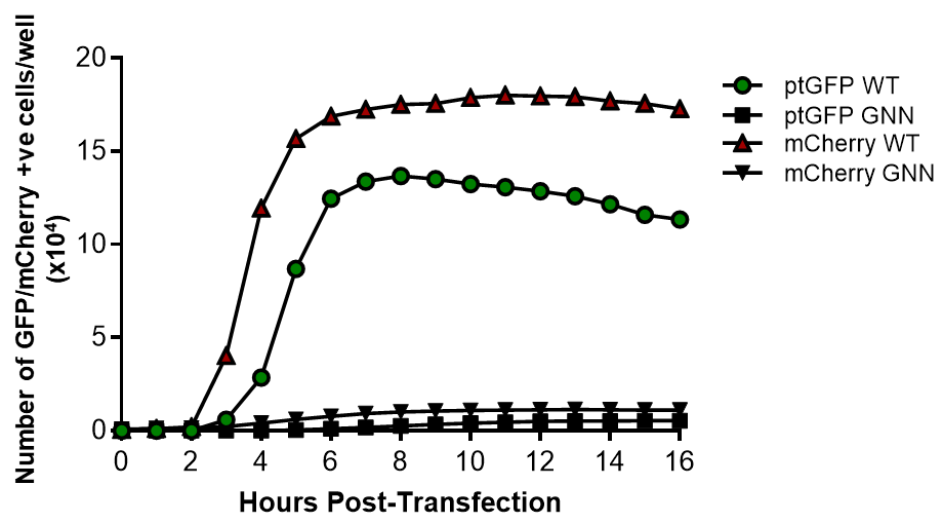


Figure 4.8 Representative data of transfected BHK-21 cells. Graph showing the mean number of ptGFP- and mCherry-expressing BHK-21 cells over time (hours) after transfection with ptGFP-and mCherry (WT and GNN). n=3, error bars removed for clarity.

Identical replicons with contrasting fluorescent reporters opened up the possibility of being able to use two replicons simultaneously as they could be easily distinguishable from each other when co-transfected (Herod et al., 2015).

4.3.3 Epitope-tagging of replication-deficient replicons

To improve the signal of GFP, two epitope tags (FLAG and HA), and mutations were introduced into the ptGFP third-generation replicon. Replication of the different replicons was assayed in BHK-21 cells alongside unmodified controls (Fig. 4.9). There is a 100-fold difference in the number of cells expressing GFP between WT ptGFP replicons and GNN ptGFP replicons.

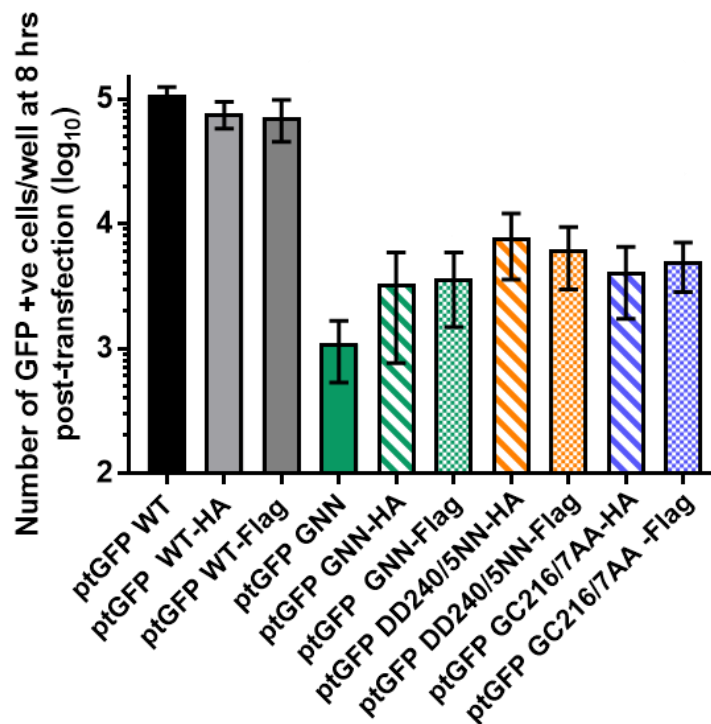


Figure 4.9 Levels of GFP-expression in BHK-21 cells transfected with ptGFP replicon RNA. A) Levels of GFP-expression at eight hours post-transfection in BHK-21 cells transfected with ptGFP-WT, ptGFP-GNN, ptGFP-WT-FLAG and -HA, ptGFP-GNN-FLAG and -HA, ptGFP-D240/5NN-FLAG and -HA, and ptGFP-GC216/7AA-FLAG and -HA replicon RNA. Levels of GFP expression of mutants GC216/7AA and DD240/5NN are compared to ptGFP-GNN. n=3, ± SEM (all statistically non-significant when compared to ptGFP-GNN).

As expected, the replicons that contained the point mutations in 3D^{pol} (DD240/5NN and GC216/7AA) were unable to replicate, resulting in significantly lower levels of GFP expression than that the WT control, and to approximately the same level of GFP expression as the ptGFP-GNN negative controls. All the mutant replicons had similar levels of GFP expression as the GNN control, within error.

4.3.4 Recovery of replication-deficient replicons

Co-transfection and use of helper replicons to recover replication-deficient replicons in *trans* is an established method to determine the function of viral proteins, particularly their role in viral genome replication. A number of studies on FMDV and other picornaviruses have used this method to demonstrate that certain non-functional, non-structural proteins can be recovered in *trans* by co-expression with replication-competent helper virus or replicon (Xuemei Cao et al., 1995; Teterina et al., 1995; Towner et al., 1998; Tiley et al., 2003; Nayak et al., 2005).

As it can be seen from previous figures (Figs. 4.2, 4.7 and 4.9), the mutant replicon 3D^{pol}-GNN is unable to replicate, producing levels of GFP expression synonymous with input translation from positive-strand template RNA. Previous work outlined in Herod et al., 2015 observed that the replication-deficient ptGFP-GNN replicon was able to be recovered by co-transfection of a WT 'helper' replicon containing the different fluorescent reporter gene, mCherry as outlined in figure 4.10. The use of different reporter genes allowed for the discrimination of replication between the WT helper replicons and the mutant replication-defective replicons.

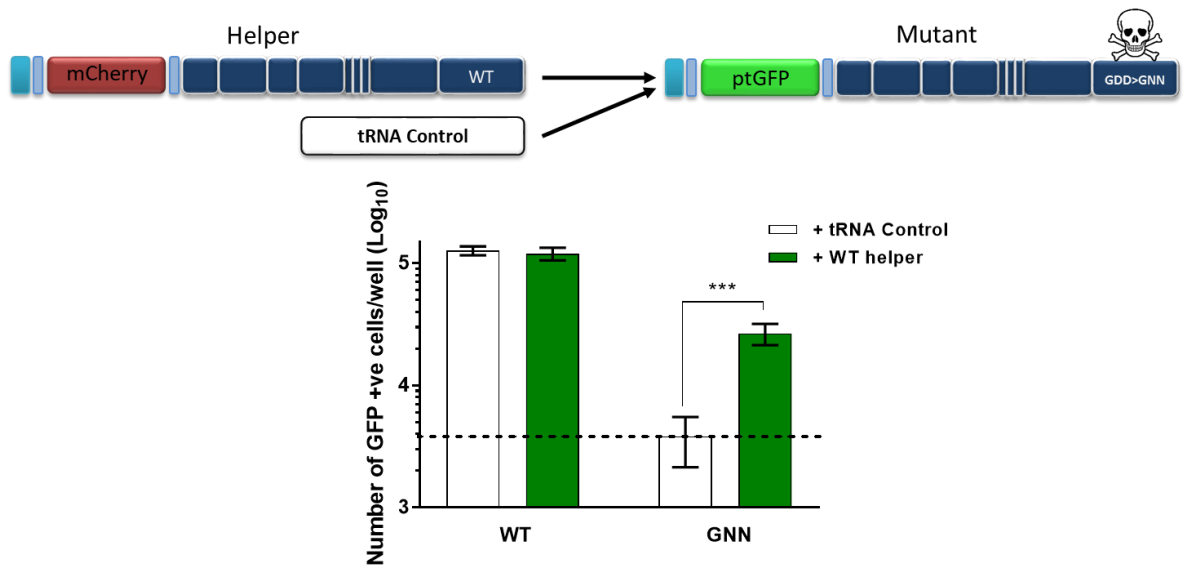


Figure 4.10 Co-transfection of mCherry-WT helper replicon RNA and control tRNA with ptGFP mutant replicon (ptGFP-GNN) or with ptGFP-WT replicon. Levels of GFP expression was measured using the IncuCyte FLR as the number of GFP-positive cells/well at eight hours post-transfection when GFP expression was maximal. $n=6 \pm$ SEM. *** = $p < 0.001$.

The levels of GFP expression produced by ptGFP-GNN replicon, when co-transfected with mCherry-WT replicon, were increased significantly when compared to the ptGFP-GNN replicon co-transfected with transfer RNA (tRNA) that is used as a control to maintain equal amounts of RNA in the transfections. The replication-deficient mutant ptGFP-GNN was unable to be recovered when co-transfected with tRNA control, highlighting that it is necessary for a fully-functional WT polymerase to be present for the recovery of replication to occur. Levels of GFP expression of ptGFP-WT replicon when co-transfected with WT mCherry helper replicon or with control tRNA were not significantly different, implying that there were no negative effects as a result of competition for cellular resources.

It has been previously mentioned in Chapter 3 that two additional replicons with mutations in 3D^{pol} were chosen to take into further functional studies: DD240/5NN

and GC216/7AA (in addition to GNN, or DD388/9NN). *In vitro* polymerase activity assays performed on recombinant his-tagged mutant 3D^{pol} (detailed in Chapter 3) showed that mutant DD240/5NN was unable to incorporate ³²P- α UTP when incubated with an RNA-primer-template as a result of the point mutations located in a catalytic site of the enzyme. Mutant GC216/7AA was, however, able to incorporate radiolabelled nucleotides to a similar level as WT his-tagged recombinant 3D^{pol} protein, showing that the mutant was still enzymatically active as a result of the mutation not being located in a catalytic domain.

Here, investigations into whether these mutations could be recovered by co-transfection with a WT helper replicon as with the ptGFP-GNN replicon were undertaken. As expected based on previous transposon mutagenesis data, all three replicons containing mutations in 3D^{pol} were unable to replicate, producing levels of GFP expression approximately equivalent to the ptGFP-GNN replicon due to input translation only (Herod et al., 2016; Herod et al., 2015) (Fig. 4.11).

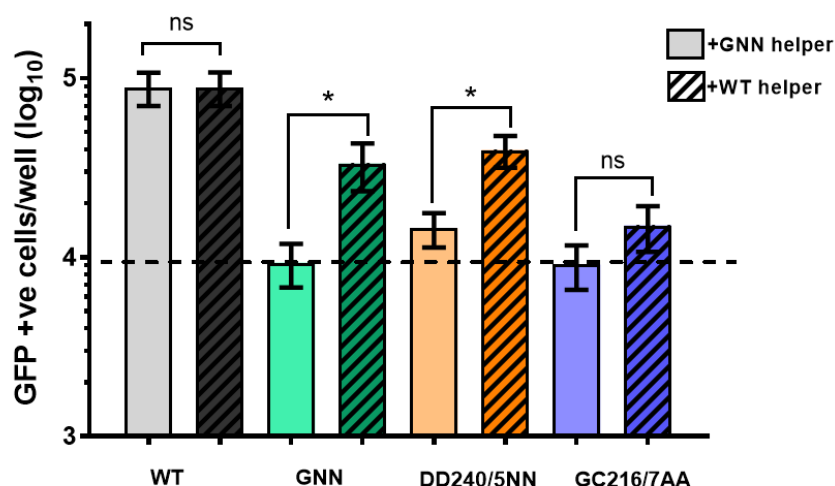


Figure 4.11 Levels of GFP expression at eight hours post-transfection of mutant polymerase ptGFP replicons (DD240/5NN, GC216/7AA, and GNN) when co-transfected with either mCherry-WT or mCherry-GNN helper replicons n=7 ± SEM. * = p < 0.05.

Levels of GFP expression in these two replicons were increased significantly when compared to the levels of GFP expression in the same replicons co-transfected with a replication-deficient helper replicon. When the mutant replicons were co-transfected with mCherry-GNN helper replicons, none of the mutants were able to replicate confirming that a fully functional 3D^{pol} is necessary for replication to occur (Fig. 4.11). Surprisingly, only two of the three mutant replicons (ptGFP-GNN and ptGFP-DD240/5NN) could be recovered when co-transfected with an mCherry-WT replicon. These two mutant replicons (DD240/5NN and GNN) contained mutations in catalytic domains of the polymerase.

Mutant replicon ptGFP-GC216/7AA, containing a mutation in the non-catalytic polymerase dsRNA exit site, was unable to be recovered when co-transfected with a WT helper replicon (Fig. 4.11). These results suggest that only catalytic mutations GNN and DD240/5NN were able to be recovered *in trans*, opening the possibility that there were certain functions of the polymerase that could only be supplied *in cis*. It is interesting to note that the non-catalytic mutant, GC216/7AA, recombinant protein was able to incorporate ³²P-αUTP in the *in vitro* assay (section 2.10, and Chapter 3), but was unable to replicate in context of the replicon (Fig. 4.9 and Fig. 4.11) suggesting that both catalytic and non-catalytic mutations were essential for the replication of RNA.

4.3.5 Cellular localisation of FMDV 3D^{pol}

One of the reasons that the WT helper replicon could not recover the non-catalytic mutant GC216/7AA could be that the two replicons were localising to different areas of the cell and were unable to come into close enough proximity for the functional

WT polymerase to be provided to the non-functional replicon *in trans*. The use of epitope-labelled replicons could be analysed successfully by confocal microscopy, therefore in order to test this hypothesis of differential localisation BHK-21 cells were transfected with mutant C-terminal FLAG-tagged replicons in a ptGFP replicon backbone (ptGFP-GNN-FLAG, ptGFP-GC216/7AA-FLAG and ptGFP-DD240/5NN-FLAG) and C-terminal HA-tagged WT (ptGFP-WT-HA) helper replicons in a *Renilla* luciferase replicon backbone.

By removing the fluorescent reporter gene, the replicons would be able to be used for confocal microscopy with the ability to probe for more than two targets as there would be no interference from the fluorescent gene. It should be noted that by removing the fluorescent reporter the same replicons could not be monitored using the IncuCyte in real-time.

The transfected cells were fixed at four hours post-transfection as detailed in section 2.7 and the epitope tags were detected by indirect immunofluorescence using commercially available antibodies (section 2.4). The cells were analysed by confocal microscopy using a Zeiss LSM-880 confocal microscope with Airyscan (Fig 4.12a).

The results of the dual colour immunofluorescence analysis show that there is clear co-localisation of both FLAG- and HA-labelled polymerases within cells (Fig 4.12b). This is indicative of both mutant and WT polymerases targeting the same intracellular compartments. This would suggest that the lack of recovery of the GC216/7AA mutant was not due to differential localisation.

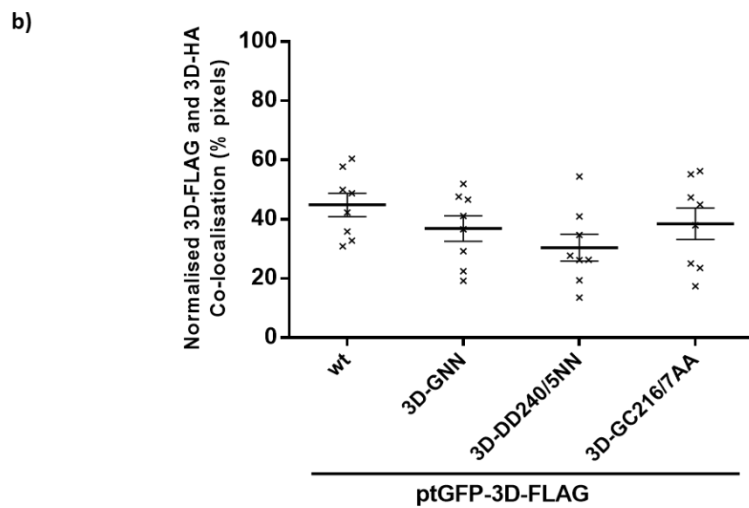
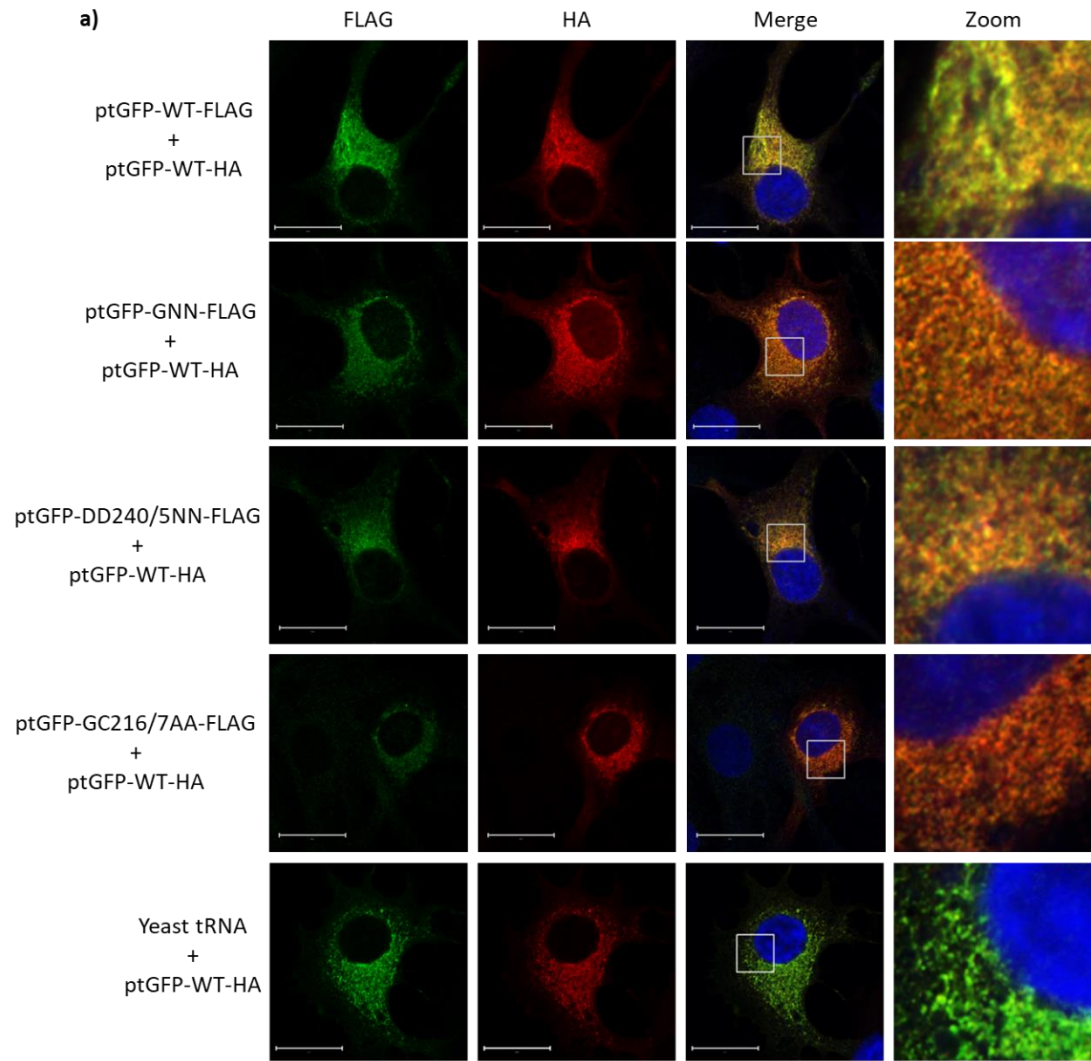


Figure 4.12 (p. 137) Dual immunofluorescence analysis showing co-localisation of WT and mutant non-structural proteins (adapted from Herod et al., 2016). A) BHK-21 cells co-transfected with FLAG-tagged mutant replicon and HA-tagged WT helper replicons. Cells were fixed at four hours post-transfection and labelled with anti-FLAG (green) and anti-HA (red) antibodies. Cell nuclei were stained with DAPI (blue). Zoomed images represent the boxed area outlined in 'merge'. Scale bar: 20 μ M. B) Quantification (%) of co-localised 3D-FLAG and 3D-HA by measuring the number of co-expressing pixels $n=8$, horizontal lines represent the mean values \pm SEM.

4.4 Role of structural RNA elements in 5' UTR in replicon recovery

There is evidence for the interaction of the non-structural proteins with the 5'UTR particularly involved in the control of translation and replication of the viral genome.

The non-structural proteins that have been identified to interact with the 5'UTR are primarily the polymerase 3D^{pol} and the precursor 3CD.

3D^{pol} and 3CD have been shown to mediate replication by binding to various structural RNA elements in the 5'UTR, such as the *cre* and the S-fragment (Nayak et al., 2005; Nayak et al., 2006; Lawrence et al., 2009). The *cre* and poly-A act as the template for VPg uridylylation which drives the production of negative strand synthesis by acting as a primer for 3D^{pol} (Paul et al., 1998; Goodfellow et al., 2000; Barton et al., 2001; Murray et al., 2003; Nayak et al., 2005; Steil et al., 2009). A current model outlined in Herod et al., 2016 suggests that 3CD, or a 3D-containing precursor, may also be able to bind to the VPg and prime for genome replication similar to the models described for the process of PV replication (Andino, Rieckhof and Baltimore, 1990; Andino, Rieckhof, Trono, et al., 1990; Andino et al., 1993; Xiang et al., 1995; Herold et al., 2001; Serrano et al., 2006; Spear et al., 2015).

A study detailed in Lawrence and Rieder, 2009 has shown that 3C binds to the S-fragment and can be co-precipitated with the large RNA structure highlighting the potential for the FMDV 3CD precursor to also be involved.

4.4.1 Role of mutations the 5' UTR in replicon recovery

To investigate the relationship of the 5' UTR structural RNA elements with non-structural proteins in the process of replicon recovery, two regions of the FMDV 5' UTR were mutated. It was hypothesised that the structured RNA elements in the 5' UTR may sequester 3D^{pol}, or its precursors, in *cis* therefore reducing their availability to assist in *trans* in the recovery of replication-deficient replicons (Herod et al., 2016).

Morgan Herod and Joseph Ward (University of Leeds) undertook mutagenesis of the first adenine nucleotide located in the conserved *cre* stem-loop sequence (AAACA) into a guanine (*cre*^{A1G}, hence GAACA) as previously described (Mason et al., 2002), and removed the S-fragment in its entirety. Both mutations to the 5' UTR structured RNA elements rendered the replicon unable to replicate (Joseph Ward, personal communication). These mutations were cloned into the helper replicon constructs and were then co-transfected with the replication-deficient polymerase mutant replicons ptGFP-GNN, ptGFP-DD340/5NN, and ptGFP-GC216/7AA.

When the replicons containing the mutations in the polymerase were co-transfected with either the tRNA control or with the mCherry-WT helper replicon, the results were the same as observed previously (Fig. 4.13). With the tRNA control, no recovery of replication was observed, as expected. When co-transfected with mCherry-WT replicon, both ptGFP-GNN and ptGFP-DD240/5NN were readily recovered. However, when the two catalytic mutant replicons ptGFP-GNN and ptGFP-DD240/5NN were co-transfected with a helper replicon mCherry- Δ S-*cre*^{A1G}, containing both mutations in the 5' UTR, levels of GFP expression was increased more than 100-fold above the tRNA control.

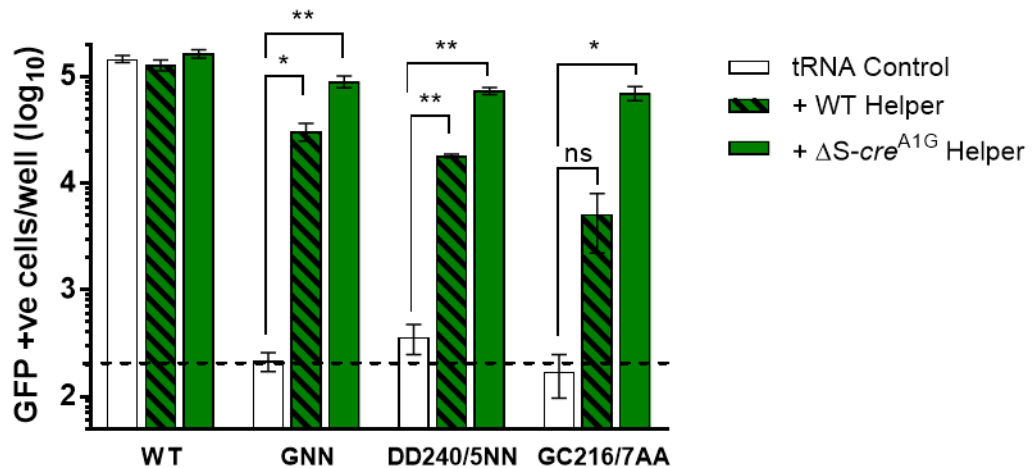


Figure 4.13 Levels of GFP expression at eight hours post-transfection of mutant polymerase ptGFP replicons (ptGFP-GNN, ptGFP-DD240/5NN and ptGFP-GC216/7AA) when co-transfected with either control tRNA, mCherry-WT or mCherry- $\Delta S\text{-cre}^{A1G}$ helper replicons. $n=3 \pm \text{SEM}$. * = $p < 0.05$, ** = $p < 0.01$.

The replicon mutant ptGFP-GC216/7AA was not recovered to the same levels as the other mutants when co-transfected with mCherry-WT helper replicon as previously observed (Fig. 4.11). However, when the replicon was co-transfected with the mCherry- $\Delta S\text{-cre}^{A1G}$ helper replicon, a greater than 100-fold increase in GFP expression was observed, similar to that seen with the catalytic mutant replicons GNN and DD240/5NN.

These data would suggest that there is a *cis* function of $3D^{pol}$ which interacts with the structured RNA elements in the 5' UTR, distinct from its catalytic polymerisation function which is provided in *trans*. By removing the RNA elements from the 5' UTR of the helper replicon that are proposed to interact with $3D^{pol}$ or with $3D^{pol}$ precursors, the WT functional polymerase would be unable to interact with the WT genome in *cis*. Conversely, it would be free to bind to the replication-deficient replicon that still has an intact 5' UTR.

4.4.2 Is 3D^{pol} sufficient to recover replication?

With the characterisation of a novel *cis* function of FMDV 3D^{pol} (Herod et al., 2016) we asked whether the presence of a functional WT 3D^{pol} was sufficient for the recovery of a replication-deficient replicon.

The FMDV genome encodes for 12 functional proteins, four structural proteins (1A-1D), followed by a short peptide sequence, 2A that is necessary for processing and separation of the structural proteins from the eight non-structural proteins (2B-3D). All 12 proteins are expressed as a single polyprotein that is co- and post-translationally processed during the replication cycle of the virus. During polyprotein processing, several precursors are formed (outlined in Fig. 4.14). The function of many of the precursors have yet to be elucidated.

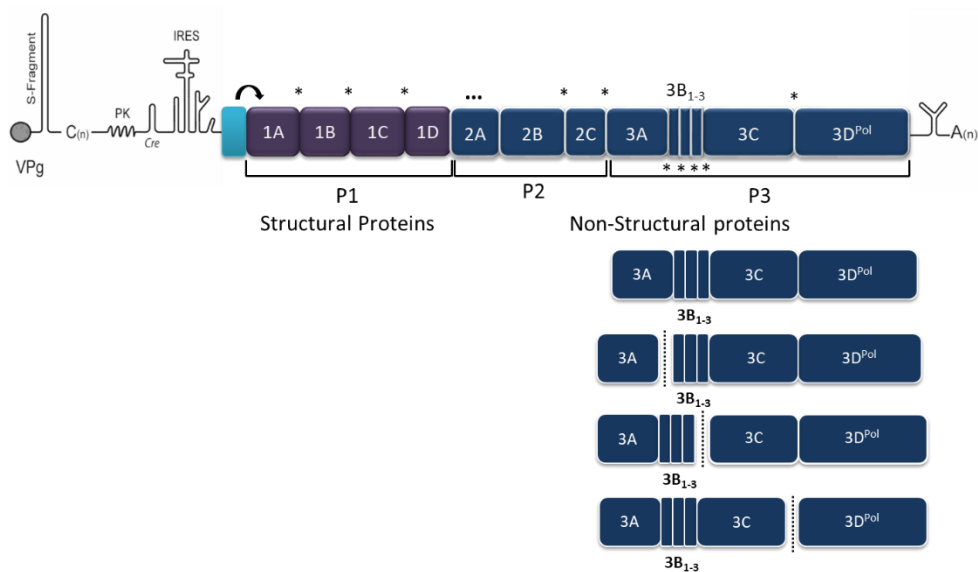


Figure 4.14 Schematic of the FMDV genome outlining the different regions (P1, P2 and P3), the structural proteins (1A-1D), and non-structural proteins (2B-3D). Arrow denotes cleavage of the polyprotein by L^{pro}. Ribosomal skipping through short peptide 2A separates the structural and non-structural proteins denoted by ellipses (...). The asterisks (*) denote cleavage by FMDV protease 3C. Schematic of some of the possible variations of P3 polyprotein processing are also shown whereby full P3 can be produced followed by 3A and 3B-3D, 3A-3B, 3A-3C, and 3C-3D before production of individual proteins.

In order to determine if 3D^{pol} was sufficient to recover a replication-deficient replicon, ptGFP-GNN, ptGFP-DD240/5NN, and ptGFP-GC216/7AA were co-transfected into BHK-21 cells with truncated replicons, as described previously. These truncated replicons (made by Morgan Herod, University of Leeds) contained the mutated 5' UTR from mCherry- ΔS -cre^{A1G} and no reporter gene. The mutated 5' UTR was linked to decreasing lengths of the genome starting from the full-length non-structural proteins 2A-3D^{pol}, successively down to just 3D^{pol} (Fig. 4.15)

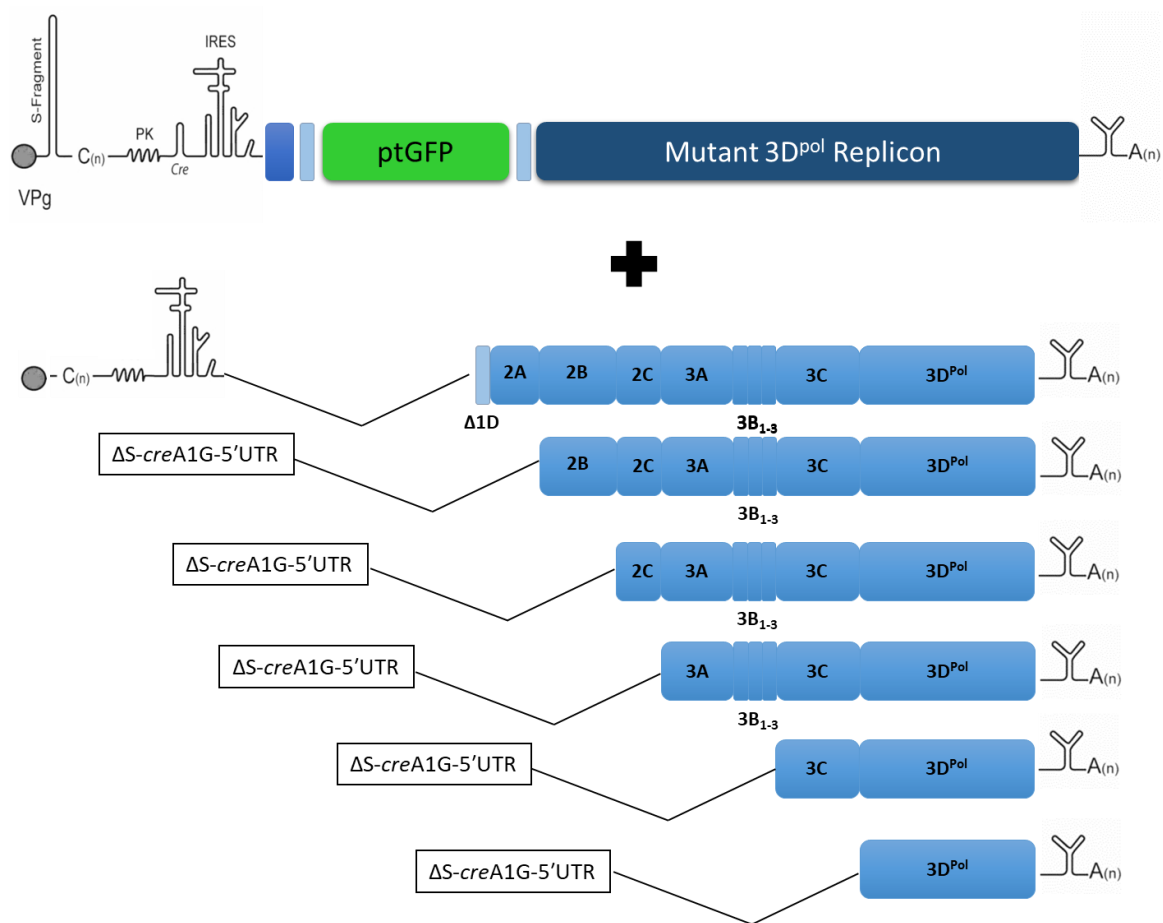
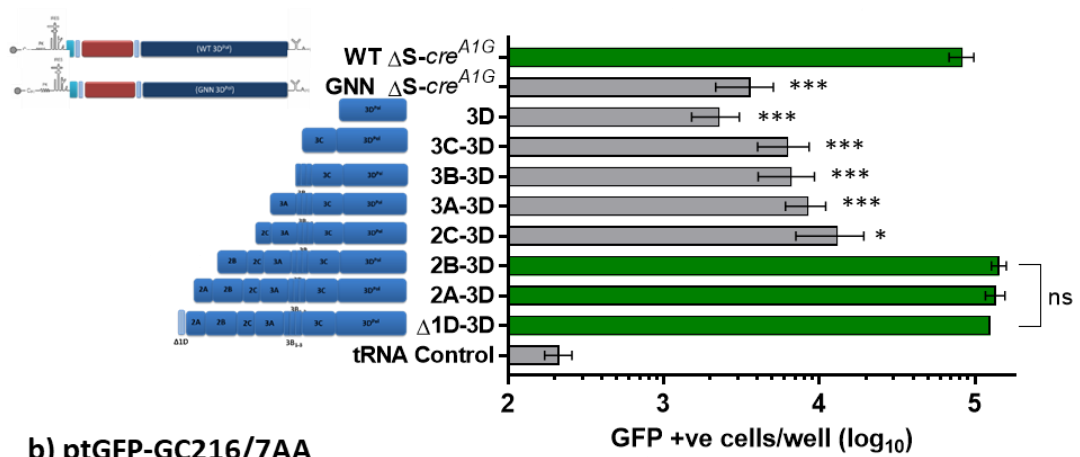


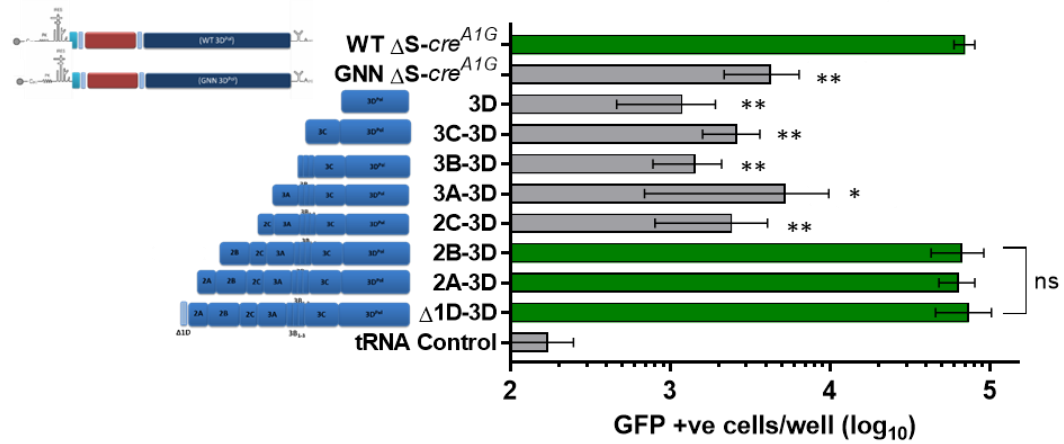
Figure 4.15 Schematic outlining the FMDV replication-deficient mutant ptGFP replicon that was co-transfected with a series of truncated helper replicons containing the mutated 5' UTR (ΔS -cre^{A1G}) into BHK-21 cells.

The replication-deficient ptGFP replicons were co-transfected with each truncated helper replicon and control helper replicons (mCherry- ΔS -*cre*^{A1G}-WT and mCherry- ΔS -*cre*^{A1G}-GNN), and tRNA. Levels of GFP expression were monitored for 24 hours using the IncuCyte FLR (Fig. 4.16). The results for the recovery of all mutant replicons with the controls were the same as previously observed with the tRNA and mCherry- ΔS -*cre*^{A1G} helper replicons as shown in figure 4.13. There was a statistically significant difference in GFP expression between all mutant replicons co-transfected with mCherry- ΔS -*cre*^{A1G}-WT and those transfected with successively truncated replicons from 2C-3D (Fig. 4.16).

a) ptGFP-GNN



b) ptGFP-GC216/7AA



c) ptGFP-DD240/5NN

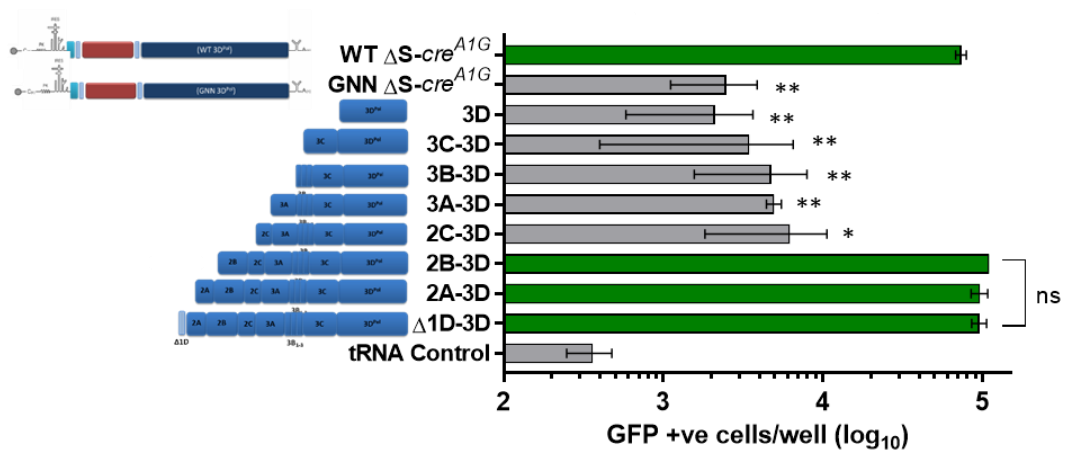


Figure 4.16 Recovery of truncated replicons. Levels of GFP expression at nine hours post-transfection of mutant polymerase ptGFP replicons co-transfected with control tRNA, control mCherry- $\Delta S\text{-cre}^{A1G}$ WT and GNN helper replicons, against truncated P2 and P3-containing replicons compared to the control mCherry- $\Delta S\text{-cre}^{A1G}$ WT replicon (A) ptGFP-GNN n = 6 \pm SEM, B) ptGFP-GC216/7AA n = 4 \pm SEM and C) ptGFP-DD240/5NN n = 2 \pm SEM. Statistical analysis performed using two-tailed unpaired t-test; * = p > 0.05, ** = p > 0.01, *** = p > 0.001.

Recovery of GFP expression in the mutant replicons ptGFP-GNN, ptGFP-GC216/7AA, and ptGFP-DD240/5AA to the levels of mCherry- Δ S-*cre*^{A1G}-WT co-transfected replicons was achieved when co-transfected with truncated replicons of increasing size from 2B-3D (Fig. 4.16).

It was interesting to observe that, although 3D^{pol} alone was not sufficient to recover replication in any of the replication-deficient mutant replicons, the full non-structural protein region was not necessary. The results across all the mutants show that when the size of the helper replicon was at least the size of 2B-3D, the replication-deficient replicon could be recovered to produce the same levels of GFP expression as when co-transfected with the mCherry- Δ S-*cre*^{A1G}-WT helper replicon. It appears from these data that 2B, 2BC, or a P2-P3 precursor may be important for the recovery of replication-deficient replicons. Alternatively, the cleavage site between 2B and 2C could also be a region of interest in the same vein as the importance of the 3B3-3C cleavage boundary as described in the recent Herod *et al.* publication (Herod et al., 2017).

4.5 Discussion

In this chapter, we have investigated the phenotype of several of the mutations in the FMDV polymerase, 3D^{pol}, that were identified by transposon mutagenesis as described in Herod et al., 2015. Two mutations in 3D^{pol} were located in catalytic sites (GNN, also termed DD388/9NN, and DD240/5NN) and one was located in a non-catalytic region (GC216/7AA). All three mutations resulted in an inability to replicate replicon RNA when transfected into cells. However, the mutations did not appear to affect the cellular localisation of the polymerase as identified by immunofluorescence.

The ability for picornaviruses to provide non-structural proteins in *trans* has been well documented, particularly the interactions between non-structural proteins 2B, 3A, and 3D with structural RNA elements such as the *cre* and the IRES (Giachetti et al., 1992; Ryan et al., 1994; Xuemei Cao et al., 1995; Teterina et al., 1995; Towner et al., 1998; Lyons et al., 2001; Tiley et al., 2003; Nayak et al., 2005).

Here, the mutant replicons, ptGFP-GNN, ptGFP-GC216/7AA, and ptGFP-DD240/5NN, were co-transfected with replicons containing a WT 3D^{pol} in an attempt to recover their activity. The two polymerase replicons that contained mutations in the catalytic domains of 3D^{pol} were shown to be readily recovered by a functional WT helper replicon when the two were co-transfected within cells, however, the non-functional mutation located in the dsRNA exit site, GC216/7AA was not able to be recovered with a functional WT helper replicon. These data would point to the existence of a necessary secondary non-catalytic function of the polymerase that could not be provided in *trans*.

It was hypothesised that the polymerase has a secondary *cis*-preferential function that interacted with the structured RNA elements within the 5' UTR. The hypothesis led to the removal of these RNA elements (S-fragment and *cre*) from the WT helper replicon. This could increase the “availability” of the WT 3D^{pol} as it would no longer be able to bind in *cis* to the parental genome and would thus be recruited by the replication-deficient replicon. Since the replication-deficient replicon would have a fully structured 5' UTR, the WT 3D^{pol} would be able to bind to those structures and provide its necessary *cis*-function in addition to its catalytic (*trans*) function. In the case of the GC216/7AA mutant, *in vitro* studies outlined in chapter 3 showed that the protein was catalytically active and could bind RNA with similar affinity to WT and could also incorporate radiolabelled UTP nucleotides to a similar rate as WT. The results would suggest that the *trans* activity within replicon could be provided by the mutant. However, replicon studies show that this mutation rendered the replicon non-functional as well as non-recoverable unless the structured 5' UTR elements were removed, suggesting that the *cis* function was vital for replication of the replicon RNA.

The two different functions of 3D^{pol} described here alongside the results discussed in chapter 3 that highlight the ability for FMDV WT 3D^{pol} to form fibrils provide an attractive hypothesis that these higher-order structures could act as “sponges” for withholding polymerase molecules and maintaining an appropriate equilibrium of enzyme to RNA. In order to test this hypothesis proposed experiments include performing complementation assays with the different mutants (catalytic and non-catalytic) and observing their ability to replicate in the context of replicon, as well as

in the context of recombinant proteins within activity assays and fibril formation assays.

The non-covalent interaction of viral non-structural proteins and host proteins with the 5' and 3' UTRs have been shown to be necessary for the formation of a ribonucleoprotein complex that may facilitate the process of replication, transcription, and translation of the PV genome (Herold et al., 2000; Barton et al., 2001; Herold et al., 2001). In FMDV, replication is thought to begin with the binding of 3D^{pol} to the uridylylated VPg in the presence of 3CD. The template for VPg uridylylation is the *cre* located in the 5' UTR. A copy of uridylylated VPg (VPg-pUpU) is covalently linked to the 5' end of the daughter strand and acts as a primer for positive strand synthesis (Goodfellow et al., 2003; Murray et al., 2003; Nayak et al., 2005; Steil et al., 2009). Studies have shown that FMDV 3CD is also able to bind to the S-fragment, equivalent to PV 3CD binding to its cloverleaf structure (Nayak et al., 2006; Lawrence et al., 2009). In PV, the switch from translation to replication on the genomic RNA is thought to be mediated by the binding of the cellular protein PCBP to the cloverleaf. This binding enhances viral translation, while the binding of the viral protein 3CD represses translation and facilitates negative-strand synthesis (Gamarnik and Andino, 1998; Serrano et al., 2006). However, biochemical studies have shown that 3CD has no polymerase activity in PV, suggesting that the processing of 3CD into active 3C and 3D^{pol} is essential for the function of 3D^{pol} (Flanegan and Baltimore, 1979; Flanegan and Van Dyke, 1979; Harris et al., 1994). The studies reported in Chapter 3 have also demonstrated no polymerase activity for FMDV 3CD.

The data presented here, and additional studies outlined in Herod et al., 2016 and Herod et al., 2015 are consistent with studies performed on both PV and HCV. A recent study in PV by Spear et al., 2015 proposed a mechanism to characterise the role of 3D^{pol} and its precursors during replication using a cell-free system. The model based on their data suggested that 3D^{pol} entered the replication complex in the form of its precursor, P3 (or 3CD), and was cleaved to release the active polymerase enzyme. One P3 molecule (or smaller precursor 3CD) binds directly to the 5' UTR, while a second precursor molecule provides the functionally active 3D^{pol} (Spear et al., 2015). In HCV, similar co-transfection studies outlined in Kazakov et al., 2015 showed that the RdRp NS5B could be supplemented in *trans*, it was also required in *cis* indicating that the polymerase had an essential *cis*-acting role distinct from its enzymatic activity (Kazakov et al., 2015; Gomes et al., 2016).

The non-recoverable mutant GC216/7AA, which has helped identify an essential *cis*-preferential role for FMDV 3D^{pol}, contains a mutation in the dsRNA binding/interacting residues located in the dsRNA exit sites. This mutant polymerase, as shown in Chapter 3, was still able to bind RNA as shown by fluorescent anisotropy assays, and was able to incorporate [α -³²P] UTP. However, in context of the FMDV replicon, it resulted in a phenotype unable to replicate.

The S-fragment, proposed to have a long stem-loop structure (Bunch et al., 1994), is inherently highly base-paired. This structure could point to a potential interaction between the polymerase and the 5' UTR. By mutating the dsRNA exit site residues, the interaction was abrogated. However, it is interesting to note that a study showed no interaction between the polymerase and the S-fragment by co-

immunoprecipitation (Lawrence et al., 2009). This may suggest that the interaction is with a polymerase precursor, or by a separate protein.

Despite both *cis* and *trans* functions of 3D^{pol} being necessary for replication to occur, the polymerase, or its precursors, were not sufficient to recover replication of a mutant replicon. For recovery to occur it appears that having a minimum size for a helper replicon that includes 2B may be important for recovery, however, it is not known if 2B alone is sufficient for replicon recovery. The function of FMDV 2B protein is still not very well understood. Recent studies have suggested that 2B may be a viroporin due to the presence of two putative transmembrane domains that target the ER membrane and induces damage to the host-cell membrane integrity (Ao et al., 2015; Gao et al., 2016). However, the viroporin activity of 2B in FMDV has still not been confirmed.

Some reports have indicated that 2B may also function synergistically with other non-structural proteins, particularly with 2C, or as the precursor 2BC. These studies have shown that the presence of 2BC or the co-expression of 2B and 2C abolished ER-to-Golgi transport of cellular proteins during infection (Moffat et al., 2005; Moffat et al., 2007; Gao et al., 2016).

There has been no evidence to date of a direct interaction between FMDV 2B and 3D^{pol} however, the potential function of 2B, or the precursor 2BC, to dysregulate the ER membrane could be necessary for FMDV replication to occur by facilitating the recruitment of cellular membranes within which a replication complex can form.

Work is ongoing to determine whether it is the RNA structure or the protein function of 2B that is important in the recovery of mutant replicon RNA. To do this, the 2B

RNA sequence has been scrambled to produce synonymous mutations of every codon, this ensures that although the native RNA structure is disrupted, the protein sequence remains the same and thus protein function should not be disrupted. Cloning of the scrambled 2B region into the helper replicon has been undertaken by Morgan Herod (University of Leeds), and ongoing studies will evaluate this construct.

Chapter 5

Foot-and-mouth disease virus genome replication is unaffected by inhibition of type III phosphatidylinositol-4-kinases

5.1 Introduction

Due to the highly infectious nature of FMDV, handling is restricted to a small number of facilities worldwide. Sub-genomic replicons were developed to allow for the study of viral replication in laboratories at lower containment level (Forss et al., 1984; McInerney et al., 2000; Tulloch et al., 2014). The FMDV replicon constructs employed here (GFP-pac-WT) have the structural proteins replaced by a GFP reporter and a puromycin acetyltransferase resistance gene cassette. Replication-deficient constructs have a GDD to GNN substitution in the catalytic active site of 3D^{pol} (GFP-pac-GNN) as described previously (refer to Chapters 3 and 4, also termed DD388/9NN). Levels of GFP expression over time can be measured using an IncuCyte Dual Colour ZOOM[®] FLR (Forrest et al., 2014; Tulloch et al., 2014; Herod et al., 2015). Replicons have also been used to study the replication of a number of other viruses. Here, we have also used hepatitis C virus (HCV) sub-genomic replicons pSGR-Luc-GFP-JFH-1 (Jones et al., 2007) and SGR-feo-JFH-1 (Wyles *et al.*, 2009), together with a Coxsackievirus B3 (CVB3) sub-genomic replicon, pRib-Fluc-CB3/T7 (Lanke et al., 2009).

Replication of a number of positive-sense RNA viruses has been shown to occur at cytoplasmic membrane-associated sites (den Boon et al., 2010). The formation of

such membrane compartments is thought to allow for the creation of a kinetically-favourable environment in which viruses can replicate rapidly and effectively, concurrently protecting the replication machinery from the hostile environment of the host cell. A number of viruses including CVB3, PV, and HCV have been shown to subvert and rearrange the membranes of the ER, Golgi, and *trans*-Golgi network in order to form discrete intracellular membranous complexes where viral replication can take place in a protected environment within the cytoplasm, as well as maintaining a region of high concentration of viral proteins for efficient virus assembly. Membranes rich in phosphatidylinositol-4-phosphate (PI4P) lipids, such as those found on the Golgi complex, have been specifically implicated in the replication of multiple members of the *Picornaviridae* and *Flaviviridae* families, including PV, enterovirus 71, CVB3, encephalomyocarditis virus (EMCV), and HCV (den Boon et al., 2010; Altan-Bonnet et al., 2012; Dorobantu, Albulescu, et al., 2015).

The relationship between PI4P and the role it plays in viral replication has been well-defined through studies with HCV (Trotard et al., 2009; Reiss et al., 2011; Bishé et al., 2012; Zhang et al., 2012). HCV, a +ve ssRNA virus in the family *Flaviviridae*, and the causative agent of hepatitis C and related sequelae including hepatocellular carcinoma, utilises a number of phosphoinositide (PI) lipids and kinases to build cytoplasmic membrane-associated replication complexes. PIs are phosphorylated derivatives of phosphatidylinositol. It has been documented that the primary kinase used by HCV for viral replication is phosphatidylinositol-4-kinase III α (PI4KIII α) (Trotard et al., 2009). HCV has also been shown to utilise another related pathway, the phosphatidylinositol-3-kinase (PI3K) pathway, especially during the formation of autophagosomes within the cells (Sir et al., 2012; Liu et al., 2012; Mohl et al., 2016).

Another well-characterised virus that utilises the PI pathway is CVB3, a +ve ssRNA virus and a related picornavirus to FMDV. It is a cardiotropic virus and is primarily known for its role as a causative agent of myocarditis (Melnick et al., 1949; Garmaroudi et al., 2015). Multiple studies have shown that CVB3 is dependent on PI4KIII α and PI4KIII β for replication as it hijacks the function of these kinases, including their interacting partners such as oxysterol binding protein and becomes able to subvert intracellular membrane formation in favour of viral replication (Greninger et al., 2012; van der Schaar et al., 2012; Arita et al., 2013; van der Schaar et al., 2013; Dorobantu et al., 2014). As a result, both HCV and CVB3 serve as excellent controls to investigate the effects of PI4K and PI3K inhibitors on FMDV translation and replication.

5.2 The role of phosphoinositides in virus RNA replication

Different intracellular membrane-bound organelles contain one of the seven distinct PI species (Matteis et al., 2004; Di Paolo et al., 2006; Krauß et al., 2007). For example, the plasma membrane contains more free phosphatidylinositol 4,5-bisphosphate than PI4P, which is found predominantly on Golgi-derived membranes (Matteis et al., 2004; Krauß et al., 2007). The distribution of PIs on the different intracellular membranes is largely determined by the enzymatic activity of specific lipid kinases and phosphatases.

Phosphorylation of PI lipids on the 4-carbon of the inositol ring which generates PI4P (Fig 5.1) is affected by the up-regulation and selective recruitment of PI4K (Fig 5.2). There are two types of well-defined families of PI4Ks: type II (PI4KII α and PI4KII β) and type III (PI4KIII α and PI4KIII β). Previous studies on PV and CVB3 have identified PI4KIII β as the host enzyme upregulated in viral replication factories (Belov et al., 2007; Lanke et al., 2009; Hsu et al., 2010; Arita et al., 2011). Depletion of PI4KIII β activity within infected cells by RNA silencing or the use of kinase inhibitors, such as PIK93 (Knight et al., 2006), were shown biochemically to be able to block PV and CVB3 viral RNA synthesis and virus replication. In contrast, HCV replication is generally accepted to be dependent on PI4KIII α activity (Berger et al., 2011; Reiss et al., 2011; Bishé et al., 2012), although there is some evidence for a dependence on PI4KIII β (Borawski et al., 2009; Arita et al., 2011; Zhang et al., 2012).

The PI4K family represents a possible pan-viral therapeutic target, however, involvement in FMDV replication has yet to be clearly defined. Using bi-cistronic

reporter constructs and sub-genomic replicons, we have compared the effects of type III PI4K and PI3K inhibitors on FMDV with other positive-sense RNA viruses. Using this approach, we have separated effects on RNA translation from direct effects on genome replication and show that FMDV replication appears not to be significantly dependent on either kinase pathway.

Another class of PIs, phosphatidylinositol 3,4-bisphosphate (PI(3,4)P₂) and its related kinase PI3K, has also been shown to be involved in viral RNA replication, particularly during HCV replication (Fig 5.1). PI(3,4)P₂ synthesis on endosomal membranes is initiated after clathrin-mediated endocytosis by PI3K. There are three classes of PI3Ks active in a mammalian cell. Class I PI3Ks (p110 α - δ) are involved in engaging the Akt pathway (a signal transduction pathway also known as the PI3K-Akt pathway) and acting as effectors to further downstream activation of the pathway required for cell growth and survival by generating PIP₃ (phosphatidylinositol (3,4,5)-triphosphate) phospholipids concentrated at the plasma membrane. Classes II and III PI3Ks are involved in intracellular trafficking through the synthesis of PI3P lipids by phosphorylating PIs.

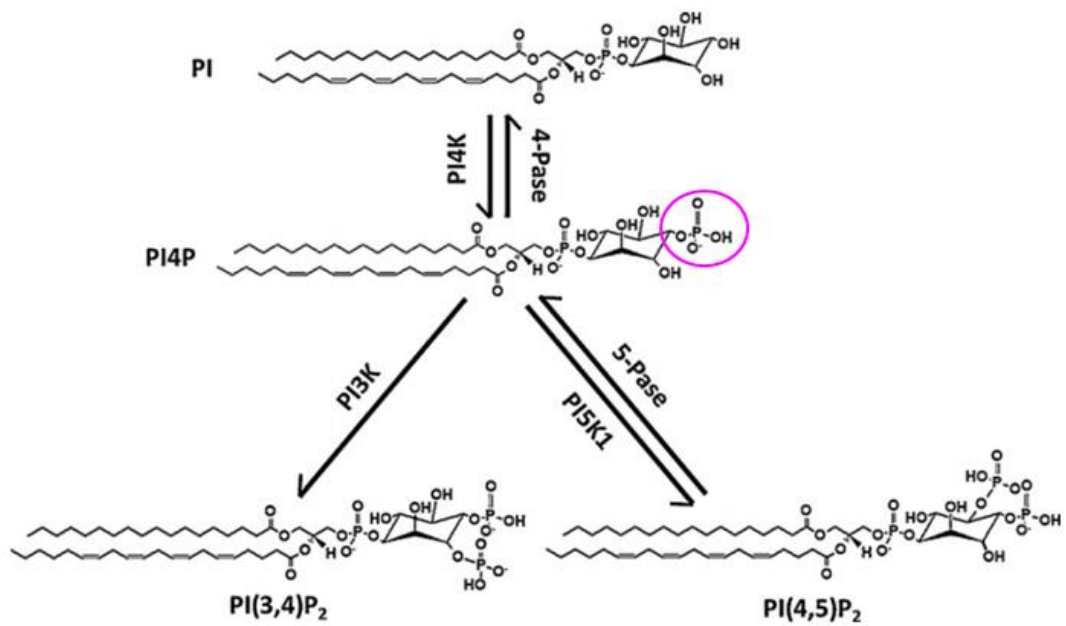


Figure 5.1 Schematic adapted from Delang et al., 2012 showing the chemical structures of the different PI phosphorylation states. PI4K phosphorylates the 4-carbon on the inositol ring (highlighted) to form PI4P, the reaction is reversible with the catalytic activity of phosphatidylinositol 4-phosphatase (4-pase). PI4P is an intermediate lipid which can be further phosphorylated into phosphatidylinositol 3,4-bisphosphate (PI(3,4)P₂) or phosphatidylinositol 4,5-bisphosphate (PI(4,5)P₂) by PI3K or phosphatidylinositol 5-kinase (PI5K1), respectively.

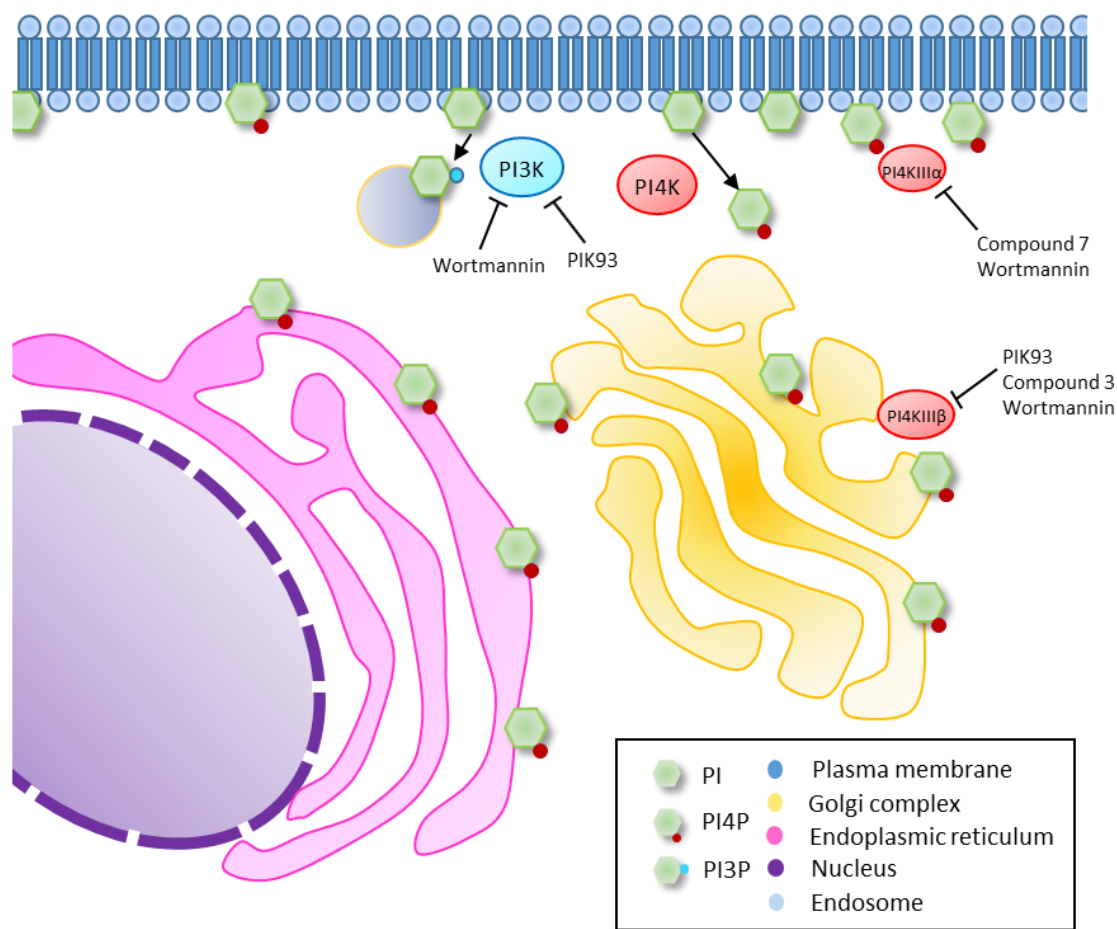


Figure 5.2 Simplified diagrammatic representation of the localisation of phosphatidylinositol (PI) lipids in the cell. Unphosphorylated PI is concentrated on the plasma membrane. PI is phosphorylated by either PI4Ks and PI3K into PI4P or PI3P, and thus translocate to intracellular membranes where the phosphorylated PIs are active. PI4P lipids are concentrated on the Golgi complex, as well as on the plasma membrane and are responsible for intracellular transport. PI4KIII α primarily is active on PIs located on the plasma membrane, whereas PI4KIII β is functional on Golgi-associated PIs. Additionally, inhibitors to each kinase is highlighted.

5.3 Inhibitors of phosphatidylinositol-4 kinases

Previous studies have identified the prominent role that the PI4KIII β pathway plays in the development of intracellular viral replication factories in cells infected with other positive-sense RNA viruses (e.g. HCV, PV and CVB3) (Altan-Bonnet et al., 2012). CVB3, HCV, and PV infection results in a dramatic remodelling of the host-cell secretory membrane pathway. During peak replication times of these viruses (approximately 6 hours post infection for enteroviruses) a large pool of viral proteins involved in genome replication are found localised within membranous organelles at the Golgi and ER membranes (Hsu et al., 2010; Limpens et al., 2011; Reiss et al., 2011; Belov et al., 2012). These membrane-bound organelles have been shown by immunofluorescence and coimmunoprecipitation to contain high levels of PI4KIII β ; the enzyme responsible for catalysing the production of PI4P lipids in the ER membrane. Depletion of PI4KIII β from the cells by either siRNA or through the use of inhibitors (such as PIK93), results in a marked reduction in PV and CVB3 RNA synthesis (Knight et al., 2006; Hsu et al., 2010; Arita et al., 2011; Greninger et al., 2012). Similarly HCV infection enhanced the production of PI4P through stimulation of both PI4KIII α and PI4KIII β , and depletion of PI4P also inhibited HCV RNA synthesis (Borawski et al., 2009; Berger et al., 2011; Zhang et al., 2012).

In order to elucidate the role of the intracellular lipid PI4P in the formation of FMDV replication factories, a number of small-molecule inhibitors of the lipid pathway were used to treat replicon-transfected BHK-21 cells. These were the well-characterised inhibitors PIK93 and wortmannin, alongside two novel compounds recently developed by AstraZeneca.

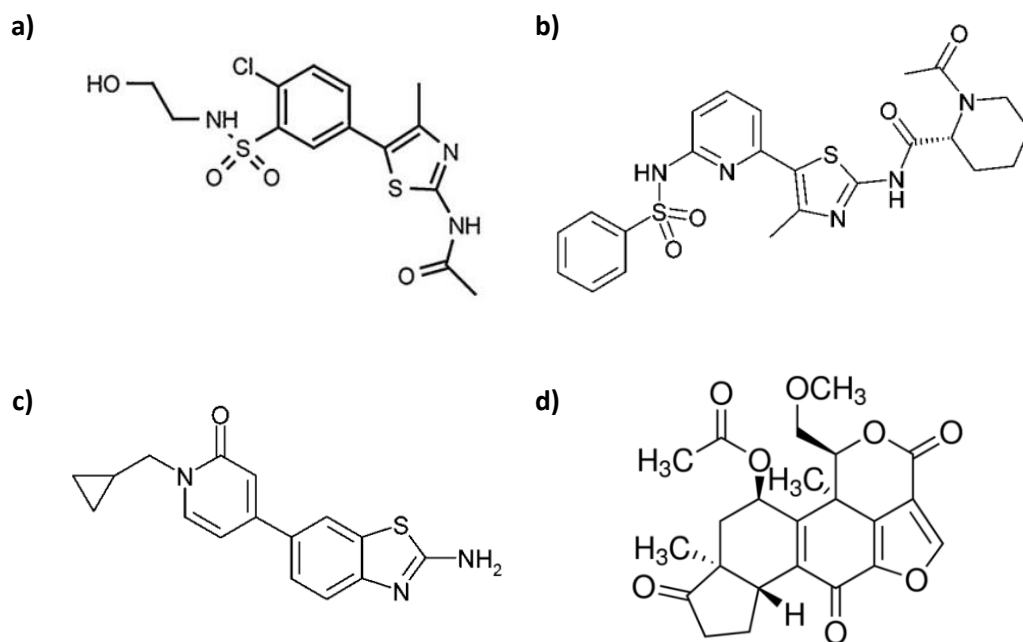


Figure 5.3 Chemical structures of the PI4K inhibitors used. A) Phenylthiazole PIK93 (adapted from Knight et al., 2006), B) AstraZeneca PI4KIII β inhibitor, compound 3 (adapted from Waring et al., 2014). C) AstraZeneca PI4KIII α inhibitor, compound 7 (adapted from Waring et al., 2014). D) Fungal steroid metabolite, wortmannin (adapted from NCBI, PubChem Substance Database; SID=24278777).

5.3.1 PIK93

PIK93 was originally developed as an inhibitor of a class I PI3K, p110 α (IC₅₀: 39 nM) as a treatment for diabetes, due to the key role the kinase plays in the downstream activity of the insulin receptor.

PIK93 is a phenylthiazole compound (Fig. 5.3a), a multi-targeted compound designed to have several target selectivities within the PI-kinase family. It was shown to have a potent effect against members of the PI4K family of enzymes, particularly on PI4KIII β (IC₅₀ PI4KIII α : 1.1 μ M, PI4KIII β : 19 nM) despite being designed as a PI3K inhibitor (Knight et al, 2006).

5.3.2 Compounds 3 and 7

Recently, the pharmaceutical company AstraZeneca (AZ) produced a number of different compounds from a 100,000-compound screen with complementary selectivities for PI4KIII α and PI4KIII β (Waring et al., 2014; Raubo et al., 2015). These compounds were designed to inhibit the phosphatidylinositol signalling cascade and cancer cell proliferation (Waring et al., 2014). Compound 7 (Fig 5.3c) exhibits selective inhibition of PI4KIII α (IC₅₀ PI4KIII α : 7 nM, PI4KIII β : 1.8 μ M), whereas Compound 3 (Fig 5.3b) exhibits a similar selectivity as PIK93 on PI4KIII β (IC₅₀ PI4KIII α : 7.3 μ M, PI4KIII β : 15 nM). These compounds are termed CMPD (7) and CMPD (3), respectively, in their literature.

5.3.3 Wortmannin

Wortmannin (Fig 5.3d) is a fungal steroid metabolite from *Penicillium funiculosum* and a potent inhibitor of PI3K (Powis et al., 1994; Wymann et al., 1996). Wortmannin functions to inhibit PI3K in a non-competitive, irreversible, and non-specific manner; as a result it is able to interact with other PI3K-related proteins, including PI4K (Powis et al., 1994; Nakanishi et al., 1995; Downing et al., 1996; Meyers et al., 1997). Its mode of action is by binding irreversibly to the catalytic domain of the enzyme inhibiting its function. It has also been used to inhibit autophagy induced by HCV replication in HCV-infected cells. (Wu et al., 2010; Mohl et al., 2016).

5.4 Effect of PI4K on IRES-mediated translation

Many positive-sense RNA viruses have been documented to replicate in membrane-associated complexes (den Boon and Ahlquist, 2010). There have been several reports demonstrating the mechanism of inhibitors affecting membrane lipid modification, such as PIK93, on viral replication. However, with the use of GFP-expressing replicons, it has been difficult to separate effects on translation of input viral RNA with those effecting genome replication. To elucidate effects of various inhibitors including PIK93 on host and viral translation, we exploited the use of bi-cistronic vectors containing *renilla* luciferase (Rluc) and firefly luciferase (Fluc) reporter genes under the control of either cap- or IRES-dependent translation mechanisms, respectively (Licursi et al., 2011) (Fig 5.4). We have employed a similar approach previously to demonstrate the absence of any non-specific effects on translation with RNA aptamers selected to FMDV 3D^{pol} (Forrest et al., 2014).

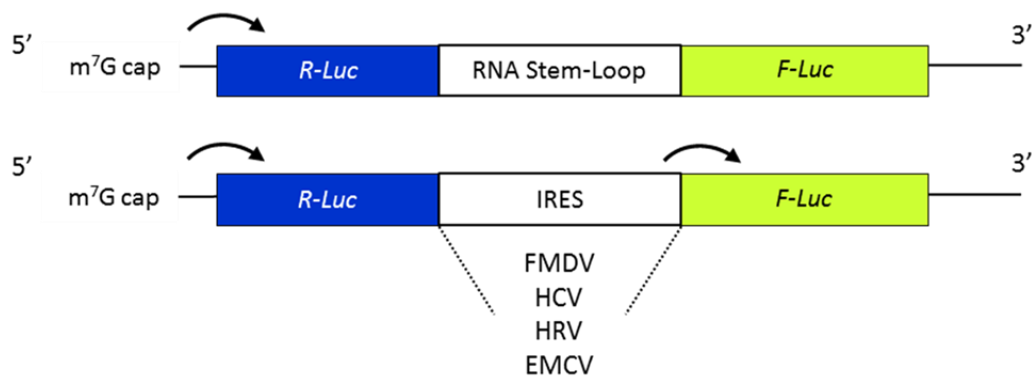


Figure 5.4 Schematic of bi-cistronic reporter constructs. The control (pRF) contains a structured RNA stem-loop element in place of an IRES resulting in minimal Fluc expression. The test constructs contain an IRES from different viruses including FMDV, HCV, HRV, and EMCV. All constructs have a 7-methylguanosine cap which allows for Rluc expression to test for efficient transfection in BHK-21 cells.

Five different constructs were used; a control (pRF) with no IRES structure, resulting in minimal Fluc expression, and constructs in which Fluc translation was controlled by the IRES from FMDV, HCV, human rhinovirus (HRV), or EMCV. The HRV IRES is type I, EMCV and FMDV are type II, and the HCV IRES is classed as a type III (Tsukiyama-Kohara et al., 1992; Belsham, 2009; Martínez-Salas et al., 2015).

Following transfection of the bi-cistronic reporter constructs into BHK-21 cells as described in sections 2.6.4 and 2.6.5, translation was assessed by measuring the levels of *renilla* and firefly luciferase luminescence produced as a result of cap-dependent and IRES-dependent translation respectively, in the presence or absence of the inhibitor PIK93 in increasing concentrations (0-5 μ M). A preliminary MTT assay did not reveal any reduction in cell viability in the presence of PIK93 at any of the concentrations used for the translation assay (Fig 5.5).

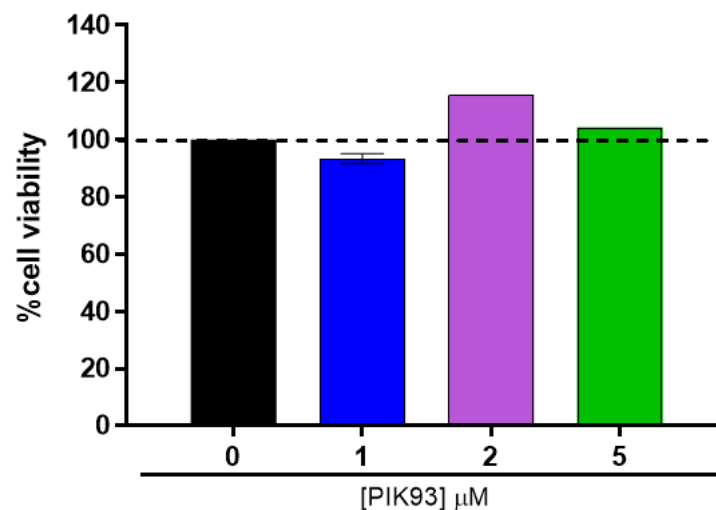


Figure 5.5 MTT cytotoxicity assay of a range of PIK93 concentrations (0-5 μ M) on BHK-21 cells. The assay shows no cytotoxicity of PIK93 on cells at the concentrations used (0-5 μ M) based on the percentage of viable cells, normalised to the untreated control (0 μ M). Data showing mean values with SEM (n = 2).

For all of the bi-cistronic constructs used, there was a modest but non-significant inhibition of cap-mediated translation in the presence of an increasing concentration of PIK93 (0–5 μ M). However, the effects of PIK93 on IRES-mediated translation (Fig. 5.6b) were more profound. There was an average decrease in luciferase signal ranging from 44.2 ± 13.5 % in constructs treated with 1 μ M to 73.3 ± 5.0 % in those treated with 5 μ M PIK93. Treatment with concentrations higher than 1 μ M of PIK93 significantly reduced FMDV, HCV, and EMCV IRES-driven luciferase expression. However, with the HRV IRES, a significant reduction in luciferase expression was only observed at 5 μ M PIK93.

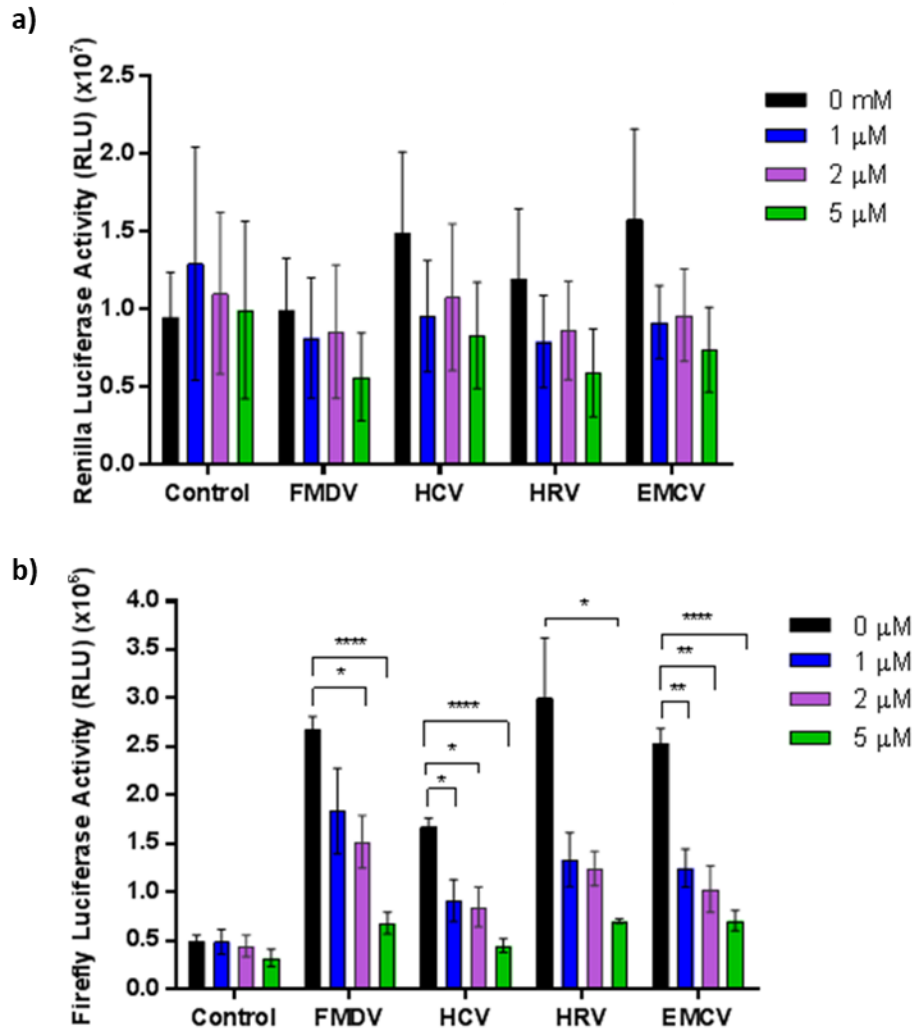


Figure 5.6 BHK-21 cells transfected with the bi-cistronic constructs and treated with varying concentrations of PIK93 for 48 hours. The data show levels of luciferase expression under the control of (a) Cap-mediated translation, and (b) IRES-mediated translation. The control (pRF) contains the Firefly reporter under the control of a non-IRES structure and the *Renilla* reporter under the control of cap-mediated translation. Data showing mean values with SEM (n = 3). Statistical analysis performed using two-tailed unpaired t-test; * = p < 0.05, ** = p < 0.01, *** = p < 0.001, **** = p < 0.0001).

5.5 Effect of PI4K on RNA replication

The result of the initial translation assay and treatment with PIK93 brings into question whether some of the documented effects of PIK93 on replication could be the result of suppression of input viral RNA translation. In order to clarify this, we compared the effects of PIK93 on the replication of wildtype (WT) and replication-deficient FMDV replicons with those of CVB3, previously shown to be dependent on PI4K activity (Lanke et al., 2009). Due to the different reporters used, replication was monitored by luciferase assay or by GFP expression.

The development of the FMDV GFP-pac replicon and optimisation of the replication assay has been previously described (Forrest et al., 2014). Replication was detected by measuring the levels of GFP expression over time using an IncuCyte Dual Colour ZOOM® FLR (Tulloch et al., 2014), with maximum fluorescence values being observed at 8-10 hours post-transfection. At this time-point up to 80 % of cells transfected with the GFP-pac-WT replicon RNA expressed high levels of GFP, and therefore replication can be equally assessed by either number of GFP positive cells or total GFP fluorescence. Use of the replication-deficient mutant replicon (GFP-pac-GNN) resulted in a markedly lower GFP signal (i.e. as a result of input translation only). Levels of GFP expression in GFP-pac-GNN replicon-transfected cells were similar to those with a second replication-deficient replicon, GFP-pac-Δ3D that contained a large deletion in the 3D^{pol} gene (data not shown) (Tulloch et al., 2014).

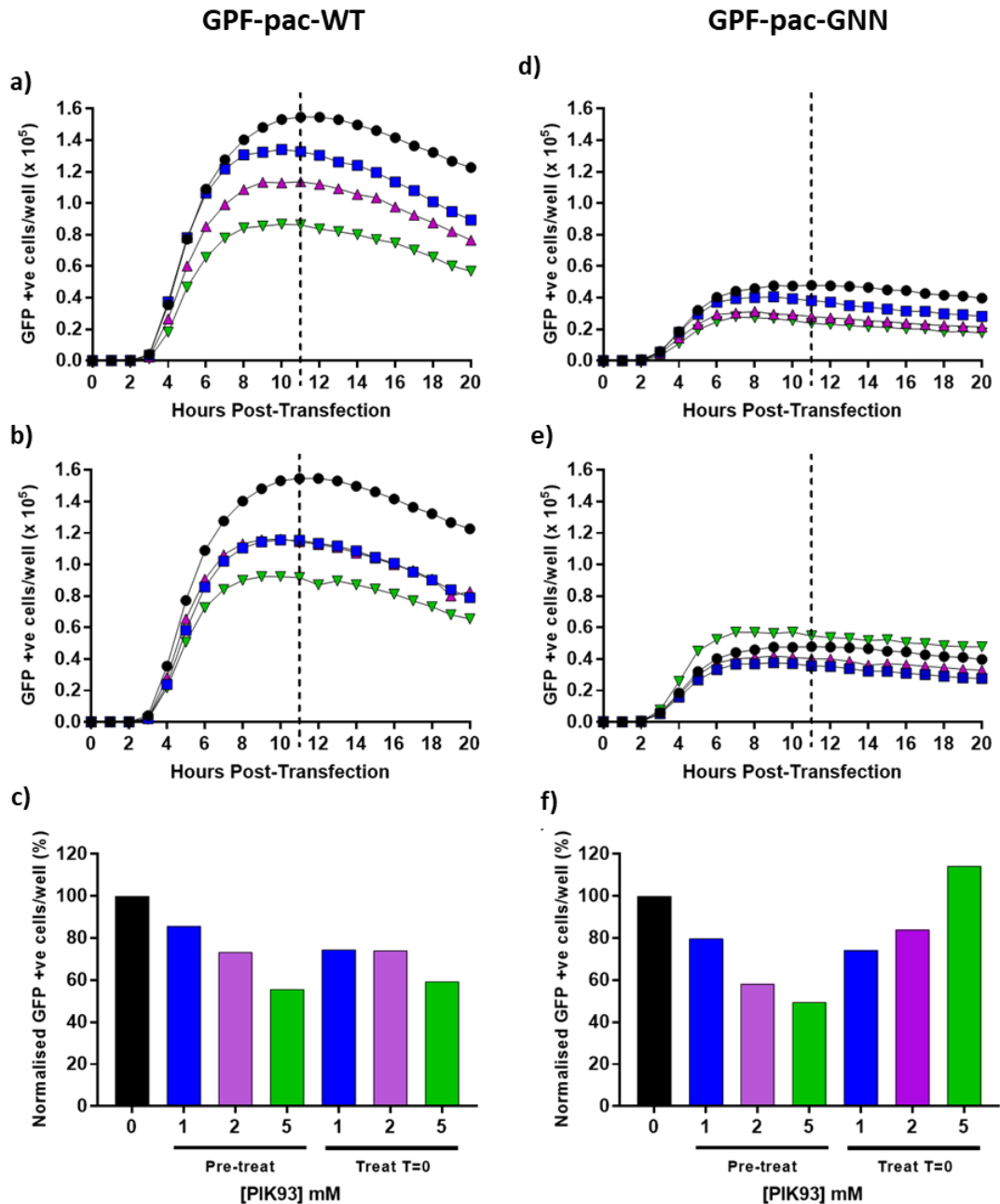


Figure 5.7 Levels of GFP expression as a measure of replication in BHK-21 cells transfected with replicon RNA. BHK-21 cells transfected with GFP-pac-WT (a, b, and c) or GFP-pac-GNN (d, e, and f) were either pre-treated for two hours with PIK93 at the indicated concentrations, or concurrently with transfection (T=0). Levels of GFP expression of pre-treated cells transfected with GFP-pac-WT and GFP-pac-GNN were measured over 20 hours (a, b, d, and f). Levels of GFP expression of the treated and untreated cells were compared against untreated controls at peak GFP expression (11 hours). GFP data were collected by imaging GFP fluorescence hourly in transfected cells using an IncuCyte Dual Colour ZOOM[®] FLR and measuring the number of GFP-expressing cells per well. (n = 1).

Due to the observed lack of cytotoxic effects of PIK93 on the cells at the concentrations used for the MTT assay (Fig 5.5), the same concentrations of PIK93 were applied to the cells at two hours prior to transfection. The effects of the addition of PIK93 prior to transfection were investigated to assess if depleting intracellular PI4P prior to transfection would further affect the ability for the replicon to replicate.

Results outlined in Fig. 5.7 show that for both GFP-pac-WT and GFP-pac-GNN, two-hour pre-treatment of cells with PIK93 results in the greatest inhibition of GFP expression than in cells treated with PIK93 at the same time as transfection (T=0). In WT-transfected cells, pre-treatment with 5 μ M PIK93 resulted in a 44.2 % decrease in the levels of GFP expression when compared to un-treated cells. Cells that were treated with PIK93 concurrently had similar reduction in GFP expression (40.7 %) (Fig 5.7a). Likewise, GNN-transfected cells showed a 50.3 % reduction in GFP expression when pre-treated with PIK93, but no inhibitory effect on GFP expression when cells were treated with PIK93 at the time of transfection (14.4 % increase in GFP expression) (Fig. 5.7d). It seems possible that PIK93 may be reducing the levels of cellular PI4P.

The addition of PIK93 at two hours pre-transfection was selected as the condition to be used for future experiments, this resulted in a dose-dependent reduction in GFP expression in cells transfected with GFP-pac-WT or -GNN replicon RNA (Fig. 5.8). Reduction of GFP expression in cells transfected with GFP-pac-WT ranged from 30.9 \pm 6.7 % to 50.0 \pm 3.9 % after treatment with 1 and 5 μ M PIK93 respectively, when compared to untreated control cells (Fig. 5.8a, b). In GFP-pac-GNN transfected cells

there was a 45.5 ± 2.3 % to 69.8 ± 5.2 % reduction (Fig. 5.8c, d). The reduction in GFP expression in cells transfected with GFP-pac-GNN in the presence of $5 \mu\text{M}$ PIK93 (69.8 ± 5.2 %) is similar to the decrease observed on FMDV IRES-mediated translation with the same concentration of PIK93 (74.1 ± 5.4 %).

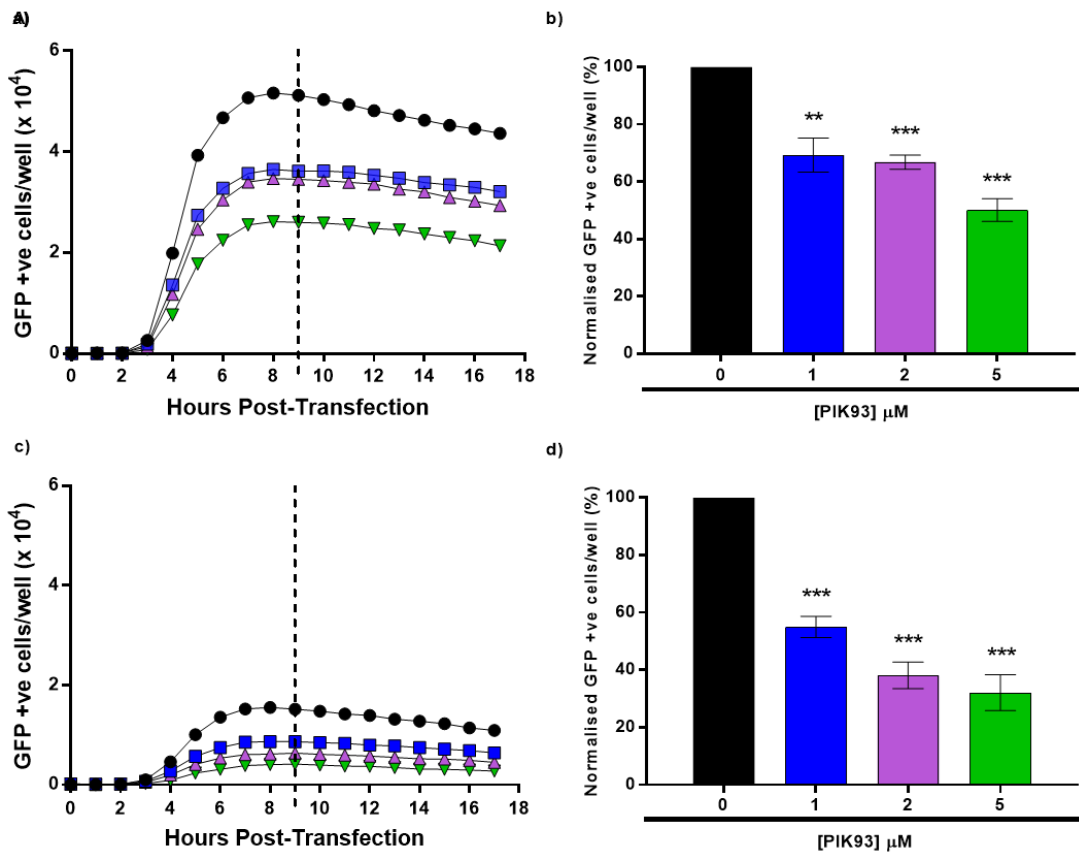


Figure 5.8 Measuring the effect of replication of FMDV replicon RNA in BHK-21 cells treated with PIK93. BHK-21 cells transfected with (a, b) GFP-pac-WT and (c, d) GFP-pac-GNN replicon RNAs. Transfected cells were pre-treated for two hours with PIK93 at the indicated concentrations and levels of GFP expression were compared against untreated controls. Data were collected by imaging GFP fluorescence hourly in transfected cells using an IncuCyte Dual Colour ZOOM® FLR. Levels of GFP expression 9 hours post-transfection are shown (b) and (d), indicated by dotted line on (a) and (c). Mean values with SEM ($n = 3$) are shown. Statistical analysis performed using two-tailed unpaired t-test; ** = $p < 0.01$, *** = $p < 0.001$, **** = $p < 0.0001$.

The effect of PIK93 was then assayed on WT and replication-deficient CVB3 replicons (Fig. 5.9). As expected, and in contrast to the results with FMDV replicons (Fig. 5.8b), there was a more pronounced dose-dependent effect of PIK93 on CVB3 replication. At 5 μ M, PIK93 treatment resulted in a 98.7 ± 0.6 % decrease in luciferase expression in cells transfected with WT Rib-Fluc-CB3/T7 RNA, compared to untreated controls (Fig. 5.9b). However, cells transfected with replication-deficient Rib-Fluc-CB3/T7-3A RNA and treated with 5 μ M PIK93 only, exhibited a 38.9 ± 13.7 % decrease in luciferase expression (Fig. 5.9c); much less than that seen with FMDV (Fig. 5.8d). It should be noted that replication of the FMDV and CVB3 constructs were assayed differently; despite this the data were consistent with the hypothesis that FMDV genome replication did not require PI4K activity, and that the effect of PIK93 was an indirect effect of inhibition of protein translation.

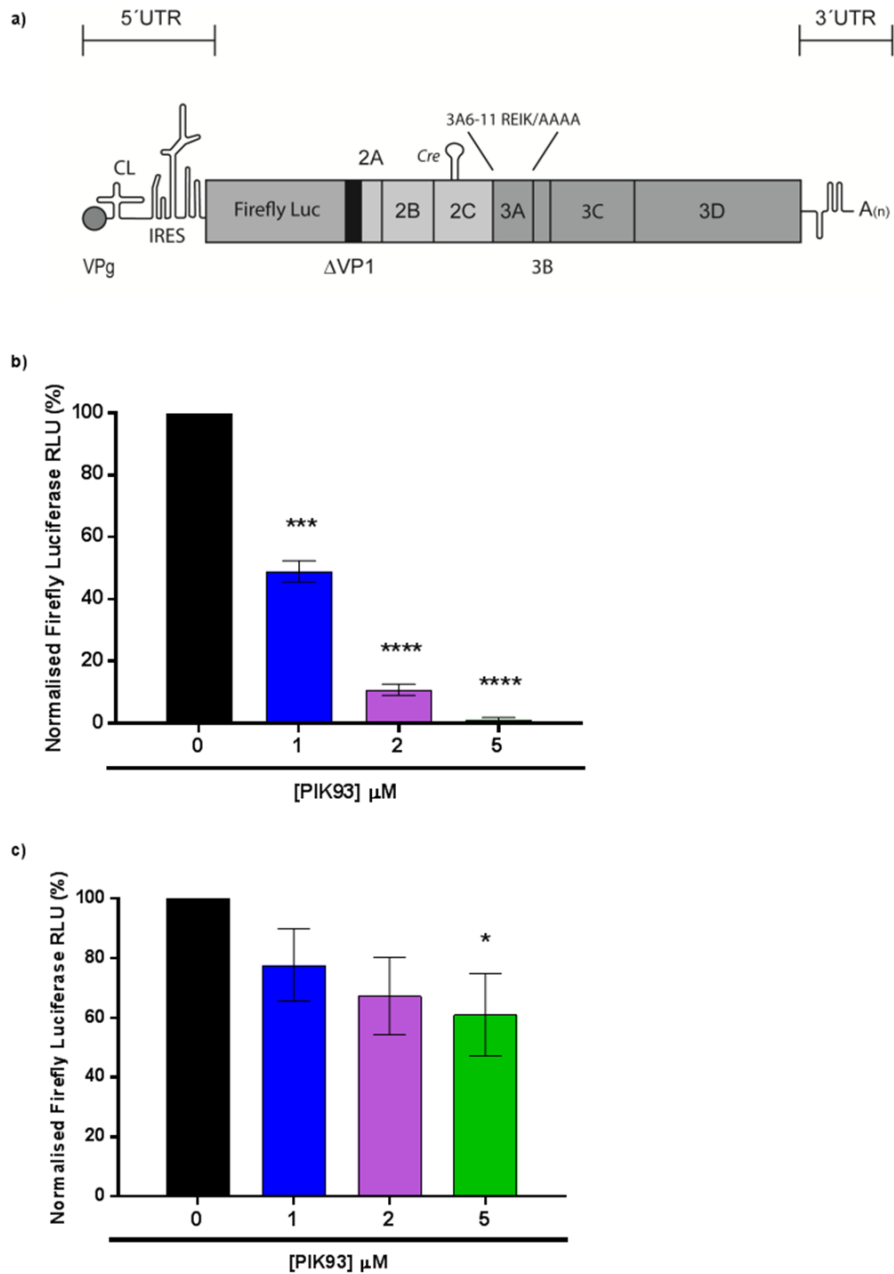


Figure 5.9 Measuring the effect of PIK93 on CVB3 replicon RNA replication in BHK-21 cells. a) Schematic diagram of the CVB3 replicon indicating location of the 5' and 3' untranslated region flanking the genes encoding replication proteins. The firefly luciferase reporter gene replaces the structural capsid proteins. Levels of luciferase expression in HeLa cells transfected with (b) Rib-Fluc-CB3/T7 or (c) Rib-Fluc-CB3/T7-3A CVB3 replicon RNAs. Transfected cells were pre-treated for two hours with PIK93 at the indicated concentrations and levels of luciferase expression were compared against an untreated control. Levels of luciferase expression were measured at eight hours post-transfection. Data show mean values with SEM (n = 3). Statistical analysis performed using two-tailed unpaired t-test; * = p < 0.05, *** = p < 0.001, **** = p < 0.001.

5.5.1 FMDV replication does not require PI4KIII α or β activity.

Given that some positive strand RNA viruses have been shown to require PI4KIII α for genome replication (e.g. HCV), it was thus formally possible that the lack of effect of PIK93 could be explained if FMDV genome replication exhibited a requirement for PI4KIII α but not PI4KIII β .

We therefore proceeded to directly test if the lack of sensitivity to PIK93 could be explained by a requirement for PI4KIII α in FMDV genome replication. As a positive control for inhibition of PI4KIII α we utilised Huh 7.5 cells transiently expressing an HCV sub-genomic replicon (SGR-Luc-GFP-JFH1), derived from the JFH-1 infectious clone and containing an insertion of GFP into domain III of NS5A (Jones et al., 2007). This allowed HCV genome replication to be assayed using the IncuCyte system, as described for FMDV above.

In order to determine if FMDV required PI4KIII α two novel compounds produced by AstraZeneca, compounds (CMPD) 3 and 7 were used. CMPD (7) was designed to have selective inhibitory activity against PI4KIII α , and CMPD (3) against PI4KIII β . Prior to any experimentation with the compounds it was first necessary to determine whether either CMPD (3) or (7) exhibited any cytotoxicity in BHK-21 cells (for FMDV experiments), or Huh 7.5 (for HCV) using an MTT assay. As shown in Figs. 5.10a and 5.10b the compounds were tolerated up to 10 μ M by both cell types, although at 20 μ M both exhibited significant cytotoxicity. We therefore tested the effects of CMPD (3) and CMPD (7) on both FMDV (Fig. 5.10c) and HCV (Fig. 5.10d) replication at 0.5 and 10 μ M. As shown in Fig. 5.10c, FMDV replication was only modestly reduced (\approx 20 %) by the higher concentration of both compounds. Reassuringly, CMPD (7) (selective

for PI4KIII α) inhibited HCV replication even at 0.5 μ M (Fig. 5.10d), CMPD (3) (selective for PI4KIII β) had no effect. We deduce that FMDV genome replication is not dependent on either PI4KIII α or PI4KIII β .

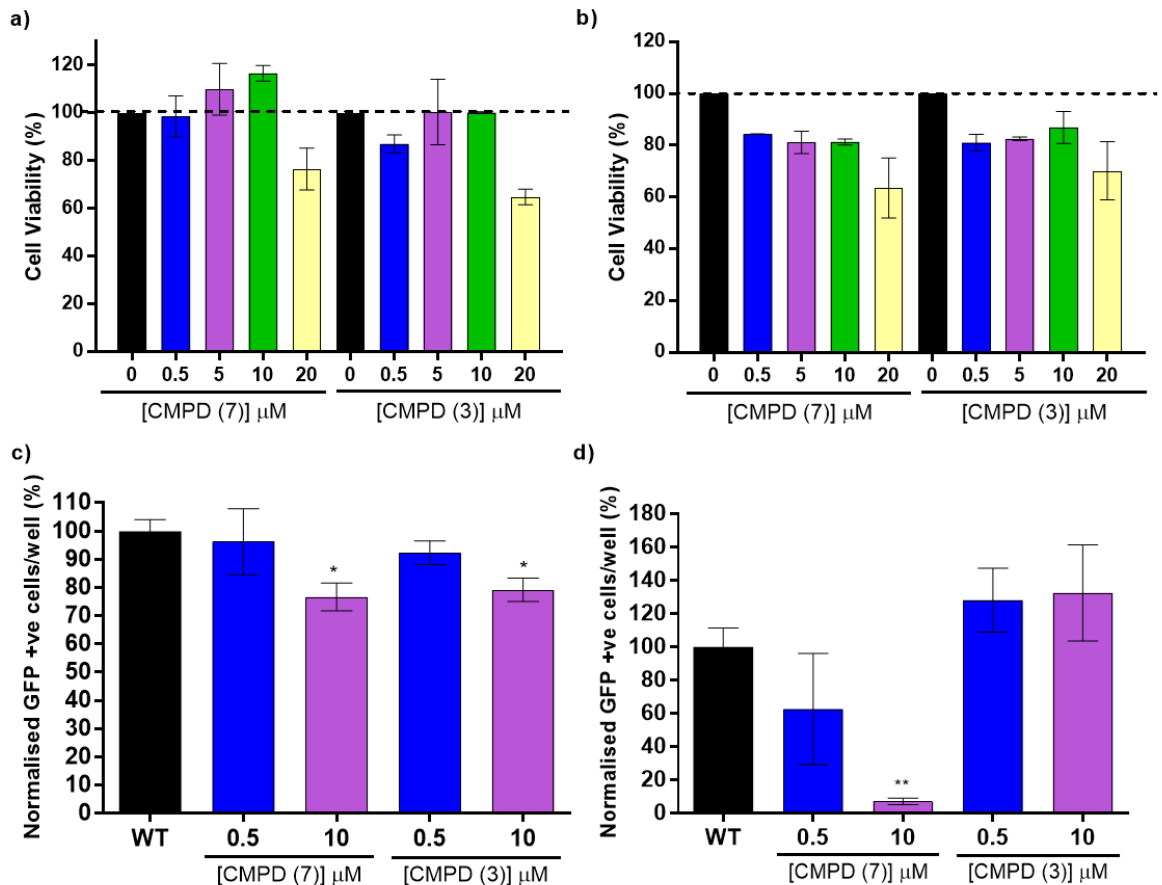
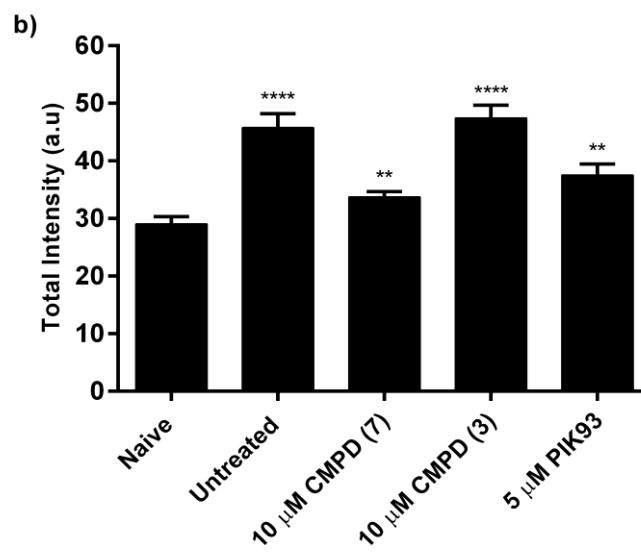
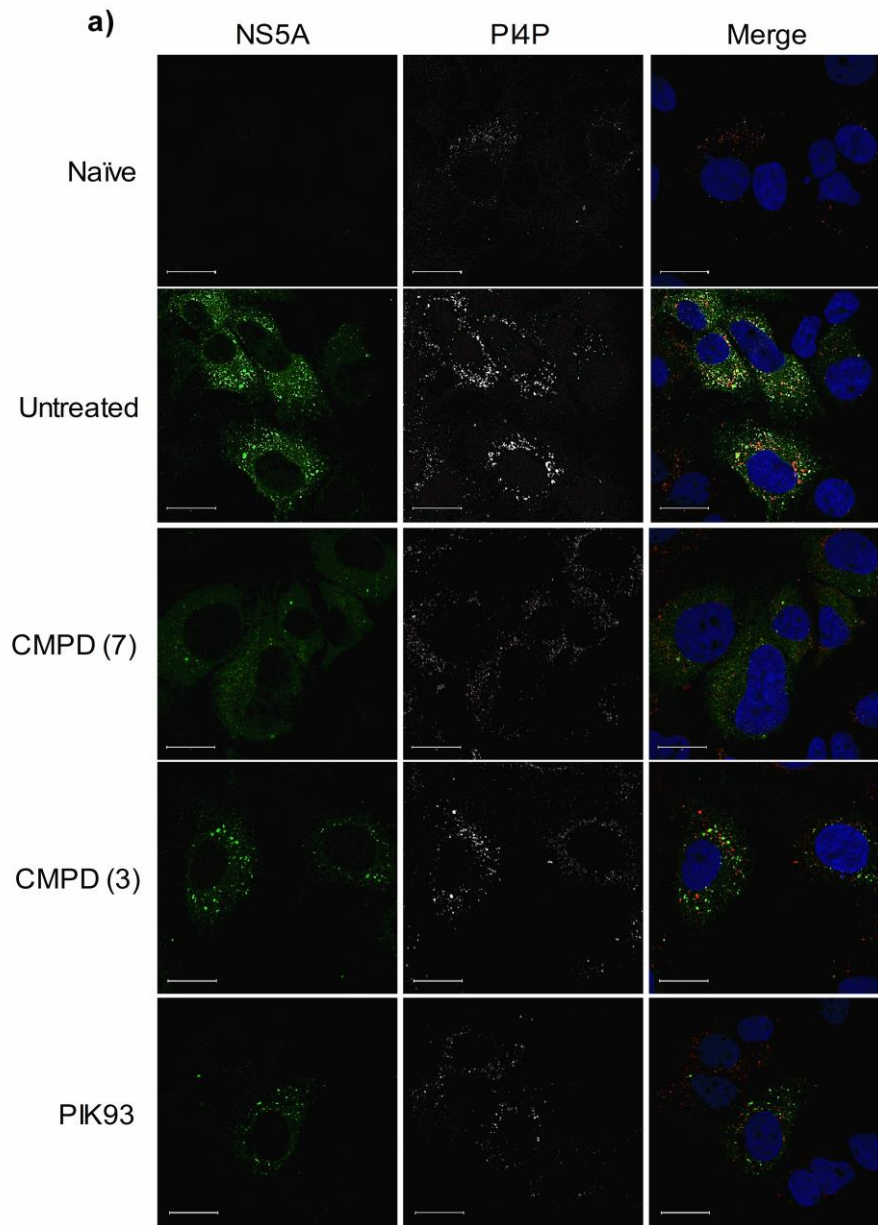


Figure 5.10 The effect of novel PI4KIII α / β compounds on the replication of FMDV and HCV replicon RNA. A) MTT assay of BHK21 cells or (B) Huh 7.5 cells treated with either a selective PI4KIII α inhibitor (compound 7), or PI4KIII β inhibitor (compound 3) at the indicated concentrations. (C) GFP-pac-WT replicon RNA-transfected BHK21 cells were treated with inhibitors as indicated and levels of GFP expression were compared against an untreated control. Levels of GFP expression was measured at eight hours post-transfection. (D) HCV SGR-Luc-GFP-JFH1 replicon RNA-electroporated Huh 7.5 cells were treated with inhibitors as indicated and levels of NS5A-GFP expression were compared against an untreated control. Levels of NS5A-GFP expression was measured at 48 hours post-electroporation. Data show mean values with SEM (n = 3). Statistical analysis performed using two-tailed unpaired t-test; * = p < 0.05, ** = p < 0.01.

5.5.2 FMDV replication does not result in upregulation of PI4P lipids.

It has previously been described (Reiss et al., 2011; Zhang et al., 2012; Ross-Thrieland et al., 2015) that HCV utilises the PI4K pathway to assist in the formation of membranous intracellular replication factories, termed the 'membranous web' and consequently the abundance of PI4P lipids is upregulated during HCV RNA replication. Due to the lack of evidence that FMDV replication is dependent on PI4K activity, it was predicted that cells harbouring FMDV replicons would not exhibit a similar upregulation of PI4P lipids. To test this, we compared the levels of PI4P lipids in cells harbouring either HCV- or FMDV-derived replicons. As shown in Fig. 5.11a and b, Huh 7.5 human hepatoma cells harbouring an HCV replicon showed high levels of PI4P lipids as judged by immunofluorescence analysis using antibodies specific for PI4P (Ross-Thrieland et al., 2015). This was lost following treatment with PIK93 and CMPD (7) (selective for PI4KIII α), consistent with the replication data shown in Fig. 5.10d.

In contrast, BHK-21 cells transfected with FMDV GFP-pac RNA did not exhibit an increase in PI4P staining compared to untransfected cells (Fig. 5.11c and d). Furthermore, there were no significant differences in the levels of PI4P staining in BHK-21 cells after treatment with any of the inhibitors tested. We propose that FMDV does not require type III PI4K activity for genome replication and consequently does not upregulate activity of these kinases.



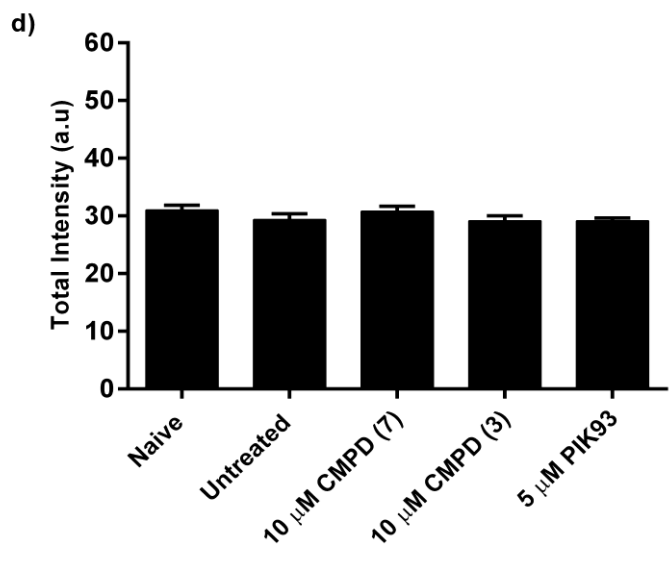
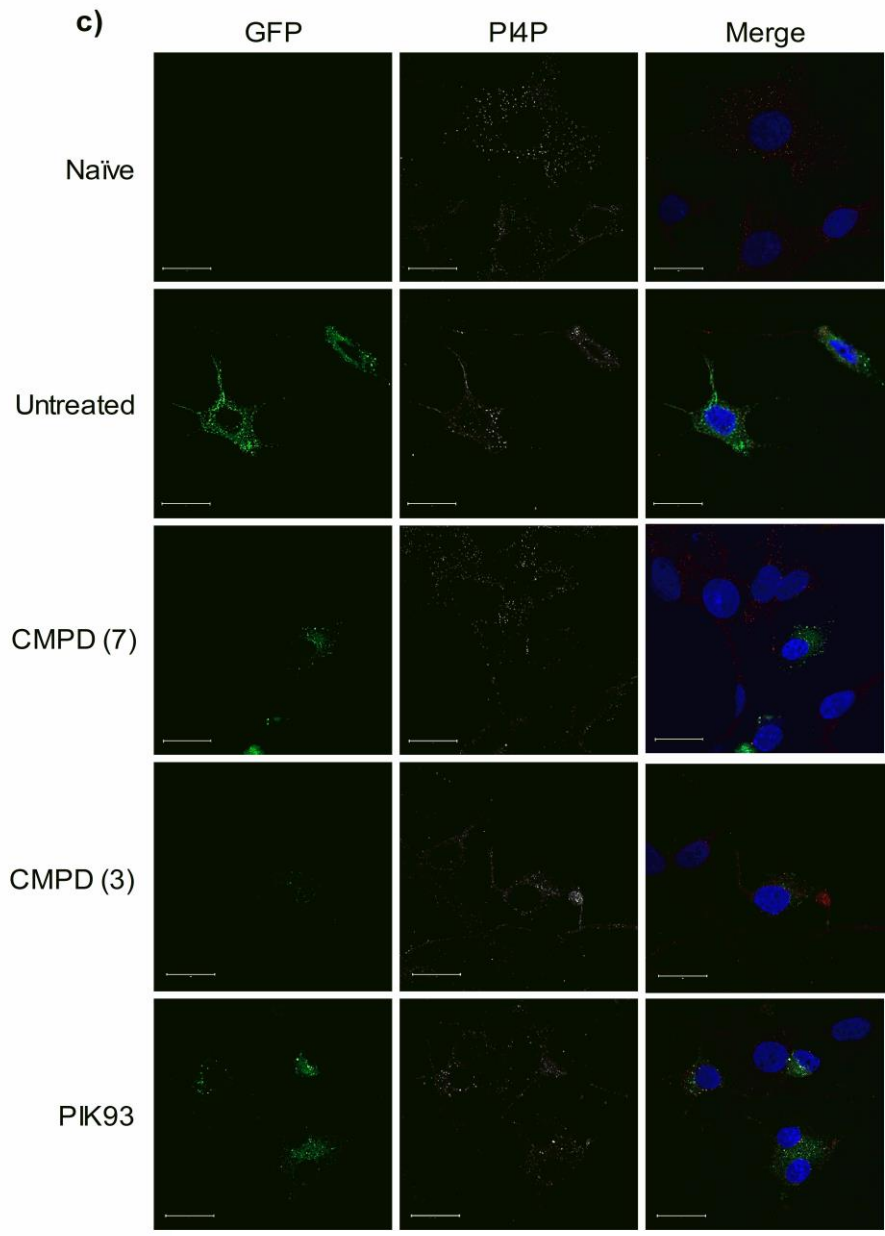


Figure 5.11 (pp. 176-177) Effect of PIK93, CMPD (3), and CMPD (7) on the levels of PI4P expression in cells. Fluorescence microscopy of (a) Huh 7.5 cells electroporated with HCV SGR-Luc-GFP-JFH1 replicon RNA, and (c) BHK21 cells transfected with GFP-pac-WT replicon RNA. Transfected cells were treated with 10 μ M PI4KIII α inhibitor (AZ13647670), PI4KIII β inhibitor (AZ13686489), or 5 μ M PIK93. Fixed cells were stained with anti-PI4P antibody (mouse). NS5A was detected by anti-NS5A antibody (sheep). Levels of PI4P expression were measured and presented as total PI4P intensity measured in arbitrary units in (b) Huh 7.5 cells and (d) BHK21 cells. Scale bar = 20 μ m. Data show mean values with SEM (n = 10).

5.5.3 Involvement of PI3K pathway in FMDV replication

The observed effects of PIK93 on translation of the FMDV replicon (Fig. 5.6), could have been as a result of non-specific interactions between the inhibitor and the host-cell translation mechanism, coupled with the colocalisation immunofluorescence studies described in Berryman et al. 2016 supported the hypothesis that FMDV did not utilise the PI4K pathway like other *Picornaviruses*.

To test if alternative PI pathways were involved in FMDV replication, wortmannin, a fungal steroid metabolite that has been shown to inhibit PI3K in a non-competitive, irreversible, and non-specific manner was used (Powis et al., 1994; Wymann et al., 1996; Meyers et al., 1997). The use of wortmannin would discern if FMDV utilised PI3K for RNA replication.

Cells transfected with GFP-pac-WT showed a reduction of GFP expression of up to 71.6 % in cells treated with 2 μ M wortmannin. Similarly, cells transfected with GFP-pac-GNN also had a decrease of GFP expression of 82.5 %. The results were inconclusive in that treatment of cells with wortmannin still resulted in a decrease in GFP-positive cells per well in both GFP-pac-WT and GFP-pac-GNN transfected cells,

similar to the effects seen in transfected cells treated with PIK93, even with lower concentrations of wortmannin (Fig. 5.12).

When the wortmannin data were combined with the PIK93 data, the wortmannin data suggest that the PI3K as well as the PI4K pathway were either affecting the translation mechanisms inside the cells, or both compounds have a non-specific effect on transfected cells degrading the replicon RNA.

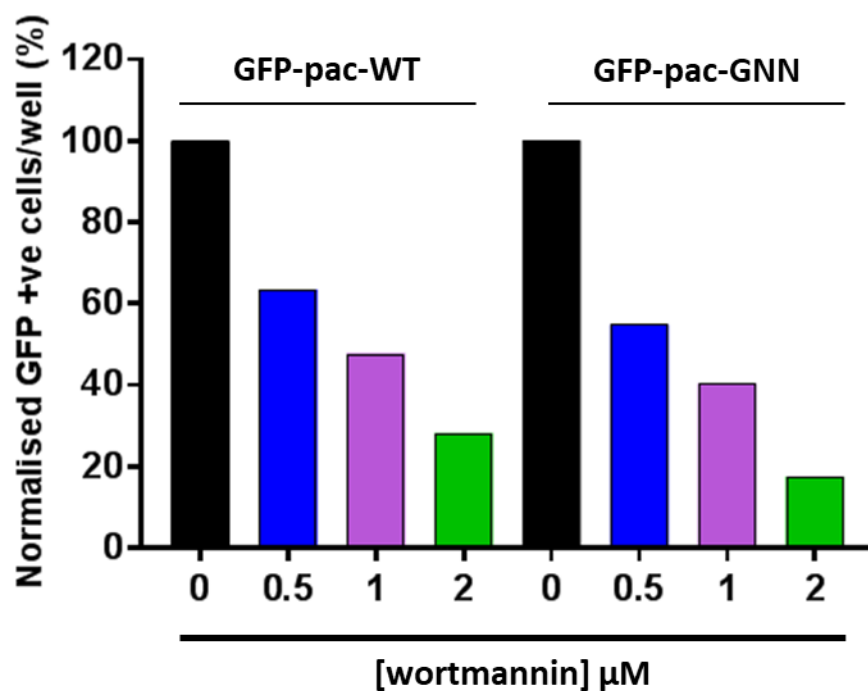


Figure 5.12 Effect of wortmannin on replication of FMDV replicon RNA. BHK-21 cells transfected with either GFP-pac-WT or GFP-pac- Δ 3D replicon RNA were treated with a titration of wortmannin (0-2 μM). Graph indicates the percentage of cells expressing GFP as an indication of replication when treated with wortmannin when compared to an untreated control (0 μM). Levels of GFP expression were measured at 8 hours post-transfection. (n=1).

5.6 Chapter discussion

The PI4K family of enzymes has been shown to be involved in the genome replication of many positive-sense RNA viruses, primarily in the formation of intracellular membranous compartments by generating PI4P lipids. These compartments are proposed to house the viral replication factories to protect the viral RNA from degradation and recognition by the host-cell innate immune response. It has also been observed that some viruses, such as HCV, upregulate PI4K expression and activity. PIK93 is a PI4KIII β small molecule inhibitor, but has shown to have an additional inhibitory effect on PI4KIII α and PI3K (Knight et al., 2006). It has been demonstrated previously that the treatment of cells with PIK93 down-regulated the generation of PI4P lipids by inhibiting the activity of PI4KIII α and β . Furthermore, studies with HCV, CVB3, and PV have shown that treating infected cells with PIK93 reduced virus genome replication (Altan-Bonnet et al., 2012). However, from the studies reported here, it appears that the apparent effect on FMDV genome replication is actually due to effects on translation. We have demonstrated that IRES-mediated translation is sensitive to PIK93. There is an additional effect on genome replication for CVB3, but not for FMDV.

We found no evidence by immunofluorescence microscopy staining for PI4P lipids that FMDV replication leads to an accumulation of these lipids. However, in cells electroporated with HCV replicon, RNA levels of PI4P were stimulated as expected. These data suggest that the PI4K pathway is not the primary pathway involved with FMDV genome replication.

Membrane reorganisation during HCV infection has been well defined and it has been reported that PI4KIII α plays an essential role in the formation of intracellular replication factories required for replication (Trotard et al., 2009; Reiss et al., 2011). PI3K has also been implicated in HCV replication by recruiting membranous compartments from the endocytic pathway (Sir et al., 2012; Liu et al., 2012; Mohl et al., 2016). It has been demonstrated that FMDV induces the formation of autophagosomes from the endocytic pathway to facilitate cell entry, but this does not appear to be involved in viral replication. In FMDV, autophagosome formation is induced in a PI3K-independent manner (Berryman et al., 2012), whereas inhibition of both PI3K and PI4KIII α significantly inhibits HCV replication (Gosert et al., 2003; Berger et al., 2009).

There is evidence from the literature that reorganisation of cellular membranes during FMDV infection is different to that seen during infection with other picornaviruses. FMDV infection results in a dramatic condensation and relocalisation of intracellular organelles to one side of the cytoplasm in the perinuclear region (Monaghan et al., 2004) and is unaffected by brefeldin A, a fungal metabolite that disrupts retrograde Golgi-ER transport. It has been shown that brefeldin A interacts with Arf1/GBF1; interference with GBF1 affects the recruitment of PI4KIII β and subsequent PI4P-lipid up-regulation. Interestingly, treatment of cells with brefeldin A has been shown to enhance FMDV infection (Midgley et al., 2013). Recent studies have shown that PV, CVB3, and HRV are able to recruit PI4KIII β in an Arf1/GBF1-independent manner highlighting the complexity of the mechanisms by which picornaviruses recruit intracellular membranes. (O'Donnell et al., 2001; Midgley et al., 2013; Dorobantu et al., 2014; Dorobantu, Ford-Siltz, et al., 2015).

Overall, these studies support the results shown here suggesting that PI4Ks are not involved in FMDV replication. The data and conclusions described here are supported by a recently published paper (Berryman et al., 2016). Therefore, it can be hypothesised that FMDV may subvert an alternative cellular pathway to affect the membrane reorganisation required to support virus replication, or may not require any upregulation of the PI4K pathway.

Chapter 6

Concluding Remarks and Future Perspectives

The primary focus of the work in this thesis was to dissect the role of FMDV 3D^{pol} in viral replication. Although the formation of a classical, discrete intracellular membrane-associated replication complex, usually associated with picornavirus replication, had yet to be identified within FMDV infected cells, the ability for FMDV to form higher-order fibril structures, which appear to require the presence of RNA, provide an attractive candidate for the nucleus of a replication complex. The fibrils could provide an enclosed, protective environment within which replication can occur in an energetically favourable manner. However, there are still outstanding questions of how FMDV fibrils form, and what is necessary for these structures to form in cells, if indeed, they are involved in whole, or as part of the proposed replication complex.

The studies described in Chapter 3 and 4 provide preliminary results concerning the function and structure of the 3D^{pol} fibrils. The results showed that although WT 3D^{pol} was able to form fibrils, none of the mutants tested here were able to do so. Mutations in the polymerase that were located within the catalytic domain of the protein (DD388/9NN and DD240/5NN) resulted in non-functional, replication-deficient replicons and were unable to form any higher-order fibril-like structures. The polymerase containing a mutation located in the non-catalytic dsRNA exit site, GC216/7AA, was also unable to replicate in context of the FMDV replicon, or form any distinctive higher-order fibril-like structures. However, the GC216/7AA mutant

was able to bind to RNA with WT affinity, and was able to incorporate radiolabelled RNA nucleotides. However, this mutation rendered the replicon non-functional and unable to be recovered when co-transfected with WT helper replicon, unlike the catalytic mutations, unless both the S-fragment was removed from the 5' UTR, and if the *cre* was inactivated.

The combination of the ability of the non-catalytic mutant GC216/7AA to incorporate RNA nucleotides, along with only being able to be recovered when the regions of the 5' UTR were removed, points to a novel, necessary *cis* function for the polymerase in addition to its catalytic polymerase activity as suggested in Herod et al., 2016.

This novel information highlights the importance to undertake further work to determine what aspects of polymerase function are important for the formation of fibrils. This process of fibril formation identified here is unique to FMDV; PV can form fibrils spontaneously even if the polymerase is catalytically inactive. This would suggest that the formation of fibrils during FMDV replication has a functional role, as opposed to simply acting as a scaffold. The natural progression of this assay would be to assess the ability of FMDV 3D^{pol} to form fibrils if a different non-catalytic site were mutated. For example, investigating whether the fibrils are able to form if the proposed protein-protein interacting residues were changed, and investigating whether these mutations hinder the ability for 3D^{pol} to bind or incorporate RNA. Additionally, it would indicate to further investigate whether these mutations affected the replication ability of FMDV in context of the replicon.

The hypothesis that the polymerase may have a primary catalytic function and a secondary non-catalytic role in replication, both of which involve binding to RNA supports the notion that RNA is necessary for the correct formation of fibrils.

Based on the orientation of the individual polymerase molecules within the fibril from the cryo-EM data, it is possible to imagine that the RNA would be replicated by the catalytic polymerase, and the newly synthesised negative-strand replicative intermediate could become coated by the other polymerase molecules, protecting it from degradation by host-cell ribonucleases or detection by the host innate immune system. However, proving this hypothesis has been challenging, primarily due to being unable to identify density corresponding to RNA associated with the fibrils as analysed by cryo-EM. The presence of RNA is necessary for the formation of fibrils but so far, no evidence of an interaction has been visualised.

A reason for the inability to identify RNA density within the fibrils could be due to low occupancy levels: if only one of 20 molecules contained RNA, RNA density would not be detected. Another reason for the inability to measure any RNA density within the fibrils could be due to the RNA primer-template that was used being too unstructured and flexible to be visualised by standard negative-stain TEM or cryo-EM as a result of the presence of flexible loops extending from the fibril. These loops, if present, could be subjected to immunogold labelling and subsequent visualisation by TEM. However, the presence of flexible RNA is unlikely as RNA density would be expected to be seen within the polymerase active site, and as yet this has not been identified.

Further work needs to be undertaken to elucidate a potential interaction between fibrils and RNA. Methods to determine this interaction include purifying fibrils by

gradient densitometry then determining if the protein and RNA appear in the same fractions, or alternatively by a particle stability thermal release (PaSTRy)-style assay (Walter et al., 2012) where identification of potentially protected RNA can occur by disassembling the fibrils and labelling the RNA that may be trapped within.

Furthermore, identifying whether there are interactions between additional non-structural proteins and fibrils *in vitro* would strengthen the hypothesis that the fibrils were central for the formation of replication complexes, particularly if there was a direct interaction with proteins such as 3A that have a known membrane-associating domain. Studies on PV have shown that its polymerase associates with precursor proteins 3AB; based on the existing similarities between PV and FMDV, it is conceivable that a similar interaction is probable, potentially even with other non-structural proteins such as 2B and 2C.

It would also be interesting to see if fibrils can be identified in replicon-containing cells. As the 3D^{pol} is his-tagged, it provides an attractive target for immunoprecipitation studies and could provide evidence for potential replication complex formation within cells if interactions with other non-structural viral proteins, cellular protein or RNA can be identified using this method. Additionally, the use of tagged constructs could be used in super-resolution microscopy studies. Preliminary confocal studies described in chapter 4 showed that WT and mutant 3D^{pol} could be identified within cells following replicon transfection. A similar process could thus be used to try and identify replication complex formation on a single molecule scale.

Identifying interactions between the P2 non-structural proteins and other non-structural proteins, particularly 3D^{pol}, may also provide answers to the apparent

importance of 2B in the recovery of replicon RNA in transfected cells. The co-transfection studies between replicons that contain a WT or a mutant polymerase showed that either the presence of 2B, or the presence of a helper RNA of a specific length was necessary for recovery to occur. However, studies have pointed to the importance of 2B, 2C, and 2BC in virus replication, particularly in the dysregulation of the ER- and Golgi-derived membranes. It is highly likely that these proteins are necessary in the formation of a replication complex.

The potential for a large protected replication complex to form involving the 3D^{pol} fibrils and non-structural proteins such as 2BC which results in the dysregulation of host-cell intracellular membrane compartments provides an attractive hypothesis for the lack of PI4K pathway involvement during replication. Our data has shown that the use of this pathway is not required for FMDV replication and that the dysregulation of the ER- and Golgi-derived membranes previously observed during FMDV replication was not due to the hijacking of the cellular kinase pathway. Further work focussing on alternative membrane trafficking pathways needs to be undertaken to identify the involvement of other host-cell mechanisms that could be involved in the rearrangement of intracellular membranes due to FMDV infection.

In conclusion, the studies outlined here have provided the scaffold for the understanding of the formation of the FMDV replication complex. As a picornavirus, the structure and formation of the replication complex is likely to share some similarities to other related viruses such as PV and CVB3. However, there are a number of key differences not only in the genome structure and organisation, but also in the formation of the 3D^{pol} higher-order complexes, as well as the ability for

the virus to replicate independently without the recruitment of host-cell membrane rearrangement factors. Therefore, it is likely that predicting the components and formation of the replication complex may be more challenging than expected.

References

- Acharya, R., Fry, E., Stuart, D., Fox, G., Rowlands, D. and Brown, F. 1989. The three-dimensional structure of foot-and-mouth disease virus at 2.9 Å resolution. *Nature*. **337**(6209), pp.709–16.
- Adams, M.J., Lefkowitz, E.J., King, A.M.Q., Harrach, B., Harrison, R.L., Knowles, N.J., Kropinski, A.M., Krupovic, M., Kuhn, J.H., Mushegian, A.R., Nibert, M., Sabanadzovic, S., Sanfaçon, H., Siddell, S.G., Simmonds, P., Varsani, A., Zerbini, F.M., Gorbalenya, A.E. and Davison, A.J. 2017. Changes to taxonomy and the International Code of Virus Classification and Nomenclature ratified by the International Committee on Taxonomy of Viruses (2017). *Archives of Virology*.
- Agudo, R., Ferrer-Orta, C., Arias, A., de la Higuera, I., Perales, C., Pérez-Luque, R., Verdaguier, N. and Domingo, E. 2010. A multi-step process of viral adaptation to a mutagenic nucleoside analogue by modulation of transition types leads to extinction-escape. *PLoS Pathogens*. **6**(8), p.e1001072.
- Ahl, R. and Rump, A. 1976. Assay of bovine interferons in cultures of the porcine cell line IB-RS-2. *Infection and Immunity*. **14**(3), pp.603–6.
- Airaksinen, A., Pariente, N., Menéndez-Arias, L. and Domingo, E. 2003. Curing of foot-and-mouth disease virus from persistently infected cells by ribavirin involves enhanced mutagenesis. *Virology*. **311**(2), pp.339–49.
- Albulescu, L., Wubbolts, R., van Kuppeveld, F.J.M. and Strating, J.R.P.M. 2015. Cholesterol shuttling is important for RNA replication of coxsackievirus B3 and encephalomyocarditis virus. *Cellular Microbiology*. **17**(8), pp.1144–1156.
- Alexandersen, S., Zhang, Z. and Donaldson, A.I. 2002. Aspects of the persistence of foot-and-mouth disease virus in animals--the carrier problem. *Microbes and Infection / Institut Pasteur*. **4**(10), pp.1099–110.
- Almeida, M.R., Rieder, E., Chinsangaram, J., Ward, G., Beard, C., Grubman, M.J. and Mason, P.W. 1998. Construction and evaluation of an attenuated vaccine for foot-and-mouth disease: difficulty adapting the leader proteinase-deleted strategy to the serotype O1 virus. *Virus Research*. **55**(1), pp.49–60.
- Altan-Bonnet, N. and Balla, T. 2012. Phosphatidylinositol 4-kinases: hostages harnessed to build panviral replication platforms. *Trends in Biochemical Sciences*. **37**(7), pp.293–302.
- Andino, R., Rieckhof, G.E., Achacoso, P.L. and Baltimore, D. 1993. Poliovirus RNA synthesis utilizes an RNP complex formed around the 5'-end of viral RNA. *The EMBO Journal*. **12**(9), pp.3587–98.
- Andino, R., Rieckhof, G.E. and Baltimore, D. 1990. A functional ribonucleoprotein complex forms around the 5' end of poliovirus RNA. *Cell*. **63**(2), pp.369–80.

- Andino, R., Rieckhof, G.E., Trono, D. and Baltimore, D. 1990. Substitutions in the protease (3Cpro) gene of poliovirus can suppress a mutation in the 5' noncoding region. *Journal of Virology*. **64**(2), pp.607–12.
- Ao, D., Guo, H.-C., Sun, S.-Q., Sun, D.-H., Fung, T.S., Wei, Y.-Q., Han, S.-C., Yao, X.-P., Cao, S.-Z., Liu, D.X. and Liu, X.-T. 2015. Viroporin activity of the foot-and-mouth disease virus non-structural 2B protein. *PLoS ONE*. **10**(5), p.e0125828.
- Ao, D., Sun, S.-Q. and Guo, H.-C. 2014. Topology and biological function of enterovirus non-structural protein 2B as a member of the viroporin family. *Veterinary Research*. **45**(1), p.87.
- Appel, N., Herian, U. and Bartenschlager, R. 2005. Efficient rescue of hepatitis C virus RNA replication by trans-complementation with nonstructural protein 5A. *Journal of Virology*. **79**(2), pp.896–909.
- Arias, A., Perales, C., Escarmís, C. and Domingo, E. 2010. Deletion mutants of VPg reveal new cytopathology determinants in a picornavirus. *PLoS ONE*. **5**(5), p.e10735.
- Arita, M. 2014. Phosphatidylinositol-4 kinase III beta and oxysterol-binding protein accumulate unesterified cholesterol on poliovirus-induced membrane structure. *Microbiology and Immunology*. **58**(4), pp.239–256.
- Arita, M., Kojima, H., Nagano, T., Okabe, T., Wakita, T. and Shimizu, H. 2013. Oxysterol-binding protein family I is the target of minor enviroxime-like compounds. *Journal of Virology*. **87**(8), pp.4252–60.
- Arita, M., Kojima, H., Nagano, T., Okabe, T., Wakita, T. and Shimizu, H. 2011. Phosphatidylinositol 4-kinase III beta is a target of enviroxime-like compounds for antipoliovirus activity. *Journal of Virology*. **85**(5), pp.2364–72.
- Armstrong, R., Davie, J. and Hedger, R.S. 1967. Foot-and-mouth Disease in Man. *British Medical Journal*. **4**, pp.529–530.
- Arnold, J.J., Ghosh, S.K. and Cameron, C.E. 1999. Poliovirus RNA-dependent RNA polymerase (3D(pol)). Divalent cation modulation of primer, template, and nucleotide selection. *Journal of Biological Chemistry*. **274**(52), pp.37060–9.
- Bablanian, G.M. and Grubman, M.J. 1993. Characterization of the foot-and-mouth disease virus 3C protease expressed in Escherichia coli. *Virology*. **197**(1), pp.320–7.
- Bachrach, H.L. 1968. Foot-and-mouth disease. *Annual Review of Microbiology*. **22**, pp.201–44.
- Baird, S.D. 2006. Searching for IRES. *RNA*. **12**(10), pp.1755–1785.
- Balla, A. and Balla, T. 2006. Phosphatidylinositol 4-kinases: old enzymes with emerging functions. *Trends in Cell Biology*. **16**(7), pp.351–361.
- Baltimore, D. and Franklin, R.M. 1962. Preliminary data on a virus-specific enzyme system responsible for the synthesis of viral RNA. *Biochemical and Biophysical Research Communications*. **9**, pp.388–92.
- Barton, D.J. and Flanagan, J.B. 1997. Synchronous replication of poliovirus RNA:

- initiation of negative-strand RNA synthesis requires the guanidine-inhibited activity of protein 2C. *Journal of Virology*. **71**(11), pp.8482–9.
- Barton, D.J., O'Donnell, B.J. and Flanagan, J.B. 2001. 5' cloverleaf in poliovirus RNA is a cis-acting replication element required for negative-strand synthesis. *The EMBO Journal*. **20**(6), pp.1439–48.
- Bauer, K. 1997. Foot- and-mouth disease as zoonosis. *Archives of Virology Supplementum*. **13**, pp.95–7.
- Baxt, B. 1987. Effect of lysosomotropic compounds on early events in foot-and-mouth disease virus replication. *Virus Research*. **7**(3), pp.257–71.
- Beales, L.P., Holzenburg, A. and Rowlands, D.J. 2003. Viral internal ribosome entry site structures segregate into two distinct morphologies. *Journal of Virology*. **77**(11), pp.6574–6579.
- Beard, C.W. and Mason, P.W. 2000. Genetic determinants of altered virulence of Taiwanese foot-and-mouth disease virus. *Journal of Virology*. **74**(2), pp.987–91.
- Beck, E. and Strohmaier, K. 1987. Subtyping of European foot-and-mouth disease virus strains by nucleotide sequence determination. *Journal of Virology*. **61**(5), pp.1621–9.
- Beckman, M.T. and Kirkegaard, K. 1998. Site size of cooperative single-stranded RNA binding by poliovirus RNA-dependent RNA polymerase. *Journal of Biological Chemistry*. **273**(12), pp.6724–30.
- Belov, G.A., Altan-Bonnet, N., Kovtunovych, G., Jackson, C.L., Lippincott-Schwartz, J. and Ehrenfeld, E. 2007. Hijacking components of the cellular secretory pathway for replication of poliovirus RNA. *Journal of Virology*. **81**(2), pp.558–67.
- Belov, G.A., Nair, V., Hansen, B.T., Hoyt, F.H., Fischer, E.R. and Ehrenfeld, E. 2012. Complex dynamic development of poliovirus membranous replication complexes. *Journal of Virology*. **86**(1), pp.302–312.
- Belsham, G.J. 2009. Divergent picornavirus IRES elements. *Virus Research*. **139**, pp.183–192.
- Belsham, G.J. 2013. Influence of the Leader protein coding region of foot-and-mouth disease virus on virus replication. *Journal of General Virology*. **94**(Pt_7), pp.1486–1495.
- Belsham, G.J. 2005. Translation and replication of FMDV RNA. *Current Topics in Microbiology and Immunology*. **288**, pp.43–70.
- Belsham, G.J. and Brangwyn, J.K. 1990. A region of the 5' noncoding region of foot-and-mouth disease virus RNA directs efficient internal initiation of protein synthesis within cells: involvement with the role of L protease in translational control. *Journal of Virology*. **64**(11), pp.5389–95.
- Belsham, G.J., McInerney, G.M. and Ross-Smith, N. 2000. Foot-and-mouth disease virus 3C protease induces cleavage of translation initiation factors eIF4A and

- eIF4G within infected cells. *Journal of Virology*. **74**(1), pp.272–80.
- Bentham, M., Holmes, K., Forrest, S., Rowlands, D.J. and Stonehouse, N.J. 2012. Formation of higher-order foot-and-mouth disease virus 3D(pol) complexes is dependent on elongation activity. *Journal of Virology*. **86**(4), pp.2371–4.
- Berger, K.L., Cooper, J.D., Heaton, N.S., Yoon, R., Oakland, T.E., Jordan, T.X., Mateu, G., Grakoui, A. and Randall, G. 2009. Roles for endocytic trafficking and phosphatidylinositol 4-kinase III alpha in hepatitis C virus replication. *Proceedings of the National Academy of Sciences of the United States of America*. **106**(18), p.7577–82.
- Berger, K.L., Kelly, S.M., Jordan, T.X., Tartell, M.A. and Randall, G. 2011. Hepatitis C virus stimulates the phosphatidylinositol 4-kinase III alpha-dependent phosphatidylinositol 4-phosphate production that is essential for its replication. *Journal of Virology*. **85**, pp.8870–8883.
- Berinstein, A., Roivainen, M., Hovi, T., Mason, P.W. and Baxt, B. 1995. Antibodies to the vitronectin receptor (integrin alpha V beta 3) inhibit binding and infection of foot-and-mouth disease virus to cultured cells. *Journal of Virology*. **69**(4), pp.2664–6.
- Berryman, S., Brooks, E., Burman, A., Hawes, P., Roberts, R., Netherton, C., Monaghan, P., Whelband, M., Cottam, E., Elazar, Z., Jackson, T. and Wileman, T. 2012. Foot-and-mouth disease virus induces autophagosomes during cell entry via a class III phosphatidylinositol 3-kinase-independent pathway. *Journal of Virology*. **86**, pp.12940–12953.
- Berryman, S., Clark, S., Monaghan, P. and Jackson, T. 2005. Early events in integrin v 6-mediated cell entry of foot-and-mouth disease virus. *Journal of Virology*. **79**(13), pp.8519–8534.
- Berryman, S., Moffat, K., Harak, C., Lohmann, V. and Jackson, T. 2016. Foot-and-mouth disease virus replicates independently of phosphatidylinositol 4-phosphate and type III phosphatidylinositol 4-kinases. *Journal of General Virology*. **97**(8), pp.1841–52.
- Bienz, K., Egger, D. and Pasamontes, L. 1987. Association of polioviral proteins of the P2 genomic region with the viral replication complex and virus-induced membrane synthesis as visualized by electron microscopic immunocytochemistry and autoradiography. *Virology*. **160**(1), pp.220–6.
- Bienz, K., Egger, D., Pfister, T. and Troxler, M. 1992. Structural and functional characterization of the poliovirus replication complex. *Journal of Virology*. **66**(5), pp.2740–7.
- Bienz, K., Egger, D., Rasser, Y. and Bossart, W. 1983. Intracellular distribution of poliovirus proteins and the induction of virus-specific cytoplasmic structures. *Virology*. **131**(1), pp.39–48.
- Birtley, J.R., Knox, S.R., Jaulent, A.M., Brick, P., Leatherbarrow, R.J. and Curry, S. 2005. Crystal structure of foot-and-mouth disease virus 3C protease. New insights into catalytic mechanism and cleavage specificity. *Journal of Biological Chemistry*. **280**(12), pp.11520–7.

- Bishé, B., Syed, G. and Siddiqui, A. 2012. Phosphoinositides in the hepatitis C virus life cycle. *Viruses*. **4**, pp.2340–2358.
- Black, D.N. and Brown, F. 1969. Effect of actinomycin D and guanidine on the formation of a ribonucleic acid polymerase induced by foot-and-mouth-disease virus and on the replication of virus and viral ribonucleic acid. *Biochemical Journal*. **112**(3), pp.317–323.
- Black, D.N., Stephenson, P., Rowlands, D.J. and Brown, F. 1979. Sequence and location of the poly C tract in aphtho- and cardiovirus RNA. *Nucleic Acids Research*. **6**(7), pp.2381–90.
- Blyn, L.B., Towner, J.S., Semler, B.L. and Ehrenfeld, E. 1997. Requirement of poly(rC) binding protein 2 for translation of poliovirus RNA. *Journal of Virology*. **71**(8), pp.6243–6.
- Bolten, R., Egger, D., Gosert, R., Schaub, G., Landmann, L. and Bienz, K. 1998. Intracellular localization of poliovirus plus- and minus-strand RNA visualized by strand-specific fluorescent In situ hybridization. *Journal of Virology*. **72**(11), pp.8578–85.
- den Boon, J. and Ahlquist, P. 2010. Organelle-like membrane compartmentalization of positive-strand RNA virus replication factories. *Annual Review of Microbiology*. **64**, pp.241–256.
- den Boon, J., Diaz, A. and Ahlquist, P. 2010. Cytoplasmic viral replication complexes. *Cell Host & Microbe*. **8**(1), pp.77–85.
- Borawski, J., Troke, P., Puyang, X., Gibaja, V., Zhao, S., Mickanin, C., Leighton-Davies, J., Wilson, C.J., Myer, V., Cornellataracido, I., Baryza, J., Tallarico, J., Joberty, G., Bantscheff, M., Schirle, M., Bouwmeester, T., Mathy, J.E., Lin, K., Compton, T., Labow, M., Wiedmann, B. and Gaither, L.A. 2009. Class III phosphatidylinositol 4-kinase alpha and beta are novel host factor regulators of hepatitis C virus replication. *Journal of Virology*. **83**(19), pp.10058–74.
- Boura, E. and Nencka, R. 2015. Phosphatidylinositol 4-kinases: Function, structure, and inhibition. *Experimental Cell Research*. **337**(2), pp.136–145.
- Brown, C.C., Piccone, M.E., Mason, P.W., McKenna, T.S. and Grubman, M.J. 1996. Pathogenesis of wild-type and leaderless foot-and-mouth disease virus in cattle. *Journal of Virology*. **70**(8), pp.5638–41.
- Brown, D.W. 2001. Foot and mouth disease in human beings. *The Lancet*. **357**(9267), p.1463.
- Brown, F., Newman, J., Stott, J., Porter, A., Frisby, D., Newton, C., Carey, N. and Fellner, P. 1974. Poly(C) in animal viral RNAs. *Nature*. **251**(5473), pp.342–344.
- Brune, W., Ménard, C., Hobom, U., Odenbreit, S., Messerle, M. and Koszinowski, U.H. 1999. Rapid identification of essential and nonessential herpesvirus genes by direct transposon mutagenesis. *Nature Biotechnology*. **17**(4), pp.360–364.
- Bryan, B.J. and Szent-Gyorgyi, C. 2001. Luciferases, fluorescent proteins, nucleic acids encoding the luciferases and fluorescent proteins and the use thereof in diagnostics, high throughput screening and novelty items.

- Bunch, T., Rieder, E. and Mason, P. 1994. Sequence of the S fragment of foot-and-mouth disease virus type A12. *Virus Genes*. **8**(2), pp.173–5.
- Burroughs, J.N., Rowlands, D.J., Sangar, D. V., Talbot, P. and Brown, F. 1971. Further Evidence for Multiple Proteins in the Foot-and-Mouth Disease Virus Particle. *Journal of General Virology*. **13**(1), pp.73–84.
- Cameron, C.E., Suk Oh, H. and Moustafa, I.M. 2010. Expanding knowledge of P3 proteins in the poliovirus lifecycle. *Future Microbiology*. **5**(6), pp.867–881.
- Cao, X., Bergmann, I.E., Füllkrug, R. and Beck, E. 1995. Functional analysis of the two alternative translation initiation sites of foot-and-mouth disease virus. *Journal of Virology*. **69**(1), pp.560–3.
- Cao, X. and Wimmer, E. 1995. Intragenomic complementation of a 3AB mutant in dicistronic polioviruses. *Virology*. **209**(2), pp.315–326.
- Carrillo, C., Lu, Z., Borca, M. V, Vagnozzi, A., Kutish, G.F. and Rock, D.L. 2007. Genetic and phenotypic variation of foot-and-mouth disease virus during serial passages in a natural host. *Journal of Virology*. **81**(20), pp.11341–51.
- Carrillo, C., Tulman, E.R., Delhon, G., Lu, Z., Carreno, A., Vagnozzi, A., Kutish, G.F. and Rock, D.L. 2005. Comparative genomics of foot-and-mouth disease virus. *Journal of Virology*. **79**(10), pp.6487–504.
- Carroll, A.R., Rowlands, D.J. and Clarke, B.E. 1984. The complete nucleotide sequence of the RNA coding for the primary translation product of foot and mouth disease virus. *Nucleic Acids Research*. **12**(5), pp.2461–2472.
- Cavanagh, D., Rowlands, D.J. and Brown, F. 1978. Early events in the interaction between foot-and-mouth disease virus and primary pig kidney cells. *Journal of General Virology*. **41**(2), pp.255–264.
- Chinnaswamy, S., Murali, A., Li, P., Fujisaki, K. and Kao, C.C. 2010. Regulation of de novo-initiated RNA synthesis in hepatitis C virus RNA-dependent RNA polymerase by intermolecular interactions. *Journal of Virology*. **84**(12), pp.5923–5935.
- Chinsangaram, J., Koster, M. and Grubman, M.J. 2001. Inhibition of L-deleted foot-and-mouth disease virus replication by alpha/beta interferon involves double-stranded RNA-dependent protein kinase. *Journal of Virology*. **75**(12), pp.5498–503.
- Chinsangaram, J., Mason, P.W. and Grubman, M.J. 1998. Protection of swine by live and inactivated vaccines prepared from a leader proteinase-deficient serotype A12 foot-and-mouth disease virus. *Vaccine*. **16**(16) ,pp.1516–22.
- Clarke, B.E., Brown, A.L., Currey, K.M., Newton, S.E., Rowlands, D.J. and Carroll, A.R. 1987. Potential secondary and tertiary structure in the genomic RNA of foot and mouth disease virus. *Nucleic Acids Research*. **15**(17), pp.7067–7079.
- Clarke, B.E. and Sangar, D. V 1988. Processing and assembly of foot-and-mouth disease virus proteins using subgenomic RNA. *Journal of General Virology*. **69** (Pt 9), pp.2313–25.

- Cold Spring Harbor Laboratory 2015. SDS-PAGE gel. *Cold Spring Harbor Protocols*. **2015**(7), p.pdb.rec087908.
- Costa Giomi, M.P., Bergmann, I.E., Scodeller, E.A., Augé de Mello, P., Gomez, I. and La Torre, J.L. 1984. Heterogeneity of the polyribocytidylic acid tract in aphthovirus: biochemical and biological studies of viruses carrying polyribocytidylic acid tracts of different lengths. *Journal of Virology*. **51**(3), pp.799–805.
- Cowan, K.M. and Graves, J.H. 1966. A third antigenic component associated with foot-and-mouth disease infection. *Virology*. **30**(3), pp.528–40.
- Cuchillo, C.M., Nogués, M.V. and Raines, R.T. 2011. Bovine pancreatic ribonuclease: Fifty years of the first enzymatic reaction mechanism. *Biochemistry*. **50**(37), pp.7835–7841.
- Delang, L., Paeshuyse, J. and Neyts, J. 2012. The role of phosphatidylinositol 4-kinases and phosphatidylinositol 4-phosphate during viral replication. *Biochemical Pharmacology*. **84**(11), pp.1400–1408.
- Devaney, M.A., Vakharia, V.N., Lloyd, R.E., Ehrenfeld, E. and Grubman, M.J. 1988. Leader protein of foot-and-mouth disease virus is required for cleavage of the p220 component of the cap-binding protein complex. *Journal of Virology*. **62**(11), pp.4407–9.
- Doedens, J.R. and Kirkegaard, K. 1995. Inhibition of cellular protein secretion by poliovirus proteins 2B and 3A. *The EMBO Journal*. **14**(5), pp.894–907.
- Doel, T.R. 2005. Natural and vaccine induced immunity to FMD. *Current Topics in Microbiology and Immunology*. **288**, pp.103–31.
- Doel, T.R., Sangar, D. V., Rowlands, D.J. and Brown, F. 1978. A re-appraisal of the biochemical map of foot-and-mouth disease virus RNA. *Journal of General Virology*. **41**(2), pp.395–404.
- Domingo, E., Escarmís, C., Lázaro, E. and Manrubia, S. 2005. Quasispecies dynamics and RNA virus extinction. *Virus Research*. **107**(2), pp.129–139.
- Domingo, E., Pariente, N., Airaksinen, A., González-Lopez, C., Sierra, S., Herrera, M., Grande-Pérez, A., Lowenstein, P.R., Manrubia, S.C., Lázaro, E. and Escarmís, C. 2005. Foot-and-mouth disease virus evolution: exploring pathways towards virus extinction. *Current Topics in Microbiology and Immunology*. **288**, pp.149–73.
- Domingo, E., Sheldon, J. and Perales, C. 2012. Viral quasispecies evolution. *Microbiology and Molecular Biology Reviews*. **76**(2), pp.159–216.
- Donnelly, M.L.L., Gani, D., Luke, G., Ryan, M.D., Mendoza, H. and Hughes, L.E. 2001. The ‘cleavage’ activities of foot-and-mouth disease virus 2A site-directed mutants and naturally occurring ‘2A-like’ sequences. *Journal of General Virology*. **82**(5), pp.1027–1041.
- Dorobantu, C.M., Albuлесcu, L., Harak, C., Feng, Q., van Kampen, M., Strating, J.R.P.M., Gorbalenya, A.E., Lohmann, V., van der Schaar, H.M. and van Kuppeveld, F.J.M. 2015. Modulation of the host lipid landscape to promote

- RNA virus replication: The picornavirus encephalomyocarditis virus converges on the pathway used by hepatitis C virus. *PLoS pathogens*. **11**(9), p.e1005185.
- Dorobantu, C.M., Ford-Siltz, L.A., Sittig, S.P., Lanke, K.H.W., Belov, G.A., van Kuppeveld, F.J.M. and van der Schaar, H.M. 2015. GBF1- and ACBD3-independent recruitment of PI4KIII β to replication sites by rhinovirus 3A proteins. *Journal of Virology*. **89**, pp.1913–1918.
- Dorobantu, C.M., van der Schaar, H.M., Ford, L. a, Strating, J.R.P.M., Ulferts, R., Fang, Y., Belov, G. and van Kuppeveld, F.J.M. 2014. Recruitment of PI4KIII β to coxsackievirus B3 replication organelles is independent of ACBD3, GBF1, and Arf1. *Journal of Virology*. **88**, pp.2725–36.
- Downing, G.J., Kim, S., Nakanishi, S., Catt, K.J. and Balla, T. 1996. Characterization of a soluble adrenal phosphatidylinositol 4-kinase reveals wortmannin sensitivity of type III phosphatidylinositol kinases. *Biochemistry*. **35**(11), pp.3587–3594.
- Duque, H. and Baxt, B. 2003. Foot-and-mouth disease virus receptors: comparison of bovine alpha(V) integrin utilization by type A and O viruses. *Journal of Virology*. **77**(4), pp.2500–11.
- Enders, J.F., Weller, T.H. and Robbins, F.C. 1949. Cultivation of the Lansing strain of poliomyelitis virus in cultures of various human embryonic tissues. *Science*. **109**(2822), pp.85–7.
- Environmental Sciences Inc. 2015. Ptilosarcus GFP. *AthenaES™*.
- Escarmís, C., Dopazo, J., Dávila, M., Palma, E.L. and Domingo, E. 1995. Large deletions in the 5'-untranslated region of foot-and-mouth disease virus of serotype C. *Virus Research*. **35**(2), pp.155–67.
- Falk, M.M., Grigera, P.R., Bergmann, I.E., Zibert, A., Multhaup, G. and Beck, E. 1990. Foot-and-mouth disease virus protease 3C induces specific proteolytic cleavage of host cell histone H3. *Journal of Virology*. **64**(2), pp.748–56.
- Falk, M.M., Sobrino, F. and Beck, E. 1992. VPg gene amplification correlates with infective particle formation in foot-and-mouth disease virus. *Journal of Virology*. **66**(4), pp.2251–60.
- Ferrer-Orta, C., Agudo, R., Domingo, E. and Verdaguer, N. 2009. Structural insights into replication initiation and elongation processes by the FMDV RNA-dependent RNA polymerase. *Current Opinion in Structural Biology*. **19**(6), pp.752–758.
- Ferrer-Orta, C., Arias, A., Agudo, R., Pérez-Luque, R., Escarmís, C., Domingo, E. and Verdaguer, N. 2006. The structure of a protein primer–polymerase complex in the initiation of genome replication. *The EMBO Journal*. **25**(4), pp.880–888.
- Ferrer-Orta, C., Arias, A., Escarmís, C. and Verdaguer, N. 2006. A comparison of viral RNA-dependent RNA polymerases. *Current Opinion in Structural Biology*. **16**(1), pp.27–34.
- Ferrer-Orta, C., Arias, A., Perez-Luque, R., Escarmis, C., Domingo, E. and Verdaguer, N. 2007. Sequential structures provide insights into the fidelity of RNA replication. *Proceedings of the National Academy of Sciences*. **104**(22),

pp.9463–9468.

- Ferrer-Orta, C., Arias, A., Perez-Luque, R., Escarmís, C., Domingo, E. and Verdaguier, N. 2004. Structure of foot-and-mouth disease virus RNA-dependent RNA polymerase and its complex with a template-primer RNA. *Journal of Biological Chemistry*. **279**(45), pp.47212–21.
- Ferrer-Orta, C., Ferrero, D. and Verdaguier, N. 2015. RNA-dependent RNA polymerases of picornaviruses: From the structure to regulatory mechanisms. *Viruses*. **7**(8), pp.4438–60.
- Ferrer-Orta, C., de la Higuera, I., Caridi, F., Sánchez-Aparicio, M.T., Moreno, E., Perales, C., Singh, K., Sarafianos, S.G., Sobrino, F., Domingo, E. and Verdaguier, N. 2015. Multifunctionality of a picornavirus polymerase domain: Nuclear localization signal and nucleotide recognition. *Journal of Virology*. **89**(13), pp.6848–6859.
- Flanegan, J.B. and Baltimore, D. 1977. Poliovirus-specific primer-dependent RNA polymerase able to copy poly(A). *Proceedings of the National Academy of Sciences*. **74**(9), pp.3677–3680.
- Flanegan, J.B. and Baltimore, D. 1979. Poliovirus polyuridylic acid polymerase and RNA replicase have the same viral polypeptide. *Journal of Virology*. **29**(1), pp.352–60.
- Flanegan, J.B. and Van Dyke, T.A. 1979. Isolation of a soluble and template-dependent poliovirus RNA polymerase that copies virion RNA in vitro. *Journal of Virology*. **32**(1), pp.155–61.
- Flint, M. and Ryan, M.D. 1997. Virus-encoded proteinases of the picornavirus supergroup. *Journal of General Virology*. **78**(4), pp.699–723.
- Forrest, S., Lear, Z., Herod, M.R., Ryan, M., Rowlands, D.J. and Stonehouse, N.J. 2014. Inhibition of the foot-and-mouth disease virus subgenomic replicon by RNA aptamers. *Journal of General Virology*. **95**, pp.2649–2657.
- Forss, S. and Schaller, H. 1982. A tandem repeat gene in a picornavirus. *Nucleic Acids Research*. **10**(20), pp.6441–6450.
- Forss, S., Strebel, K., Beck, E. and Schaller, H. 1984. Nucleotide sequence and genome organization of foot-and-mouth disease virus. *Nucleic Acids Research*. **12**(16), pp.6587–601.
- Fowler, V.L., Bashiruddin, J.B., Maree, F.F., Mutowembwa, P., Bankowski, B., Gibson, D., Cox, S., Knowles, N. and Barnett, P.V. 2011. Foot-and-mouth disease marker vaccine: Cattle protection with a partial VP1 G–H loop deleted virus antigen. *Vaccine*. **29**(46), pp.8405–8411.
- Fowler, V.L., Knowles, N.J., Paton, D.J. and Barnett, P.V. 2010. Marker vaccine potential of a foot-and-mouth disease virus with a partial VP1 G-H loop deletion. *Vaccine*. **28**(19), pp.3428–3434.
- Fowler, V.L., Paton, D.J., Rieder, E. and Barnett, P.V. 2008. Chimeric foot-and-mouth disease viruses: Evaluation of their efficacy as potential marker vaccines in cattle. *Vaccine*. **26**(16), pp.1982–1989.

- Fox, G., Parry, N.R., Barnett, P. V., McGinn, B., Rowlands, D.J. and Brown, F. 1989. The cell attachment site on foot-and-mouth disease virus includes the amino acid sequence RGD (Arginine-Glycine-Aspartic Acid). *Journal of General Virology*. **70**(3), pp.625–637.
- Gamarnik, A. V and Andino, R. 1998. Switch from translation to RNA replication in a positive-stranded RNA virus. *Genes & Development*. **12**(15), pp.2293–304.
- Gamarnik, A. V and Andino, R. 1997. Two functional complexes formed by KH domain containing proteins with the 5' noncoding region of poliovirus RNA. *RNA*. **3**(8), pp.882–92.
- Gao, Y., Sun, S.-Q. and Guo, H.-C. 2016. Biological function of foot-and-mouth disease virus non-structural proteins and non-coding elements. *Virology Journal*. **13**(1), p.107.
- García-Briones, M., Rosas, M.F., González-Magaldi, M., Martín-Acebes, M.A., Sobrino, F. and Armas-Portela, R. 2006. Differential distribution of non-structural proteins of foot-and-mouth disease virus in BHK-21 cells. *Virology*. **349**(2), pp.409–21.
- García-Nuñez, S., Gismondi, M.I., König, G., Berinstein, A., Taboga, O., Rieder, E., Martínez-Salas, E. and Carrillo, E. 2014. Enhanced IRES activity by the 3'UTR element determines the virulence of FMDV isolates. *Virology*. **448**, pp.303–313.
- Garmaroudi, F.S., Marchant, D., Hendry, R., Luo, H., Yang, D., Ye, X., Shi, J. and McManus, B.M. 2015. Coxsackievirus B3 replication and pathogenesis. *Future Microbiology*. **10**(4), pp.629–653.
- George, M., Venkataramanan, R., Pattnaik, B., Sanyal, A., Gurumurthy, C.B., Hemadri, D. and Tosh, C. 2001. Sequence analysis of the RNA polymerase gene of foot-and-mouth disease virus serotype Asia1. *Virus Genes*. **22**(1), pp.21–6.
- Giachetti, C., Hwang, S.S. and Semler, B.L. 1992. cis-acting lesions targeted to the hydrophobic domain of a poliovirus membrane protein involved in RNA replication. *Journal of Virology*. **66**(10), pp.6045–57.
- Giraud, A.T., Sagedahl, A., Bergmann, I.E., La Torre, J.L. and Scodeller, E.A. 1987. Isolation and characterization of recombinants between attenuated and virulent aphthovirus strains. *Journal of Virology*. **61**(2), pp.419–25.
- Gladue, D.P., O'Donnell, V., Baker-Branstetter, R., Holinka, L.G., Pacheco, J.M., Fernandez-Sainz, I., Lu, Z., Brocchi, E., Baxt, B., Piccone, M.E., Rodriguez, L. and Borca, M. V 2012. Foot-and-mouth disease virus nonstructural protein 2C interacts with Beclin1, modulating virus replication. *Journal of Virology*. **86**(22), pp.12080–90.
- Gomes, R.G.B., Isken, O., Tautz, N., McLauchlan, J. and McCormick, C.J. 2016. Polyprotein-driven formation of two interdependent sets of complexes supporting hepatitis C virus genome replication. *Journal of Virology*. **90**(6), pp.2868–2883.
- González-Magaldi, M., Martín-Acebes, M.A., Kremer, L. and Sobrino, F. 2014.

- Membrane topology and cellular dynamics of foot-and-mouth disease virus 3A protein. *PLoS ONE*. **9**(10), p.e106685.
- González-Magaldi, M., Postigo, R., de la Torre, B.G., Vieira, Y.A., Rodríguez-Pulido, M., López-Viñas, E., Gómez-Puertas, P., Andreu, D., Kremer, L., Rosas, M.F. and Sobrino, F. 2012. Mutations that hamper dimerization of foot-and-mouth disease virus 3A protein are detrimental for infectivity. *Journal of Virology*. **86**(20), pp.11013–23.
- González-Magaldi, M., Vázquez-Calvo, Á., de la Torre, B.G., Valle, J., Andreu, D. and Sobrino, F. 2015. Peptides interfering 3A protein dimerization decrease FMDV multiplication. *PLoS ONE*. **10**(10), p.e0141415.
- Goodfellow, I., Chaudhry, Y., Richardson, A., Meredith, J., Almond, J.W., Barclay, W. and Evans, D.J. 2000. Identification of a cis-acting replication element within the poliovirus coding region. *Journal of Virology*. **74**(10), pp.4590–600.
- Goodfellow, I.G., Polacek, C., Andino, R. and Evans, D.J. 2003. The poliovirus 2C cis-acting replication element-mediated uridylylation of VPg is not required for synthesis of negative-sense genomes. *Journal of General Virology*. **84**(Pt 9), pp.2359–63.
- Gorbalenya, A.E., Koonin, E. V. and Wolf, Y.I. 1990. A new superfamily of putative NTP-binding domains encoded by genomes of small DNA and RNA viruses. *FEBS Letters*. **262**(1), pp.145–148.
- Gosert, R., Egger, D. and Bienz, K. 2000. A cytopathic and a cell culture adapted hepatitis A virus strain differ in cell killing but not in intracellular membrane rearrangements. *Virology*. **266**(1), pp.157–169.
- Gosert, R., Egger, D., Lohmann, V., Bartenschlager, R., Blum, H.E., Bienz, K. and Moradpour, D. 2003. Identification of the hepatitis C virus RNA replication complex in Huh-7 cells harboring subgenomic replicons. *Journal of Virology*. **77**, pp.5487–5492.
- Graci, J.D. and Cameron, C.E. 2002. Quasispecies, error catastrophe, and the antiviral activity of ribavirin. *Virology*. **298**(2), pp.175–80.
- Greninger, A.L., Knudsen, G.M., Betegon, M., Burlingame, A.L. and Derisi, J.L. 2012. The 3A protein from multiple picornaviruses utilizes the golgi adaptor protein ACBD3 to recruit PI4KIII β . *Journal of Virology*. **86**(7), pp.3605–16.
- Grigera, P.R. and Tisminetzky, S.G. 1984. Histone H3 modification in BHK cells infected with foot-and-mouth disease virus. *Virology*. **136**(1), pp.10–9.
- Grubman, M.J. and Baxt, B. 2004. Foot-and-Mouth Disease. *Clinical Microbiology Reviews*. **17**(2), pp.465–493.
- Grubman, M.J. and Mason, P.W. 2002. Prospects, including time-frames, for improved foot and mouth disease vaccines. *Revue Scientifique et Technique (International Office of Epizootics)*. **21**(3), pp.589–600.
- Grubman, M.J., Robertson, B.H., Morgan, D.O., Moore, D.M. and Dowbenko, D. 1984. Biochemical map of polypeptides specified by foot-and-mouth disease virus. *Journal of Virology*. **50**(2), pp.579–86.

- Hansen, J.L., Long, A.M. and Schultz, S.C. 1997. Structure of the RNA-dependent RNA polymerase of poliovirus. *Structure*. **5**(8), pp.1109–1122.
- Harris, K.S., Xiang, W., Alexander, L., Lane, W.S., Paul, A. V and Wimmer, E. 1994. Interaction of poliovirus polypeptide 3CDpro with the 5' and 3' termini of the poliovirus genome. Identification of viral and cellular cofactors needed for efficient binding. *Journal of Biological Chemistry*. **269**(43), pp.27004–14.
- Harris, T.J. 1980. Comparison of the nucleotide sequence at the 5' end of RNAs from nine aphthoviruses, including representatives of the seven serotypes. *Journal of Virology*. **36**(3), pp.659–64.
- Harris, T.J. 1979. The nucleotide sequence at the 5' end of foot-and-mouth disease virus RNA. *Nucleic Acids Research*. **7**(7), pp.1765–85.
- Harris, T.J. and Brown, F. 1977. Biochemical analysis of a virulent and an avirulent strain of foot-and-mouth disease virus. *Journal of General Virology*. **34**(1), pp.87–105.
- Hellen, C.U.T. and Sarnow, P. 2001. Internal ribosome entry sites in eukaryotic mRNA molecules. *Genes & Development*. **15**(13), pp.1593–612.
- Herod, M.R., Ferrer-Orta, C., Loundras, E.-A., Ward, J.C., Verdaguer, N., Rowlands, D.J. and Stonehouse, N.J. 2016. Both cis and trans activities of foot-and-mouth disease virus 3D polymerase are essential for viral RNA replication. *Journal of Virology*. **90**(15), pp.6864–6883.
- Herod, M.R., Gold, S., Lasecka-Dykes, L., Wright, C., Ward, J.C., McLean, T.C., Forrest, S., Jackson, T., Tuthill, T.J., Rowlands, D.J. and Stonehouse, N.J. 2017. Genetic economy in picornaviruses: Foot-and-mouth disease virus replication exploits alternative precursor cleavage pathways. *PLoS Pathogens*. **13**(10), p.e1006666.
- Herod, M.R., Loundras, E.-A., Ward, J.C., Tulloch, F., Rowlands, D.J. and Stonehouse, N.J. 2015. Employing transposon mutagenesis to investigate foot-and-mouth disease virus replication. *Journal of General Virology*. **96**(12), pp.3507–3518.
- Herod, M.R., Schregel, V., Hinds, C., Liu, M., McLauchlan, J., McCormick, C.J. and Sandri-Goldin, R.M. 2014. Genetic complementation of hepatitis C virus nonstructural protein functions associated with replication exhibits requirements that differ from those for virion assembly. *Journal of Virology*. **88**(5), pp.2748–2762.
- Herold, J. and Andino, R. 2000. Poliovirus requires a precise 5' end for efficient positive-strand RNA synthesis. *Journal of Virology*. **74**(14), pp.6394–400.
- Herold, J. and Andino, R. 2001. Poliovirus RNA replication requires genome circularization through a protein-protein bridge. *Molecular Cell*. **7**(3), pp.581–91.
- Hicks, B.W. 2002. *Green Fluorescent Protein* New Jersey: Humana Press.
- Hogbom, M., Jager, K., Robel, I., Unge, T. and Rohayem, J. 2009. The active form of the norovirus RNA-dependent RNA polymerase is a homodimer with cooperative activity. *Journal of General Virology*. **90**(2), pp.281–291.

- Hogle, J.M., Chow, M. and Filman, D.J. 1985. Three-dimensional structure of poliovirus at 2.9 Å resolution. *Science*. **229**(4720), pp.1358–65.
- Hsu, N.-Y., Ilnytska, O., Belov, G., Santiana, M., Chen, Y.-H., Takvorian, P.M., Pau, C., van der Schaar, H., Kaushik-Basu, N., Balla, T., Cameron, C.E., Ehrenfeld, E., van Kuppeveld, F.J.M. and Altan-Bonnet, N. 2010. Viral reorganization of the secretory pathway generates distinct organelles for RNA replication. *Cell*. **141**(5), pp.799–811.
- ICTV 2016. ICTV Master Species List 2016 v1.3 - Master Species Lists - Master Species Lists - International Committee on Taxonomy of Viruses (ICTV).
- Ilnytska, O., Santiana, M., Hsu, N.-Y., Du, W.-L., Chen, Y.-H., Viktorova, E.G., Belov, G., Brinker, A., Storch, J., Moore, C., Dixon, J.L. and Altan-Bonnet, N. 2013. Enteroviruses harness the cellular endocytic machinery to remodel the host cell cholesterol landscape for effective viral replication. *Cell Host & Microbe*. **14**(3), pp.281–293.
- Jablonski, S.A., Luo, M. and Morrow, C.D. 1991. Enzymatic activity of poliovirus RNA polymerase mutants with single amino acid changes in the conserved YGDD amino acid motif. *Journal of Virology*. **65**(9), pp.4565–72.
- Jackson, T., Clark, S., Berryman, S., Burman, A., Cambier, S., Mu, D., Nishimura, S. and King, A.M.Q. 2004. Integrin alphavbeta8 functions as a receptor for foot-and-mouth disease virus: role of the beta-chain cytodomain in integrin-mediated infection. *Journal of Virology*. **78**(9), pp.4533–40.
- Jackson, T., Mould, A.P., Sheppard, D. and King, A.M.Q. 2002. Integrin alphavbeta1 is a receptor for foot-and-mouth disease virus. *Journal of Virology*. **76**(3), pp.935–41.
- Jackson, T., Sheppard, D., Denyer, M., Blakemore, W. and King, A.M. 2000. The epithelial integrin alphavbeta6 is a receptor for foot-and-mouth disease virus. *Journal of Virology*. **74**(11), pp.4949–56.
- Jamal, S.M. and Belsham, G.J. 2013. Foot-and-mouth disease: past, present and future. *Veterinary Research*. **44**(1), p.116.
- Jang, S.K., Krausslich, H.-G., Nicklin, M.J.H., Duke, G.M., Palmenberg, A.C. and Wimmer, E. 1988. A segment of the 5' nontranslated region of encephalomyocarditis virus RNA directs internal entry of ribosomes during In vitro translation. *Journal of Virology*. **62**(8), pp.2636–2643.
- Jecht, M., Probst, C. and Gauss-Müller, V. 1998. Membrane permeability induced by hepatitis A virus proteins 2B and 2BC and proteolytic processing of HAV 2BC. *Virology*. **252**(1), pp.218–227.
- Jones, D.M., Gretton, S.N., McLauchlan, J. and Targett-Adams, P. 2007. Mobility analysis of an NS5A-GFP fusion protein in cells actively replicating hepatitis C virus subgenomic RNA. *Journal of General Virology*. **88**, pp.470–475.
- Jones, D.M., Patel, A.H., Targett-Adams, P. and McLauchlan, J. 2009. The hepatitis C virus NS4B protein can trans-complement viral RNA replication and modulates production of infectious virus. *Journal of Virology*. **83**(5), pp.2163–2177.

- Kazakov, T., Yang, F., Ramanathan, H.N., Kohlway, A., Diamond, M.S. and Lindenbach, B.D. 2015. Hepatitis C virus RNA replication depends on specific cis- and trans-acting activities of viral nonstructural proteins. *PLoS Pathogens*. **11**(4), p.e1004817.
- Kieft, J.S. 2008. Viral IRES RNA structures and ribosome interactions. *Trends in Biochemical Sciences*. **33**(6), pp.274–283.
- Kim, Y.K., Lee, S.H., Kim, C.S., Seol, S.K. and Jang, S.K. 2003. Long-range RNA-RNA interaction between the 5' nontranslated region and the core-coding sequences of hepatitis C virus modulates the IRES-dependent translation. *RNA*. **9**(5), pp.599–606.
- Kirchweger, R., Ziegler, E., Lamphear, B.J., Waters, D., Liebig, H.D., Sommergruber, W., Sobrino, F., Hohenadl, C., Blaas, D. and Rhoads, R.E. 1994. Foot-and-mouth disease virus leader proteinase: purification of the Lb form and determination of its cleavage site on eIF-4 gamma. *Journal of Virology*. **68**(9), pp.5677–84.
- Kleid, D.G., Yansura, D., Small, B., Dowbenko, D., Moore, D.M., Grubman, M.J., McKercher, P.D., Morgan, D.O., Robertson, B.H. and Bachrach, H.L. 1981. Cloned viral protein vaccine for foot-and-mouth disease: responses in cattle and swine. *Science*. **214**(4525), pp.1125–9.
- Klein, M., Zimmermann, H., Nelsen-Salz, B., Hadaschik, D. and Eggers, H.J. 2000. The picornavirus replication inhibitors HBB and guanidine in the echovirus-9 system: the significance of viral protein 2C. *Journal of General Virology*. **81**(4), pp.895–901.
- Klump, W., Marquardt, O. and Hofschneider, P.H. 1984. Biologically active protease of foot and mouth disease virus is expressed from cloned viral cDNA in *Escherichia coli*. *Proceedings of the National Academy of Sciences of the United States of America*. **81**(11), pp.3351–5.
- Knight, Z.A., Gonzalez, B., Feldman, M.E., Zunder, E.R., Goldenberg, D.D., Williams, O., Loewith, R., Stokoe, D., Balla, A., Toth, B., Balla, T., Weiss, W.A., Williams, R.L. and Shokat, K.M. 2006. A Pharmacological map of the PI3-K family defines a role for p110 α in insulin signaling. *Cell*. **125**(4), pp.733–747.
- Knowles, N. 2017. Aphthovirus.
- Knowles, N., Hovi, T., Hyypiä, T., King, A.M., Lindberg, A., Pallansch, M., Palmenberg, A., Simmonds, P., Skern, T., Stanway, G., Yamashita, T. and Zell, R. 2012. *Virus Taxonomy: Classification and Nomenclature of Viruses: Ninth Report of the International Committee on Taxonomy of Viruses*. Elsevier, pp. 855–880.
- Knowles, N.J., Davies, P.R., Henry, T., O'Donnell, V., Pacheco, J.M. and Mason, P.W. 2001. Emergence in Asia of foot-and-mouth disease viruses with altered host range: characterization of alterations in the 3A protein. *Journal of Virology*. **75**(3), pp.1551–1556.
- Knowles, N.J., Samuel, A.R., Davies, P.R., Midgley, R.J. and Valarcher, J.-F. 2005. Pandemic strain of foot-and-mouth disease virus serotype O. *Emerging Infectious Diseases*. **11**(12), pp.1887–1893.

- Knox, C., Moffat, K., Ali, S., Ryan, M. and Wileman, T. 2005. Foot-and-mouth disease virus replication sites form next to the nucleus and close to the Golgi apparatus, but exclude marker proteins associated with host membrane compartments. *Journal of General Virology*. **86**(Pt 3), pp.687–96.
- Konan, K. V and Sanchez-Felipe, L. 2014. Lipids and RNA virus replication. *Current Opinion in Virology*. **9**, pp.45–52.
- Krauß, M. and Haucke, V. 2007. Phosphoinositide-metabolizing enzymes at the interface between membrane traffic and cell signalling. *EMBO Reports*. **8**(3), pp.241–246.
- Krieger, N., Lohmann, V. and Bartenschlager, R. 2001. Enhancement of hepatitis C virus RNA replication by cell culture-adaptive mutations. *Journal of Virology*. **75**(10), pp.4614–24.
- Ku, B.-K., Kim, S.-B., Moon, O.-K., Lee, S.-J., Lee, J.-H., Lyoo, Y.-S., Kim, H.-J. and Sur, J.-H. 2005. Role of apoptosis in the pathogenesis of Asian and South American foot-and-mouth disease viruses in swine. *Journal of Veterinary Medical Science*. **67**(11), pp.1081–8.
- Kühn, R., Luz, N. and Beck, E. 1990. Functional analysis of the internal translation initiation site of foot-and-mouth disease virus. *Journal of Virology*. **64**(10), pp.4625–31.
- van Kuppeveld, F.J., Hoenderop, J.G., Smeets, R.L., Willems, P.H., Dijkman, H.B., Galama, J.M. and Melchers, W.J. 1997. Coxsackievirus protein 2B modifies endoplasmic reticulum membrane and plasma membrane permeability and facilitates virus release. *The EMBO Journal*. **16**(12), pp.3519–3532.
- van Kuppeveld, F.J., Melchers, W.J., Kirkegaard, K. and Doedens, J.R. 1997. Structure-function analysis of coxsackie B3 virus protein 2B. *Virology*. **227**(1), pp.111–8.
- Lama, J., Paul, A. V, Harris, K.S. and Wimmer, E. 1994. Properties of purified recombinant poliovirus protein 3AB as substrate for viral proteinases and as co-factor for RNA polymerase 3Dpol. *Journal of Biological Chemistry*. **269**(1), pp.66–70.
- Lanke, K.H.W., van der Schaar, H.M., Belov, G.A., Feng, Q., Duijsings, D., Jackson, C.L., Ehrenfeld, E. and van Kuppeveld, F.J.M. 2009. GBF1, a guanine nucleotide exchange factor for Arf, is crucial for coxsackievirus B3 RNA replication. *Journal of Virology*. **83**, pp.11940–11949.
- Laporte, J. 1969. The structure of foot-and-mouth disease virus protein. *Journal of General Virology*. **4**(4), pp.631–634.
- Lawrence, P. and Rieder, E. 2009. Identification of RNA helicase A as a new host factor in the replication cycle of foot-and-mouth disease virus. *Journal of Virology*. **83**(21), pp.11356–66.
- Lawson, M.A. and Semler, B.L. 1992. Alternate poliovirus nonstructural protein processing cascades generated by primary sites of 3C proteinase cleavage. *Virology*. **191**(1), pp.309–20.

- Le, S.-Y., Chen, J.-H., Sonenberg, N. and Maizel, J. V. 1993. Conserved tertiary structural elements in the 5' nontranslated region of cardiovirus, aphthovirus and hepatitis A virus RNAs. *Nucleic Acids Research*. **21**(10), pp.2445–2451.
- Leippert, M., Beck, E., Weiland, F. and Pfaff, E. 1997. Point mutations within the betaG-betaH loop of foot-and-mouth disease virus O1K affect virus attachment to target cells. *Journal of Virology*. **71**(2), pp.1046–51.
- Licursi, M., Christian, S.L., Pongnopparat, T. and Hirasawa, K. 2011. In vitro and in vivo comparison of viral and cellular internal ribosome entry sites for bicistronic vector expression. *Gene Therapy*. **18**(6), pp.631–6.
- Licursi, M., Komatsu, Y., Pongnopparat, T. and Hirasawa, K. 2012. Promotion of viral internal ribosomal entry site-mediated translation under amino acid starvation. *Journal of General Virology*. **93**(Pt 5), pp.951–62.
- Limpens, R.W.A.L., van der Schaar, H.M., Kumar, D., Koster, A.J., Snijder, E.J., van Kuppeveld, F.J.M. and Barcena, M. 2011. The transformation of enterovirus replication structures: a three-dimensional study of single- and double-membrane compartments. *mBio*. **2**(5), pp.e00166-11-e00166-11.
- Lin, J.-Y., Chen, T.-C., Weng, K.-F., Chang, S.-C., Chen, L.-L. and Shih, S.-R. 2009. Viral and host proteins involved in picornavirus life cycle. *Journal of Biomedical Science*. **16**(1), p.103.
- Liu, Z., Tian, Y., Machida, K., Lai, M.M.C., Luo, G., Fong, S.K.H. and Ou, J.J. 2012. Transient activation of the PI3K-AKT pathway by hepatitis C virus to enhance viral entry. *Journal of Biological Chemistry*. **287**(50), pp.41922–41930.
- Loeffler, F. and Frosch, P. 1897. Summarischer Bericht über die Ergebnisse der Untersuchungen zur Erforschung der Maul-und Klauenseuche. *Zentralbl. Bakteriol. Parasitenkd Abt.* **1**(22), pp.257–259.
- López de Quinto, S. and Martínez-Salas, E. 2000. Interaction of the eIF4G initiation factor with the aphthovirus IRES is essential for internal translation initiation in vivo. *RNA*. **6**(10), pp.1380–92.
- López de Quinto, S., Sáiz, M., de la Morena, D., Sobrino, F. and Martínez-Salas, E. 2002. IRES-driven translation is stimulated separately by the FMDV 3'-NCR and poly(A) sequences. *Nucleic Acids Research*. **30**(20), pp.4398–405.
- de Los Santos, T., de Avila Botton, S., Weiblen, R. and Grubman, M.J. 2006. The leader proteinase of foot-and-mouth disease virus inhibits the induction of beta interferon mRNA and blocks the host innate immune response. *Journal of Virology*. **80**(4), pp.1906–14.
- de los Santos, T., Diaz-San Segundo, F. and Grubman, M.J. 2007. Degradation of nuclear factor kappa B during foot-and-mouth disease virus infection. *Journal of Virology*. **81**(23), pp.12803–12815.
- Lowe, P.A. and Brown, F. 1981. Isolation of a soluble and template-dependent foot-and-mouth disease virus RNA polymerase. *Virology*. **111**(1), pp.23–32.
- Lu, Z., Zhang, X., Fu, Y., Cao, Y., Tian, M., Sun, P., Li, D., Liu, Z. and Xie, Q. 2010. Expression of the major epitope regions of 2C integrated with the 3AB non-

- structural protein of foot-and-mouth disease virus and its potential for differentiating infected from vaccinated animals. *Journal of Virological Methods*. **170**(1–2), pp.128–133.
- Lubroth, J. and Brown, F. 1995. Identification of native foot-and-mouth disease virus non-structural protein 2C as a serological indicator to differentiate infected from vaccinated livestock. *Research in Veterinary Science*. **59**(1), pp.70–8.
- Lubroth, J., Grubman, M.J., Burrage, T.G., Newman, J.F. and Brown, F. 1996. Absence of protein 2C from clarified foot-and-mouth disease virus vaccines provides the basis for distinguishing convalescent from vaccinated animals. *Vaccine*. **14**(5), pp.419–27.
- Luo, G., Hamatake, R.K., Mathis, D.M., Racela, J., Rigat, K.L., Lemm, J. and Colonno, R.J. 2000. De novo initiation of RNA synthesis by the RNA-dependent RNA polymerase (NS5B) of hepatitis C virus. *Journal of Virology*. **74**(2), pp.851–63.
- Luz, N. and Beck, E. 1991. Interaction of a cellular 57-kilodalton protein with the internal translation initiation site of foot-and-mouth disease virus. *Journal of Virology*. **65**(12), pp.6486–94.
- Lyle, J.M., Bullitt, E., Bienz, K. and Kirkegaard, K. 2002. Visualization and functional analysis of RNA-dependent RNA polymerase lattices. *Science*. **296**(5576), pp.2218–22.
- Lyle, J.M., Clewell, A., Richmond, K., Richards, O.C., Hope, D.A., Schultz, S.C. and Kirkegaard, K. 2002. Similar structural basis for membrane localization and protein priming by an RNA-dependent RNA polymerase. *Journal of Biological Chemistry*. **277**(18), pp.16324–16331.
- Lyons, T., Murray, K.E., Roberts, A.W. and Barton, D.J. 2001. Poliovirus 5'-terminal cloverleaf RNA is required in cis for VPg uridylylation and the initiation of negative-strand RNA synthesis. *Journal of virology*. **75**(22), pp.10696–708.
- Macejak, D.G. and Sarnow, P. 1991. Internal initiation of translation mediated by the 5' leader of a cellular mRNA. *Nature*. **353**(6339), pp.90–94.
- Martín-Acebes, M.A., González-Magaldi, M., Sandvig, K., Sobrino, F. and Armas-Portela, R. 2007. Productive entry of type C foot-and-mouth disease virus into susceptible cultured cells requires clathrin and is dependent on the presence of plasma membrane cholesterol. *Virology*. **369**(1), pp.105–118.
- Martínez-Salas, E. 2008. The impact of RNA structure on picornavirus IRES activity. *Trends in Microbiology*. **16**, pp.230–237.
- Martínez-Salas, E., Francisco-Velilla, R., Fernandez-Chamorro, J., Lozano, G. and Diaz-Toledano, R. 2015. Picornavirus IRES elements: RNA structure and host protein interactions. *Virus Research*, pp.1–12.
- Mason, P.W., Bezborodova, S. V and Henry, T.M. 2002. Identification and characterization of a cis-acting replication element (cre) adjacent to the internal ribosome entry site of foot-and-mouth disease virus. *Journal of Virology*. **76**(19), pp.9686–94.

- Mason, P.W., Grubman, M.J. and Baxt, B. 2003. Molecular basis of pathogenesis of FMDV. *Virus Research*. **91**(1), pp.9–32.
- Mason, P.W., Piccone, M.E., Mckenna, T.S., Chinsangaram, J. and Grubman, M.J. 1997. Evaluation of a live-attenuated foot-and-mouth disease virus as a vaccine candidate. *Virology*. **227**(1), pp.96–102.
- Mason, P.W., Rieder, E. and Baxt, B. 1994. RGD sequence of foot-and-mouth disease virus is essential for infecting cells via the natural receptor but can be bypassed by an antibody-dependent enhancement pathway. *Proceedings of the National Academy of Sciences of the United States of America*. **91**(5), pp.1932–6.
- Matteis, M.A. De and Godi, A. 2004. PI-loting membrane traffic. *Nature Cell Biology*. **6**(6), pp.487–492.
- McCullough, K.C., Parkinson, D. and Crowther, J.R. 1988. Opsonization-enhanced phagocytosis of foot-and-mouth disease virus. *Immunology*. **65**(2), pp.187–91.
- McInerney, G.M., King, A.M.Q., Ross-Smith, N. and Belsham, G.J. 2000. Replication-competent foot-and-mouth disease virus RNAs lacking capsid coding sequences. *Journal of General Virology*. **81**(7), pp.1699–1702.
- McMahon, C.W., Traxler, B., Grigg, M.E. and Pullen, A.M. 1998. Transposon-mediated random insertions and site-directed mutagenesis prevent the trafficking of a mouse mammary tumor virus superantigen. *Virology*. **243**(2), pp.354–365.
- Melnick, J.L., Shaw, E.W. and Curnen, E.C. 1949. A virus isolated from patients diagnosed as non-paralytic poliomyelitis or aseptic meningitis. *Proceedings of the Society for Experimental Biology and Medicine*. **71**(3), pp.344–9.
- Mesmin, B., Bigay, J., Moser von Filseck, J., Lacas-Gervais, S., Drin, G. and Antony, B. 2013. A Four-step cycle driven by PI(4)P hydrolysis directs sterol/PI(4)P exchange by the ER-Golgi tether OSBP. *Cell*. **155**(4), pp.830–843.
- Meyer, R.F., Babcock, G.D., Newman, J.F., Burrage, T.G., Toohey, K., Lubroth, J. and Brown, F. 1997. Baculovirus expressed 2C of foot-and-mouth disease virus has the potential for differentiating convalescent from vaccinated animals. *Journal of Virological Methods*. **65**(1), pp.33–43.
- Meyers, R. and Cantley, L.C. 1997. Cloning and Characterization of a Wortmannin-sensitive Human Phosphatidylinositol 4-Kinase. *Journal of Biological Chemistry*. **272**(7), pp.4384–4390.
- Midgley, R., Moffat, K., Berryman, S., Hawes, P., Simpson, J., Fullen, D., Stephens, D.J., Burman, A. and Jackson, T. 2013. A role for endoplasmic reticulum exit sites in foot-and-mouth disease virus infection. *Journal of General Virology*. **94**(Pt 12), pp.2636–46.
- Mirzayan, C. and Wimmer, E. 1994. Biochemical Studies on Poliovirus Polypeptide 2C: Evidence for ATPase Activity. *Virology*. **199**(1), pp.176–187.
- Modrow, I. 1929. Filtration und Ultrafiltration des Maul- und Klauenseuchevirus. *Zeitschrift für Hygiene und Infektionskrankheiten*. **110**(4), pp.618–643.

- Moffat, K., Howell, G., Knox, C., Belsham, G.J., Monaghan, P., Ryan, M.D. and Wileman, T. 2005. Effects of foot-and-mouth disease virus nonstructural proteins on the structure and function of the early secretory pathway: 2BC but not 3A blocks endoplasmic reticulum-to-Golgi transport. *Journal of Virology*. **79**(7), pp.4382–95.
- Moffat, K., Knox, C., Howell, G., Clark, S.J., Yang, H., Belsham, G.J., Ryan, M. and Wileman, T. 2007. Inhibition of the secretory pathway by foot-and-mouth disease virus 2BC protein is reproduced by coexpression of 2B with 2C, and the site of inhibition is determined by the subcellular location of 2C. *Journal of Virology*. **81**(3), pp.1129–1139.
- Mohl, B.-P., Bartlett, C., Mankouri, J. and Harris, M. 2016. Early events in the generation of autophagosomes are required for the formation of membrane structures involved in hepatitis C virus genome replication. *Journal of General Virology*. **97**(3), pp.680–693.
- Monaghan, P., Cook, H., Jackson, T., Ryan, M. and Wileman, T. 2004. The ultrastructure of the developing replication site in foot-and-mouth disease virus-infected BHK-38 cells. *Journal of General Virology*. **85**(Pt 4), pp.933–46.
- Morgan, D.O., Moore, D.M. and McKercher, P.D. 1978. Purification of foot-and-mouth disease virus infection-associated antigen. *Proceedings, Annual Meeting of the United States Animal Health Association*. (82), pp.277–83.
- Murray, K.E. and Barton, D.J. 2003. Poliovirus CRE-dependent VPg uridylylation is required for positive-strand RNA synthesis but not for negative-strand RNA synthesis. *Journal of Virology*. **77**(8), pp.4739–50.
- Myers, R.M., Larin, Z. and Maniatis, T. 1985. Detection of single base substitutions by ribonuclease cleavage at mismatches in RNA:DNA duplexes. *Science*. **230**(4731), pp.1242–6.
- Nakanishi, S., Catt, K.J. and Balla, T. 1995. A wortmannin-sensitive phosphatidylinositol 4-kinase that regulates hormone-sensitive pools of inositolphospholipids. *Proceedings of the National Academy of Sciences*. **92**(12), pp.5317–5321.
- Di Nardo, A., Knowles, N.J. and Paton, D.J. 2011. Combining livestock trade patterns with phylogenetics to help understand the spread of foot and mouth disease in sub-Saharan Africa, the Middle East and Southeast Asia. *Revue Scientifique et Technique (International Office of Epizootics)*. **30**(1), pp.63–85.
- Nayak, A., Goodfellow, I.G. and Belsham, G.J. 2005. Factors required for the uridylylation of the foot-and-mouth disease virus 3B1, 3B2, and 3B3 peptides by the RNA-dependent RNA polymerase (3Dpol) in vitro. *Journal of Virology*. **79**(12), pp.7698–7706.
- Nayak, A., Goodfellow, I.G., Woolaway, K.E., Birtley, J., Curry, S. and Belsham, G.J. 2006. Role of RNA structure and RNA binding activity of foot-and-mouth disease virus 3C protein in VPg uridylylation and virus replication. *Journal of Virology*. **80**(19), pp.9865–9875.
- Neff, S., Sá-Carvalho, D., Rieder, E., Mason, P.W., Blystone, S.D., Brown, E.J. and

- Baxt, B. 1998. Foot-and-mouth disease virus virulent for cattle utilizes the integrin alpha(v)beta3 as its receptor. *Journal of Virology*. **72**(5), pp.3587–94.
- Newton, S.E., Carroll, A.R., Campbell, R.O., Clarke, B.E. and Rowlands, D.J. 1985. The sequence of foot-and-mouth disease virus RNA to the 5' side of the poly(C) tract. *Gene*. **40**(2–3), pp.331–6.
- Niepmann, M. 2009. Internal translation initiation of picornaviruses and hepatitis C virus. *Biochimica et Biophysica Acta (BBA) - Gene Regulatory Mechanisms*. **1789**(9–10), pp.529–541.
- Nieva, J.L., Madan, V. and Carrasco, L. 2012. Viroporins: structure and biological functions. *Nature Reviews Microbiology*. **10**(8), pp.563–574.
- Novoa, R.R., Calderita, G., Arranz, R., Fontana, J., Granzow, H. and Risco, C. 2005. Virus factories: associations of cell organelles for viral replication and morphogenesis. *Biology of the Cell*. **97**(2), pp.147–72.
- O'Donnell, V., LaRocco, M. and Baxt, B. 2008. Heparan sulfate-binding foot-and-mouth disease virus enters cells via caveola-mediated endocytosis. *Journal of Virology*. **82**(18), pp.9075–9085.
- O'Donnell, V., LaRocco, M., Duque, H. and Baxt, B. 2005. Analysis of foot-and-mouth disease virus internalization events in cultured cells. *Journal of Virology*. **79**(13), pp.8506–18.
- O'Donnell, V., Pacheco, J.M., LaRocco, M., Burrage, T., Jackson, W., Rodriguez, L.L., Borca, M. V. and Baxt, B. 2011. Foot-and-mouth disease virus utilizes an autophagic pathway during viral replication. *Virology*. **410**(1), pp.142–150.
- O'Donnell, V.K., Pacheco, J.M., Henry, T.M. and Mason, P.W. 2001. Subcellular distribution of the foot-and-mouth disease virus 3A protein in cells infected with viruses encoding wild-type and bovine-attenuated forms of 3A. *Virology*. **287**(1), pp.151–62.
- O'Reilly, E.K. and Kao, C.C. 1998. Analysis of RNA-dependent RNA polymerase structure and function as guided by known polymerase structures and computer predictions of secondary structure. *Virology*. **252**(2), pp.287–303.
- Oh, H.S., Pathak, H.B., Goodfellow, I.G., Arnold, J.J. and Cameron, C.E. 2009. Insight into poliovirus genome replication and encapsidation obtained from studies of 3B-3C cleavage site mutants. *Journal of Virology*. **83**(18), pp.9370–9387.
- Otto, P. 1994. Veterinary Virology. *Journal of Basic Microbiology*, pp.56–56.
- Pacheco, J.M., Gladue, D.P., Holinka, L.G., Arzt, J., Bishop, E., Smoliga, G., Pauszek, S.J., Bracht, A.J., O'Donnell, V., Fernandez-Sainz, I., Fletcher, P., Piccone, M.E., Rodriguez, L.L. and Borca, M. V. 2013. A partial deletion in non-structural protein 3A can attenuate foot-and-mouth disease virus in cattle. *Virology*. **446**(1–2), pp.260–267.
- Pacheco, J.M., Henry, T.M., O'Donnell, V.K., Gregory, J.B. and Mason, P.W. 2003. Role of nonstructural proteins 3A and 3B in host range and pathogenicity of foot-and-mouth disease virus. *Journal of Virology*. **77**(24), pp.13017–27.

- Pallansch, M.A., Kew, O.M., Semler, B.L., Omilianowski, D.R., Anderson, C.W., Wimmer, E. and Rueckert, R.R. 1984. Protein processing map of poliovirus. *Journal of Virology*. **49**(3), pp.873–80.
- Palmenberg, A.C. 1987. Comparative organization and genome structure in picornaviruses. *Positive Strand RNA Viruses (UCLA Symposia on Molecular and Cellular Biology)*., pp.25–34.
- Palmenberg, A.C. 1990. Proteolytic processing of picornaviral polyprotein. *Annual Review of Microbiology*. **44**(1), pp.603–623.
- Di Paolo, G. and De Camilli, P. 2006. Phosphoinositides in cell regulation and membrane dynamics. *Nature*. **443**(7112), pp.651–657.
- Park, J.H., Lee, K.N., Ko, Y.J., Kim, S.M., Lee, H.S., Park, J.Y., Yeh, J.Y., Kim, M.J., Lee, Y.H., Sohn, H.J., Cho, I.S. and Kim, B. 2013. Diagnosis and control measures of the 2010 outbreak of foot-and-mouth disease A type in the Republic of Korea. *Transboundary and Emerging Diseases*. **60**(2), pp.188–192.
- Parsley, T.B., Cornell, C.T. and Semler, B.L. 1999. Modulation of the RNA binding and protein processing activities of poliovirus polypeptide 3CD by the viral RNA polymerase domain. *Journal of Biological Chemistry*. **274**(18), pp.12867–76.
- Pata, J.D., Schultz, S.C. and Kirkegaard, K. 1995. Functional oligomerization of poliovirus RNA-dependent RNA polymerase. *RNA*. **1**(5), pp.466–77.
- Paul, A. V. 2002. Possible unifying mechanism of picornavirus genome replication. *Molecular Biology of Picornavirus (American Society of Microbiology)*. pp.227–246.
- Paul, A. V., van Boom, J.H., Filippov, D. and Wimmer, E. 1998. Protein-primed RNA synthesis by purified poliovirus RNA polymerase. *Nature*. **393**(6682), pp.280–4.
- Paul, A. V., Rieder, E., Kim, D.W., van Boom, J.H. and Wimmer, E. 2000. Identification of an RNA hairpin in poliovirus RNA that serves as the primary template in the in vitro uridylylation of VPg. *Journal of Virology*. **74**(22), pp.10359–70.
- Pelletier, J. and Sonenberg, N. 1988. Internal initiation of translation of eukaryotic mRNA directed by a sequence derived from poliovirus RNA. *Nature*. **334**(6180), pp.320–325.
- Pfister, T. and Wimmer, E. 1999. Characterization of the nucleoside triphosphatase activity of poliovirus protein 2C reveals a mechanism by which guanidine inhibits poliovirus replication. *Journal of Biological Chemistry*. **274**(11), pp.6992–7001.
- Piccone, M.E., Rieder, E., Mason, P.W. and Grubman, M.J. 1995. The foot-and-mouth disease virus leader proteinase gene is not required for viral replication. *Journal of Virology*. **69**(9), pp.5376–82.
- Pilipenko, E. V, Gmyl, A.P., Maslova, S. V, Svitkin, Y. V, Sinyakov, A.N. and Agol, V.I. 1992. Prokaryotic-like cis elements in the cap-independent internal initiation of translation on picornavirus RNA. *Cell*. **68**(1), pp.119–31.
- Pilipenko, E. V, Pestova, T. V, Kolupaeva, V.G., Khitrina, E. V, Poperechnaya, A.N.,

- Agol, V.I. and Hellen, C.U. 2000. A cell cycle-dependent protein serves as a template-specific translation initiation factor. *Genes & Development*. **14**(16), pp.2028–45.
- Pogue, G.P., Huntley, C.C. and Hall, T.C. 1994. Common replication strategies emerging from the study of diverse groups of positive-strand RNA viruses. *Archives of Virology: Supplementum*. **9**, pp.181–94.
- Polatnick, J. and Arlinghaus, R.B. 1967. Foot-and-mouth disease virus-induced ribonucleic acid polymerase in baby hamster kidney cells. *Virology*. **31**(4), pp.601–8.
- Polatnick, J. and Wool, S. 1983. Association of foot-and-mouth disease virus induced RNA polymerase with host cell organelles. *Comparative Immunology, Microbiology and Infectious Diseases*. **6**(3), pp.265–272.
- Polatnick, J. and Wool, S.H. 1983. Correlation of surface and internal ultrastructural changes in cells infected with foot-and-mouth disease virus. *Canadian Journal of Comparative Medicine*. **47**(4), pp.440–4.
- Porta, C., Kotecha, A., Burman, A., Jackson, T., Ren, J., Loureiro, S., Jones, I.M., Fry, E.E., Stuart, D.I. and Charleston, B. 2013. Rational Engineering of Recombinant Picornavirus Capsids to Produce Safe, Protective Vaccine Antigen. *PLoS Pathogens*. **9**(3), p.e1003255.
- Porta, C., Xu, X., Loureiro, S., Paramasivam, S., Ren, J., Al-Khalil, T., Burman, A., Jackson, T., Belsham, G.J., Curry, S., Lomonossoff, G.P., Parida, S., Paton, D., Li, Y., Wilsden, G., Ferris, N., Owens, R., Kotecha, A., Fry, E., Stuart, D.I., Charleston, B. and Jones, I.M. 2013. Efficient production of foot-and-mouth disease virus empty capsids in insect cells following down regulation of 3C protease activity. *Journal of Virological Methods*. **187**(2), pp.406–12.
- Porter, A.G., Fellner, P., Black, D.N., Rowlands, D.J., Harris, T.J.R. and Brown, F. 1978. 3'-Terminal nucleotide sequences in the genome RNA of picornaviruses. *Nature*. **276**(5685), pp.298–301.
- Powis, G., Bonjouklian, R., Berggren, M.M., Gallegos, A., Abraham, R., Ashendel, C., Zalkow, L., Matter, W.F., Dodge, J. and Grindey, G. 1994. Wortmannin, a potent and selective inhibitor of phosphatidylinositol-3-kinase. *Cancer Research*. **54**(9), pp.2419–23.
- Racaniello, V.R. 2007. Picornaviridae: The Viruses and their Replication *In*: D. M. Knipe, P. M. Howley, D. E. Griffin, M. A. Martin, R. A. Lamb, B. Roizman and S. E. Straus, eds. *Fields Virology Volume 1*, pp.795–838.
- Raubo, P., Andrews, D.M., McKelvie, J.C., Robb, G.R., Smith, J.M., Swarbrick, M.E. and Waring, M.J. 2015. Discovery of potent, selective small molecule inhibitors of α -subtype of type III phosphatidylinositol-4-kinase (PI4KIII α). *Bioorganic & Medicinal Chemistry Letters*. **25**(16), pp.3189–3193.
- Reiss, S., Rebhan, I., Backes, P., Romero-Brey, I., Erfle, H., Matula, P., Kaderali, L., Poenisch, M., Blankenburg, H., Hiet, M.S., Longerich, T., Diehl, S., Ramirez, F., Balla, T., Rohr, K., Kaul, A., Bühler, S., Pepperkok, R., Lengauer, T., Albrecht, M., Eils, R., Schirmacher, P., Lohmann, V. and Bartenschlager, R. 2011. Recruitment

- and activation of a lipid kinase by hepatitis C virus NS5A is essential for integrity of the membranous replication compartment. *Cell Host and Microbe*. **9**, pp.32–45.
- Remenyi, R., Qi, H., Su, S.-Y., Chen, Z., Wu, N.C., Arumugaswami, V., Truong, S., Chu, V., Stokelman, T., Lo, H.-H., Olson, C.A., Wu, T.-T., Chen, S.-H., Lin, C.-Y. and Sun, R. 2014. A comprehensive functional map of the hepatitis C virus genome provides a resource for probing viral proteins. *mBio*. **5**(5), pp.e01469-14-e01469-14.
- Rieder, E., Bunch, T., Brown, F. and Mason, P.W. 1993. Genetically engineered foot-and-mouth disease viruses with poly(C) tracts of two nucleotides are virulent in mice. *Journal of Virology*. **67**(9), pp.5139–45.
- Robertson, B.H., Grubman, M.J., Weddell, G.N., Moore, D.M., Welsh, J.D., Fischer, T., Dowbenko, D.J., Yansura, D.G., Small, B. and Kleid, D.G. 1985. Nucleotide and amino acid sequence coding for polypeptides of foot-and-mouth disease virus type A12. *Journal of Virology*. **54**(3), pp.651–60.
- Rodríguez Pulido, M., Serrano, P., Sáiz, M. and Martínez-Salas, E. 2007. Foot-and-mouth disease virus infection induces proteolytic cleavage of PTB, eIF3a,b, and PABP RNA-binding proteins. *Virology*. **364**(2), pp.466–74.
- Ross-Thriepland, D., Mankouri, J. and Harris, M. 2015. Serine phosphorylation of the hepatitis C virus NS5A protein controls the establishment of replication complexes. *Journal of Virology*. **89**, pp.3123–35.
- Rossmann, M.G. 1989. The canyon hypothesis. Hiding the host cell receptor attachment site on a viral surface from immune surveillance. *Journal of Biological Chemistry*. **264**(25), pp.14587–90.
- Roulin, P.S., Lötzerich, M., Torta, F., Tanner, L.B., van Kuppeveld, F.J.M., Wenk, M.R. and Greber, U.F. 2014. Rhinovirus uses a phosphatidylinositol 4-phosphate/cholesterol counter-current for the formation of replication compartments at the ER-Golgi interface. *Cell Host & Microbe*. **16**(5), pp.677–690.
- Rowlands, D.J., Harris, T.J. and Brown, F. 1978. More precise location of the polycytidylic acid tract in foot and mouth disease virus RNA. *Journal of Virology*. **26**(2), pp.335–43.
- Rueckert, R. and Wimmer, E. 1984. Systematic nomenclature of picornavirus proteins. *Journal of Virology*. **50**(3), pp.957–9.
- Rweyemamu, M., Roeder, P., Mackay, D., Sumption, K., Brownlie, J., Leforban, Y., Valarcher, J.-F., Knowles, N.J. and Saraiva, V. 2008. Epidemiological patterns of foot-and-mouth disease worldwide. *Transboundary and Emerging Diseases*. **55**(1), pp.57–72.
- Ryan, M.D., Belsham, G.J. and King, A.M. 1989. Specificity of enzyme-substrate interactions in foot-and-mouth disease virus polyprotein processing. *Virology*. **173**(1), pp.35–45.
- Ryan, M.D. and Drew, J. 1994. Foot-and-mouth disease virus 2A oligopeptide

- mediated cleavage of an artificial polyprotein. *The EMBO Journal*. **13**(4), pp.928–33.
- Ryan, M.D., Flint, M., Donnelly, M.L., Gani, D. and Monaghan, S. 1997. The cleavage activities of aphthovirus and cardiovirus 2A proteins. *Journal of General Virology*. **78**(1), pp.13–21.
- Ryan, M.D., King, A.M. and Thomas, G.P. 1991. Cleavage of foot-and-mouth disease virus polyprotein is mediated by residues located within a 19 amino acid sequence. *Journal of General Virology*. **72 (Pt 11)**, pp.2727–32.
- Ryan, M.D., Mehrotra, A., Gani, D., Donnelly, M.L.L., Hughes, L.E., Luke, G. and Li, X. 2001. Analysis of the aphthovirus 2A/2B polyprotein 'cleavage' mechanism indicates not a proteolytic reaction, but a novel translational effect: a putative ribosomal 'skip'. *Journal of General Virology*. **82**(5), pp.1013–1025.
- Saeed, M., Scheel, T.K.H., Gottwein, J.M., Marukian, S., Dustin, L.B., Bukh, J. and Rice, C.M. 2012. Efficient replication of genotype 3a and 4a hepatitis C virus replicons in human hepatoma cells. *Antimicrobial Agents and Chemotherapy*. **56**(10), pp.5365–5373.
- Sáiz, M., Gómez, S., Martínez-Salas, E. and Sobrino, F. 2001. Deletion or substitution of the aphthovirus 3' NCR abrogates infectivity and virus replication. *Journal of General Virology*. **82**(Pt 1), pp.93–101.
- Sáiz, M., Núñez, J.I., Jimenez-Clavero, M.A., Baranowski, E. and Sobrino, F. 2002. Foot-and-mouth disease virus: biology and prospects for disease control. *Microbes and Infection / Institut Pasteur*. **4**(11), pp.1183–92.
- Saleh, L., Rust, R.C., Füllkrug, R., Beck, E., Bassili, G., Ochs, K. and Niepmann, M. 2001. Functional interaction of translation initiation factor eIF4G with the foot-and-mouth disease virus internal ribosome entry site. *Journal of General Virology*. **82**(Pt 4), pp.757–63.
- Sanchez-Aparicio, M.T., Rosas, M.F. and Sobrino, F. 2013. Characterization of a nuclear localization signal in the foot-and-mouth disease virus polymerase. *Virology*. **444**(1–2), pp.203–210.
- Sangar, D. V., Black, D.N., Rowlands, D.J. and Brown, F. 1977. Biochemical mapping of the foot-and-mouth disease virus genome. *Journal of General Virology*. **35**(2), pp.281–297.
- Sangar, D. V., Rowlands, D.J., Harris, T.J.R. and Brown, F. 1977. Protein covalently linked to foot-and-mouth disease virus RNA. *Nature*. **268**(5621), pp.648–650.
- Sangar, D. V., Black, D.N., Rowlands, D.J., Harris, T.J. and Brown, F. 1980. Location of the initiation site for protein synthesis on foot-and-mouth disease virus RNA by in vitro translation of defined fragments of the RNA. *Journal of Virology*. **33**(1), pp.59–68.
- Sangar, D. V., Newton, S.E., Rowlands, D.J. and Clarke, B.E. 1987. All foot and mouth disease virus serotypes initiate protein synthesis at two separate AUGs. *Nucleic Acids Research*. **15**(8), pp.3305–15.
- Sanz-Parra, A., Ley, V. and Sobrino, F. 1998. Infection with foot-and-mouth disease

- virus results in a rapid reduction of MHC class I surface expression. *Journal of General Virology*. **79**(3), pp.433–436.
- Sarnow, P. 1989. Translation of glucose-regulated protein 78/immunoglobulin heavy-chain binding protein mRNA is increased in poliovirus-infected cells at a time when cap-dependent translation of cellular mRNAs is inhibited. *Proceedings of the National Academy of Sciences of the United States of America*. **86**(15), pp.5795–9.
- Saunders, K. and King, A.M. 1982. Guanidine-resistant mutants of aphthovirus induce the synthesis of an altered nonstructural polypeptide, P34. *Journal of Virology*. **42**(2), pp.389–94.
- Saunders, K., King, A.M., McCahon, D., Newman, J.W., Slade, W.R. and Forss, S. 1985. Recombination and oligonucleotide analysis of guanidine-resistant foot-and-mouth disease virus mutants. *Journal of Virology*. **56**(3), pp.921–9.
- van der Schaar, H.M., Leyssen, P., Thibaut, H.J., de Palma, A., van der Linden, L., Lanke, K.H.W., Lacroix, C., Verbeken, E., Conrath, K., Macleod, A.M., Mitchell, D.R., Palmer, N.J., van de Poël, H., Andrews, M., Neyts, J. and van Kuppeveld, F.J.M. 2013. A novel, broad-spectrum inhibitor of enterovirus replication that targets host cell factor phosphatidylinositol 4-kinase III β . *Antimicrobial Agents and Chemotherapy*. **57**(10), pp.4971–81.
- van der Schaar, H.M., van der Linden, L., Lanke, K.H.W., Strating, J.R.P.M., Pürstinger, G., de Vries, E., de Haan, C.A.M., Neyts, J. and van Kuppeveld, F.J.M. 2012. Coxsackievirus mutants that can bypass host factor PI4KIII β and the need for high levels of PI4P lipids for replication. *Cell Research*. **22**(11), pp.1576–92.
- Schlegel, A., Giddings, T.H., Ladinsky, M.S. and Kirkegaard, K. 1996. Cellular origin and ultrastructure of membranes induced during poliovirus infection. *Journal of Virology*. **70**(10), pp.6576–88.
- Sellers, R.F., Donaldson, A.I. and Herniman, K.A.J. 2009. Inhalation, persistence and dispersal of foot-and-mouth disease virus by man. *Journal of Hygiene*. **68**(4), p.565.
- Semler, B.L., Anderson, C.W., Kitamura, N., Rothberg, P.G., Wishart, W.L. and Wimmer, E. 1981. Poliovirus replication proteins: RNA sequence encoding P3-1b and the sites of proteolytic processing. *Proceedings of the National Academy of Sciences of the United States of America*. **78**(6), pp.3464–8.
- Serrano, P., Pulido, M.R., Sáiz, M. and Martínez-Salas, E. 2006. The 3' end of the foot-and-mouth disease virus genome establishes two distinct long-range RNA-RNA interactions with the 5' end region. *The Journal of General Virology*. **87**(Pt 10), pp.3013–22.
- Sierra, S., Dávila, M., Lowenstein, P.R. and Domingo, E. 2000. Response of foot-and-mouth disease virus to increased mutagenesis: influence of viral load and fitness in loss of infectivity. *Journal of Virology*. **74**(18), pp.8316–23.
- Sir, D., Kuo, C., Tian, Y., Liu, H.M., Huang, E.J., Jung, J.U., Machida, K. and Ou, J.J. 2012. Replication of hepatitis C virus RNA on autophagosomal membranes.

- Journal of Biological Chemistry*. **287**(22), pp.18036–18043.
- Sizova, D. V, Kolupaeva, V.G., Pestova, T. V, Shatsky, I.N. and Hellen, C.U. 1998. Specific interaction of eukaryotic translation initiation factor 3 with the 5' nontranslated regions of hepatitis C virus and classical swine fever virus RNAs. *Journal of Virology*. **72**(6), pp.4775–82.
- Sobrino, F., Saíz, M., Jiménez-Clavero, M.A., Núñez, J.I., Rosas, M.F., Baranowski, E. and Ley, V. 2001. Foot-and-mouth disease virus: a long known virus, but a current threat. *Veterinary Research*. **32**(1), pp.1–30.
- Spagnolo, J.F., Rossignol, E., Bullitt, E. and Kirkegaard, K. 2010. Enzymatic and nonenzymatic functions of viral RNA-dependent RNA polymerases within oligomeric arrays. *RNA*. **16**(2), pp.382–93.
- Spear, A., Ogram, S.A., Morasco, B.J., Smerage, L.E. and Flanagan, J.B. 2015. Viral precursor protein P3 and its processed products perform discrete and essential functions in the poliovirus RNA replication complex. *Virology*. **485**, pp.492–501.
- Stanway, G. 1990. Structure, function and evolution of picornaviruses. *Journal of General Virology*. **71**(11), pp.2483–2501.
- Steil, B.P. and Barton, D.J. 2009. Conversion of VPg into VPgpUpUOH before and during poliovirus negative-strand RNA synthesis. *Journal of Virology*. **83**(24), pp.12660–12670.
- Steitz, T.A. 1998. A mechanism for all polymerases. *Nature*. **391**(6664), pp.231–2.
- Stewart, S.R. and Semler, B.L. 1997. RNA Determinants of picornavirus cap-independent translation initiation. *Seminars in Virology*. **8**(3), pp.242–255.
- Suhy, D.A., Giddings, T.H. and Kirkegaard, K. 2000. Remodeling the endoplasmic reticulum by poliovirus infection and by individual viral proteins: an autophagy-like origin for virus-induced vesicles. *Journal of Virology*. **74**(19), pp.8953–65.
- Summerfield, A., Guzylack-Piriou, L., Harwood, L. and McCullough, K.C. 2009. Innate immune responses against foot-and-mouth disease virus: Current understanding and future directions. *Veterinary Immunology and Immunopathology*. **128**(1–3), pp.205–210.
- Sweeney, T.R., Cisnetto, V., Bose, D., Bailey, M., Wilson, J.R., Zhang, X., Belsham, G.J. and Curry, S. 2010. Foot-and-mouth disease virus 2C is a hexameric AAA+ protein with a coordinated ATP hydrolysis mechanism. *Journal of Biological Chemistry*. **285**(32), pp.24347–24359.
- Taboga, O., Tami, C., Carrillo, E., Núñez, J.I., Rodríguez, A., Saíz, J.C., Blanco, E., Valero, M.L., Roig, X., Camarero, J.A., Andreu, D., Mateu, M.G., Giralto, E., Domingo, E., Sobrino, F. and Palma, E.L. 1997. A large-scale evaluation of peptide vaccines against foot-and-mouth disease: lack of solid protection in cattle and isolation of escape mutants. *Journal of Virology*. **71**(4), pp.2606–14.
- Tami, C., Taboga, O., Berinstein, A., Núñez, J.I., Palma, E.L., Domingo, E., Sobrino, F. and Carrillo, E. 2003. Evidence of the coevolution of antigenicity and host cell

- tropism of foot-and-mouth disease virus in vivo. *Journal of Virology*. **77**(2), pp.1219–26.
- Tellez, A.B., Wang, J., Tanner, E.J., Spagnolo, J.F., Kirkegaard, K. and Bullitt, E. 2011. Interstitial contacts in an RNA-dependent RNA polymerase lattice. *Journal of Molecular Biology*. **412**(4), pp.737–750.
- Tesar, M., Berger, H.G. and Marquardt, O. 1989. Serological probes for some foot-and-mouth disease virus nonstructural proteins. *Virus Genes*. **3**(1), pp.29–44.
- Tesar, M. and Marquardt, O. 1990. Foot-and-mouth disease virus protease 3C inhibits cellular transcription and mediates cleavage of histone H3. *Virology*. **174**(2), pp.364–74.
- Teterina, N.L., Gorbalenya, A.E., Egger, D., Bienz, K., Rinaudo, M.S. and Ehrenfeld, E. 2006. Testing the modularity of the N-terminal amphipathic helix conserved in picornavirus 2C proteins and hepatitis C NS5A protein. *Virology*. **344**(2), pp.453–467.
- Teterina, N.L., Lauber, C., Jensen, K.S., Levenson, E.A., Gorbalenya, A.E. and Ehrenfeld, E. 2011. Identification of tolerated insertion sites in poliovirus non-structural proteins. *Virology*. **409**(1), pp.1–11.
- Teterina, N.L., Zhou, W.D., Cho, M.W. and Ehrenfeld, E. 1995. Inefficient complementation activity of poliovirus 2C and 3D proteins for rescue of lethal mutations. *Journal of Virology*. **69**(7), pp.4245–54.
- Tiley, L., King, A.M.Q. and Belsham, G.J. 2003. The foot-and-mouth disease virus cis-acting replication element (cre) can be complemented in trans within infected cells. *Journal of Virology*. **77**(3), pp.2243–2246.
- Towner, J.S., Mazanet, M.M. and Semler, B.L. 1998. Rescue of defective poliovirus RNA replication by 3AB-containing precursor polyproteins. *Journal of Virology*. **72**(9), pp.7191–200.
- Trotard, M., Lepère-Douard, C., Régeard, M., Piquet-Pellorce, C., Lavillette, D., Cosset, F.-L., Gripon, P. and Le Seyec, J. 2009. Kinases required in hepatitis C virus entry and replication highlighted by small interference RNA screening. *FASEB journal : Official Publication of the Federation of American Societies for Experimental Biology*. **23**(11), pp.3780–9.
- Troxler, M., Egger, D., Pfister, T. and Bienz, K. 1992. Intracellular localization of poliovirus RNA by in situ hybridization at the ultrastructural level using single-stranded riboprobes. *Virology*. **191**(2), pp.687–97.
- Tsukiyama-Kohara, K., Iizuka, N., Kohara, M. and Nomoto, A. 1992. Internal ribosome entry site within hepatitis C virus RNA. *Journal of Virology*. **66**(3), pp.1476–1483.
- Tulloch, F., Pathania, U., Luke, G.A., Nicholson, J., Stonehouse, N.J., Rowlands, D.J., Jackson, T., Tuthill, T., Haas, J., Lamond, A.I. and Ryan, M.D. 2014. FMDV replicons encoding green fluorescent protein are replication competent. *Journal of Virological Methods*. **209C**, pp.35–40.
- Vakharia, V.N., Devaney, M.A., Moore, D.M., Dunn, J.J. and Grubman, M.J. 1987.

- Proteolytic processing of foot-and-mouth disease virus polyproteins expressed in a cell-free system from clone-derived transcripts. *Journal of Virology*. **61**(10), pp.3199–207.
- Valdazo-González, B., Timina, A., Scherbakov, A., Abdul-Hamid, N., Knowles, N.J. and King, D.P. 2013. Multiple introductions of serotype O foot-and-mouth disease viruses into East Asia in 2010–2011. *Veterinary Research*. **44**(1), p.76.
- Villaverde, A., Martínez-Salas, E. and Domingo, E. 1988. 3D gene of foot-and-mouth disease virus. Conservation by convergence of average sequences. *Journal of Molecular Biology*. **204**(3), pp.771–6.
- Villordo, S.M., Alvarez, D.E. and Gamarnik, A. V. 2010. A balance between circular and linear forms of the dengue virus genome is crucial for viral replication. *RNA*. **16**(12), pp.2325–2335.
- Walter, T.S., Ren, J., Tuthill, T.J., Rowlands, D.J., Stuart, D.I. and Fry, E.E. 2012. A plate-based high-throughput assay for virus stability and vaccine formulation. *Journal of Virological Methods*. **185**(1), pp.166–170.
- Wang, D., Fang, L., Li, K., Zhong, H., Fan, J., Ouyang, C., Zhang, H., Duan, E., Luo, R., Zhang, Z., Liu, X., Chen, H. and Xiao, S. 2012. Foot-and-mouth disease virus 3C protease cleaves NEMO to impair innate immune signaling. *Journal of Virology*. **86**(17), pp.9311–9322.
- Wang, H., Perry, J.W., Lauring, A.S., Neddermann, P., De Francesco, R. and Tai, A.W. 2014. Oxysterol-binding protein is a phosphatidylinositol 4-kinase effector required for HCV replication membrane integrity and cholesterol trafficking. *Gastroenterology*. **146**(5), p.1373–1385.e11.
- Wang, J., Lyle, J.M. and Bullitt, E. 2013. Surface for catalysis by poliovirus RNA-dependent RNA polymerase. *Journal of Molecular Biology*. **425**(14), pp.2529–2540.
- Wang, J., Wang, Y., Liu, J., Ding, L., Zhang, Q., Li, X., Cao, H., Tang, J. and Zheng, S.J. 2012. A critical role of N-myc and STAT interactor (Nmi) in foot-and-mouth disease virus (FMDV) 2C-induced apoptosis. *Virus Research*. **170**(1–2), pp.59–65.
- Waring, M.J., Andrews, D.M., Faulder, P.F., Flemington, V., McKelvie, J.C., Maman, S., Preston, M., Raubo, P., Robb, G.R., Roberts, K., Rowlinson, R., Smith, J.M., Swarbrick, M.E., Treinies, I., Winter, J.J.G. and Wood, R.J. 2014. Potent, selective small molecule inhibitors of type III phosphatidylinositol-4-kinase α -but not β -inhibit the phosphatidylinositol signaling cascade and cancer cell proliferation. *Chemical Communications*. **50**(40), pp.5388–5390.
- Westaway, E.G., Khromykh, A.A. and Mackenzie, J.M. 1999. Nascent flavivirus RNA colocalized in situ with double-stranded RNA in stable replication complexes. *Virology*. **258**(1), pp.108–117.
- Wu, Q., Brum, M.C.S., Caron, L., Koster, M. and Grubman, M.J. 2003. Adenovirus-mediated type I interferon expression delays and reduces disease signs in cattle challenged with foot-and-mouth disease virus. *Journal of Interferon & Cytokine Research*. **23**(7), pp.359–68.

- Wu, Y.-T., Tan, H.-L., Shui, G., Bauvy, C., Huang, Q., Wenk, M.R., Ong, C.-N., Codogno, P. and Shen, H.-M. 2010. Dual role of 3-methyladenine in modulation of autophagy via different temporal patterns of inhibition on class I and III phosphoinositide 3-kinase. *Journal of Biological Chemistry*. **285**(14), pp.10850–10861.
- Wymann, M.P., Bulgarelli-Leva, G., Zvelebil, M.J., Pirola, L., Vanhaesebroeck, B., Waterfield, M.D. and Panayotou, G. 1996. Wortmannin inactivates phosphoinositide 3-kinase by covalent modification of Lys-802, a residue involved in the phosphate transfer reaction. *Molecular and Cellular Biology*. **16**(4), pp.1722–33.
- Xia, H., Wang, P., Wang, G.-C., Yang, J., Sun, X., Wu, W., Qiu, Y., Shu, T., Zhao, X., Yin, L., Qin, C.-F., Hu, Y. and Zhou, X. 2015. Human enterovirus nonstructural protein 2CATPase functions as both an RNA helicase and ATP-independent RNA chaperone. *PLoS Pathogens*. **11**(7), p.e1005067.
- Xiang, W., Harris, K.S., Alexander, L. and Wimmer, E. 1995. Interaction between the 5'-terminal cloverleaf and 3AB/3CDpro of poliovirus is essential for RNA replication. *Journal of Virology*. **69**(6), pp.3658–67.
- Xiao, Y., Chen, H.-Y., Wang, Y., Yin, B., Lv, C., Mo, X., Yan, H., Xuan, Y., Huang, Y., Pang, W., Li, X., Yuan, Y.A. and Tian, K. 2016. Large-scale production of foot-and-mouth disease virus (serotype Asia1) VLP vaccine in *Escherichia coli* and protection potency evaluation in cattle. *BMC Biotechnology*. **16**(1), p.56.
- Yu, Y., Abaeva, I.S., Marintchev, A., Pestova, T. V and Hellen, C.U.T. 2011. Common conformational changes induced in type 2 picornavirus IRESs by cognate trans-acting factors. *Nucleic Acids Research*. **39**(11), pp.4851–4865.
- Zhang, L., Hong, Z., Lin, W., Shao, R.X., Goto, K., Hsu, V.W. and Chung, R.T. 2012. ARF1 and GBF1 generate a PI4P-Enriched environment supportive of hepatitis C virus replication. *PLoS ONE*. **7**(2), p.e32135.